Tampere University

RIIKKA NIEMI

Preoperative Evaluation of Ovarian Tumors

Tampere University Dissertations 27

Tampere University Dissertations 27

RIIKKA NIEMI

Preoperative Evaluation of Ovarian Tumors

ACADEMIC DISSERTATION
To be presented, with the permission of
the Faculty Council of the Faculty of Medicine and Health Technology
of the Tampere University,
for public discussion in the Jarmo Visakorpi auditorium
of the Arvo building, Arvo Ylpön katu 34, Tampere,
on 15 March 2019, at 12 o'clock.

ACADEMIC DISSERTATION
Tampere University, Faculty of Medicine and Health Technology
Tampere University Hospital, Department of Obstetrics and Gynecology
Finland

Responsible supervisor and Custos
Professor Johanna Mäenpää
Tampere University
Finland

Pre-examiners
Professor Kari Punnonen
University of Eastern Finland
Finland

Docent Maarit Anttila
University of Eastern Finland
Finland

Opponent
Docent Antti Perheentupa
University of Turku
Finland

Cover design: Roihu Inc.

ISBN 978-952-03-0952-7 (print)
ISBN 978-952-03-0953-4 (pdf)
ISSN 2489-9860 (print)
ISSN 2490-0028 (pdf)
http://urn.fi/URN:ISBN:978-952-03-0953-4

PunaMusta Oy – Yliopistopaino
Tampere 2019

To my dearest ones
Esa, Helmi, Saimi & Vilho

ABSTRACT

Ovarian tumors involve a wide range of neoplasms, from innocuous benign tumors to aggressive cancers. Not seldom are they found by chance, without any notable symptoms, and, as cancers, they may already have metastasized at that point. The diagnostic golden standard includes vaginal ultrasound (US) along with serum biomarkers, traditionally CA125, to assess tumor characteristics. The correct preoperative diagnosis of cancer is essential, as it allows a prompt referral to a center, where the operations are performed by gynecologic oncologists. In ovarian cancer (OC), effective and correct primary surgery is the most important prognostic factor. On the other hand, conservative follow-up may be sufficient for benign tumors.

Against this background, the aim of this thesis was to study advanced US modalities and to discover new possible biomarkers or methods to distinguish ovarian pathology preoperatively. First, we examined 100 at least 50-year-old women scheduled for surgery with an unclear ovarian tumor using traditional US and comparing it to various US scoring methods and three-dimensional ultrasound (3D US) with power Doppler (PD). The findings were compared with the results of examinations made by another experienced US examiner and also with histopathological diagnoses. None of the advanced US methods exceeded the accuracy of the subjective opinion of an expert. In addition, the 3D US with PD added no significant value to traditional methods. However, the results produced by two examiners were in good agreement.

To extend our investigation, we collected urine samples from 71 women with indefinite adnexal masses and from 22 controls, and analyzed urinary polyamines using liquid chromatography-tandem mass spectrometry (LC-MS/MS). Polyamines are naturally occurring components of all mammalian cells and have many functions, including cell growth. They are linked to carcinogenesis, and especially their diacetylated forms are found to be elevated in many cancers, although not previously in OC. In Study II, we showed that diacetylated spermine (DiAcSpm) was significantly elevated in urine from OC patients. While the levels of DiAcSpm differed even between low-stage OCs and benign ovarian tumors, the highest levels were found in high-grade OCs. Urinary DiAcSpm was even more sensitive than

serum CA125 with its commonly used cutoff value (35 U/mL): their respective sensitivities were 86.5% and 75.7%.

Based on previous experiments on the ability of dogs to detect the odor of cancer, urine samples (60 from women with adnexal tumors and 18 from controls) were also examined using field asymmetric waveform ion mobility spectrometry (FAIMS), a novel artificial olfactory technology. In our proof-of-concept Study III, we used FAIMS to differentiate between ovarian malignancy and benign tumors or controls with respective accuracies of 77.3% and 81.3%. When only high-grade cancers were taken into account, the accuracy in distinguishing them from low-grade cancers was 88.7%. Even low-grade cancers were differentiated from benign tumors with an accuracy of 83.9%.

Metabolic alterations, including lipid changes, in blood and tissues are associated with OC. However, it is unclear which specific lipids or lipid species are altered. A previous study showed decreases in levels of nearly all lipid species in blood samples from high-grade serous ovarian carcinoma patients, compared with women with benign gynecological disorders. In Study IV, our aim was to validate those previous results in a larger population, including also low-grade and early-stage cancers and histological pathology other than only serous. Lipidomic analysis was performed on 354 blood samples from women with OCs or benign gynecological pathologies; the women were from Finland or Germany. The results were compared with the previous results from 250 women. A total of 39 lipids were altered consistently and significantly in both early and late stages in all three cohorts (Finnish, German and previous study), 23 of them in all histological subtypes. Results showed lower levels of most of the lipids; there were higher levels of only one ceramide (Cer[d18:1/18:0]) and triacylglycerol (TAG[18:1/18:1/20:4]) in all stages and histologies. Combinations of some lipids and lipid ratios with CA125 improved the diagnostic value of serum CA125.

In conclusion, the subjective evaluation of two-dimensional US by an expert remains the most reliable preoperative diagnostic tool of adnexal masses. Emerging objective biochemical and biophysical methods include urinary polyamine analysis, FAIMS technology, and serum lipidomic profile.

TIIVISTELMÄ

Munasarjakasvaimet ovat ryhmä hyvin erilaisia kasvaimia viattomasta hyvänlaatuisesta kasvaimesta aggressiiviseen syöpään. Ne ovat usein sattumalöydöksiä oireettomilla naisilla, jopa levinneessä syövässä. Diagnostiikan kulmakivi on emättimen kautta tehtävä ultraäänitutkimus yhdistettynä verestä mitattaviin merkkiaineisiin, joista perinteisesti käytetyin on CA125-merkkiaine. Oikea ja mahdollisimman varhainen diagnoosi vaikuttaa kasvaimen hoitolinjoihin ja ennusteeseen, joka heikkenee merkittävästi levinneessä syövässä verrattuna alkuvaiheen munasarjasyöpään. Riittävän laaja leikkaushoito on merkittävin munasarjasyövän ennusteeseen vaikuttava tekijä. Toisaalta hyvänlaatuisten kasvaimien kohdalla konservatiivinen seurantalinja voi olla riittävä hoito, jolloin voidaan välttää turhia leikkausriskejä.

Väitöskirjan tavoitteena oli tutkia kehittyneempiä ultraäänitutkimusmenetelmiä ja -luokitteluja verrattuna perinteiseen kaksiulotteiseen ultraäänitutkimukseen, sekä etsiä uusia menetelmiä ja mahdollisia merkkiaineita munasarjakasvaimien erotusdiagnostiikkaan. Ensimmäisessä osatyössä tutkittiin 100 vähintään 50-vuotiasta naista, jotka odottivat munasarjakasvaimen vuoksi tehtävää leikkausta. Naiset tutkittiin ennen leikkausta kolmiulotteisella ultraäänitutkimuksella sekä moderneilla kaksiulotteiseen ultraäänitutkimukseen perustuvilla luokitteluilla, ja löydöksiä verrattiin keskenään. Mikään menetelmä ei ollut parempi kuin kokeneen ultraäänitutkijan oma arvio (ns. expert opinion) kaksiulotteisesta ultraäänitutkimuksesta. Kolmiulotteinen ultraäänitutkimus ei tuonut merkittävää lisäarvoa perinteisiin menetelmiin verrattuna. Jälkikäteen toinen kokenut ultraäänitutkija arvioi samat potilaat tallennettujen ultraäänikuvien perusteella, ja löydösten arviointi oli hyvin yhteneväistä tutkijoiden kesken.

Tutkimuksia laajennettiin keräämällä ennen leikkausta 71 munasarjakasvain- ja 22 kontrollipotilailta virtsanäytteitä, joista analysoitiin ja mitattiin nestekromatografia-massaspektrometrialla polyamiineja. Polyamiinit ovat nisäkässoluissa esiintyviä mm. solujen kasvulle välttämättömiä molekyylejä, joiden on todettu liittyvän myös karsinogeneesiin. Erityisesti asetyloituneiden polyamiinien kohonneita pitoisuuksia elimistön nesteissä on todettu useissa syövissä. Toisessa osatyössä osoitettiin ensimmäistä kertaa diasetyloituneen spermiinin (DiAcSpm) pitoisuuden olevan

kohonneen myös munasarjasyöpäpotilaiden virtsassa verrattuna kontrolleihin ja naisiin, joilla on hyvänlaatuinen munasarjakasvain. Korkeimmat virtsan DiAcSpm-pitoisuudet mitattiin potilailla, joilla oli huonosti erilaistunut ja levinnyt munasarjasyöpä (high-grade syöpä). Virtsan DiAcSpm oli tutkimuksessa jopa herkempi merkkiaine kuin yleisesti käytetty seerumin CA125 raja-arvolla 35 U/ml (86.5% vs. 75.7%).

Koirakokeissa on todettu, että koulutettu koira tunnistaa hajuaistin avulla syöpäkudoksen ja syöpäpotilaan eritteet. Nykyteknologia mahdollistaa analytiikan, jolla näytteen sisältämien orgaanisten yhdisteiden muodostama hajuspektri analysoidaan mm. koneellisen nenän (elektroninen nenä, eNose) avulla. Kolmannessa osatyössä virtsanäytteet (51 munasarjakasvain- ja 18 kontrollipotilailta) tutkittiin FAIMS (field asymmetric waveform ion mobility spectrometry)-teknologialla, joka on ionimobiliteettispektrometrian muunnelma sijoittuen massaspektrometrian ja elektronisen nenän välimaastoon. FAIMS-teknologian avulla munasarjasyöpäpotilaiden virtsa erotettiin kontrollien sekä hyvänlaatuisten kasvainpotilaiden virtsasta 81.3%:n ja 77.3%:n tarkkuuksilla. High-grade munasarjasyöpää sairastavien potilaiden virtsa oli erotettavissa varhaisvaiheen (low-grade) munasarjasyöpää sairastavien naisten virtsasta, joka puolestaan erosi hyvänlaatuisten kasvainpotilaiden virtsasta.

Munasarjasyövän metaboliatutkimuksissa on todettu muutoksia myös rasva-aineiden (lipidi) aineenvaihdunnassa syöpäpotilailla. On kuitenkin ollut epäselvää, mitkä lipidiryhmät muuttuvat erityisesti. Aiemmassa suomalais-saksalaisessa tutkimuksessa todettiin lähes kaikkien lipidien pitoisuuden laskevan high-grade seröösiä munasarjasyöpää sairastavien potilaiden veressä verrattuna naisiin, joilla oli hyvänlaatuinen gynekologinen sairaus. Neljännessä osatyössä lipidiaineenvaihdunnan muutoksia tutkittiin 354 verinäytteestä, jotka oli otettu varhais- ja levinneen vaiheen sekä erilaisia syöpäkasvaintyyppejä (muitakin kuin seröösi) sairastavilta munasarjasyöpäpotilailta ja hyvänlaatuista gynekologista sairautta sairastavilta naisilta. Yhteensä 39 lipidiä oli samansuuntaisesti ja pääosin tilastollisesti merkitsevästi muuttunut sekä varhais- että myöhäisasteen syövissä, ja 23 näistä lipideistä oli muuttunut myös kaikissa kasvaintyypeissä. Pääosin lipidipitoisuudet olivat vähentyneet syöpäpotilaiden veressä verrattuna ei-syöpäpotilaiden verinäytteisiin. Vain yksi keramidi (Cer[d18:1/18:0]) ja triasyyliglyseroli (TAG[18:1/18:1/20:4]) olivat kohonneet kaikissa levinneisyysasteissa ja kudostyypeissä. Lipidiyhdistelmät yhdessä seerumin CA125-pitoisuuden kanssa paransivat diagnostista osuvuutta yksittäiseen CA125-arvoon verrattuna.

Kokeneen tutkijan oma arvio kasvaimen laadusta perinteisessä kaksiulotteisessa ultraäänitutkimuksessa on edelleen luotettavin ultraäänitutkimusmenetelmä munasarjakasvaimien laatua arvioitaessa. Virtsan polyamiinien mittaaminen, FAIMS-teknologia ja seerumin lipidiprofiilin tutkiminen ovat lupaavia uusia objektiivisia tutkimusmenetelmiä munasarjakasvainten arvioinnissa.

TABLE OF CONTENTS

LIST OF ORIGINAL PUBLICATIONS

This thesis is based on the following original publications, which are referred to by the Roman numerals I-IV as assigned below.

I. Niemi RJ, Saarelainen SK, Luukkaala TH, Mäenpää JU. Reliability of preoperative evaluation of postmenopausal ovarian tumors. Journal of Ovarian Research 2017; 10(1): 15.

II. Niemi RJ, Roine AN, Häkkinen MR, Kumpulainen PS, Keinänen TA, Vepsäläinen JJ, Lehtimäki T, Oksala NK, Mäenpää JU. Urinary polyamines as biomarkers for ovarian cancer. International Journal of Gynecological Cancer 2017; 27(7): 1360-1366.

III. Niemi RJ, Roine AN, Eräviita E, Kumpulainen PS, Mäenpää JU, Oksala NK. FAIMS analysis of urine gaseous headspace is capable of differentiating ovarian cancer. Gynecologic Oncology 2018; 151(3): 519-524.

IV. Niemi RJ, Braicu EI, Kulbe H, Koistinen KM, Sehouli J, Puistola U, Mäenpää JU, Hilvo M. Ovarian tumors of different histologic type and clinical stage induce similar changes in lipid metabolism. British Journal of Cancer 2018; 119(7): 847-854.

 In addition, some unpublished data are presented.

ABBREVIATIONS

2D US	Two-dimensional ultrasound
3D US	Three-dimensional ultrasound
3D-PD	Three-dimensional power Doppler
ADC	Apparent diffusion coefficient
ADNEX	Assessment of different neoplasias in the adnexa
ATX	Autotoxin
AUC	Area under the curve
BEP	Bleomycin-etoposide-cisplatin
BOT	Borderline ovarian tumor
CA125	Cancer antigen 12-5
CEA	Carcinoembryonic antigen
Cer	Ceramide
CI	Confidence interval
CT	Computed tomography
DCE MRI	Dynamic contrast-enhanced magnetic resonance imaging
DFMO	DL-α-difluoromethylornithine
DiAcSpd	N^1, N^8-diacetylspermidine
DiAcSpm	N^1, N^{12}-diacetylspermine
DWI	Diffusion-weighted imaging
ELISA	Enzyme-linked immunosorbent assay
eNose	Electronical nose
FAIMS	Field asymmetric waveform ion mobility spectrometry
FAS	Fatty acid synthase
FDA	Food and Drug Administration
FI	Flow index
FIGO	International Federation of Gynecology and Obstetrics
GC	Gas chromatography
HDL	High density lipoprotein

HGSOC	High-grade serous ovarian carcinoma
HE4	Human epididymis protein 4
HPLC	High-performance liquid chromatography
IOTA	International Ovarian Tumor Analysis
IS	Internal standard
LC	Liquid chromatography
LC-MS(/MS)	Liquid chromatography-mass spectrometry (-tandem mass spectrometry)
LDA	Linear discriminant analysis
LGSC	Low-grade serous carcinoma
LPA	Lysophosphatidic acid
LR1 & 2	Logistic regression models 1 & 2
MRI	Magnetic resonance imaging
MS	Mass spectrometry
OC	Ovarian cancer
PD	Power Doppler
PET	Position emission tomography
PI	Pulsatility index
PLA2	Phospholipase A2
QDA	Quadratic discriminant analysis
RI	Resistance index
RMI	Risk of malignancy index
ROC	Receiver operating characteristics
ROMA	Risk of malignancy algorithm
SSAT	Spermidine/spermine N^1-acetyltransferase
TAG	Triacylglycerol
TATI	Tumor-associated trypsin inhibitor
US	Ultrasound
VFI	Vascularity flow index
VI	Vascularity index
VOC	Volatile organic compound
VOCAL	Virtual Organ Computer-Aided Analysis
WHO	World Health Organization

1 INTRODUCTION

Approximately 239,000 new ovarian cancer (OC) cases are found annually worldwide, and the peak incidence rate is among postmenopausal women (Ferlay et al. 2015). At the same time, OC is the most lethal gynecological cancer and the fifth leading cause of cancer deaths in the U.S.. The five-year relative survival rate has improved significantly in the U.S., from 36% to 46% in 1975-2011, a rate that is still quite poor compared to the localized OC survival rate of 92% (Siegel et al. 2016). In Finland, the published overall five-year survival for OC patients was 43% in 2013-2015 (Finnish Cancer Registry 2018). Because the prognosis improves remarkably when OC is diagnosed at an early-stage, better diagnostic methods are urgently needed.

Accurate preoperative classification of ovarian tumors is necessary for the appropriate treatment of tumors, especially classification into benign and malignant tumors. Women with suspected OC should be operated on and treated in specialized centers because optimal cytoreductive surgery is one of the main prognostic factors in the treatment (Bristow et al. 2002). On the other hand, a majority of ovarian neoplasms are benign, and an accurate diagnosis is needed to avoid unnecessary or overly radical surgery in order to reduce the risk of surgical procedures.

The symptoms of OC are non-specific and can mimic other conditions such as upper-abdominal disease. At early stages of the disease, most women are asymptomatic. Large ovarian tumors can be palpable in a clinical examination, but often a further evaluation of the pelvis using vaginal ultrasound (US) is performed to diagnose and classify the ovarian mass as either benign or malignant. Previous studies have determined sonographic morphological and vascular features of adnexal masses that specify their nature. The gold standard of ovarian tumor markers is CA125, which – together with US findings – is typically used in predicting the malignancy of an adnexal tumor. The disadvantage of CA125 is that increased serum levels are associated more with advanced and serous OCs than with low-stage cancers or other histological subtypes. Also, serum CA125 has a quite poor

specificity for OC because it can also be elevated in some non-ovarian cancers and in benign gynecological conditions (Jacobs & Bast 1989).

Several predictive models have been created to optimize the diagnostic performance of sonography, including different scoring systems, logistic regression analysis and neural networks. The risk of malignancy index (RMI) is the first score criterion that takes into consideration US findings, serum CA125 level, and patient age and menopausal status (Jacobs et al. 1990). In 2008, the International Ovarian Tumor Analysis (IOTA) group published simple US-based rules which can be used to correctly classify most ovarian tumors (Timmerman et al. 2008).

Polyamines are molecules necessary for eukaryotes and essential for cellular proliferation, also in carcinogenesis. Increased polyamine concentrations have been found in many cancers (Gerner & Meyskens 2004). New technology has permitted the simultaneous large-pattern analysis of both acetylated and unacetylated polyamines from urine (Häkkinen et al. 2013).

Some cancers have distinct odors caused by volatile organic compounds (VOCs) which can be detected in urine, blood and breath by a canine's olfactory sense (Lippi & Cervellin 2012). In addition to canine studies, various new technical methods have been studied, e.g. the so-called electronic nose (eNose) and lately more modern variants such as field asymmetric waveform ion mobility spectrometry (or FAIMS) (Covington et al. 2015).

Several metabolic alterations occur in cancer cells due to the increased demand for energy. Metabolomic profiling is a new diagnostic tool in understanding these metabolic changes. In OC, altered serum metabolites have been shown to include ketone bodies, carbohydrates, amino acids, lipids and fatty acids (Hilvo et al. 2016). Especially alterations in the phospho- and sphingolipid metabolism are associated with malignancies, and changes in those lipids have also been found in OC (Furuya et al. 2011; Tania et al. 2010). To date, there are no validation studies of the most-altered lipids in OC (Ke et al. 2015).

In this thesis, new preoperative diagnostic methods are demonstrated to distinguish between benign and malignant ovarian processes. First, women with unclear ovarian masses were examined using various sonographic predictive methods, including three-dimensional power Doppler (3D-PD) US before surgery. Preoperatively collected urine samples were investigated, employing liquid chromatography-tandem mass spectrometry (LC-MS/MS) to explore the polyamine concentrations in women with and without ovarian neoplasms. The urine samples

were also tested using FAIMS to determine the ability of the system to detect volatile compounds in the urine of OC patients. Finally, lipidomic analysis of blood samples from women with ovarian tumors and benign gynecological diseases was performed to identify possible alterations in lipidomic profiling.

2 REVIEW OF THE LITERATURE

2.1 Ovarian neoplasms

Primary ovarian tumors can be categorized into three main types: surface epithelial-stromal, sex cord-stromal and germ cell. Each category contains many subgroups, and some tumors are mixed tumors consisting of different types of cells (V. W. Chen et al. 2003).

Figure 1. Origin of the main types of ovarian tumors (modified from V. W. Chen et al. 2003).

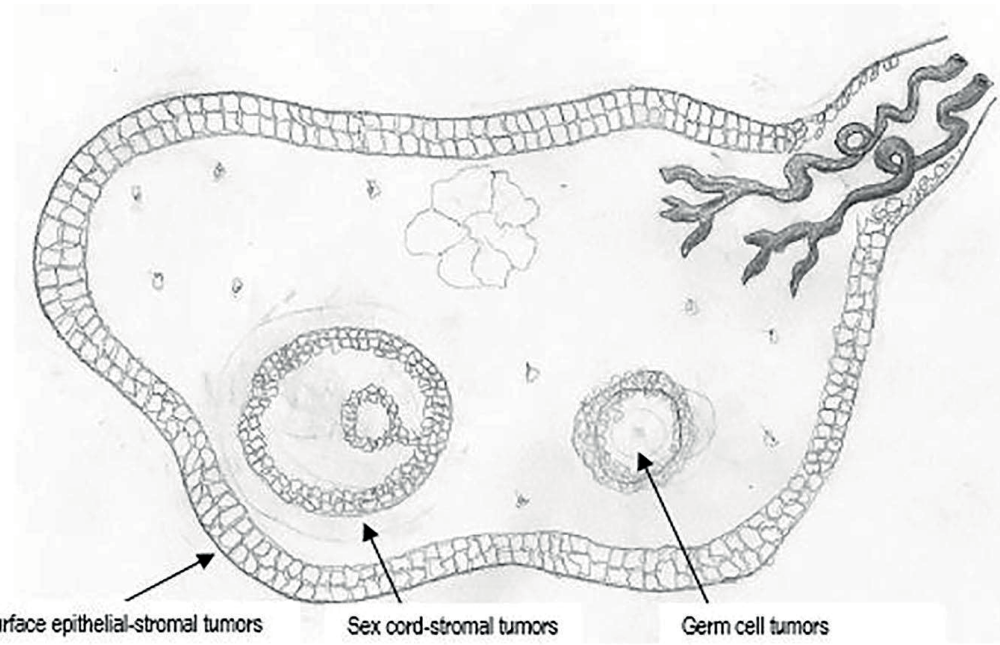

In recent years, molecular, genetic and epigenetic studies have improved knowledge about the pathology of ovarian tumors, so the World Health Organization (WHO) revised the classification of cancers of the ovaries, fallopian tubes and peritoneum in 2014 (Kurman et al. 2014; see Table 1). It is based mainly on histopathological findings and takes into account the pathogenesis and prognosis of the OC subtypes (Meinhold-Heerlein et al. 2015; Meinhold-Heerlein et al. 2016). In parallel with WHO reclassification, the International Federation of Gynecology and Obstetrics (FIGO) introduced a new surgical staging classification for cancers of the ovary, fallopian tubes and peritoneum. It recognizes that OCs are a heterogenous group of malignant tumors with different characteristics and outcomes (Zeppernick & Meinhold-Heerlein 2014).

Table 1. The current (2014) WHO classification of epithelial ovarian tumors (Kurman et al. 2014).

Serous tumors	**Benign type**	**Borderline (SBOT)**	**Malignant type**
	Cystadenoma Adenofibroma Surface papilloma	SBOT/atypical proliferating tumor SBOT, micropapillary type/ non-invasive, serous low-grade carcinoma	Serous low-grade carcinoma Serous high-grade carcinoma
Mucinous tumors	**Benign type**	**Borderline (MBOT)**	**Malignant type**
	Cystadenoma Adenofibroma	MBOT/atypical proliferating mucinous tumor	Mucinous carcinoma
Endometrioid tumors	**Benign type**	**Borderline (EBOT)**	**Malignant type**
	Endometriosis cyst Endometrioid cystadenoma Endometrioid cystadenofibroma	EBOT/atypical proliferating endometrioid tumor	Endometrioid carcinoma
Clear cell tumors	**Benign type**	**Borderline (CBOT)**	**Malignant type**
	Cystadenoma	CBOT/atypical proliferating clear cell tumor	Clear cell carcinoma
Brenner tumors	**Benign type**	**Borderline**	**Malignant type**
	Brenner tumor	Borderline Brenner tumor/atypical proliferating Brenner tumor	Malignant Brenner tumor
Seromucinous tumors	**Benign type**	**Borderline**	**Malignant type**
	Seromucinous cystadenoma Seromucinous adenofibroma	Seromucinous borderline tumor/atypical proliferating seromucinous tumor	Seromucinous carcinoma
Undifferentiated carcinoma			

2.1.1 Benign ovarian tumors

While epithelial tumors form the majority of ovarian malignancies, germ cell tumors, or mature cystic teratomas (dermoid cysts), represent the most common benign ovarian neoplasms, appearing mainly among youth and younger women of reproductive age (Koonings et al. 1989; Park et al. 2015). They are assumed to originate from primordial germ cells of yolk sac migrated along the coelomic cavity to the ovary (Koonings et al. 1989).

The most common benign ovarian tumor among women over 50 years old is serous cystadenoma (Koonings et al. 1989). Mucinous cystadenomas often occur as large cystic masses and represent approximately 10-15% of benign ovarian neoplasms. Epithelial cystadenomas are believed to be formed from coelomic inclusion cysts that undergo metaplasia (Brown & Frumovitz 2014; Koonings et al. 1989).

2.1.2 Borderline ovarian tumors

Borderline ovarian tumors (BOTs) are neoplasms classified between the benign and malignant categories. They are low-malignancy potential tumors that have an elevated mitotic activity and slight nuclear atypia without marked stromal invasion. Most of them are serous and mucinous subtypes (Silverberg et al. 2004). BOTs occur also in younger women, when correct diagnosis and treatment options must also take into account fertility preservation issues. Serous BOTs share molecular and genetic similarities with low-grade serous carcinomas (LGSCs), and they can exist at advanced stages with peritoneal implants and/or lymph node involvement. Non-serous BOTs occur mainly at Stage I. The new WHO classification reformed the terminology of microinvasion: microinvasive foci have dimensions of maximum 5 mm, but if they have solid nests or cribriform glands histologically reminiscent of LGSCs, they are classified as LGSCs despite the size of the microinvasion (Hauptmann et al. 2017).

The recent classification of WHO also mentioned micropapillary serous BOT as a distinct variant of BOT. It is also determined as a non-invasive LGSC. Micropapillary pattern of serous BOT is not an independent prognostic factor, but it is more often associated with poor clinicopathological factors e.g. found at advanced stages (Hauptmann et al. 2017). Previously the peritoneal implants of

serous BOT were divided into invasive and non-invasive while the new WHO classification considers the invasive foci as peritoneal LGSC (Meinhold-Heerlein et al. 2016).

2.1.3 Ovarian cancer

One in 75 women develops OC during her lifetime. The risk is higher in the U.S. and Europe than in Asia (Reid et al. 2017).

At least 90% of ovarian malignancies are of epithelial origin, and the main subtype is high-grade serous (HGSC; 70%), followed by endometrioid (10%), clear cell (10%), mucinous (3%), and LGSC (<5%) (Zeppernick & Meinhold-Heerlein 2014). Malignant sex cord-stromal (mainly granulosa cell tumors) and germ cell tumors (dysgerminomas, yolk sac tumors and immature teratomas) represent respectively 1-2% and 3% of OCs (Prat & FIGO Committee on Gynecologic Oncology 2014).

Nowadays epithelial OC is roughly divided into two groups: type I and type II (Koshiyama et al. 2017; Kurman & Shih 2016; Labidi-Galy et al. 2017).

Table 2. The characteristics of type I and II epithelial ovarian carcinoma.

	Type I ovarian cancer	**Type II ovarian cancer**
Behavior	Slow-growing	Aggressive
Origin → Histological subtype	Endometriosis → Endometrioid carcinoma, Clear cell carcinoma, Seromucinous carcinoma Fallopian tube → LGSC Germ cell (via mature teratoma) → Mucinous carcinoma? Transitional cell → Mucinous carcinoma?, Malignant Brenner tumor	Fallopian tube → HGSC, Carcinosarcoma, Undifferentiated carcinoma
Stage	Frequently early stage	Mostly advanced stage
Precursor	A benign precursor cyst or atypical proliferative (borderline) tumor	Mostly STICs (*de novo* starting)
Proliferative activity	Usually low	Always high
BRCA1 / BRCA2 mutation	Low	High
TP53 mutation	Low	High
Chromosomal instability	Low	High
Homologous recombination repair	Rarely defective	Often defective
Clinical outcome	Usually good	Often poor

LGSC: low-grade serous carcinoma; HGSC: high-grade serous carcinoma; STIC: serous tubal intraepithelial carcinoma.

2.1.4 Treatment

2.1.4.1 Benign ovarian tumors

Examination by an experienced sonographist is essential for the accurate diagnosis of ovarian tumors and making decisions regarding their treatment. Asymptomatic adnexal tumors can be managed conservatively by appropriate follow-up, which diminishes surgical risks by minimizing unnecessary surgery. The effect of a tumor or surgery on hormonal status should also be considered. On the other hand, ovarian tumors with a suspicion of malignancy must be referred to a gynecologic oncologist.

An international panel of experts has drafted consensus recommendations for the clinical assessment and management of asymptomatic ovarian tumors (Glanc et al. 2017). Based on this and other publications, treatment of simple cysts (Greenlee et al. 2010; Modesitt et al. 2003) or cysts with solid components, septated tumors (Saunders et al. 2010), solid tumors (Alcazar et al. 2017; Timmerman et al. 2008; S. Wang & Johnson 2012), dermoid cysts (Park et al. 2015) and endometrioid cysts (He et al. 2017) are summarized in Table 3 below.

Table 3. Treatment recommendations for asymptomatic sonographically benign ovarian tumors.

Ultrasound finding	Risk of malignancy	Recommended treatment
Simple cyst <10 cm	Minimal	Conservative follow-up
Thin (<3 mm) septas of a cyst	Minimal	Conservative follow-up
Cysts with a few solid (<3 mm) components	Minimal More or larger components increase risk of malignancy	Conservative follow-up
Solid tumor	Tumors with acoustic shadows, non-detectable or minimal blood flow in color Doppler without ascites bear minimal risk (2% in postmenopausal women)	Conservative follow-up
Dermoid cyst	Older age, elevated CA125 levels, postmenopausal status, or large tumors increase the risk	Surgery for large tumors or for those with changes in follow-up
Endometrioid cyst	Postmenopausal status and size of >8 cm increase the risk OR for clear cell cancer =3.05 OR for endometrioid cancer =2.04 OR for low-grade serous cancer =2.11	No evidence that early surgical treatment reduces the risk for cancer; surgery or careful follow-up for women with risk factors

OR: Odds ratio.

2.1.4.2 Borderline ovarian tumors

Borderline ovarian tumors occur in younger women than epithelial OC, and therefore more conservative surgery is often discussed in order to retain fertility. The prognosis for BOTs is generally excellent because they are mainly diagnosed at a non-advanced stage. The five-year survival for Stage I patients is 95-97%; because recurrences can appear late, the ten-year survival is 70-95%. In turn, the five-year survival for women with Stage II or III BOT is 65-87% (Fischerova et al. 2012).

Recurrences are associated more often with conservative treatment than with radical surgery. In the study of Suh-Burgmann (2006), 193 women with BOTs, mainly Stage I disease, were treated conservatively. The patients who underwent cystectomy relapsed more often than the patients who underwent oophorectomy (23% vs. 7% respectively). Two women (1%) saw a recurrence with malignant OC in the three years after their first surgery.

The standard surgery for BOTs remains bilateral salpingo-oophorectomy with or without hysterectomy, including FIGO staging procedures, and it is recommended for women without wish to remain fertile. In these cases, preoperative counselling before conservative surgery is important. Routine lymphadenectomy is not recommended (Fischerova et al. 2012; Gershenson 2017). Adequate staging includes appendicectomy in the case of mucinous BOTs (Morice et al. 2012).

To date, there is no data evidencing the benefits of adjuvant chemotherapy, even at advanced stages of BOTs (Fischerova et al. 2012). Still, for women with serous BOTs and invasive peritoneal implants, platinum-based chemotherapy is recommended. Increasingly, these BOTs are called low-grade carcinomas (Gershenson 2017).

2.1.4.3 Epithelial ovarian cancer

The histopathological evaluation of tissue samples is needed to confirm the diagnosis of OC; surgery is often required to obtain such samples. The main targets of the surgery are to verify the diagnosis, determine the stage of the cancer and achieve maximal removal of the tumor. Both the histopathological type of tumor (WHO classification) and the surgical stage of tumor (FIGO classification) are important in therapeutic decisions regarding OC. The FIGO staging classification from 2014 is shown in Table 4 (Prat & FIGO Committee on Gynecologic Oncology 2014).

Table 4. The FIGO staging classification (2014) of ovarian cancer.

Stage	Description
I	Tumor confined to the ovaries
IA	Tumor restricted to one ovary (capsule is intact); no tumor on ovarian surface; no malignant cells in the ascites or peritoneal washings
IB	Tumor is restricted to both ovaries (capsule is intact), no tumor on ovarian surface, no malignant cells in the ascites or peritoneal washings
IC	Tumor is restricted to one or both ovaries with one of the following:
IC1	• capsule rupture intraoperatively
IC2	• capsule rupture preoperatively or tumor on ovarian surface
IC3	• malignant cells in the ascites or peritoneal washings
II	Tumor involves one or both ovaries with pelvic involvement
IIA	Extension and/or implants on uterus and/or fallopian tubes and/or ovaries
IIB	Extension to other pelvic intraperitoneal tissue
III	Tumor involves one or both ovaries with cytologically or histologically verified peritoneal metastases outside the pelvis and/or in retroperitoneal lymph nodes
IIIA1	(Cytologically or histologically verified) metastases in retroperitoneal lymph nodes (i) maximum diameter 10 mm (ii) maximum diameter >10 mm
IIIA2	Microscopic peritoneal metastases outside the pelvis with or without metastases in retroperitoneal lymph nodes
IIIB	Macroscopic peritoneal metastases ≤2 cm outside the pelvis with or without metastases in retroperitoneal lymph nodes
IIIC	Macroscopic peritoneal metastases >2 cm outside the pelvis with or without metastases in retroperitoneal lymph nodes (including capsule of the liver/spleen but excluding parenchymatous metastases)
IV	Distant metastasis without peritoneal metastases
IVA	Pleural effusion with positive cytology
IVB	Parenchymal metastases and metastases in extra-abdominal organs (including inguinal and extra-abdominal lymph node metastases)

The cornerstones of epithelial OC treatment are surgery and postoperative chemotherapy. The surgery consists of staging laparotomy (longitudinal incision), including a total hysterectomy with bilateral salpingo-oophorectomy, peritoneal cytology, biopsies from the peritoneum and/or resection of suspicious lesions of the peritoneum, omentectomy, and pelvic and para-aortal lymphadenectomies. The aim of the surgery is an optimal debulking removing all the visible tumor manifestations, which is the main prognostic factor in patient survival (Meinhold-Heerlein et al.

2015). Neoadjuvant chemotherapy may decrease postoperative morbidity in patients in poor condition or with co-morbidities and may improve the likelihood of optimal surgery, but it cannot improve the prognosis of a patient (Hacker & Rao 2017).

A review of Chiva et al. (2016) collected information from 12,000 patients with Stage III-IV OC. The patients with completely resected disease had a median overall survival of 70 months compared with patients with a minimal macroscopic residual disease of 0.1-0.5 cm or suboptimal debulking (residual disease >0.5-1 cm), who survived 53 and 30-40 months respectively. Melamed et al. (2017) established that optimal cytoreductive surgery was an important prognostic factor in Stage IIIC-IV OC of the serous, clear cell and mucinous histological subtypes. To achieve complete primary cytoreduction, extensive ultra-radical surgery is performed in the management of advanced OCs. This aggressive surgery may include procedures such as diaphragm peritonectomy, splenectomy, bowel resection and liver resection (Chang et al. 2015).

Platinum- and taxane-based chemotherapy is the standard first-line treatment for early- and advanced-stage epithelial OC after primary surgery. Adjuvant chemotherapy is not recommended for patients whose disease is restricted to the ovary (Stage IA or IB) and of a low histological grade, because they have a five-year survival of >90% after successful surgery (Young et al. 1990). The chemotherapy is received in six cycles every three weeks, although shorter courses of chemotherapy may be sufficient for patients with a non-serous histology (Webber & Friedlander 2017). The addition of bevacizumab to standard chemotherapy has improved the overall survival of OC patients with a high risk of cancer progression (Oza et al. 2015).

2.1.4.4 Non-epithelial malignant ovarian tumors

Malignant germ cell ovarian tumors are mainly unilateral and restricted only to the ovary, which enables fertility-sparing surgery such as unilateral salpingo-oophorectomy. The extent of surgical staging depends, for example, on the age of the patient. A careful evaluation of the abdominal cavity is performed with cytological samples, peritoneal biopsies, palpation of the omentum or omentectomy, and lymph node biopsies or lymphadenectomies are performed as in epithelial OC staging (Brown et al. 2014; Gershenson 2007). Cisplatin-based adjuvant chemotherapy, bleomycin-etoposide-cisplatin (BEP), has been a postoperative

standard (Brown et al. 2014). However, women with Stage IA dysgerminomas and highly differentiated Stage IA immature teratomas can be treated with surgery alone (Colombo et al. 2012).

The surgical treatment of malignant sex cord-stromal ovarian tumors is similar to that of epithelial OCs, but systematic lymphadenectomies are not recommended. Young women with localized tumors (Stage IA) can have conservative surgery that spares the contralateral adnex. According to the recommendations, postoperative chemotherapy (e.g. BEP) is utilized only in advanced stages: granulosa cell tumors Stages IIA-IV and Sertoli-Leydig cell tumors with poor differentiation (Colombo et al. 2012).

2.1.5 Ovarian cancer screening

Screening for OC has thus far turned out to be quite ineffective. The results of the UK Collaborative Trial of Ovarian Cancer Screening (UKCTOCS) were published recently. In that randomized controlled trial, they recruited 200,000 postmenopausal women and divided them in a ratio of 1:1:2 into three groups: one with annual multimodal screening with CA125 measuring with a transvaginal US as a secondary test for women with increased CA125 levels, one with annual transvaginal US screening and one without any screening. The primary analysis of UKCTOCS did not reveal any significant reduction in OC mortality in the screening groups, although a subgroup analysis excluding prevalent OCs did (Jacobs et al. 2016).

MicroRNAs are small, non-coding RNA molecules found circulating in peripheral blood and shown to be deregulated in cancer, also in OC. Therefore, they have been studied as potential early biomarkers of OC, but large population studies are still lacking (Prahm et al. 2016). Liquid-based Pap smear specimens, which can reveal previously identified DNA mutations indicating OC, have also been tested for OC diagnostics. These tests will have to be improved before they can be used in routine screening (Kinde et al. 2013).

2.2 Preoperative assessment of ovarian tumors with biomarkers

2.2.1 Cancer antigen 125

Cancer antigen 125 (CA125) is the most studied OC biomarker; it was described as elevated in epithelial OC patients in 1983 by Bast et al. (Jacobs & Bast 1989). CA125 is an antigen on a high-molecular-weight membrane glycoprotein recognized by the corresponding monoclonal antibody OC125, which was discovered when mice were immunized with an ovarian cancer cell line. It is expressed in Müllerian and coelomic epithelia, but originally it was not found on normal adult and fetal ovarian surfaces. Later studies showed immunohistochemical CA125 expression also in normal ovarian epithelium tissue (Jacobs & Bast 1989). In turn, CA125 promotes ovarian cancer cell proliferation and suppresses an anti-cancer immune response, and is therefore overexpressed in epithelial cancers (Bast & Spriggs 2011). It has been detected in, for example, normal seminal fluid, fallopian tubes and the endometrium, but also in the lungs and conjunctiva, although its physiological function remains unclear (Bast & Spriggs 2011). The original CA125 test reacts only to OC125, and serum levels of CA125 are considered to be normal if ≤35 U/mL (van Nagell & Miller 2016).

The serum CA125 marker is used to distinguish OC from benign ovarian tumors, to check therapeutic response and to detect recurrence of OC (Bast et al. 2005). It is elevated in over 80% of epithelial OC patients, but mucinous or early-stage (FIGO Stage I) cancers are associated with lower CA125 values (Duffy et al. 2005). CA125 detects epithelial OC in postmenopausal women at an early- and advanced-stage with a specificity of 90% and a respective sensitivity of 50-60% and 80-90% (Muinao et al. 2018). In a study by Chen et al., women with type II OC were shown to have higher CA125 levels than women with type I OC: the respective median CA125 levels were 937 U/mL and 171 U/mL (X. Chen et al. 2013).

CA125 levels may be elevated due to many benign or extraovarian malignant causes, which attenuates its usefulness as a diagnostic biomarker (Duffy et al. 2005; Jacobs & Bast 1989; Sevinc et al. 2007; see Table 5). The predictive value of CA125 is better for postmenopausal than premenopausal women, who can be healthy and still have higher CA125 levels. Pregnancy increases CA125 levels, which also fluctuate during the menstrual cycle (Duffy et al. 2005; Jacobs & Bast 1989). In a

pooled analysis of 13 studies, it was concluded that a higher body mass index and non-white race may be factors in higher CA125 values (Babic et al. 2017). Monitoring CA125 values over time may give a more reliable view of the disease: benign or non-gynecological causes may result in fluctuating or stable values, whereas, with OC, CA125 values tend to increase (Bast et al. 2005).

Table 5. Benign and malignant conditions other than ovarian cancer affecting elevated CA125 concentrations.

Benign gynecological disorders	Benign non-gynecological disorders	Malignant gynecological disorders	Malignant non-gynecological disorders*
Endometriosis	Pancreatitis	Advanced uterine cancer	Breast cancer
Uterine myomas	Renal failure		Lung cancer
Adenomyosis	Liver cirrhosis		Pancreatic cancer
Pelvic inflammatory disease	Some lung and pleural diseases		Gastro-intestinal cancer
Ovarian hyperstimulation syndrome	Other conditions associated with ascites		Hepato-biliary cancer
Meig`s syndrome			Bladder cancer
(Pregnancy)			Lymphoma with peritoneal involvement

* Especially with peritoneal metastasis.

2.2.2 Human epididymis protein 4

Human epididymis protein 4 (HE4) is encoded by the WFDC2 gene, which was originally found in epithelial cells of the human epididymis (Hellstrom et al. 2003). HE4 is expressed in normal reproductive and respiratory tracts and in salivary gland secretions, but minimal expression is found in normal ovarian tissues. The overexpression of HE4 is seen in epithelial OCs, especially in serous and endometrioid adenocarcinomas. Benign and borderline ovarian tumors have lower levels of HE4 (N. S. Karlsen et al. 2014).

The first experiment showing that serum HE4 could act as an OC biomarker was published in 2003. In that study, HE4 was shown to be comparable with CA125 in distinguishing localized and advanced OC (Hellstrom et al. 2003). Later studies have reported HE4 to be as good as CA125 or even better in detecting OC. Moore et al. compared multiple ovarian biomarkers for detecting OC. HE4 had the highest sensitivity (72.9%) in finding OC, with a specificity of 95%, but the combination of

CA125 and HE4 improved the sensitivity to 76.4%. HE4 was found to be also the best biomarker to differentiate Stage I OC from benign tumors, although the sensitivity of HE4 was quite low, 45.9%, with a specificity of 95%, and a combination with CA125 did not improve the results (Moore et al. 2008). In a study by Holcomb et al. (2011), serum HE4 performed better (sensitivity 88.9% and specificity 91.8%) compared with CA125 (83.3% and 59.5% respectively) in distinguishing between benign and malignant adnexal masses in premenopausal women

In 2008, the Food and Drug Administration (FDA) in the U.S. approved serum HE4 as a diagnostic tool for OC (N. S. Karlsen et al. 2014). Urinary HE4 has also been proven to be a feasible non-invasive diagnostic biomarker for OC. One meta-analysis of seven studies estimated a sensitivity of 76% and specificity of 92% for urine HE4 in detecting OC (Jia et al. 2017).

The advantage of HE4 over CA125 is its very low production in normal ovarian tissue. Consequently, while CA125 levels are often elevated in premenopausal women with endometriomas or other benign ovarian tumors, serum levels of HE4 remain normal (Huhtinen et al. 2009; Moore et al. 2008). The commonly used cutoff value for serum HE4 concentration is 70 pmol/L (Moore et al. 2008). Serum levels of HE4 increase along age and smoking (Bolstad et al. 2012). Pregnant women in every trimester have lower levels of HE4 than other premenopausal women (Moore et al. 2012). In contrast with HE4, serum levels of CA125 in postmenopausal women are significantly lower than in premenopausal women (Bon et al. 1996), which means it is more useful than HE4 with postmenopausal women. The guidelines of the Royal College of Obstetricians and Gynaecologists do not recommend the routine use of serum HE4 instead of CA125 in the diagnosis of postmenopausal ovarian neoplasms due to insufficient data (Royal College of Obstetricians and Gynaecologists 2016).

Higher HE4 levels can be associated with some non-malignant diseases, of which renal failure is the most significant, featuring HE4 levels that increase with the serum creatine concentration (Escudero et al. 2011). Serum HE4 levels are elevated in acute and chronic heart failure correlating with severity of the disease and renal function (de Boer et al. 2013; Piek et al. 2017). Significantly elevated HE4 levels are also found in malignancies, not only in epithelial OC but also in endometrial cancer, lung adenocarcinoma and transitional cell carcinoma. Patients with liver metastases from any cancer origin have been found to have elevated HE4 levels (Escudero et al. 2011; N. S. Karlsen et al. 2014).

2.2.3 The risk of malignancy algorithm

The serum HE4 biomarker has been studied and used mostly as a complementary biomarker for CA125. Moore et al. evaluated the risk of malignancy algorithm (ROMA) as a diagnostic marker for the prediction of ovarian tumors and combined serum CA125 and HE4 into two logistic regression algorithms depending on patients' menopausal status. The ROMA algorithm classified tumors as a low or high risk in post- and premenopausal groups with sensitivities of 92% and 77% respectively and specificities of 75% in both groups (Moore et al. 2009). FDA approved ROMA as a preoperative test in evaluating ovarian tumors in 2011 (Miller & Ueland 2012).

Meta-analyses of 11 (F. Li et al. 2012) and 32 studies (J. Wang et al. 2014) evaluated the diagnostic performance of ROMA, single HE4 and CA125 parameters in predicting OC (Table 6).

Table 6. Summary of pooled/mean estimates for prediction of ovarian cancer.

Reference		CA125	HE4	ROMA
Li et al. 2012	Overall			
	Sensitivity (95% CI)	0.73 (0.63-0.81)	0.77 (0.72- 0.81)	0.86 (0.82-0.89)
	Specificity (95% CI)	0.86 (0.81-0.90)	0.88 (0.82-0.93)	0.78 (0.75-0.81)
	Epithelial ovarian cancer			
	Sensitivity (95% CI)	0.77 (0.58-0.89)	0.79 (0.74-0.84)	0.89 (0.84-0.93)
	Specificity (95% CI)	0.84 (0.76-0.90)	0.93 (0.87-0.96)	0.83 (0.77-0.88)
	Premenopausal women			
	Sensitivity (95% CI)	0.88 (0.59-0.99)	0.87 (0.65-0.99)	0.82 (0.67-0.91)
	Specificity (95% CI)	0.59 (0.47-0.71)	0.93 (0.86-0.98)	0.82 (0.74-0.88)
	Postmenopausal women			
	Sensitivity (95% CI)	0.95 (0.83-0.99)	0.82 (0.68-0.94)	0.93 (0.89-0.96)
	Specificity (95% CI)	0.86 (0.73-0.96)	0.95 (0.81-1.00)	0.79 (0.73-0.83)
Wang et al. 2014	Overall			
	Sensitivity (95% CI)	0.79 (0.74-0.84)	0.76 (0.72-0.80)	0.85 (0.81-0.89)
	Specificity (95% CI)	0.82 (0.77-0.87)	0.94 (0.90-0.96)	0.82 (0.77-0.87)
	Premenopausal women			
	Sensitivity (95% CI)	0.80 (0.70-0.88)	0.71 (0.64-0.78)	0.76 (0.70-0.81)
	Specificity (95% CI)	0.76 (0.63-0.86)	0.94 (0.88-0.97)	0.85 (0.80-0.89)
	Postmenopausal women			
	Sensitivity (95% CI)	0.86 (0.79-0.91)	0.78 (0.71-0.85)	0.91 (0.87-0.93)
	Specificity (95% CI)	0.85 (0.79-0.90)	0.90 (0.78-0.97)	0.79 (0.74-0.84)
	Epithelial ovarian cancer			
	Sensitivity (95% CI)	0.81 (0.74-0.87)	0.77 (0.71-0.82)	0.90 (0.86-0.93)
	Specificity (95% CI)	0.81 (0.73-0.87)	0.94 (0.90-0.96)	0.77 (0.69-0.84)

In a prospective study of 1,218 patients with an adnexal tumor, HE4 and CA125 were measured and combined in a ROMA index. All three biomarkers were compared with the RMI, which considers CA125 value, menopausal status and US findings. Both ROMA and RMI indices improved the specificities of single CA125 and HE4 markers with a similar sensitivity. The areas under the curve (AUCs) of ROMA and the RMI were equivalent in distinguishing between OC and benign tumors but did not differ considerably from AUCs of CA125 or HE4 alone, whereas RMI was slightly more sensitive and specific than ROMA among premenopausal women (M. A. Karlsen et al. 2012).

2.2.4 Other biomarkers

CA125 lacks specificity in premenopausal ovarian tumors and sensitivity in the diagnosis of early-stage and mucinous OC, which is why many ovarian tumor markers have been tested together with CA125 to complement it (Duffy et al. 2005).

In 2009, the FDA approved a multivariate index assay, OVA1, to help in the clinical decision of whether to refer patients with undetermined ovarian tumors to a gynecologic oncologist. The OVA1 test includes five biomarkers: two upregulated (CA125 and β-2 microglobulin) and three downregulated proteins (transferrin, prealbumin and apolipoprotein A1). An appropriate software program, OvaCalc, combines the values of each protein and uses a multivariate index assay logarithm to form an ovarian malignancy risk index. The numeric results vary from 0.0 to 10.0, indicating a high probability of OC in premenopausal and postmenopausal women with respective values ≥5.0 and 4.4 (Miller & Ueland 2012).

In a study of Ueland et al. (2011), the sensitivity of OVA1 in identifying epithelial OC was 99%, compared to 83% with CA125. Even in premenopausal early-stage OCs (FIGO Stage I or II), the sensitivity was 93%, compared to 36% with CA125. It has been emphasized that the OVA1 test should be used only for decision-making regarding where ovarian tumor surgery should be performed. The cost of the test limits its availabity (Muller 2010).

Subsequently, a second-generation multivariate index assay has been developed that includes three OVA1 markers (CA125, transferrin and apolipoprotein A1) and two other markers (follicle-stimulating hormone and HE4). It achieved better specificity and positive predictive values than the previous OVA1 test, although the sensitivity and negative predictive value did not change (Coleman et al. 2016).

There are no good serum biomarkers for mucinous ovarian tumors. However, carcinoembryonic antigen (CEA) is considered to be the most applicable tumor marker (Brown & Frumovitz 2014), and tumor-associated trypsin inhibitor (TATI) combined with CA125 have achieved better accuracy than CA125 or TATI alone (Medl et al. 1995; Mogensen et al. 1990).

The most common malignant sex cord-stromal tumors are adult-type granulosa cell tumors that produce estrogen, which causes their most typical symptoms. In turn, Sertoli-Leydig cell tumors (androblastomas) are usually associated with virilization and elevated serum androgen levels. The most-used biomarkers for preoperative diagnosis and follow-up, also for malignant germ cell tumors, are presented in Table 7 (Al-Hussaini et al. 2017; Färkkilä et al. 2015; Goyal et al. 2014; Haltia et al. 2017).

Table 7. Most commonly used serum biomarkers for non-epithelial ovarian tumors.

	Sex cord-stromal tumors		Germ cell tumors
	Adult-type granulosa cell tumor	Sertoli-Leydig cell tumor	Dysgerminoma Yolk sac tumor Immature teratoma
Biomarker	Inhibin B	Androgens	hCG
	AMH	AFP	LDH
			AFP

AMH: anti-Müllerian hormone; AFP: alpha-fetoprotein; hCG: human chorionic gonadotrophin; LDH: lactate dehydrogenase.

2.3 Preoperative assessment of ovarian tumors with imaging

2.3.1 Two-dimensional sonography with Doppler

Transvaginal US alone or combined with serum biomarkers is considered to represent the best method to detect an ovarian tumor and determine its benign or malignant nature. Ovarian tumors are classified by US into benign, malignant or indeterminate, depending on their morphological findings. The entire tumor must be visualized, also by transabdominal US if the tumor is too large for the transvaginal scan. The presence of cystic or solid lesions, as well as septations, cystic wall abnormalities and possible ascites in the abdominal cavity, must be recognized. To

optimize the diagnostic performance of transvaginal US, many scoring and predicting models have been developed. In order to standardize the morphological terms, definitions and the US measurement and examination techniques, an international IOTA group of, currently, approximately 50 contributing clinical centers was founded in 1999 (Abramowicz & Timmerman 2017), and a consensus paper was published (Timmerman et al. 2000).

The assessment of the vascularity of ovarian tumors by color or power Doppler is combined with gray-scale morphologic sonography in the differential diagnosis of ovarian tumors. It is based on the increased neovascularization of malignant tumors, leading to low-impedance blood flow due to anatomical differences between normal blood vessels and those developed by tumor angiogenesis, which lack smooth muscle in their walls, resulting in a reduced resistance to flow (Miller & Ueland 2012). The impedance of the vascularity can be measured by using pulsatility (PI) and resistance indices (RI).

There have been attempts to determine cutoff levels for PI and RI, but the levels of benign and malignant tumors have been overlapping (Fleischer et al. 1991; Salem et al. 1994; Tekay & Jouppila 1992). While the entire tumor should be examined with color Doppler, PIs and RIs can be measured only from the areas selected. Additionally, the measurements are angle-dependent, which means decreased intra- and interobserver reproducibility.

Vascularization of ovarian tumors can be detected also from benign tumors, and then it more often occurs in the peripherical areas of the tumor, whereas vascularization in the central or solid areas of a tumor is more indicative of malignant processes. Nevertheless, most non-vascularized tumors are benign (Guerriero et al. 2002; Schelling et al. 2000). The higher the color content of the tumor assessed by color Doppler, the greater the risk of malignancy. The subjective evaluation of the color content of the tumor is used to determine the nature of the ovarian tumor (Valentin 1997). In the IOTA consensus paper, the vascularity of ovarian tumors is divided into four scores: a score of 1 is for tumors with no found blood flow, 2 for tumors with minimal flow, 3 for tumors with moderate flow and 4 for highly vascularized tumors (Timmerman et al. 2000). The intra- and interobserver agreement of the assessment of the color content of adnexal masses was, respectively, good to very good and moderate to good in a study with 100 tumors and seven US examiners with different degrees of experience (Zannoni et al. 2013).

Figure 2. Vascularization of an ovarian tumor examined using color Doppler.

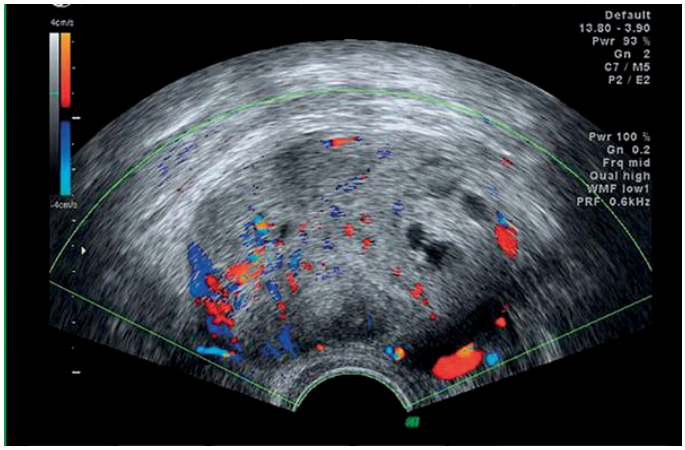

2.3.1.1 Risk of malignancy index

Jacobs et al. developed a scoring system in 1990, the RMI, as a tool for differentiating between different types of adnexal masses in less specialized centers to help treatment decisions. The RMI was the first prediction model combining menopausal status, US findings and CA125 measurement in order to characterize ovarian tumors (Jacobs et al. 1990). Subsequent modifications of RMI include RMI 2 and 3 (Tingulstad et al. 1996; Tingulstad et al. 1999), and RMI 4 (Yamamoto et al. 2009). The formulas for RMI 1-4 are presented in Table 8 below.

Table 8. Variants of risk of malignancy index (RMI).

Variant	Ultrasound score (U)*	Menopausal score (M)	Tumor size (S), mm (single greatest diameter)
RMI 1 (U x M x CA125)	U = 0 (0 parameter) U = 1 (1 parameter) U = 2 (≥2 parameters)	M = 1 (premenopausal) M = 3 (postmenopausal)	Not applicable
RMI 2 (U x M x CA125)	U = 1 (0-1 parameter) U = 4 (≥2 parameters)	M = 1 (premenopausal) M = 4 (postmenopausal)	Not applicable
RMI 3 (U x M x CA125)	U = 1 (0–1 parameter) U = 3 (≥2 parameters)	M = 1 (premenopausal) M = 3 (postmenopausal)	Not applicable
RMI 4 (U x M x S x CA125)	U = 1 (0-1 parameter) U = 4 (≥2 parameters)	M = 1 (premenopausal) M = 4 (postmenopausal)	S = 1 (<70 mm) S = 2 (≥70 mm)

*Parameters: presence of a multilocular cystic lesion, solid areas, bilateral lesions, ascites, intra-abdominal metastases.

RMI 1 and RMI 2 have been assessed in 16 and seven clinical studies respectively. With a cutoff value of 200, their pooled sensitivity was 78% and specificity 87% (Geomini et al. 2009). The RMI may be above the threshold of 200 in many benign conditions and, on the other hand, may not in early malignancies. Therefore a cutoff level of 250 for the RMI is sometimes utilized, with a poorer sensitivity, 70%, but a better specificity, i.e. 90% (Royal College of Obstetricians and Gynaecologists 2016).

Three variants of RMI (RMI 1-3) were validated in a retrospective study of 152 women with pelvic masses. There were no significant differences between those three variants in identifying OC (Manjunath et al. 2001). RMI 4 proved to be the most accurate of all RMI variants in differentiating OC (Yamamoto et al. 2009), but later no significant differences were found in the performances of RMI 1-4 in another study (Campos et al. 2016). The original, RMI 1, is the most validated, and the other RMIs have not been found to be clinically more beneficial than RMI 1; therefore it is recommended as the scoring system for triaging ovarian tumors (Royal College of Obstetricians and Gynaecologists 2016).

2.3.1.2 IOTA Logistic regression models 1 and 2

After the standardization of the US terms and examination protocols (Timmerman et al. 2000), the IOTA group developed and internally validated, in 1999-2002, various risk prediction models from their database of 1,066 women for the preoperative evaluation of ovarian tumors. Subsequently, the most workable models were temporally and later externally validated in a new patient data set and compared with the other existing scoring models such as the RMI between 2002 and 2007 (Kaijser et al. 2013). A total of 11 mathematical prediction models developed by IOTA were validated using different statistical models and compared with various previously developed scoring and mathematical models. In an external validation study, the IOTA models performed similarly to and better than non-IOTA models (Van Holsbeke et al. 2012). However, the more complex statistical techniques did not improve the diagnostic performances of two more simple logistic regression models designed by IOTA called LR1 and LR2 (see Table 9; Kaijser et al. 2013).

Table 9. The LR1 model features 12 and the LR2 model six variables.

LR1	LR2
Personal history of ovarian cancer (yes/no)	
Current hormonal therapy (yes/no)	
Age of the patient (in years)	Age of the patient (in years)
Presence of pain during the examination (yes/no)	
Maximum diameter of the ovarian tumor (mm)	
Appearance of a solely solid tumor (yes/no)	
Maximum diameter of the solid lesion of tumor (in millimeters)	Maximum diameter of the solid lesion of tumor (in millimeters)
Appearance of blood flow in the solid or papillary lesion of the tumor (yes/no)	Appearance of blood flow in the solid or papillary lesion of the tumor (yes/no)
Color content of the tumor (score 1-4)	
Irregular internal cyst walls (yes/no)	Irregular internal cyst walls (yes/no)
Appearance of acoustic shadows (yes/no)	Appearance of acoustic shadows (yes/no)
Appearance of ascites (yes/no)	Appearance of ascites (yes/no)

The risk of malignancy is derived by using specific logistic regression analysis. The results from development and test data from IOTA studies achieved the sensitivity and specificity for LR1 of 93% and 76-77%, by choosing a 10% risk of malignancy (Timmerman et al. 2005), which has subsequently been the most usable cutoff level.

The following IOTA temporal and external validation studies showed an equal reliability of LR1 and LR2. As a simpler and more user-friendly method, LR2 may be recommended as the main mathematical prediction model in the future (Timmerman et al. 2010b). The IOTA studies, which comprised 5,191 women, improved the usability of LR models in differentiating between benign and malignant ovarian lesions preoperatively. The sensitivities and specificities of LR2, using the cutoff risk level of 10%, varied between 88-95% and 74-90% (Kaijser 2015).

2.3.1.3 IOTA Simple rules

Besides the mathematical scoring systems, the IOTA group established simple, clinically useful US-based rules for the preoperative discrimination of ovarian tumors which were based on the fact that many benign and malignant adnexal masses have typical US features. The rules provide no risk estimate for malignancy but categorize the mass as benign, malignant or inconclusive without any need for a computer. Numerous combinations of US variables and their ability to predict a tumor's malignant or benign nature were tested in a development study. Finally, a combination of five rules for malignancy (M-rules) and five for predicting benign tumors (B-rules) were presented in Table 10.

Table 10. Ten simple ultrasound-based rules for classifying ovarian tumors.

Appearances that indicate benign tumors (B-rules)	Appearances that indicate malignant tumors (M-rules)
B1: Unilocular cyst	**M1**: Irregular solid tumor
B2: Presence of solid components with a maximum diameter of <7 mm	**M2**: Presence of ascites
B3: Presence of acoustic shadows	**M3**: At least four papillary structures
B4: Smooth multilocular tumor with a maximum diameter of <100 mm	**M4**: Irregular multilocular solid tumor with a maximum diameter of ≥100 mm
B5: No blood flow (color score: 1)	**M5**: Very strong blood flow (color score: 4)

If only B-rules and no M-rules apply, the tumor is categorized as benign. In turn, if M-rules and no B-rules apply, the tumor is categorized as malignant. In the case of both or neither of these rules applying, the tumor is unclassifiable, i.e. the results are considered inconclusive (Timmerman et al. 2008).

Development, temporal and external validation studies by IOTA accomplished similar results: the simple rules were usable in 76-77% of masses with sensitivities of 92-93% and specificities of 90-96% (Timmerman et al. 2008; Timmerman et al. 2010a). Expert opinion was recommended as a secondary test (the so-called two-step strategy) with tumors to which the simple rules provided inconclusive results achieving a sensitivity of 91% (95% CI 88-93) and specificity of 93% (95% CI 91-94). An alternative for inconclusive tumors is to classify them as malignant tumors (Timmerman et al. 2010a). Results from various studies using these two alternatives as a secondary test for inconclusive tumors are seen in Table 11.

Initially, the IOTA models (LR1, LR2 and simple rules) were validated by US experts, although the original idea was to utilize them as predictive tools for inexperienced clinicians for referrals to tertiary centers. Sayasneh et al. (2013) validated the LR models and simple rules in examiners with variable US experience and training. Their findings were in accordance with previous results from IOTA external studies showing IOTA predicting models working well also among non-experts. In fact, IOTA models demonstrated a better test performance than the RMI among examiners.

2.3.1.4 The Assessment of different neoplasias in the adnexa (ADNEX) model

The IOTA group also developed a mathematical polytomous risk-scoring model in order to distinguish between not only benign and malignant ovarian tumors but also to differentiate between benign, borderline, Stage I invasive, Stage II-IV, and secondary metastatic adnexal masses from each other. The need to categorize into four different types of malignancy arises from the desire to provide the optimal treatment and surgery and to plan it better preoperatively. The data from the first prospective diagnostic study originated in 5,909 nonpregnant women with adnexal tumors waiting for the surgery. The prediction model was designed to contain nine variables. The predictors included three clinical findings (age, serum CA125 level and the type of treatment center, i.e. tertiary oncological hospitals vs. other hospital types) and six US findings (maximum diameter of lesion, proportion of solid tissue, more than ten cystic locules, existence of acoustic shadows or/and ascites, and the number of papillary projections): the CA125 value and the solid portion of the tumor were the strongest ones. The ADNEX model calculates a total risk of malignancy and probabilities of the four types of malignancy. The developed risk scoring model is available for use on the website of the IOTA group and in mobile applications. When the 10% prediction level for malignancy was used, it yielded a sensitivity of 96.5% and a specificity of 71.3%. The AUCs classifying the four subtypes of malignancies varied from 0.71 to 0.95 (Van Calster et al. 2014). The cutoff level for malignancy can be modified depending on the local protocols in order to choose either a higher sensitivity, i.e. lower than 10% as the cutoff level, or a higher specificity, i.e. higher than 10% as the cutoff level (Van Calster et al. 2015).

A recent validation study compared the subjective assessment of an expert US examiner and four malignancy prediction models in differentiating the nature of an ovarian tumor preoperatively (Meys et al. 2017). The results are shown in Table 11.

2.3.1.5 Subjective assessment by an expert ultrasound examiner and comparison of various predictive methods

One of the best methods for preoperative analysis of ovarian tumors is subjective assessment (also called pattern recognition) of US findings after an accurate transvaginal examination by an experienced US examiner using two-dimensional (2D) sonography with Doppler (Valentin et al. 2001). However, in the hands of an expert, about 7% of the adnexal masses examined could not be distinguished as benign or malignant tumors, and the RMI or LR did not improve the classification. Tumors difficult to classify were multilocular cystic tumors with solid components, and histopathological diagnoses were borderline tumors, cystadeno(fibro)mas and fibromas (Valentin et al. 2011).

The IOTA methods and other scoring systems have been compared with subjective assessment, although they were developed more as diagnostic tools to help relatively inexperienced clinicians using US in primary and secondary centers. Table 11 shows the sensitivities and specificities of different scoring methods from three publications, or the IOTA Phase III study (Testa et al. 2014), the meta-analysis of 47 articles (Meys et al. 2016) and the external validation study of the ADNEX model (Meys et al. 2017).

Table 11. Summary of results from various scoring methods (LR2 and ADNEX at cutoff point 10% and RMI 200).

Author	Patients	Method	Sensitivity, % (95% CI)	Specificity, % (95% CI)
Testa et al. 2014	2,403	RMI 1	67.1 (61.4-72.4)	90.6 (87.3-93.1)
		LR2	90.2 (86.9-92.8)	78.9 (73.2-83.7)
		SA	92.5 (89.4-94.8)	87.7 (83.2-91.2)
		SR(mal)	95.3 (93.1-96.9)	74.1 (67.7-79.7)
		SR+SA (two-step strategy)	91.8 (89.1-93.9)	89.0 (85.2-92.0)
Meys et al. 2016	6,970	RMI 1	75 (72-79)*	92 (88-94)*
	1,544	LR2	93 (89-95)*	84 (78-89)*
	12,294	SA	93 (92-95)*	89 (86-92)*
	3,073	SR(mal)	93 (91-95)*	80 (77-82)*
	2,231	SR+SA	91 (89-93)*	91 (87-94)*
Meys et al. 2017	326	RMI 1	71 (62-79)	79 (72-84)
		LR2	93 (86-97)	79 (73-84)
		SA	90 (83-95)	91 (86-94)
		SR(mal)	93 (86-97)	68 (61-70)
		SR+SA	89 (81-94)	90 (85-94)
		ADNEX	98 (93-100)	62 (55-68)

RMI 1: risk of malignancy index 1; LR2: logistic regression model 2; SA: subjective assessment; SR(mal): simple rules, and when the result is inconclusive, the tumor is classified as malignant; SR+SA: simple rules, and when results are inconclusive, the tumor is classified by subjective assessment; ADNEX: assessment of different neoplasias in the adnexa model.
* Pooled sensitivity and specificity.

The approaches to assessment of an adnexal tumor by ultrasonography according to the IOTA studies are presented in Figure 3 (Kaijser et al. 2013; Kaijser 2015).

Figure 3. The flowchart for the use of ultrasonographic assessment methods for ovarian tumors.

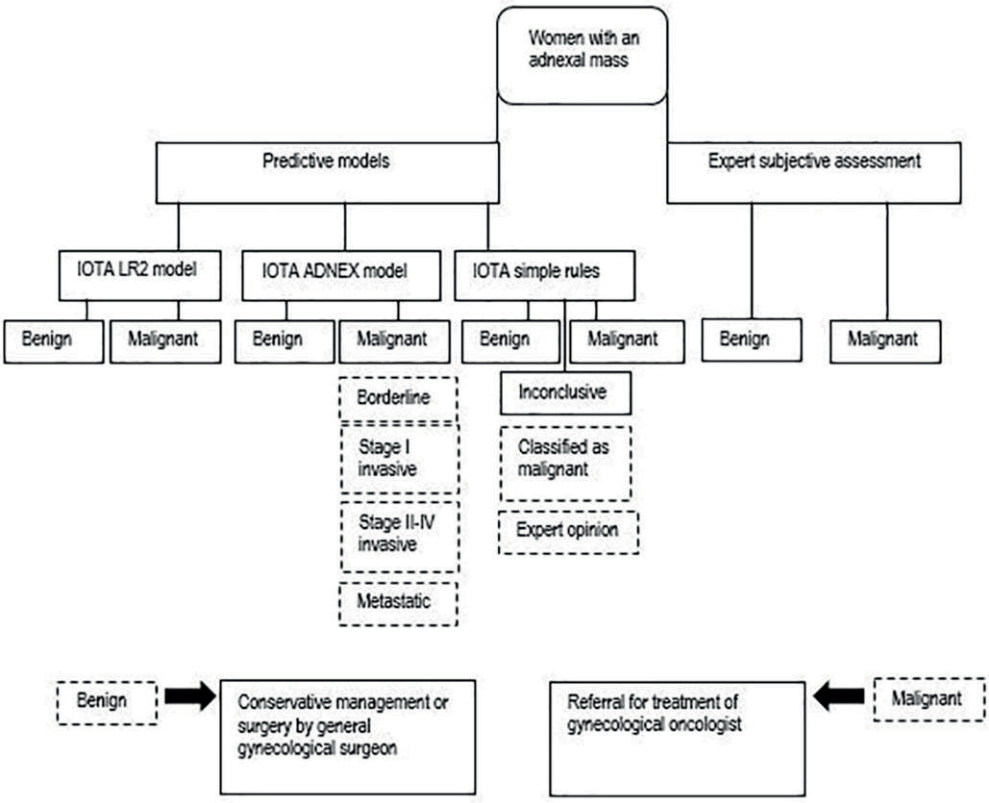

Mobile applications of IOTA models (LR1, LR2, simple rules and ADNEX) have been developed to facilitate their use in a clinical setting (Kaijser 2015).

2.3.2 Three-dimensional sonography

At the beginning of the century, 3D US for the characterization of ovarian lesions was introduced, a new tool that allowed visualization of the assessed lesion in three planes (coronal, sagittal and frontal) and permitted data on its volume to be acquired, stored and later analyzed. The internal structure of the lesion can be examined thoroughly. For volume calculation, an application named Virtual Organ Computer-Aided Analysis (VOCAL) can be used (Alcazar & Jurado 2011).

In addition to its morphology, the vascularization and flow pattern of the entire adnexal mass can be visualized using 3D-PD and VOCAL software. The term "Doppler imaging" usually refers to normal or color Doppler, which is based on Doppler frequency shifts relative to the velocity of blood flow. In turn, PD is based on the amplitude shift proportional to the number of blood cells detected. Compared to normal color Doppler, PD has some benefits like its sensitivity in noticing blood flow and characterizing vascular patterns (Alcazar & Castillo 2005). With the aid of 3D-PD, the architecture and density of the vascularity of the target can be described. Using the clinically popular 4D View software (GE Medical Systems, Zipf, Austria) and its histogram facility, the PD signal can be quantitatively measured. First, the examiner specifies the volume of interest whose PD signal intensities are demonstrated by histogram using VOCAL. Secondly, three vascular indices, vascularization index (VI), flow index (FI) and vascularization-flow index (VFI) are calculated with the aid of histogram utility. VI reflects the proportion of blood vessels within the assessed volume and is reported as a percentage. FI represents the mean PD intensity during the 3D sweep and is presented as a value of 0-100, as is the VFI, which is a combination of VI and FI. These indices are influenced by various internal and external factors: the local erythrocyte concentration, flow rate and number of vessels in the examined lesion, including its distance from the transducer, can affect them. Nevertheless, VI and VFI seemed to have a linear relationship with the changes in confounding factors in a phantom study (Raine-Fenning et al. 2008a). Many Doppler settings – especially gain, signal power and pulse repetition frequency – seem to have significant effects on the 3D-PD indices. Therefore, it is important to perform examinations using similar settings when comparing indices between persons and for the same patient (Raine-Fenning et al. 2008b).

2.3.2.1 Three-dimensional gray-scale morphologic ultrasound

Several studies comparing 3D US with traditional 2D US in determining malignant ovarian tumors have been published. These reports used 3D rendering or a multiplanar view to determine benign or malignant morphological characteristics such as irregular inner wall surface, papillary projection or thick septa, mostly solid tumor and echogenity of the tumor (Alcazar et al. 2003; Alcazar et al. 2007; Bonilla-Musoles et al. 1995; Chan et al. 1997; Hata et al. 1999; Kurjak et al. 2001).

The results are conflicting. Some studies found 3D US to provide positive additional value compared with 2D US (Bonilla-Musoles et al. 1995; Hata et al. 1999; Kurjak et al. 2001); other studies failed to demonstrate significant benefits over 2D US in classifying adnexal lesions (Alcazar et al. 2003; Alcazar et al. 2007). An explanation for this discrepancy may be that both the 2D US and 3D gray scale US methods are based on the subjective opinion of the examiner (Hata et al. 2011).

2.3.2.2 Three-dimensional power Doppler angiography

There are two approaches to the use of 3D-PD in evaluating adnexal tumors. One is evaluating the morphological changes in vessels suspected of malignancy, and the other is using an objective quantification of vascularity by the VOCAL program or some other software. The characteristics in vessels that can change with malignancy are density, caliber, tortuosity, irregular branching, and bridges between vessels (Sladkevicius et al. 2007).

The sensitivities and specificities of 3D-PD vs. 2D US varied between 77-100% vs. 94-100% and 50-99% vs. 50-97% in a review of seven studies involving the use of 3D-PD vascular tree assessment in detecting OC (Alcazar & Jurado 2011). Only one of seven studies showed a significant difference ($p < 0.05$) between the detection ability of 3D-PD and 2D US, but it indicated that 2D US had an advantage (Dai et al. 2008). Nor did the review by Hata et al. (2011) find any significant or reported differences in the accuracies of 2D US and 3D-PD.

Alcazar et al. reported their results regarding quantification of 3D-PD vascular indices. They used a focused sampling from the most vascularized and suspected areas, and the indices were calculated automatically from that area using the VOCAL program. All PD indices differed significantly in ovarian malignancies compared with benign tumors (Alcazar et al. 2005), but the VIs and VFIs from ovarian tumors were significantly higher in advanced or metastasized OC than in early-stage cancers (Alcazar 2006). In a subsequent study of Geomini et al. (2007), only FI – and not VI or VFI – showed significantly higher levels in malignant tumors than in benign tumors when assessed from the whole tumor.

Modified approaches to vascular sampling have been developed based on automatically calculated 1-5 cm^3 spherical samples from the most vascularized areas. The 3D-PD indices significantly separated benign and malignant tumors (Jokubkiene et al. 2007; Kudla & Alcazar 2010). Vascular sampling can also take place by manually

outlining the highly vascularized areas. Both methods can be used, but spherical sampling is not possible in all small tumors (Alcazar & Prka 2009).

Repeatability in assessments of 3D-PD indices in offline analyses from the stored 3D volumes has proved to be good, as is the intra- and interobserver agreement, regardless of the method used for vascular sampling (Alcazar et al. 2008; Alcazar & Prka 2009; Jokubkiene et al. 2007). The agreement of offline analysis with the real-time US results in the diagnosis of benign or malignant tumor was good, with a similar diagnostic performance (Alcazar et al. 2012). The IOTA US rules, color score system (scores 1-4), simple rules, LR1 and LR2 models, and expert opinion were analyzed later by other US examiners using stored 3D data. The intra- and interobserver agreement, also between examiners with different experience, varied mainly between moderate and good (Guerriero et al. 2013; Pineda et al. 2014; Ruiz de Gauna et al. 2014; Sladkevicius & Valentin 2013). However, it has been stated that offline analyses are not comparable with real-time US because they lack the interactive nature of examinations (Sladkevicius & Valentin 2013). In general, the use of 3D-PD indices and their importance in practical work is restricted by a lack of standardization and complete understanding of their significance (Guerriero et al. 2015).

2.3.3 Ultrasound contrast agents

Neovascularization, i.e. increased intratumoral microvascularization, is characteristic of malignancies, and color and power Doppler sonography is used to describe it. However, these techniques cannot detect vessels with a diameter of less than 0.1 mm. Intratumoral Doppler signals can be enhanced with the aid of intravascular sonographic contrast agents, which may promote earlier detection of OC (Testa et al. 2005).

Ultrasound contrast agents used intravenously contain microbubbles that are smaller than erythrocytes and can flow into capillaries, allowing the depiction of low volume blood flow. Pulse-inversion techniques with related software enable the description of contrast agent microbubbles in normal and neovascularized tumor tissues (Fleischer et al. 2010).

With the aid of modern software, second-generation contrast agents such as Definity® (perflutren, Lantheus Medical Imaging, North Billerica, MA), available in the U.S., and SonoVue® (sulfur hexafluoride, Bracco Imaging S.p.A, Milan, Italy)

can be detected by the harmonic response of microbubbles to US signals at a low acoustic pressure (Fleischer et al. 2010). The major advantage of SonoVue® is that microbubbles insonated by US persist in the blood for a few minutes (Testa et al. 2005).

The preliminary study by Testa et al. (2005) showed that SonoVue®, together with contrast-tuned imaging technology, allows for a higher number of intratumoral vessels in ovarian tumors to be detectable in a PD examination than without contrast media. Studies evaluating the kinetic parameters of second-generation contrast agents in US examinations have shown significantly different results in malignant and benign tumors (Fleischer et al. 2008; Testa et al. 2009; J. Wang et al. 2011), although the AUC of the best contrast variable was smaller than that of an expert opinion (Testa et al. 2009). The benefit of contrast-enhanced US appears to be uncertain because there is overlapping in the parameters of benign, borderline and malignant ovarian tumors; contrast agents are also rather expensive (Testa et al. 2009).

The ability of SonoVue®-enhanced US in discriminating ovarian tumors has also been studied in 3D sonography in small study series, also compared with 2D-enhanced US (Hu et al. 2014; Xiang et al. 2013). 3D-enhanced US may help especially in classifying early diagnoses of small ovarian malignancies, but larger validation studies are warranted to evaluate the possible advantages of combining 3D US technology and contrast-enhanced US.

2.3.4 Magnetic resonance imaging

The advantage of magnetic resonance imaging (MRI) is its high-contrast resolution, especially soft tissue contrast, without an exposure to ionizing radiation (Foti et al. 2016). The European Society of Urogenital Radiology has published guidelines that recommend the use of MRI together with an algorithm approach as an additional tool in identifying indeterminate ovarian masses. This protocol divides the unclear tumors into three categories based on the findings in T1- and T2- weighted sequences. The categories include additional imaging sequences – for example, fat-saturated T1-weighted or oblique sequences – or the assessment of intravenous gadolium-contrast enhancement (Spencer et al. 2010).

A meta-analysis of various preoperative methods determined the optimal method in presurgical identification of ovarian masses. The pooled sensitivity and specificity

from 24 datasets for conventional MRI techniques was 91.9% and 88.4% respectively and was similar to transvaginal 2D and 3D US (Dodge et al. 2012). In turn, earlier meta-analysis demonstrated that contrast-enhanced MRI appears to be more sensitive and specific than unenhanced MRI but increases only specificity as compared with 2D Doppler US (sensitivities 81% vs. 76% vs. 84%, and specificities 98% vs. 97% vs. 82% respectively) (Kinkel et al. 2005).

The addition of functional imaging via diffusion-weighted imaging (DWI) has provided controversial results in the literature. DWI measures randomly moving water molecules in tissues affected by hypercellularity and changes in cellular membrane integrity. The apparent diffusion coefficient (ADC) values derived from DWI provide information on the diffusivity of the imaged tissue (Sharma et al. 2016). A meta-analysis of 21 studies revealed no significant difference between the ADC values of benign and malignant ovarian tumors, although subgroup analysis of benign tumors produced higher ADC values than malignant ones. However, overlapping of ADC values was seen, as especially endometriomas and teratomas produced the very low ADCs typical of malignant tumors (Kim et al. 2016).

The use of dynamic contrast-enhanced MRI (DCE MRI) produces information on the vascularity and permeability of tumor as time-intensity curves after the injection of contrast agent (Sharma et al. 2016). The use of DWI and DCE MRI enables a morphologic and vascular assessment of tumors and improves the differentiation of complex ovarian lesions as well as peritoneal dissemination (Fujii et al. 2008; Sala et al. 2010; Thomassin-Naggara et al. 2008; Thomassin-Naggara et al. 2009; Thomassin-Naggara et al. 2011). The use of functional sequences, DWI and DCE MRI provided new criteria for ovarian tumor imaging and resulted in the development of an MRI scoring system for adnexal tumors (ADNEX MR scoring) (Thomassin-Naggara et al. 2013).

By virtue of these additional tools for ovarian tumor imaging, the guidelines by the European Society of Urogenital Radiology were reconsidered in 2016. The new guidelines recommend the use of DWI and DCE MRI especially in the cases of solid and complex cystic adnexal tumors (Forstner et al. 2016).

2.3.5 Computed tomography

Contrast-enhanced computed tomography (CT) is preferred for a preoperative evaluation of the extent of suspected OC and the likelihood of successful cytoreductive surgery, and for postoperative assessment of residual tumor tissue after surgery. The advantages of CT are its easy availability, shorter duration of examinations, and lower cost compared with MRI. In turn, the use of iodine-based contrast agent may be contraindicated, and exposure to radiation restricts its use (Fischerova & Burgetova 2014).

CT has a lower soft-tissue contrast than MRI, and will only miss small early-stage adnexal lesions (Bharwani et al. 2011). Contrast-enhanced MRI and CT are equally accurate modalities in the preoperative staging of OC. Their accuracy in detecting metastasized lymph nodes and peritoneal implants depends on their size, location and possible ascites. In one series, MRI was superior to CT in detecting pathological lymph nodes (p <0.04) while being equivalent for peritoneal implants (p <0.91) (Tempany et al. 2000).

2.3.6 Positron emission tomography/Computed tomography

Positron emission tomography (PET) uses a positron-emitting radiolabeled tracer, commonly ^{18}F-2-fluoro-2-deoxy-D-glucose, which accumulates in the tissues and cells whose glucose metabolism is high, such as cancer cells. If PET is combined with CT (PET-CT), this enhanced glucose uptake can be anatomically localized to specific areas (Fischerova & Burgetova 2014).

PET-CT is not recommended for the primary diagnosis of OC due to a reported sensitivity of only 58% and a specificity of 76%. Elevated metabolic activity has been reported in inflammatory processes, endometriomas and premenopausal ovaries, depending on the phase of the menstrual cycle, resulting in false-positive results. In turn, false-negative results have been reported in borderline tumors and early-stage OCs (Fenchel et al. 2002).

PET-CT may, however, be of some use in the preoperative staging of OC. PET-CT is accurate in detecting regional lymph node and distant metastasis. There are studies showing better sensitivity for PET-CT in diagnosing pathological lymph nodes, especially retroperitoneal or supradiaphragmatic, than CT or MRI (Fischerova & Burgetova 2014; Khiewvan et al. 2017).

A summary of various imaging modalities and their main roles in imaging ovarian tumors is seen Table 12 (Fischerova et al. 2012; Fleischer et al. 2010; Guerriero et al. 2015; Khiewvan et al. 2017; Tempany et al. 2000).

Table 12. Summary of imaging modalities in ovarian cancer.

Imaging modality	2D ultrasound	3D ultrasound	Contrast-enhanced ultrasound	CT	Dynamic contrast-enhanced MRI	PET-CT
	First line evaluation of adnexal masses	Potential aid in preoperative discrimination of indeterminate tumors	Potential aid in preoperative discrimination of indeterminate tumors	Preoperative staging in advanced cancer (especially evaluation of peritoneal implants, sub-diaphragmatic space and hepatic surface)	Potential aid in preoperative discrimination of indeterminate tumors	Preoperative staging in advanced cancer? (especially evaluation of supra-diaphragmatic and retroperitoneal space)
	Preoperative staging in advanced cancer as a supplement for CT or MRI (especially evaluation of liver and lymph nodes)				Preoperative staging in advanced cancer (especially evaluation of peritoneal implants, sub-diaphragmatic space, and hepatic surface)	In recurrent cancer

2.4 Polyamines

2.4.1 Overview of polyamine metabolism

Polyamines are low-molecular-weight polycations derived from amino acids, predominantly ornithine and methionine (Miller-Fleming et al. 2015). They are found in most living organisms, and nearly all cells can produce them. In addition to biosynthesis, polyamines are acquired from dietary sources and produced by the intestinal bacteria (Hussain et al. 2017). The most common polyamines in mammals

are putrescine, spermidine and spermine with respectively two, three and four amino groups in a hydrocarbon chain, followed by cadaverine and 1,3-diaminopropane (Miller-Fleming et al. 2015).

Ornithine, produced from arginine in the urea cycle, is converted to putrescine, which is the precursor for spermidine and spermine. Intracellular polyamine quantity is regulated by the monoacetylation of spermidine and the mono- and diacetylation of spermine. These acetylated polyamines can be either excreted to the urine or converted back to putrescine. Putrescine, spermidine and spermine can also be transported into the intracellular space (Gerner & Meyskens 2004). Synopsis of polyamine metabolism and key enzymes are presented in Figure 4.

Figure 4. Polyamine metabolism (modified from Gerner & Meyskens 2004; Seiler 2004; Soda 2011).

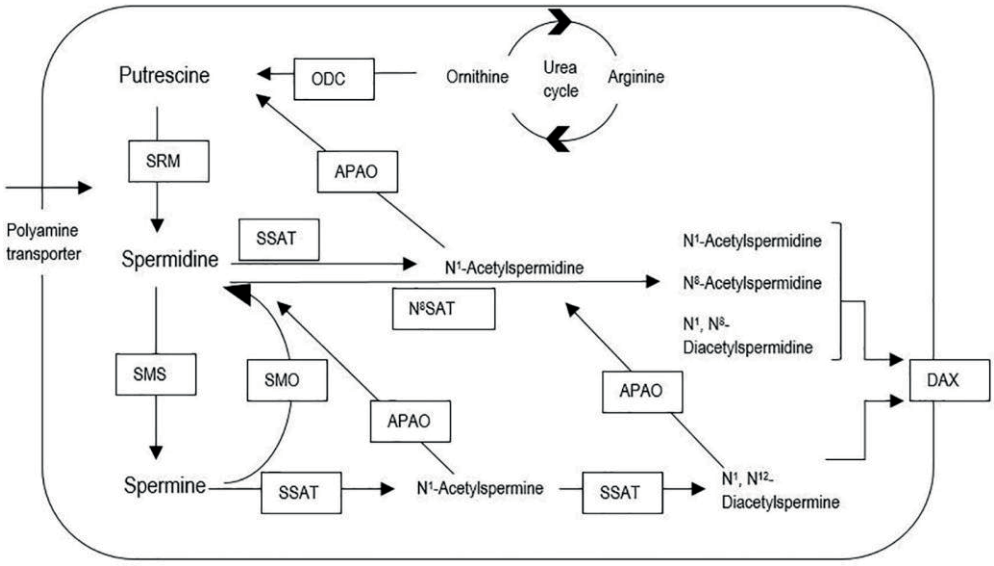

ODC: ornithine decarboxylase; N^8SAT: spermidine-N^8-acetyltransferase; SRM: spermidine synthase; SMS: spermine synthase; SSAT: spermidine/spermine N^1-acetyltransferase; SMO: spermine oxidase; APAO: acetylpolyamine oxidase; DAX: diamine exporter.

Polyamines are involved in many body functions affecting cellular proliferation, tissue growth and development, including gene transcription, posttranscriptional regulation, cell apoptosis, the control of ion channel activity, and the modulation of cell cycles, cell membrane structure and cell function. Polyamines also have anti-inflammatory properties and effects on protein synthesis (Hussain et al. 2017; Igarashi & Kashiwagi 2010; Pegg & Casero 2011).

2.4.1.1 Polyamines in cancer

An overactivation of polyamine synthesis is associated with carcinogenesis. It leads to elevated polyamine concentrations and the overexpression of genes and enzymes involved in polyamine biosynthesis in cancer cells (Thomas & Thomas 2003). Levels of the enzyme ornithine decarboxylase are increased in cancer tissues, and it is not only a target for Myc- and Ras-oncogenes, but also a potential oncogene itself because its overexpression can alter cell lines alone or together with other oncogenes (Casero et al. 2018; Gerner & Meyskens 2004; Miller-Fleming et al. 2015). Increased polyamine levels stimulate cell proliferation and decrease apoptosis, both of which are characteristic of cancer. Polyamines are also needed for angiogenesis in tumorigenesis (Gerner & Meyskens 2004).

In a hypoxic situation, cancer cells advance metastasizing and invasion by decreasing cell adhesion. Also, polyamine uptake from extracellular space is elevated due to hypoxia. The expression of the adhesion molecules CD44 and E-cadherin is reportedly diminished in malignancies, which promotes invasion and metastatic potential. Increased spermine levels in cells are shown to be involved in decreased CD44 expression (Tsujinaka et al. 2011), and they may also prevent normal antitumor immune cell function by decreasing the chemokine and cytokine production of immune cells and enabling tumor progression (Kano et al. 2007).

Arising from the association between cancer and polyamine metabolism, many therapeutical cancer treatments have been developed, albeit without great clinical success thus far. The most studied one is DL-α-difluoromethylornithine (DFMO), an irreversible binding inhibitor of ornithine decarboxylase (Bae et al. 2018; Murray-Stewart et al. 2016). DFMO has been found to reduce tumor growth in animal experiments and to have chemopreventive properties, also in clinical trials and mainly combined with other chemotherapeutic medications, e.g. in gliomas (Alexiou et al. 2017; Casero et al. 2018).

Elevated polyamine concentrations in the urine of cancer patients were first reported by Russell et al. over 45 years ago (Russell et al. 1971). They analyzed 24-hour urine samples using liquid chromatography-mass spectrometry (LC-MS), but, interestingly, the highest concentrations of putrescine, spermine and spermidine were found in a patient with a large solid benign ovarian teratoma. Polyamine levels dropped after tumor removal. Increased polyamine levels in the blood of cancer patients have also been found (Russell 1983; Uehara et al. 1980). Serum polyamine concentrations are correlated with urinary levels (Durie et al. 1977), demonstrating

that polyamines produced by malignancies are delivered to the circulation and excreted via the kidneys to urine (Soda 2011).

Polyamines are also produced in non-cancerous tissues and transferred to various organs such as the intestinal mucosa, where they can also be produced by the intestinal microbiota (Soda 2011; Timmons et al. 2012). In one study, an elevated polyamine nutritional intake over two months increased serum polyamine levels in mice and in humans (Soda et al. 2009). Thus, these factors must be taken into account in analyzing the polyamine levels in cancer patients. In addition, the individual variation in polyamine concentrations in healthy people is high, which makes it difficult to determine whether values are abnormal (Hiramatsu et al. 1995; Soda 2011). Furthermore, benign diseases such as polymyositis, hemolytic anemia and inflammatory bowel diseases can increase polyamine levels (Hiramatsu et al. 2005; Suh et al. 1997). Urinary polyamine concentrations are highest in the morning and higher in men than in women (Pöyhönen et al. 1990). In women, estrogen may affect at least some polyamine levels: premenopausal women with breast cancer have been found to have higher polyamine concentrations in serum, in contrast to postmenopausal patients and healthy controls (Byun et al. 2009).

2.4.2 Analysis of polyamines

Polyamines are found in cells in free and conjugated forms, and, in physiological fluids, mainly in acetylated forms. In healthy people, monoacetylated polyamines form the major component of polyamines in urine. Levels of N^1, N^{12}-diacetylspermine (DiAcSpm) and N^1, N^8-diacetylspermidine (DiAcSpd) in normal urine are 0.46% and 1.4% of total polyamines (Hiramatsu et al. 1995).

Several analytical methods used for polyamine analysis are based on LC and gas chromatography (GC). Most of these methods require pre- or post-column derivatization, and these different derivates can be detected with selective detectors, e.g. by measuring ultraviolet absorbance or fluorescence, or using mass spectrometry (MS). However, diacetylated polyamines without a free amino group cannot be derivatized and detected using conventional methods (Häkkinen et al. 2013; Jeevanandam & Petersen 2001).

For a long time, the polyamine field lacked a method of analyzing free, mono- and diacetylated amines simultaneously. Byun et al. (2008) reported a LC/MS method using an extractive carbamoylation to analyze ten polyamines simultaneously

from serum and urine of healthy women and patients with breast cancer. However, these polyamines did not include diacetylated forms. Häkkinen et al. (2013) published a LC-MS/MS method for the concurrent analysis of 14 urinary polyamines (free, mono- and diacetylated forms) without any derivatization.

DiAcSpd and DiAcSpm were first identified in normal human urine using high-performance liquid chromatography (HPLC) combined with an enzyme reactor (Hiramatsu et al. 1995). Because these diacetylated polyamines are studied as diagnostic and prognostic biomarkers, there was a demand for convenient and less-time-consuming analytics. Highly specific antibodies for DiAcSpd and DiAcSpm have been produced and enzyme-linked immunosorbent assays (ELISA) developed for urinary detection as alternatives to HPLC analysis (Hiramatsu et al. 1997; Hiramatsu et al. 1998). Concentrations of DiAcSpm and DiAcSpd measured by these ELISA-based methods have been shown to be comparable to concentrations obtained with HPLC. However, minimal cross-reaction with monoacetylated spermine and spermidine should be taken account in the analysis (Hamaoki et al. 2002). Subsequently, a kit for urinary DiAcSpm detection based on colloidal gold aggregation with automatic analyzers was developed for commercial use (Kawakita et al. 2011).

2.4.3 Polyamines as tumor markers

As a consequence of the first finding of elevated polyamine concentrations in the urine of cancer patients (Russell et al. 1971), the potential of polyamines to act as tumor markers for cancer was evaluated. Levels of monoacetylated polyamines, or the amount of N^1-acetylspermidine and the ratio of N^1-acetylspermidine to N^8-acetylspermidine, were higher in the urine of patients with lymphoma (Abdel-Monem et al. 1982). However, their clinical use was proven to be limited due to their elevated concentrations also in benign disorders and a wide normal variation in the population (Kawakita & Hiramatsu 2006). Sugimoto et al. (1995) showed that the total amount of urinary polyamines and N^1-acetylspermidine did not differ significantly in patients with and without cancer, and N^1-acetylspermidine levels were often elevated in patients with benign diseases. However, the concentrations of DiAcSpd and DiAcSpm in cancer patients were significantly higher than in controls or people with benign disorders. This strongly promoted further research into DiAcSpd and DiAcSpm as tumor markers.

The metabolism of DiAcSpm and DiAcSpd is not totally clear: several mechanisms may lead to increased excretion. The source of DiAcSpm in cancer patients may be spermine produced either by cancerous or non-cancerous tissues (Takahashi, Sakaguchi et al. 2015). Levels of DiAcSpm are elevated in colorectal cancer tissues and even in precancerous lesions, which could be a sign that cancer cells produce DiAcSpm (Kuwata et al. 2013). The increased activity of the SSAT enzyme may also stimulate cancer cells to increase the excretion of acetylated polyamines as a feedback mechanism for elevated intracellular polyamine levels to control the polyamine homeostasis (Kawakita & Hiramatsu 2006). Despite the secretion of DiAcSpm into the circulation, its content in urine remains quite stable without any relevant decrease because it is not reabsorbed from the kidneys (Miki et al. 2005). Therefore, the glomerular clearance of DiAcSpm is analogous with that of creatinine, and the DiAcSpm concentrations are usually normalized in relation to creatinine concentrations (Takahashi, Horio et al. 2015). Provided this normalization with creatinine has been undertaken, single urine samples taken at any time of day, can be considered to reflect the general urinary concentration level of DiAcSpm of a given individual. However, the gender, age and menstrual cycle of the patient have effect on the concentrations (Hiramatsu et al. 2014).

The molecular character of the enzyme responsible for DiAcSpd is not identified, which may explain why studies of DiAcSpd as a tumor marker have waned (Kawakita & Hiramatsu 2006). On the other hand, DiAcSpm has been widely studied as a tumor and prognostic factor in malignancies including leukemias and urogenital, hepatocellular, colorectal, breast, pancreaticobiliary and non-small cell lung cancers (see Table 13). It is notable that, in studies of colorectal cancer, urinary DiAcSpm seems to be a more reliable tumor marker than CEA (Hiramatsu et al. 2005; Nakayama et al. 2012; Umemori et al. 2010).

Although increased concentrations of free and monoacetylated polyamines have previously been found in the urine of OC patients (Lawton et al. 1989; Suh et al. 1997), to the best of my knowledge, no previous literature on diacetylated polyamines involving OC is available.

Table 13. Overview of studies involving urinary N^1, N^{12}-diacetylspermine (DiAcSpm) as a tumor or prognostic marker in various cancers.

Study	Patients	Method	Results	Extra
Hiramatsu et al. 1997	31 urogenital cancers 42 benign urogenital disorders	HPLC with electrochemical detection	↑ significantly in cancers	DiAcSpd also ↑ in cancers. Prognosis of cancer was good when DiAcSpm and DiAcSpd normalized after treatment.
Lee et al. 1998	43 leukemias 32 healthy controls	GC with nitrogen-phosphorus detection	↑ significantly in leukemias	
Enjoji et al. 2004	53 hepatocellular cancers (Stages I-IV) 182 benign liver diseases	ELISA	65.5% sensitivity and 76.0% specificity in cancers	63.8% sensitivity for AFP. DiAcSpm values increased along the stage.
Hiramatsu et al. 2005	248 colon cancers (Stages 0-IV) 83 breast cancers (Stages I-IV) 51 benign gastrointestinal diseases	ELISA	75.8% sensitivity in all colon cancers (62.5% and 90.5% in Stage I and IV colon cancers) and 61.4% sensitivity in all breast cancers	39.5% sensitivity for CEA in all colon cancers. (10.0% and 66.7% in Stage I and Stage IV cancers).
Yamaguchi et al. 2005	32 pancreaticobiliary cancers (Stages IIb-IV) 52 benign pancreaticobiliary diseases	ELISA	75% sensitivity and 81% specificity in cancers	44% sensitivity and 92% specificity for CEA. 75% sensitivity and 80% specificity for CA 19-9.
Umemori et al. 2010	33 colorectal cancers (Stages I-IV) 28 breast cancers (Stages 0-IV)	ELISA	69.6% sensitivity in colorectal cancers and 46.4% sensitivity in breast cancers	46.8% of sensitivity for CEA in colorectal cancers.
Nakayama et al. 2012	113 colorectal cancers	Colloidal gold aggregation	69.0% of cancers had positive ratios of DiAcSpm (66.7% in early and 69.2% in advanced cancers)	44.2% of cancers had positive ratios of serum CEA (11.1% in early and 47.1% in advanced cancers).

Kato et al. 2014	251 NSCLCs	Reagent kit with automatic analyzer	DiAcSpm was a significant prognostic factor for disease-free and overall survival	
Takahashi, Sakaguchi, et al. 2015	260 NSCLCs 99 benign lung diseases 140 healthy controls	Colloidal gold aggregation	↑ significantly in cancers, especially in squamous cell cancers	Increased DiAcSpm levels correlated with stage and unfavourable prognostic factors.
Takahashi, Horio, et al. 2015	516 NSCLCs	Colloidal gold aggregation	Patients with invasive cancers had significantly higher levels than non-invasive cancers	
Nakajima et al. 2018	201 colorectal cancers 31 healthy controls or benign colorectal diseases	LC-MS	↑ significantly in cancers (AUC=0.79 for discriminating cancers)	59 samples were re-collected and -analyzed to profile seven kinds of polyamines showing good reproducibility. A machine-learned method was developed to predict the cancer risk by using various markers.
Venäläinen et al. 2018	57 colorectal cancers 25 benign colorectal diseases 34 healthy controls	LC-MS/MS	78.0% sensitivity and 70.6% specificity in cancers	

HPLC: high-performance liquid chromatography; DiAcSpd: N^1, N^8-diacetylspermidine; GC: gas chromatography; ELISA: enzyme-linked immunosorbent assay; AFP: alpha-fetoprotein; CEA: carcinoembryonic antigen; NSCL: non-small cell lung cancer; LC-MS: liquid chromatography-mass spectrometry; AUC: area under the curve; LC-MS/MS: liquid chromatography-tandem mass spectrometry.

2.5 Detection of volatile organic compounds

2.5.1 Overview

Historically dogs are known to have a superior olfactory apparatus. A letter to the editor of *The Lancet* in 1989 laid the foundation for medical research on "sniffer dogs" to detect malignancy by its odor. The letter was about a dog who was desperately interested in its owner's mole, which proved to be malignant (Williams & Pembroke 1989). Consequently, studies on whether dogs could be trained to detect the odor of cancers were initiated. The first published studies of trained canine experiments were the detection of bladder cancer from urine and melanoma from tissue samples (Pickel et al. 2004; Willis et al. 2004). Subsequently, canines were taught to differentiate breath samples from breast and lung cancer patients (McCulloch et al. 2006) and urine samples from breast and prostatic cancer patients (Gordon et al. 2008). Horvath et al. began to examine whether OC also has a typical odor that dogs can detect. The first study showed that one trained dog could make the distinction between 31 OC tissue samples representing different histopathologies and stages, and healthy control tissues in a double-blind test with a sensitivity of 100% and specificity of 97.5%. For the discrimination between OC and other gynecological cancers the sensitivity was also 100%, while the specificity was 91% (G. Horvath et al. 2008). Later, two trained dogs discriminated between the blood samples of OC patients and those from healthy controls with a sensitivity of 100% and specificity of 95% (G. Horvath et al. 2010). In the following study, dogs detected distinct features of OC from blood samples during chemotherapy. Three and six months after the chemotherapy, dogs were able to detect from patient blood samples which patients had relapsed (G. Horvath et al. 2013).

These studies have proved that various cancers may produce some cancer-specific molecules and volatile organic compounds (VOCs) which are released into the urine, stool and blood and into the surrounding air by breath and sweat (Lippi & Cervellin 2012; Sonoda et al. 2011). Arasaradnam et al. (2011) proposed that colonic fermentation products such as volatile gases and their alterations could be changed, at least in colonic and metabolic diseases. These gases would exist as VOCs

and be detected in the urine of patients with colorectal inflammatory disease and diabetes.

Clinical use of the excellent canine sense of olfaction is challenging, because the dogs require highly specified and intensive training and, even then, their ability to detect odors differs from individual to individual, even in the case of the same dog. Therefore, artificial methods to replace the canine olfactory system have been developed.

2.5.2 Technical analytical methods

The gold standard for the analysis of VOCs is GC-MS. Analyzing volatile molecules by MS is a quantitative method; however, it has limitations in clinical settings, e.g. large and expensive equipment which requires well-trained operators and time-consuming procedures. Due to these restrictions, there has been an interest in developing new non-invasive, simple and rapid methods of detecting VOCs. The utilization of the eNose in the medical field began in the nineties; a range of applications have subsequently been developed (D'Amico et al. 2012). An eNose consists of an array of non-selective sensors which recognize not simply one VOC but, rather, respond to all the volatile information from the sample by creating a qualitative spectrum reflecting it (Bernabei et al. 2008; Z. Zhang & Li 2010). The principles for all techniques that mimic human olfactory system are similar (Wilson & Baietto 2011).

Figure 5. The process of VOC analytics.

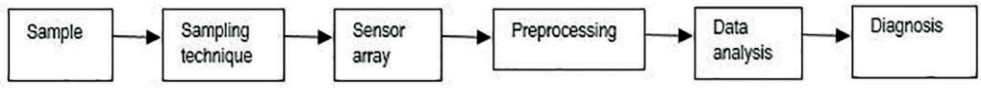

First, the sample is processed by a sampling technique responsible for introducing odors to the analyzer. The aim of such a technique is to collect an optimal and homogenous sample by enriching and cleaning the sample, and then amplifying it. Static headspace extraction is one of the most common ways of delivering the sample to the sensor. The sample is stored in a hermetic container from which accumulated volatile gases can be extracted when an equilibrium has been reached between the

matrix and the gas phase in the headspace. In the dynamic headspace technique, the VOCs of the sample are removed by the continuous gas flow that conveys the molecules to the sensor. Solid-phase microextraction employs a fiber-coated solid material in the headspace of the sample in which volatile compounds are adsorbed. The volatile molecules are extracted from the headspace and released from the material via heating (S. Chen et al. 2013).

The first eNose sensor arrays were metal oxide semiconductor sensors, and more advanced technologies for gas sensing have since been established (S. Chen et al. 2013). Information generated from sensor arrays is analyzed by data computing systems using pattern recognition methods. The analysis begins when signals from sensors are obtained and stored in the computer. Signal preprocessing is conducted to remove noise, optimize signal quality and select the descriptive patterns of the arrays and create a vector from them for further processing. Pattern recognition methods are unsupervised and supervised learning procedures. In unsupervised learning, different algorithms learn to extract features from the vectors that might classify these odor vectors without any knowledge of the status of the samples. Principal component analysis is the technique most often used to accomplish this. In supervised learning, the unknown odor is classified according to the previously existing knowledge about the feature. Typically, this pattern recognition method requires several samples in order to form this knowledge basis. With supervised learning, the classifier is given the information regarding the status of the sample (eg. healthy or diseased). The classifier then attempts to find the features that distinguish the two groups from each other with maximum accuracy. Linear discriminant analysis (LDA) is an example of supervised learning methods. When the classifier of the odor data has been found, it must be cross-validated to avoid overfitting, a phenomenon in which samples are discriminated according to unique features of the dataset that do not generalize to another population. Thus, all eNose results should be cross-validated by an independent sample population or in smaller datasets by leave-one-out cross-validation (S. Chen et al. 2013).

2.5.2.1 Field asymmetric waveform ion mobility spectrometry

ENose technology suffers from poor repeatability and sensitivity due to indiscriminate chemical interactions between the sample and the sensors. Ion mobility spectrometry is a variant of eNose technology between MS and traditional

eNose. It measures the ion mobility in an atmospheric pressure using air as a carrier gas, compared to MS, which needs vacuum (Covington et al. 2015). The gas with the sample is first ionized and then passed through an orthogonal electric field in which ions collide with the air molecules, discriminating ions by their mobility. The time that an ion spends in an electric channel is the parameter measured by ion mobility spectrometry and detected by an electrometer at the end of the channel. FAIMS is a variant of ion mobility spectrometry (see Figure 6 below). It applies an alternating voltage between the plates and thus can select only certain ions to pass through the alternating electric field to the sensor, which improves its discrimination ability (Covington et al. 2015; Kolakowski & Mester 2007).

Figure 6. Schema of the FAIMS procedure (adapted from Kolakowski & Mester 2007).

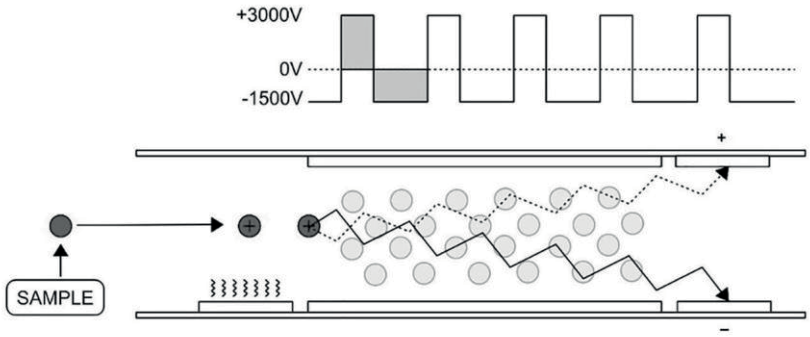

2.5.3 Detection of cancer

Some VOCs associated with cancer have been identified by GC-MS or nano-particle-polymer sensor arrays. Using GC-MS, Amal et al. (2015) found a total of 133 different VOCs from 182 breath samples from OC patients, healthy women and women with benign gynecological neoplasia. Two VOCs which significantly distinguished cancer samples from benign samples were decanal and 2-butanone. Also, nonanal, styrene and hexadecane were found to be possible volatile markers for OC. They also used nanoarrays as sensors for analyzing the same breath samples, achieving a 71% accuracy, sensitivity and specificity, in distinguishing between

samples from OC patients and all other samples. Subsequently, another breath array for OC diagnostics was reported, based on modified gold nanoparticles as sensors. An array of ten sensors was exposed to the VOCs previously linked to OC. The researchers analyzed breath samples from 26 healthy controls and 17 women with epithelial OC. The analysis of all sensors separated the groups with an accuracy of 83.7%, a sensitivity of 82.3% and a specificity of 84.6% (Kahn et al. 2015).

The ability of various applications of the eNose to detect cancer has been investigated with various malignancies. Lung cancer has been studied most by eNose. The first examination of breath samples discriminated lung cancer patients from controls with an accuracy of 90.3% (Di Natale et al. 2003). Later, bladder (Bernabei et al. 2008; Weber et al. 2011) and prostate (Bernabei et al. 2008; Roine et al. 2014) cancers were detected from urinary headspace and breast, colorectal and prostatic cancers from breath samples (Peng et al. 2010), as well as colorectal cancer from fecal headspace (de Meij et al. 2014) with the eNose.

Horvath et al. tested the capability of eNose to discriminate OC tissue odor from that of healthy gynecological tissue. A total of 23 tissue samples from grade 3 seropapillary carcinomas were analyzed in a pilot and external validation study. The overall sensitivity of the results was 84% and the specificity 86.8% (G. Horvath, Chilo et al. 2010).

There are only two studies published in which FAIMS was used as a detector of cancer. With the aid of FAIMS, colorectal cancer was detected in urine samples of 83 cancer patients compared to 50 healthy controls, with a sensitivity of 88% and specificity of 60% (Arasaradnam et al. 2014). From urine headspace, FAIMS differentiated between pancreatic cancer patients (N=81) and healthy controls (N=81) with a sensitivity of 91% and specificity of 83%. Even the urine from early-stage cancer patients was differentiated significantly from that from controls (Arasaradnam et al. 2018).

2.6 Lipidomics

2.6.1 Overview of lipids

Lipids are a large structurally and biologically diverse group of hydrophobic or amphipathic molecules (Sethi & Brietzke 2017). They accomplish three main roles in cells. First, they store energy, mainly as triacylglycerol and cholesterol esters in lipid droplets. Second, they make up cellular membranes, which is the most common location of cellular lipids. The main membrane lipids in eukaryotic cells are glycerophospholipids, of which phosphatidylcholines and phosphatidyletholamines are the most prominent. Third, they function as first and second messengers for molecular signaling and identification processes (S. E. Horvath & Daum 2013; van Meer et al. 2008).

In 2005, Fahy et al. (2005) published a classification for lipids to standardize the information on lipid data. Lipids were divided into eight categories depending on their chemical structures and biochemical properties (see Table 14 below). Each lipid category is divided into subclasses using a variety of molecular differences in acyl carbon chain lengths and the number and positions of double bonds. With new analytical approaches, more than 40,000 lipid structures have already been listed in the LIPID MAPS database, and new lipids will certainly be found in the future (Lydic & Goo 2018).

Table 14. Lipid categories and examples of their classes (Lydic & Goo 2018; Y. Y. Zhao et al. 2015).

Category	Example classes
Fatty Acyls	Fatty acids and conjugates
Glycerolipids	Monoacylglycerols Triacylglycerols
Glycerophospholipids	Glycerophosphocholines Glycerophosphoinositols
Sphingolipids	Phosphosphingolipids Ceramides
Sterol lipids	Cholesterol and derivates
Prenol lipids	Isoprenoids
Saccharolipids	Acylaminosugars
Polyketides	Flavonoids Cytochalasins

Daily nutrition, genetic background and diseases have an influence on lipid contents and concentrations in plasma. Plasma lipids are transported by lipoproteins into the circulation and tissues. Lipoproteins, which consist of lipids and apolipoproteins, are separated into different classes: chylomicron, very low-density lipoprotein (VLDL), low-density lipoprotein (LDL) and high-density lipoprotein (HDL). Each lipoprotein has its own function in plasma lipid delivery (Lydic & Goo 2018).

2.6.2 Analytical methods for lipidomics

Lipidomics is a branch of metabolomics that characterizes, identifies and quantifies lipid species and their multiple biological roles (Y. Y. Zhao et al. 2015). It emerged in the literature in 2003 (Han & Gross 2003; Lagarde et al. 2003) and has progressed since then, especially with recent technological advancements. Lipid profiling from cells, biological fluids and tissues provides new insights into pathophysiology, diagnostics and treatment of different diseases (Lydic & Goo 2018).

There are two ways to analyze lipids: targeted and non-targeted analysis. In targeted analysis, specific lipids are investigated using an accurate method for quantification. The principle behind non-targeted analysis is to analyze all possible lipid species simultaneously (Sethi & Brietzke 2017). A lipidomic analysis involves multiple processes in the workflow to identify and quantify many lipids at the same time (Figure 7).

Figure 7. The workflow for lipidomics (modified from Lydic & Goo 2018; Yang & Han 2016).

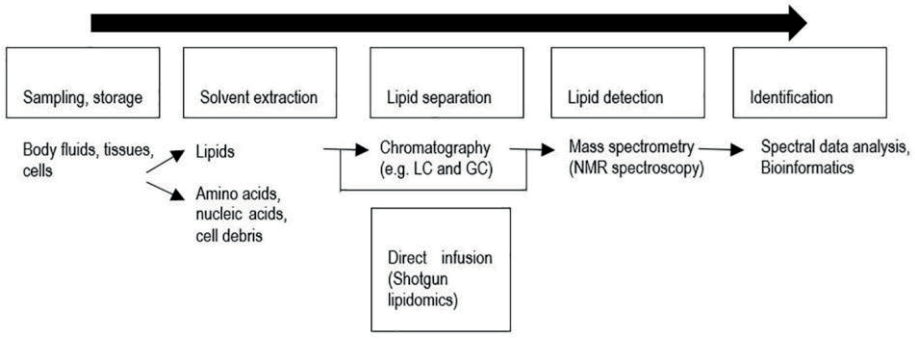

LC: liquid chromatography; GC: gas chromatography; NMR: nuclear magnetic resonance.

Normally, a 5-100 μL of plasma or serum or 1-100 mg of tissue is required for lipid profiling. The first step in lipidomic analysis is the extraction of lipids from the sample to remove proteins, saccharides and other compounds (Sethi & Brietzke 2017). Liquid-liquid extraction developed by Folch et al. (1957) is the most common method of isolating lipids, and the organic solvent used is a combination of chloroform and methanol. Other solvents have also been used for extraction, depending on the hydrophobicity and amount of lipids in the sample. Liquid-liquid extraction is well-suited for a diverse spectrum of lipids in non-targeted lipidomics. Other extraction methods have also been developed in recent years, e.g. solid-phase extraction, a rapid method that performs better in targeted lipidomics (Lydic & Goo 2018; Y. Y. Zhao et al. 2015).

MS- or non-MS-based methods such as nuclear magnetic resonance (NMR) spectroscopy are utilized in lipidomics to detect lipids. After lipid extraction, various chromatographic methods such as GC, LC, thin layer chromatography and HPLC are often used to separate a broad range of lipids from complex samples before detection. Another option is to infuse lipids after ionization directly into MS for detection without prior separation. This method, called shotgun lipidomics, is rapid but more suitable for untargeted lipid profiling than chromatography with MS. These two methods are considered to complement each other (Lydic & Goo 2018; Sethi & Brietzke 2017; Y. Y. Zhao et al. 2015).

The profusion of lipid species is identified from the chromatographic (e.g. LC-MS) and MS/MS spectral data and quantified by comparisons of peak areas and ion peak intensities against standards (Lydic & Goo 2018). The data processed by lipidomics is enormous because each sample can contain a large number of lipid species. Therefore, there are several data-processing software options, in addition to analytical lipid databases, that can be used to aid such efforts (Sethi & Brietzke 2017). Pathway analysis is one method used to understand lipidomics findings in a biological context; there are biotechnological software platforms available to facilitate lipid pathway analysis (Lydic & Goo 2018).

2.6.3 Lipid metabolism in cancer

Cancer cells share characteristic metabolic alterations as a response to increased cellular growth and proliferation. The Warburg effect is the well-known metabolic adaptation in cancer cells: cells produce energy by non-oxidative glycolysis, i.e.

fermentation of pyruvate to lactate in cytoplasm, in contrast to the oxidative phosphorylation in mitochondria in healthy cells (Warburg 1956). An increased glutamine metabolism is also a commonly detected disturbance in cancer cells. Glutamine can be converted to citrate, which is needed by acetyl groups for fatty acid synthesis (Currie et al. 2013).

There are several reported changes in lipid metabolism in cancer in response to cellular proliferation and the increased need for lipids. Most human cells obtain lipids from blood circulation as free fatty acids or combined with proteins such as lipoproteins. These lipids are acquired from dietary sources or synthesized *de novo* mainly in the liver, adipose tissue and lactating breasts. As early as the 1950s, it was noted that human neoplastic tissues can produce lipids through *de novo* synthesis (C. R. Santos & Schulze 2012; Swinnen et al. 2006). Increased lipogenesis in cancer leads to the elevated expression and activity of lipogenic enzymes. The enzymes showing increased activity in malignancies, also in OC, include ATP citrate lyase, acetyl-CoA carboxylase and fatty acid synthase (FAS), which are regulated by several signaling pathways (Pyragius et al. 2013). The increased expression of FAS is shown to correlate with the aggressiveness of OC (Ueda et al. 2010). Lipid rafts in cellular membranes which are synthesized from cholesterol and phospholipids, are increased in number in cancer cells. They are specialized microdomains which act as platforms for signaling molecules and receptors (Beloribi-Djefaflia et al. 2016; A. L. Santos & Preta 2018). One of the most studied pro-oncogenic signaling pathway is phosphatidylinositol-3-kinase (PI3K)-AKT which can enhance the expression of FAS (Yellen & Foster 2014). Oncoproteins and tumor suppressors such as p53 regulate fatty acid synthesis by influencing the fatty acid precursors created from glucose and glutamine metabolism (Pyragius et al. 2013). The mevalonate pathway, which facilitates cholesterol synthesis, belongs to important processes in cancer. Cholesterol is especially needed for membranes. Lipid droplets, which contain triacylglycerols and cholesteryl esters, are more abundant in malignant cells than in healthy ones (C. R. Santos & Schulze 2012; Swinnen et al. 2006; see Figure 8). Inhibitory molecules targeting lipogenic enzymes are being developed for inhibiting tumor growth and metastatic spread (Beloribi-Djefaflia et al. 2016; Cha & Lee 2016; Q. Liu et al. 2017).

Obesity is a contributing factor in many cancers, mainly due to its insulin resistance. An excess of adipose tissue leads to increased insulin secretion from pancreatic beta cells and the enhanced availability of insulin-like growth factor 1,

both of which stimulate the proliferation of tumor cells and protect them from apoptosis. Inflammatory cytokines secreted by adipose tissue can enhance tumor cell proliferation (C. R. Santos & Schulze 2012). A recent meta-analysis showed that a high consumption of nutritional fats may increase the risk of OC, which could be partly due to a stimulated secretion of extra-ovarian estrogen, which may promote tumor activity (Qiu et al. 2016). On the other hand, the cachexia commonly seen in connection with advanced cancer is caused by the reduction of fat stores through an increased lipolysis in adipose tissue. The breakdown of lipids leads to an increased amount of circulating free fatty acids and production of glycerol for gluconeogenesis in the liver, which supplies energy to the tumor cells (C. R. Santos & Schulze 2012).

An altered lipid metabolism and increased synthesis of long-chain fatty acids promotes cancer development in many ways. Cancer cells need more lipids for membrane building, which is also essential for tumor cell growth and proliferation. *De novo* lipid synthesis and the elevated levels of available lipid droplets support the survival of tumor cells under oxidative and energy stress. An increase in fatty acid and cholesterol synthesis may stimulate signaling in tumorigenesis. Cancer cells have a high glycolysis rate due to their energy demand and therefore an increased lactate production. Lipids may also play a stabilizing role in the oxidation-reduction balance (C. R. Santos & Schulze 2012).

Figure 8. Lipid metabolism in cancer cells (modified from C. R. Santos & Schulze 2012; Swinnen et al. 2006).

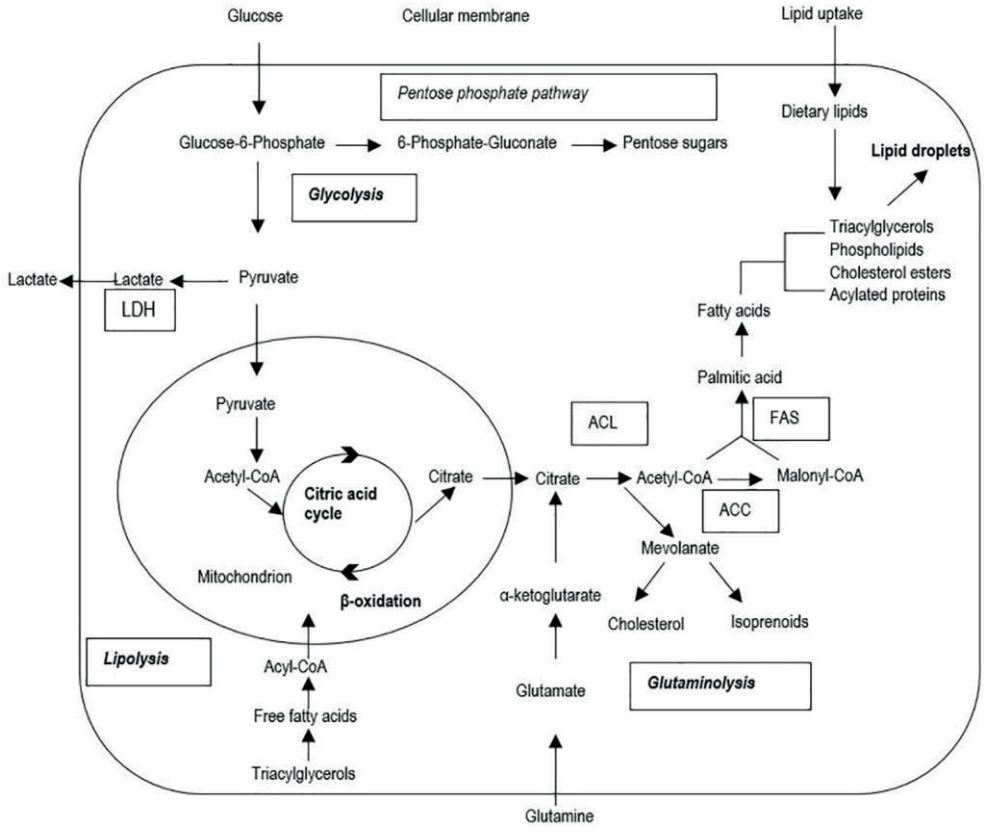

LDH: lactate dehydrogenase; ACL: ATP citrate lyase; ACC: acetyl-CoA carboxylase; FAS: fatty acid synthase.

2.6.3.1 Lipidomics in ovarian cancer

Phospholipids, the major component of cellular membranes, are associated with malignancies. They are associated with OC in many forms, such as increased levels of lysophosphatidic acid (LPA) and altered activity of phospholipase A2 (PLA2), phospholipase D and autotoxin (ATX) (Tania et al. 2010). LPA acts as an extracellular signaling molecule that binds to cell surface G protein-coupled receptors and activates the proliferation, survival and migration of cancer cells

(Pyragius et al. 2013), and LPA levels are elevated in the ascites and plasma of OC patients (Ren et al. 2006). LPA is produced by the activity of PLA2 and ATX enzymes. Elevated levels of PLA2 have been found in ascites and tissue samples in patients with epithelial OC (Cai et al. 2012), and blocking the ATX enzyme seems to inhibit the production of LPA. Phospholipase D is an enzyme essential for the formation of phosphatidic acid, a precursor of LPA (Tania et al. 2010).

Altered sphingolipids have also been connected to malignancies. Ceramides (Cers), short-chain sphingolipids, are most often studied in carcinogenesis due to their role in the induction of apoptosis. Another sphingolipid, sphingosine-1-phosphate, plays an opposite role in promoting cancer cell survival (Furuya et al. 2011). Cers are formed by the hydrolysis of sphingomyelin or by *de novo* synthesis, and they can be converted back to sphingomyelin or to glycosphingolipids, including e.g. sulphatides (Furuya et al. 2011; Hajj et al. 2015). Sulphatides are shown to be elevated in OC tissues, although their role in the development of OC is unclear (Y. Liu et al. 2010).

Activation of lipid metabolism is involved in early carcinogenesis, but lipids also feature in cancer development and progression. Therefore, lipid profiling of the body fluids, tissues and cells of cancer patients has been researched in recent years to detect novel biomarkers for the early diagnosis (Yang & Han 2016) and prognosis of cancer, as well as to find therapeutic targets (Lydic & Goo 2018). Table 15 summarizes the lipid studies in human samples as potential diagnostic or prognostic factors in OC, showing alteration (decrease or increase) of lipids in cancer patients compared with controls.

Table 15. Overview of lipids studied as potential diagnostic or prognostic factors in OC.

Study	Name of lipid	Sample type	N	Decrease (↓) or Increase (↑)	Diagnostic factor	Prognostic factor
Xu 1998	LPA	Plasma	48 controls 48 OCs	↑	x	
Xiao 2000	LPAs 16:0, 18:2, 18:1 & 18:0 LPIs 16:0, 18:0 & 20:4	Plasma	10 controls 8 OCs	↑	x	
Sutphen 2004	LPAs, LPIs, LPCs, S1P	Plasma	27 controls 117 EOCs	↑	x	
Sedlakova 2008	LPA	Plasma	43 controls 30 benign tumors 60 OCs	↑	x	
Liu Y 2010	Sulphatides	Tissue	12 controls 12 EOCs	↑	x	
Sedlakova 2011	LPA	Plasma	27 controls 51 benign tumors 81 OCs	↑	x	
Kang 2011	PCs 32:3, 34:1 & 36:2	Tissue	6 controls 23 OCs	↑	x	
Shan 2012	LPA, LPC, PPE	Serum	212 controls 211 EOCs	↑ (LPA) ↓ (LPC, PPE)	x (combined with CA125)	
Zhang T 2012	LPCs 18:3 & 14:0	Plasma	90 benign tumors 80 EOCs	↓	X	
Gaul 2015	LPCs 18:3 & 14:0, LPI 18:1, Cer(d18:1/16:0), LPE 22:6, PI 20:4/18:1	Serum	49 controls 46 Stage I-II serous EOCs	↑	X	

Ke 2015	LPC 14:0, LPC 18:2(9Z,12Z), LPC 18:3(9Z,12Z,15Z), LPE 0:0/18:1(9Z), LPE 0:0/16:0, LPE 20:2(11Z,14Z)/0:0	Plasma	158 benign tumors 150 uterine fibroids 140 EOCs	↑ (in localized OC) ↓ (in metastatic OC)	x	x
Buas 2016	16 GPLs, 8 TAGs, 1 SL, 1 sterol lipid, 8 unknown lipids	Plasma	50 serous benign tumors and 50 serous EOCs	↓	x	
Zhang Y 2016	LPCs, PCs, TAGs	Plasma	11 controls 27 benign tumors 27 OCs	↑ (LPCs) ↓ (PCs & TAGs)	x	
Zhao Z 2016	TAGs 50:2, 50:1, 52:2, 54:4 & 54:3	Cell lines	low vs. highly aggressive EOCs	↑ (in highly aggressive cell lines)		x
Braicu 2017	PCs, PIs, PEs, CEs, DAGs, SMs, Cerebrosides, LacCers, Gb3s, S1Ps, LPCs, LPEs, Cers, TAGs, plasmalogens	Serum	98 controls 147 HGSOCs	↓ ↑ (specific lipids of LPCs, LPEs, Cers, TAGs and plasmalogens)	x	x
Knapp 2017	C16-Cer, C18:1-Cer, C18-Cer, C24:1-Cer, C24-Cer, S1P	Plasma, tissue	81 controls 74 HGSOCs	↑ (C16-Cer, C18:1-Cer & C18-Cer in plasma and tissue, C24:1-Cer, C24-Cer & S1P in tissue)	x	
Li J 2017	31 lipids, including LPCs, PEs, PCs, PIs, Cer(d18:1/23:0), SMs	Plasma	31 non-recurrent EOCs 39 recurrent EOCs	↓ (in recurrent EOCs) ↑ (only PC 31:2 & PE[P-42:4] in recurrent EOCs)		x

OC: ovarian cancer; LPA: lysophosphatidic acid; LPI: lysophosphatidylinositol; EOC: epithelial ovarian cancer; LPC: lysophosphatidylcholine; S1P: sphingosine-1-phosphate; PC: phosphatidylcholine; PPE: plasmenylphosphoethanolamine; LPE: lysophosphatidyletholamine; Cer: ceramide; PI: phosphatidylinositol; GPL: glycerophospholipid; TAG: triacylglycerol; SL: sphingolipid; PE: phosphatidyletholamine; CE: cholesterylester; DAG: diacylglycerol; SM: sphingomyelin; LacCer: lactosylceramide; Gb3: globotriasoylceramide; HGSOC: high-grade serous ovarian carcinoma; PE(P): 1Z-alkenyl phosphatidyletholamine.

3 AIMS OF THE STUDY

This study was undertaken to assess whether new methods could improve preoperative diagnostics of ovarian cancer. The specific aims of the study were:

1. To evaluate the feasibility of the various ultrasound scoring systems and three-dimensional power Doppler sonography in the assessment of ovarian tumors (Study I).
2. To explore whether urinary polyamines analyzed by liquid chromatography-tandem mass spectrometry discriminate benign and malignant ovarian tumors (Study II).
3. To test whether field asymmetric ion mobility spectrometry can distinguish between the urine of women with benign and malignant ovarian tumors (Study III).
4. To examine if there are alterations in lipid metabolism that can be found in serum/plasma samples obtained from patients with early- and advanced-stage ovarian cancer of various histological subtypes (Study IV).

4 PATIENTS, MATERIALS AND METHODS

4.1 Patients and study design (Studies I-IV)

A total of 119 women aged at least 50 years with an indefinite ovarian tumor scheduled for surgery were prospectively enrolled into Study I. Obviously benign or malignant-looking ovarian tumors were not included, such as simple cysts or tumors with abundant ascites (the diameter of the largest ascites pouch was >10 cm). In addition, the entire tumor had to be visible in the transvaginal US assessment which was performed during the period of two weeks immediately prior to surgery. However, the stored US data of 19 women was lost due to the breakdown of the hard disk of the US machine. In connection with the preoperative laboratory tests, which included a CA125 sample, an extra serum sample was obtained from 111 women to be stored in a freezer.

The study population was partly the same in the three studies: 22 women in Study I were also in Study II, and 13 women in Study I were in Study III. For Studies II and III, we recruited postmenopausal women 50 and older with an unspecified adnexal mass waiting for surgery along with women scheduled for genital prolapse or urinary incontinence operations as controls. A total of 107 women gave their informed consent to the study, but only 98 women gave a urine sample; of them, 93 were eligible for the Study II polyamine analysis and, later, 78 were eligible for the Study III FAIMS analysis. Sixty-six women were included in both Studies II and III. All women provided a urine sample on the morning of their operation, and the samples were stored in two tubes at -70°C to be analyzed later. All the operations in Studies I-III were performed at the Tampere University Hospital.

Study IV was conducted in cooperation with the Oulu University Hospital in Finland and the Charitè Medical University in Berlin, Germany. Serum samples from Study I were included in the Study IV population. Also included were 54 preoperatively collected plasma samples from the Oulu University Hospital and 189 serum samples from the Tumor Bank-Ovarian Cancer Network of the Charité Medical University from women with adnexal masses. These were the two study

cohorts (Finland and Charité in Germany). The blood samples from these two cohorts were compared with previously analyzed data from 250 serum samples from Charitè (Braicu et al. 2017).

The characteristics of the study groups after exclusions are presented in Table 16.

Table 16. Study population, main objectives and main outcome measures in Studies I-IV.

	Study I	Study II	Study III	Study IV
Study design	Prospective	Prospective	Prospective	Retrospective
Number of patients	98[a]	81[b]	69[c]	354 250 (Reference Study Cohort)
Study population	32 malignant ovarian tumors and 66 benign ovarian tumors	37 malignant ovarian tumors, 23 benign ovarian tumors and 21 healthy controls	33 malignant ovarian tumors, 18 benign ovarian tumors and 18 healthy controls	138 malignant ovarian tumors, 25 borderline tumors and 191 controls with benign gynecologic pathologies 152 malignant ovarian tumors (Reference Study Cohort) and 98 controls with benign gynecologic pathologies (Reference Study Cohort)
Age (years) Md (range)	61 (50-84)	66 (51-86)	64 (51-83)	56 (18-85) 54 (17-92; Reference Study Cohort)
Study objectives	To compare various US scoring systems, serum CA125 and 3D-PD in assessing the nature of ovarian tumors	To examine whether urine polyamine levels differ in women with benign and malignant ovarian tumors and healthy controls	To clarify whether urine from women with benign and malignant ovarian tumors and from controls can be differentiated using FAIMS	To validate the former findings of lipidomic alterations in serum of women with advanced HGSOC and to investigate whether the lipid changes occur also in serum/plasma of women with early-stage cancer and in other histological subtypes
Sample collection	FEB 2011 – NOV 2014	MAY 2013 – MAR 2016	MAY 2013 – MAR 2016	JAN 2009 – DEC 2015
Main outcome measures	The sensitivities, specificities and accuracies of each predictive model in detecting ovarian malignancy	Changes in urinary polyamine concentrations in the different study groups	The sensitivities, specificities and accuracies of FAIMS in finding differences between the study groups	Lipidomic changes in early- and late-stage ovarian cancer vs. controls, and serous and histological subtypes vs. controls

[a] Two patients excluded (tumors were of appendiceal origin).

[b] 12 patients excluded: six malignant tumors were of colorectal origin; one tumor was a metastasis of uterine leiomyosarcoma; four patients had concurrent other malignancies; and one was not postmenopausal.

[c] Nine patients excluded: six malignant tumors were of colorectal origin and one was metastasis of uterine leiomyosarcoma, two patients had concurrent other malignancy).

US: ultrasound; 3D-PD: three-dimensional power Doppler; FAIMS: field asymmetric waveform ion mobility spectrometry; HGSOC: high-grade serous ovarian carcinoma.

4.2 Methods

The results from the assessed diagnostic methods were correlated with the final histopathology of the tumors. The offline evaluation of stored sonography data and 3D volumes (Study I), the analysis of polyamines by LC-MS/MS (Study II) and the FAIMS urinary analysis (Study III) were performed blinded to the histopathological results. In Study IV, blood samples were randomized within each cohort before LC-MS/MS lipidomic analyses were performed.

4.2.1 Two- and three-dimensional sonography with power Doppler (Study I)

All US examinations were conducted using a Voluson 730 Expert unit (GE Medical Systems, Zipf, Austria) with a multifrequency endovaginal probe (5-9 MHz) by one examiner (R.N.) The routine B-mode examination was performed first and the dimensions of the ovarian tumor were measured. If bilateral ovarian tumors existed, the more complex tumor was included in the study. The adnexal tumor was first evaluated using 2D US, and the vascularization of tumor was scored from 1 to 4 using the IOTA classification system: 1 was no Doppler signal detected, and 4 was a highly vascularized tumor with abundant Doppler signals detected (Timmerman et al. 2000). The following PD settings were used: a frequency of 6 MHz, a power Doppler gain of -0.6, the wall motion filter on low 1, and a pulse repetition frequency of 0.6 kHz.

In the beginning of the 3D evaluation, the size of the volume box was adjusted to cover the contours of the ovarian mass. The acquisition angle was set to 85 degrees. The women hyperventilated briefly and then held their breath during the 3D sweep. Once a volume was obtained and accepted as fulfilling the requirements (no movement artifacts, and the entire tumor was within the volume box), it was stored on a hard disk with the previously stored 2D data to be analyzed later offline.

4.2.1.1 Ultrasound-based scoring methods

After each US examination, the investigator categorized the tumor as benign or malignant (expert opinion). The RMI was calculated using the original formula (Jacobs et al. 1990). Tumors were analyzed from stored 2D data using the IOTA

simple rules (Timmerman et al. 2008). In the case of non-classifiable tumors, i.e. tumors to which none of the rules or both M- and B-rules applied, the tumor was classified by expert opinion. In addition, the probability of tumor malignancy was calculated using IOTA LR2 (Timmerman et al. 2005) with various cutoff levels, with the aid of the Predictive IOTA models for ovarian cancer application software, version 2013 (an app for IOS operating systems).

4.2.1.2 Three-dimensional power Doppler angiography

Offline analyses of stored 3D volumes were performed using the VOCAL imaging utility and 4DView software version 9.1 (GE Medical Systems, Zipf, Austria). With the aid of these programs, the visual and quantitative evaluation of 3D data was feasible on a Windows-based computer. Volumes of all tumors were constructed by manually outlining the contours of tumors inside the volume box in a mid-sagittal plane (Plane A) with 15-degree rotations. With the help of the histogram feature of the VOCAL utility, the vascular indices VI, FI and VFI were obtained from the selected tumor volume.

Figure 9. Volume analysis of an ovarian tumor using the VOCAL utility.

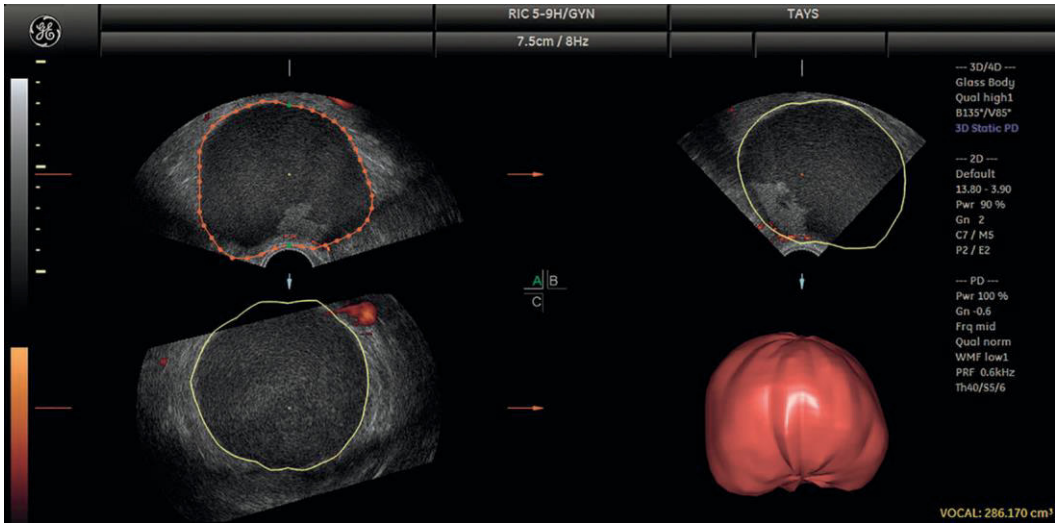

Figure 10. Histogram feature with the respective vascular indices for the same volume.

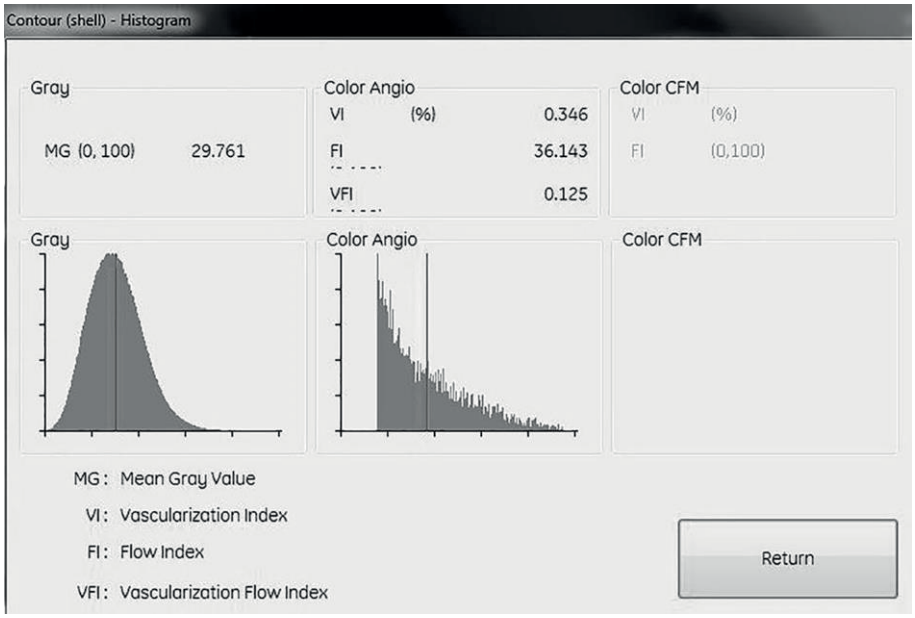

4.2.1.3 Interobserver agreement

To estimate the agreement between two examiners, the stored 2D data from the ovarian tumors was re-evaluated offline and classified as either benign or malignant by another independent US examiner (S.S.) The volumes and vascular indices were also re-analyzed using 3D US data as previously described. The analyses were performed blinded to each other`s interpretations.

4.2.2 Polyamine analysis by liquid chromatography-tandem mass spectrometry (Study II)

The creatinine concentration was quantified enzymatically in Fimlab laboratory (Tampere, Finland) from a portion of each urine sample. The stored urine samples were thawed at room temperature and centrifuged. The LC-MS/MS analyses were performed at the University of Eastern Finland.

Urine specimens were first mixed with water and an internal standard (IS) working solution, which contained isotope-labeled molecules for each analyzed polyamine mimicking the target molecules in the LC but still distinguishable from them. The urine samples were filtered through the solid-phase extraction cartridge before LC-MS/MS analysis.

The chromatographic separations of polyamines were performed using a reversed phase column with 0.1% heptafluorobutyric acid as an evaporative ion-pairing agent. The samples were ionized using a positive electrospray ionization source and then detected with an Agilent 6410 Triple Quadrupole MS. Deuterated ISs of each polyamine were used in the quantification, and the polyamine concentrations were normalized using creatinine concentrations. The obtained data was processed and quantified using Agilent Masshunter Workstation software (Agilent Technologies, Palo Alto, CA, USA).

A detailed description of this LC-MS/MS technique has been reported by Häkkinen et al. (2013). This technique was validated and calibrated for quantitation limits for each polyamine. The amounts of polyamines remained stable in urine matrix and in water dilutions and did not change even after longer storages or several freezing-thawing procedures. Water dilution is needed in case polyamine concentrations are very high. Some urine compounds may have effect on sensitivity of the analyte (matrix effect) which was compensated using deuterated ISs. Also, the accuracy and precision of this technique were tested in intra- and inter-day analysis according to the FDA validation guideline using <15% as an acceptable variation value.

4.2.3 The FAIMS analytical technique (Study III)

For the FAIMS analysis, we used a commercial Lonestar (Owlstone, Cambridge, United Kingdom) device with an ATLAS sampling unit to standardize the analytical circumstances. The stored urine specimens were thawed to room temperature. The urine samples were mixed using a vortex and 5 mL of urine sample was pipetted into a 30 mL glass vial, which was heated to 40°C. Clean air was streamed over the sample, transferring VOCs into the device at a total flow rate of 2500 mL/min. Inside the Lonestar, the sample stream was ionized with nickel-63 isotope. Subsequently, the sample was passed into the electric field where it was analyzed by alternating the compensation voltage range between -6V and +6V in 512 steps for

field strengths of 0-90% in 51 steps. Each sample was scanned three times; afterwards, five scans with sterilized water were made to clean the device and reduce carryover.

The FAIMS technique used has not been standardized due to its experimental nature but the other published studies have also utilized the same technique (Arasaradnam et al. 2014; Arasaradnam et al. 2018). I am not aware of previous studies of repeatability of FAIMS analysis. However, the urine samples were randomized before analysis in order to prevent any systematic bias.

4.2.4 Lipidomic analysis by liquid chromatography-tandem mass spectrometry (Study IV)

The blood samples stored at -70°C were thawed to a temperature of +4°C. Two lipidomic platforms, a global screening method and a phosphosphingolipid platform were used to perform the lipidomic profiling at the laboratory of Zora Biosciences Oy (Espoo, Finland). The isolation of lipids for the global screening method was performed by modified Folch extraction (Folch et al. 1957). A 10 μL sample was aliquoted into 96 wells of the plate, and a solvent containing chloroform, methanol and a mixture of synthetic ISs was added to the plate to extract lipids. In turn, a 25 μL sample was aliquoted into a 96-well plate to which methanol and 0.1% butylated hydroxytoluene with a mixture of synthetic ISs was added for phosphosphingolipid extraction.

A hybrid triple quadrupole/linear ion trap mass spectrometer with ultra-high-performance liquid chromatography was used. Lipid detection was performed by MS analysis in the positive ion mode for both platforms. The data from the lipidomics screening platform was collected using a scheduled multiple reaction monitoring algorithm and from the phosphosphingolipid platform using multiple reaction monitoring. The lipidomics data was analyzed using Analyst and MultiQuant 3.0 software (AB Sciex, Concors, Canada), and normalization with IS amount and sample volume was done in relation to the area or height ratios of each analyte and its respective IS peak. The analyzed lipid species and the mean coefficient of variation of each analyzed lipid, which varied between the analyses, are shown in Table 17.

Table 17. Analyzed lipids

Lipid class	Number of lipids	Coefficient of variation
Acylcarnitine (AC)	8	15%
Cholesteryl ester (CE)	21	24%
Ceramide (d16:1-d20:1)	37	22-36%*
Diacylglycerol (DAG)	18	29%
Globotriasoylceramide (Gb3)	4	41%
Glucosyl/galactosylceramide (Glc/GalCer)	22	29%
Lactosylceramide (LacCer)	10	28%
Lysophosphatidylcholine (LPC)	53	11%
Lysophosphatidylethanolamine (LPE)	13	12-13%*
Phosphatidylcholine (PC)	116	20-23%*
Phosphatidylethanolamine (PE)	38	27-30%*
Phosphatidylglycerol (PG)	4	23%
Phosphatidylinositol (PI)	19	19%
Phosphosphingolipids (S1P/SA1P)	4	9%
Sphingomyelin (SM)	41	16%
Triacylglycerol (TAG)	42	11%
Total	**450**	

*depending on the specific lipid class

Braicu et al. (2017) gave a detailed description of this lipidomic analysis which was modified from the previously described method (Weir et al. 2013). The analysis technique used is a so-called high throughput screening method which has to be validated to specific targeted lipid molecules before using as a clinical test. The effect of thawing and freezing on the lipid concentrations should also be studied as part of the validation.

4.3 Statistical analysis

Sample sizes were not calculated due to the preliminary nature of all studies. In Study I, statistical analyses were performed using IBM SPSS Statistics version 22 (IBM Corp., Armonk, NY, USA). The Kolmogorov-Smirnov test was used to assess the normal distribution of continuous variables. The groups were compared using the Mann-Whitney U-test, and correlations were assessed using Spearman's correlation tests. Receiver operating characteristic (ROC) analyses were carried out

for each continuous variable to evaluate its performance as a predictive test. Appropriate cutoff levels for variables were calculated based on sensitivity, specificity, negative and positive predictive values. Categorical variables were tested using Pearson's chi-square test or Fisher's exact test. The concordance of US features as noted by two observers was calculated using Cohen's kappa index, and the concordance of 3D-PD vascular indices using the related-samples Wilcoxon signed rank test.

In Study II, MATLAB Version R2016b (Mathworks Inc., Natick, MA, USA) was used for statistical analysis. The distributions of continuous variables were evaluated using the Kolmogorov-Smirnov test. The comparisons in polyamine concentrations were assessed between all groups (controls, benign tumors and malignant tumors) using the Wilcoxon rank sum test; $p < 0.05$ between the groups was considered statistically significant. The ROC curves for predictive biomarkers, urinary DiAcSpm and serum CA125 were computed and used to identify the optimal cutoff level for DiAcSpm. For CA125, the cutoff level selected was the commonly used 35 kU/L. Sensitivities and specificities for these threshold levels were measured.

In Study III, data from the third scan of each urine sample, including both positive and negative ion channels, were discovered to be comparable with the average of all three scans. The data were processed using LDA and quadratic discriminant analysis (QDA) to create classification parameters. Subsequently, the data were cross-validated by 10-fold cross-validation to avoid overfitting. The statistical analyses were conducted using MATLAB Version R2017b (Mathworks Inc, Natick, MA, USA).

In Study IV, we used R version 3.4.2, which is non-commercial software, for statistical analyses. Two groups (women with tumors vs. women controls) were compared by calculating the mean relative differences between the groups, and *p*-values were calculated by unpaired t-tests on log-transformed concentrations. Heatmaps were visualized by Tableau software version 10.1. Logistic regression models obtained from the Charité cohort were tested in the Finnish cohort, and the AUC values were calculated using a pROC package.

4.4 Ethical considerations

In conducting our studies, we complied with the Declaration of Helsinki. The sample collection and protocols for Studies I-IV were approved by the Pirkanmaa Hospital District Ethics Committee. Each patient gave written informed consent for the study. The local ethics committees of the Oulu University Hospital (Finland) and the Charitè Medical University (Berlin, Germany) also approved Study IV.

5 RESULTS

A few recruited patients were excluded from the final analysis after the final histopathological diagnosis of a non-ovarian neoplasm. The detailed exclusions from each study are presented in the explanatory legends of Table 16 above. The histological diagnoses from Studies I-III are presented below in Table 18 and from Study IV in Table 19.

Table 18. Histopathological diagnoses from Studies I-III.

Histology	Study I	Study II	Study III
Benign	**66**	**23**	**18**
Serous cystadenoma / adenofibroma	39	11	9
Mucinous cystadenoma	3	2	1
Fibroma / thecoma	5	2	2
Teratoma	7		
Serous / hemorrhagic / simple/ necrotized cyst	7	6	4
Endometriotic cyst	3	2	2
Brenner tumor	1		
Bizarre leiomyoma	1		
Borderline	**7**	**9**	**9**
Serous	5	4	4
Mucinous	2	5	5
FIGO Stage			
I & II	7	8	9
III & IV		1	
Malignant	**25**	**28**	**24**
Serous			
Low-grade	3		
High-grade	9	18	17
Mucinous			
Adenocarcinoma	3	3	2
Endometrioid			
Adenocarcinoma		1	1
Other			
Clear cell carcinoma	1		
Granulosa cell tumor	4	4	2
Sertoli-Leydig cell tumor	1	1	1
Carcinosarcoma	2	1	1
Metastatic	2		
FIGO Stage			
I & II	14	10	7
III & IV	9	18	17

Table 19. Histopathological diagnoses in various study cohorts from Study IV.

Histology	Charitè	Finland	Charité Reference Study Cohort
Benign	**109**	**82**	**98**
Uterine fibroid	7	1	25
Cyst / functional cyst / inclusion cyst	29	9	1
Cystic teratoma	12	8	5
Endometrioid cyst / endometriosis	14	1	2
Non-ovarian cyst		4	
Cystadenoma / cystadenofibroma	39	12	6
Mucinous cystadenoma		3	2
Serous cystadenoma		34	3
Brenner tumor	1	2	1
Fibroma / thecoma / fibroadenoma		6	
Incomplete abortion			5
Adnexitis			5
Other	7	2	43
Borderline	**18**	**7**	
Serous	13	5	
Mucinous	2	2	
Other	3		
FIGO Stage			
I & II	12	7	
III & IV	3		
NA	3		
Malignant	**62**	**76**	**152**
Serous	41	29	147
Mucinous	6	18	
Endometrioid	9	14	5
Other	6	15	
FIGO Stage			
I & II	26	52	8
III & IV	33	22	133
NA	3	2	11

NA: not applicable.

5.1 Ultrasound scoring methods (Study I)

The calculated RMI values (and CA125 serum levels) of benign and malignant ovarian tumors differed to a statistically significant degree (p <0.001). The accuracies in detecting a malignancy were quite similar with CA125 (with the commonly used threshold value of 35 U/mL) and the RMI (with the most common used threshold value of 200), or 76.5% and 77.6% respectively.

Using the IOTA simple rules, 76 of 98 tumors could be classified, 68 of which were correct. The 22 remaining unclassifiable tumors were evaluated by an US examiner (R.N.), and 17 of 22 were correctly classified. The accuracy of the IOTA simple rules with the aid of expert opinion was 86.7%, compared with the accuracy of expert opinion alone, which was 90.8%. The sensitivity of the IOTA simple rules together with an expert opinion reached 90.6% but the specificity was poorer than expert opinion alone, i.e. 84.6% vs. 92.4% respectively. Attention must also be paid to the number of patients, which means that the difference between these two methods is not that great.

Another IOTA method, LR2 (with a threshold value of 25%), achieved a sensitivity in detecting malignancies that was similar to that of the simple rules. However, LR2 failed – by comparison with the simple rules – in its specificity and accuracy. The vascularity of the tumors as analyzed by 2D PD was significantly higher in malignant than in benign tumors (p <0.001), and this method was as accurate and sensitive as LR2.

The diagnostic performances of all the methods studied in Study I are presented in Table 20 below.

Table 20. Ultrasound-based scoring methods, including serum CA125, of differentiating between benign and malignant ovarian tumors.

Method	**Sensitivity** (%) (95% CI)	**Specificity** (%) (95% CI)	**Accuracy (%)**
CA125[a]	59.4 (40.6-76.3)	84.9 (73.9-92.5)	76.5
RMI[b]	71.9 (53.3- 86.3)	80.3 (68.7-89.1)	77.6
Simple rules[c]	90.6 (75.0-98.0)	84.6 (73.9-92.5)	86.7
Expert opinion	87.5 (71.0-96.5)	92.4 (83.2-97.5)	90.8
Tumor vascularity[d]	90.6 (75.0-98.0)	77.3 (65.3-86.7)	81.6
LR2[e]	90.6 (75.0-98.0)	77.3 (65.3-86.7)	81.6

CI: confidence interval.

[a] Cutoff value 35 kU/L.

[b] Cutoff value 200.

[c] When the result was inconclusive, the expert evaluated the tumor.

[d] Two-dimensional vascular score 1-2 vs. 3-4.

[e] Cutoff value 25%.

5.1.1 Three-dimensional power Doppler angiography

Three-dimensional vascular indices differed significantly between malignant and benign tumors (p <0.001). The VI and VFI were the most specific and accurate indices, comparable with the RMI, the simple rules and LR2. However, the combination of VFI value with the RMI/simple rules/LR2 did not improve their diagnostic performances. Table 21 below shows the diagnostic performances of 3D-PD vascular indices and the combination of the VFI with other scoring methods.

Table 21. Diagnostic performances of 3D-PD vascular indices and combined methods.

3D-PD indices Cutoff value	**Sensitivity** (%) (95% CI)	**Specificity** (%) (95% CI)	**PPV** (%) (95% CI)	**NPV** (%) (95% CI)	**Accuracy** (%)
VI (%)	67.7	90.9	77.8	85.7	83.5
1.00	(48.6-83.3)	(81.3-96.6)	(57.7-91.4)	(75.3-92.9)	
FI	83.9	51.5	44.8	87.2	61.9
30	(66.3-94.6)	(38.9-64.0)	(31.7-58.5)	(72.6-95.7)	
VFI	71.0	89.4	75.9	86.8	83.5
0.31	(52.0-85.8)	(79.4- 95.6)	(56.5-89.7)	(76.4-93.8)	
Combination methods					
RMI >200 and VFI	51.6	95.5	84.2	80.8	81.4
>0.31	(33.1-69.9)	(87.3-99.1)	(60.4-96.6)	(70.3-88.8)	
Simple rules with	71.0	95.5	88.0	87.5	86.7
expert opinion and	(52.0-85.8)	(87.3-99.1)	(68.8-97.5)	(77.6-94.1)	
VFI >0.31					
LR2 and VFI	64.5	97.0	90.9	85.3	86.5
>0.31	(45.4-80.8)	(89.5-99.6)	(70.8-98.9)	(75.3-92.4)	

PPV: positive predictive value.
NPV: negative predictive value.

The diagnostic performances of CA125, the RMI, LR2 and the 3D-PD vascular indices (VI, FI, VFI) are presented in ROC curves in Figure 11. The respective AUCs for these methods are 0.80, 0.81, 0.93, 0.86, 0.72 and 0.87.

Figure 11. The ROC curves for CA125, the RMI, LR2 and the 3D-PD vascular indices.

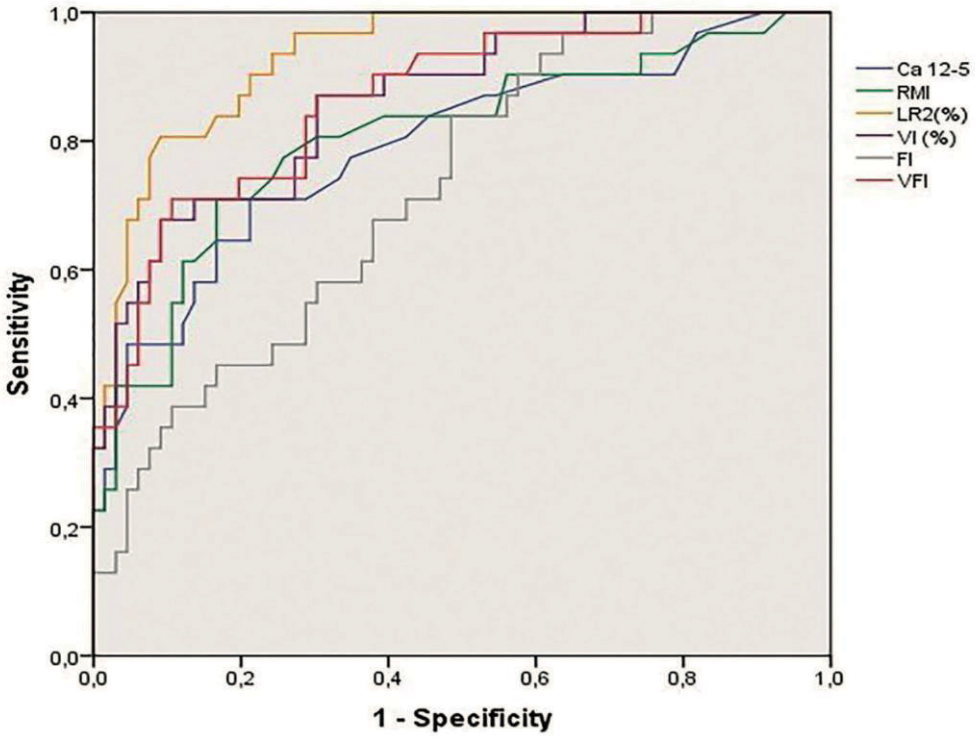

5.1.2 Interobserver agreement

The expert opinions of two US examiners (R.N. and S.S.) were compared, and they disagreed in only five cases, all of which turned out to be histopathologically benign. Both of the experts missed four malignant tumors: a Stage IA endometrioid adenocarcinoma, a granulosa cell tumor and two serous BOTs. The agreement between the conclusions of the two observers was very good regarding tumor malignancy (Cohen's $\kappa = 0.89$; 95% CI 0.79-0.98).

The 3D-PD vascular indices measured by both examiners did not differ from each other ($p > 0.1$), which indicates a good level of interobserver agreement.

5.2 Urinary polyamines (Study II)

A total of 12 polyamines (cadaverine, acetylated cadaverine, diacetylated cadaverine, acetylated putrescine, diacetylated putrescine, spermidine, N^1-acetylated spermidine, N^8-acetylated spermidine, DiAcSpd, spermine, acetylated spermine and DiAcSpm) were found in urine samples from the controls, the women with benign tumors and those with malignant tumors. However, only six of these polyamines were found in all samples (see Table 22 below).

Table 22. The polyamines found in all urine samples and their concentrations (µmol/g creatinine).

Polyamine	Controls (*N* = 21)	Benign ovarian tumors (*N* = 23)	Low-grade malignant tumors (*N* = 18)	High-grade malignant ovarian tumors (*N* = 19)
		Range (µmol/g creatinine)		
AcCad	0.04-5.64	0.08-14.26	0.11-13.08	0.17-5.57
AcPut	6.57-19.28	5.60-28.10	9.15-41.45	8.54-50.16
N^1AcSpd	1.78-8.92	1.04-8.17	1.39-6.50	2.52-18.50
N^8AcSpd	1.84-4.75	1.15-4.69	1.65-5.03	2.18-5.99
DiAcSpd	0.18-0.65	0.14-1.32	0.16-1.34	0.23-1.20
DiAcSpm	0.06-0.20	0.04-1.02	0.06-0.37	0.14-2.37

AcCad: acetylated cadaverine; AcPut: acetylated putrescine; N^1AcSpd: N^1-acetylated spermidine; N^8AcSpd: N^8-acetylated spermidine; DiAcSpd: N^1,N^8-diacetylspermidine; DiAcSpm: N^1,N^{12}-diacetylspermine.

5.2.1 Diagnostic performance of urinary diacetylspermine

Urinary DiAcSpm was the only polyamine which showed statistically significant differences between all studied groups, except between controls and women with benign ovarian tumors (see Table 23). The concentrations of DiAcSpm were highest in women with malignant ovarian tumors, especially high-grade and advanced cancers. The DiAcSpm concentrations in the different groups are presented in Figures 12 and 13. In addition, there were statistically significant differences between study groups in the urinary concentrations of DiAcSpd, N^1AcSpd and N^8AcSpd.

Table 23. Comparisons between study groups in differences in urinary DiAcSpm concentrations.

Comparisons	*p-value*
Benign ovarian tumors vs. all malignant ovarian tumors	<0.001
Benign ovarian tumors vs. low-malignant potential ovarian tumors	0.020
Benign ovarian tumors vs. Stage I-II tumors	0.017
All malignant ovarian tumors vs. controls	<0.001
Low-malignant potential ovarian tumors vs. high-grade tumors	<0.001
Stage I-II vs. Stage III-IV tumors	<0.001

Figure 12. Concentrations of urine DiAcSpm (µmol/g creatinine) by study group. Reprinted from the International Journal of Gynecological Cancer, Vol. 27, Niemi et al., "Urinary polyamines as biomarkers for ovarian cancer", pp. 1360-1366, Copyright (2017), with permission from Wolters Kluwer.

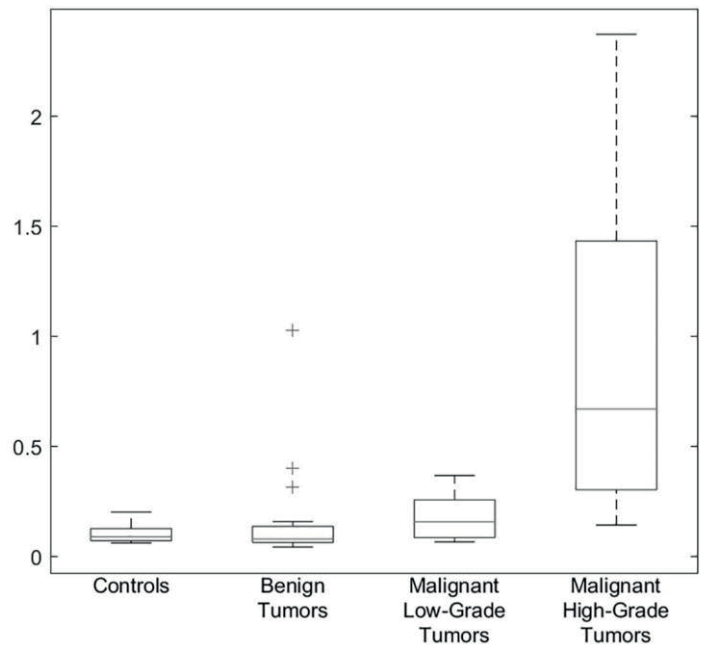

Figure 13. Concentrations of urine DiAcSpm (µmol/g creatinine) by study group. Reprinted from the International Journal of Gynecological Cancer, Vol. 27, Niemi et al., "Urinary polyamines as biomarkers for ovarian cancer", pp. 1360-1366, Copyright (2017), with permission from Wolters Kluwer.

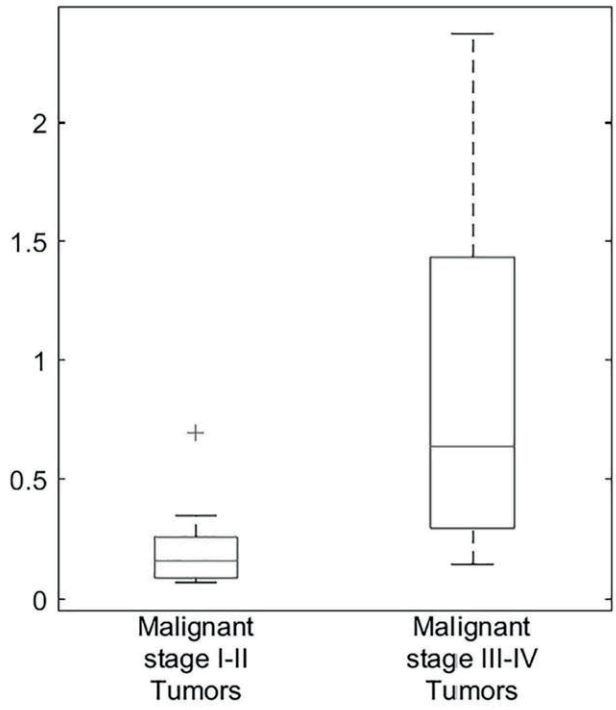

Serum CA125 levels in all women with ovarian tumors had a sensitivity of 75.7% and specificity of 69.6% in distinguishing malignant tumors. Urinary DiAcSpm proved to be at least as good tumor marker as CA125, with a sensitivity of 86.5% and specificity of 65.2% (Figure 14).

Figure 14. The ROC curves for urinary DiAcSpm and serum CA125. Reprinted from the International Journal of Gynecological Cancer, Vol. 27, Niemi et al., "Urinary polyamines as biomarkers for ovarian cancer", pp. 1360-1366, Copyright (2017), with permission from Wolters Kluwer.

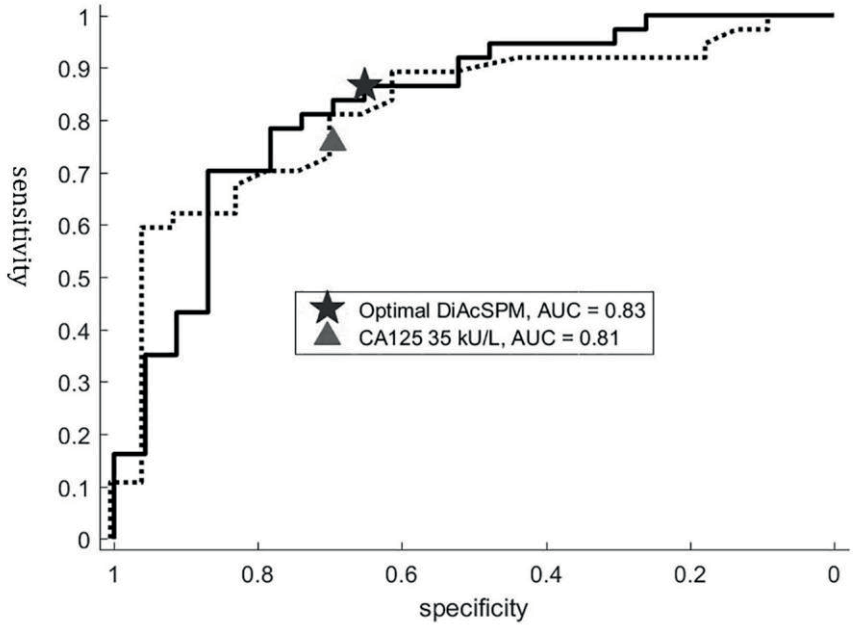

5.3 FAIMS analysis of urine (Study III)

The FAIMS analysis produces numerical data consisting of pixels with three values: compensating voltage, percentage of asymmetric radio frequency waveform and ion current. As many complex samples with various VOCs are impractical to be analyzed manually in order to find out non-linear peaks of each VOC, the data analysis is commonly performed by using multivariate analysis.

The VOC analysis of urine using FAIMS technology was performed with QDA and LDA and validated using 10-fold cross-validation as described above. The main results from the data are shown in Table 24.

Table 24. Results from the FAIMS signal data using both QDA and LDA classification.

Classification pairs	QDA			LDA		
	Sensitivity (%) (±2 Std)	Specificity (%) (±2 Std)	Accuracy (%) (±2 Std)	Sensitivity (%) (±2 Std)	Specificity (%) (±2 Std)	Accuracy (%) (±2 Std)
Benign ovarian tumors vs. controls	93.4 (±11.4)	90.4 (±14.4)	91.9 (±9.8)	86.0 (±11.2)	86.1 (±12.2)	86.1 (±9.6)
Controls vs. malignant ovarian tumors	91.2 (±7.2)	63.1 (±16.0)	81.3 (±8.2)	90.4 (±5.2)	64.3 (±12.8)	81.2 (±5.8)
Controls vs. high-grade ovarian cancers	89.1 (±2.8)	74.6 (±9.6)	81.9 (±5.2)	88.7 (±3.2)	75.6 (±11.8)	82.1 (±6.0)
Benign vs. malignant ovarian tumors	91.5 (±6.4)	51.4 (±32.0)	77.3 (±13.8)	87.1 (±9.0)	27.1 (±38.6)	65.9 (±13.8)
Benign ovarian tumors vs. low-grade ovarian cancers	73.1 (±41.4)	92.9 (±11.4)	83.9 (±23.4)	35.9 (±14.0)	78.8 (±5.8)	59.3 (±7.0)
Benign ovarian tumors vs. high-grade ovarian cancers	85.3 (±15.0)	79.7 (±12.0)	82.5 (±10.0)	85.0 (±15.0)	79.9 (±11.2)	82.5 (±9.6)
Low-grade vs. high-grade ovarian cancers	87.8 (±12.8)	89.6 (±16.6)	88.7 (±11.2)	84.3 (±16.0)	79.7 (±13.4)	82.0 (±10.8)

QDA: quadratic data analysis.
LDA: linear data analysis.

5.4 Lipidomic analysis (Study IV)

A total of 450 lipids were analyzed, 155 of which were found to discriminate between OC patients and controls in the Charité and Finland study cohorts, as well as in the Charité Reference Study Group. The alteration between patients and controls was significant at least in two of those study cohort groups. This range of lipids was analyzed further.

5.4.1 Lipidomic changes in early- and advanced-stage ovarian cancer and in various histological subtypes

To examine whether lipidomic changes occur in earlier stages of OC (FIGO I-II), we selected lipids that showed a consistent increase or decrease in both FIGO Stage I-II vs. controls and FIGO Stage III-IV vs. controls, and were also significantly altered, at least in the Stage III-IV groups in the Finnish and Charité cohorts. With this approach, we found 39 lipids that were mainly decreased in OC patients. Only some ceramide and triacylglycerol species, depending on their fatty acid chains, showed increases in samples from OC patients. Typically, these lipid changes were more often statistically significant in samples from patients with advanced OC.

In order to investigate whether these lipid alterations also exist in histological subtypes (endometrioid and mucinous) other than serous OC, we selected the lipids that showed same direction of change in both the Charité and Finnish cohorts in all histological subtypes. We found 23 lipids that were significant in either endometrioid or mucinous subtypes in both of the cohorts, and all of them were significant in serous OC. Levels of only two of these 23 lipids, Cer(d18:1/18:0) and TAG(18:1/18:1/20:4), were elevated in all subtypes of OC. Levels of all other lipids were decreased.

Figure 15 shows all the lipids that were altered in early-stage OC, also in different histological subtypes.

Figure 15. The most promising lipids showing alterations in all stages and various histologies.

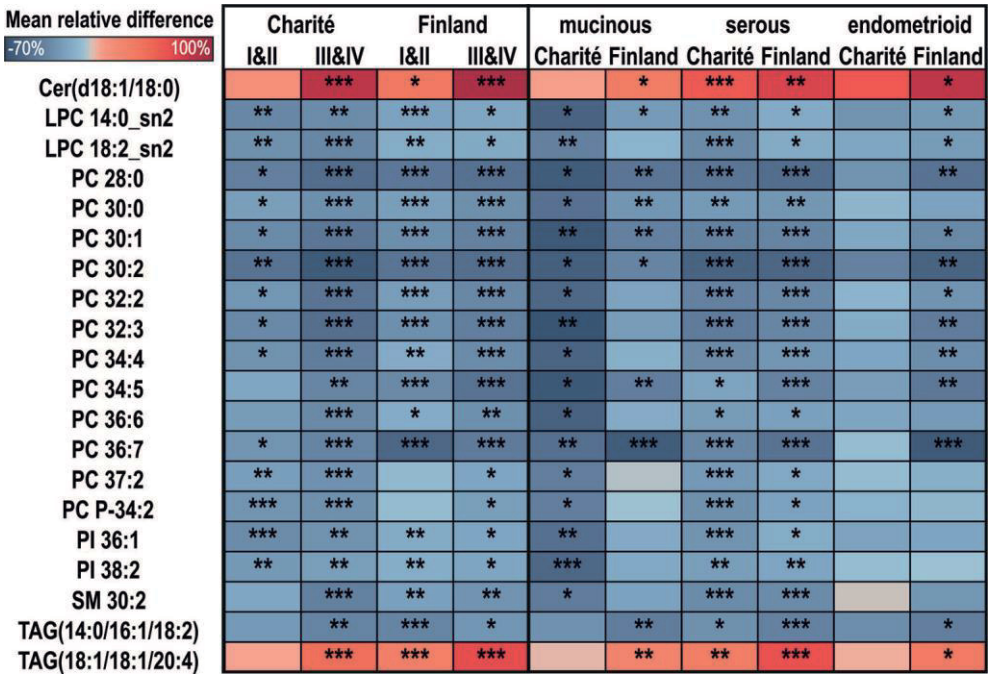

Cer: ceramide; LPC: lysophosphatidylcholine; PC: phosphatidylcholine; PC P: alkenyl-linked phosphatidylcholine; PI: phosphatidylinositol; SM: sphingomyelin; TAG: triacylglycerol.

To investigate whether lipid changes in ovarian malignancies could improve the diagnostic value of serum CA125, we added lipids or lipid ratios to CA125. The increased serum/plasma levels of lipids in OC and CA125 were used as numerators in ratio calculations, and decreased lipids as denominators. Adding lipid data to CA125 improved the AUC values both in the Charité and Finnish study cohorts, and the increases were seen especially in Stage I-II ovarian tumors. Some of the models with the greatest improvements are presented in Table 25.

Table 25. AUC values with 95% confidence intervals for the logistic regression models incorporating lipids and CA125, and also for CA125 alone and CA125 as a binary variable with its commonly used cutoff value.

Variable 1	Variable 2	Charitè			Finland		
		All	Stages I-II	Stages III-IV	All	Stages I-II	Stages III-IV
CA125 / Glc/GalCer(d18:1/26:0)	Cer(d18:1/24:1) / LPC 14:0_sn2	0.93 (0.89-0.96)	0.87 (0.80-0.94)	0.98 (0.96-1.00)	0.76 (0.68-0.85)	0.74 (0.64-0.83)	0.93 (0.84-1.00)
Cer(d18:1/24:1) / LPC 14:0_sn2	CA125 / PC 37:2	0.93 (0.89-0.96)	0.87 (0.81-0.94)	0.98 (0.95-1.00)	0.76 (0.68-0.85)	0.73 (0.64-0.83)	0.95 (0.89-1.00)
Cer(d20:1/24:1) / LPC 14:0_sn2	CA125 / PC 37:2	0.92 (0.87-0.96)	0.85 (0.77-0.93)	0.98 (0.95-1.00)	0.77 (0.68-0.85)	0.74 (0.64-0.83)	0.95 (0.90-1.00)
Cer(d18:1/24:1) / LPC 14:0_sn2	CA125 / PI 38:2	0.92 (0.89-0.96)	0.87 (0.81-0.94)	0.97 (0.94-1.00)	0.77 (0.69-0.85)	0.75 (0.66-0.84)	0.95 (0.88-1.00)
CA125	TAG(18:1/18:1/22:6) / LPC 14:0_sn2	0.91 (0.86-0.96)	0.83 (0.73-0.92)	0.98 (0.96-1.00)	0.78 (0.70-0.86)	0.75 (0.66-0.84)	0.89 (0.77-1.00)
CA125		0.90 (0.84-0.95)	0.81 (0.71-0.90)	0.97 (0.94-1.00)	0.72 (0.62-0.81)	0.67 (0.57-0.78)	0.95 (0.91-1.00)
CA125 (35 U/mL cutoff)		0.80 (0.73-0.86)	0.69 (0.59-0.80)	0.89 (0.84-0.94)	0.71 (0.64-0.79)	0.68 (0.60-0.76)	0.91 (0.87-0.95)

Glc/GalCer: glucosyl/galactosylceramide; Cer: ceramide; LPC: lysophosphatidylcholine; PC: phosphatidylcholine; PI: phosphatidylinositol; TAG: triacylglycerol.

5.4.2 Lipidomic analysis in borderline ovarian tumors

There were only eight lipids with significant changes in either Charité or Finnish cohorts, which showed an alteration in the same direction in both: the phosphatidylcholines, the phosphatidyletholamines and sphinganine-1-phosphate. Overall, the lipid changes in borderline tumors were minor compared with those in overtly malignant tumors.

6 DISCUSSION

Further investigations are still necessary in preoperative OC diagnostics so that early diagnosis can improve and lead to better treatment results and survival rates for the patients. Serum biomarkers tend to increase as late as in the advanced stages, and the possibility of using imaging modalities is restricted in symptomless early-stage tumors.

6.1 Three-dimensional sonography does not seem to offer significantly more benefit than two-dimensional sonographic scoring methods (Study I)

Several 2D US-based prediction models and algorithms have been developed since the RMI was published in 1990 (Jacobs et al. 1990) in order to improve diagnostics of ovarian tumors. The IOTA study is the largest diagnostic study which has first standardized morphological and Doppler US features, and secondly collected a large database to test and compare former developed models and the subjective assessment of an experienced US examiner to novel IOTA US models and logarithms, which include simple rules, LR1 and 2 and ADNEX model. These IOTA models have been externally validated in various study groups after development and internal validation tests to discover the most optimal model for clinicians to triage suspected ovarian malignancies for appropriate surgery and on the other hand find out the tumors which may be treated conservatively or with minimal invasive surgery (Kaijser 2015).

According to the literature, the benefit of 3D US for the evaluation of ovarian tumors is conflicting. The assessment of 3D-PD vascularity has shown some value in estimating adnexal masses (Alcazar & Jurado 2011). Our purpose was to collect many validated 2D US prediction models and examine if 3D-PD vascular indices have advantages alone or together with 2D US models in ovarian tumor discrimination.

In our series of 100 ovarian tumors, we found that expert opinion possessed the best accuracy (90.8%) and specificity (92.4%) in diagnosing ovarian malignancy. However, the sensitivities of the IOTA simple rules, LR2 and evaluation of tumor vascularity by 2D vascular scores were slightly better than that of expert opinion, although they could not achieve the accuracy and specificity of that method. The diagnostic performance of the RMI and serum CA125, with accuracies below 80%, was poorer than that of the IOTA models.

Of the 3D-PD vascular indices, the VI and VFI were as accurate as and even more specific than LR2 and 2D US evaluation of vascularity, but they were distinctly less sensitive. The specificity of the test improved when the VFI was combined with the RMI, simple rules and LR2, with a coincidental decrease of sensitivity.

Another US expert re-evaluated the stored data by giving his opinion of each tumor and re-measured the 3D-PD vascular indices. The interobserver agreement on the nature of the tumors (expert opinion) and on the 3D-PD measurements was very good/good.

Our results indicating the superiority of subjective assessment by an expert are in concordance with a large-scale meta-analysis that proved expert opinion to be the best predictive US method in discriminating ovarian tumors preoperatively with a pooled sensitivity of 94% and specificity of 85% for postmenopausal women. LR2 proved to be as good a diagnostic as expert opinion for postmenopausal women in this meta-analysis (Meys et al. 2016). When preoperative US examinations were performed by examiners with broad and varied experience, the RMI and simple rules were more reliable than subjective assessment (Sayasneh et al. 2013). The general recommendation is to use the RMI, simple rules and LR2 as a first-stage test and refer the unclear or inconclusive tumors for a second-opinion US examination by an expert (a two-step strategy). Another two-step strategy (simple rules and expert opinion) in a group of 1,049 postmenopausal women led to a sensitivity of 93% and specificity of 83% (Testa et al. 2014), which is comparable to our respective results of 91% and 85%.

The 3D-PD vascular indices have been found to be elevated in ovarian malignancies (Alcazar et al. 2005), which our study also showed. Our results resembled those of a previous study which showed that 3D-PD vascular indices did not improve the results of 2D evaluation of vascularity (Silvestre et al. 2015). However, that study did not consider the menopausal status of patients.

Future studies should concentrate on combining different multimodal risk-scoring models to test them as screening tests for ovarian malignancies in symptomatic and asymptomatic women in large populations. Future IOTA studies will include the validation tests for the ADNEX model and the use of MRI and 3D-PD as a secondary test for inconclusive tumors. There is currently an ongoing large-scale IOTA-based follow-up cohort study of conservatively treated ovarian cysts. The objective of the study is to add information to be used in decision-making regarding surgical intervention and on the risks of conservative treatment (Kaijser 2015). Large-scale multicenter studies are needed to discover the most effective, reliable and safe method of making decisions regarding patient treatment and, in the future, hopefully also screening.

6.2 Urinary DiAcSpm as a possible biomarker in ovarian cancer (Study II)

Studies have found elevated levels of polyamines during highly proliferative processes such as those occurring in connection with cancer (Bae et al. 2018). They exist mainly in acetylated forms in urine (Hiramatsu et al. 1995), and especially diacetylated forms increase most in cancer, although their amounts in urine are very small (Kawakita et al. 2011; Sugimoto et al. 1995). However, the mechanism for elevated urinary polyamines such as DiAcSpm is unclear. It is assumed that the body can increase secretion of DiAcSpm as a response to the higher intracellular concentrations of DiAcSpm caused by tumor proliferation (Kawakita & Hiramatsu 2006; Umemori et al. 2010).

In our study, we used a previously described method, LC-MS/MS, for polyamine analysis (Häkkinen et al. 2013). We managed to measure all polyamines simultaneously, as opposed to previous studies, which have suffered from incomplete polyamine arrays and poor reproducibility. DiAcSpm from the urine of ovarian cancer patients was elevated compared with the levels found in women with benign ovarian tumors. Although the concentration of DiAcSpm intensifies as the cancer advances, even early-stage and low-malignant potential ovarian tumors showed higher concentrations than did benign tumors and controls. These novel OC results are concordant with previous results from other cancers (Enjoji et al. 2004; Hiramatsu et al. 2005; Yamaguchi et al. 2005). Our study showed that urinary

DiAcSpm was even more sensitive than serum CA125 in distinguishing between benign and malignant ovarian tumors.

In some cancers, DiAcSpm has proved to be not only a diagnostic biomarker, but also a prognostic biomarker for evaluating the efficacy of cancer treatment and the possibility of recurrence (Casero et al. 2018; Kato et al. 2014). Commercial kits for determining urinary DiAcSpm levels are available, which increases the potential of DiAcSpm as a non-invasive biomarker also in the early diagnosis of cancer (Kawakita et al. 2011). However, DiAcSpm is not a tumor-specific marker, as it may be elevated also in some benign proliferative processes (Kawakita & Hiramatsu 2006).

Polyamines seem to amplify the progression of cancer by increasing the metastatic capability of cancer cells and inhibiting the immune response against tumors (Soda 2011). Thus, one potential target of future anti-cancer treatment could be to diminish the polyamine uptake by cells, as an inhibition of polyamine synthesis by DFMO has had some preliminary efficacy in clinical trials (Alexiou et al. 2017; Murray-Stewart et al. 2016).

6.3 Detection of volatile organic compounds from urine of ovarian cancer patients is possible with the aid of FAIMS (Study III)

In canine studies, it has been discovered that cancers may have distinct odors that can be detected by dogs. The source of odors characteristic to cancer is released into the surrounding air in the form of VOCs (Lippi & Cervellin 2012). Tissue and blood samples from OC patients were also detected by trained dogs with a good sensitivity and specificity (G. Horvath et al. 2008; G. Horvath et al. 2010; G. Horvath et al. 2013). These studies demonstrate that also OC may have its own distinct smell. Nevertheless, training of canines is time-consuming and the validation of studies also rather difficult. Therefore, more effortless and validated methods for the artificial recognition of VOCs have been developed for clinical use.

Further studies generated technical counterparts such as the eNose to mimic the olfactory system and detect VOCs. Several studies have been published on various eNose applications aimed at detecting different cancers from exhaled breath, urine and blood (Bernabei et al. 2008; Turner & Magan 2004; Xue et al. 2008). Also OC

was identified from tissue and breath samples using the eNose (G. Horvath et al. 2010) and nanoarray analysis (Amal et al. 2015).

FAIMS is a special variant of ion mobility spectrometry based on measurements of the different movements of ionized molecules in samples in very high electric fields. It provides a qualitative spectrum derived from the complex chemical structures found in biological samples. Compared to the traditional eNose apparatus, FAIMS is more reproducible and sensitive. Also, FAIMS technology is better suited for portable equipment, which is beneficial for practical use (Arasaradnam et al. 2014; Arasaradnam et al. 2018).

Our third study demonstrated the potential of FAIMS in distinguishing urine from women with OC from controls and women with benign ovarian tumors. The sensitivity was good (91.2% and 91.5% respectively) but the specificity was weaker – improving, however, when only high-grade tumors were being distinguished from controls and benign tumors. FAIMS also seemed to differentiate urine from patients with low- and high-grade ovarian tumors. Our study reproduced the feasibility of using FAIMS for cancer detection in urine that was shown in previous positive results from patients with colorectal and pancreatic cancers (Arasaradnam et al. 2014; Arasaradnam et al. 2018).

Future research should explore the potential of FAIMS in using urine samples to monitor the effect of therapy and recognize any recurrences of cancer after treatment. As a sensitive and non-invasive method, the FAIMS analysis of urine could even have potential as a screening method. First, however, a large collection of data from urine samples of OC patients should be analyzed to form a database.

6.4 Lipidomic changes in blood occur even in early stages of ovarian cancer (Study IV)

Many cancers cause the same metabolic changes in order to provide more energy for the abnormally rapid growth and proliferation of cancer cells (Currie et al. 2013). Metabolic profiling of blood and tissue samples from OC patients has been performed to identify the main metabolic pathways in OC: these investigations have shown alterations also in lipid metabolism (Buas et al. 2016; Denkert et al. 2006; Fong et al. 2011; Ke et al. 2015). A study by Braicu et al. (2017) showed specific lipid

changes in blood from HGSOC patients. Study IV was conducted to validate those results at an early-stage and in non-HGSOC, or in endometrioid and mucinous OC.

Our results are in line with earlier studies showing that levels of most of the analyzed lipids were decreased in OC (Bachmayr-Heyda et al. 2017; Buas et al. 2016). Only some Cers and TAGs showed higher levels in the blood samples from OC patients. Study IV confirms that levels of Cer(d18:1/18:0), Cer(d18:0/18:0) and TAG(18:1/18:1/20:4) are higher even in the early stages (Stages I-II) of OC, but their concentrations intensify further in the advanced stages (Stages III-IV). Levels of Cer(d18:1/18:0) and TAG(18:1/18:1/20:4) were elevated not only in serous but also in mucinous and endometrioid OCs.

Earlier results from other studies of lipids in OC vary, but phospho- and sphingolipids have been studied most. Phospholipids form the cellular membrane and take part in cellular signaling (Pyragius et al. 2013). Sphingolipids, especially Cers, induce apoptosis and may thus affect cancer development (Hajj et al. 2015). In pathway analysis, glycerophospholipid metabolism proved to be the main dysregulated pathway in OC, but also glycerolipid (including TAGs) and sphingolipid metabolism was altered (Y. Zhang et al. 2016). There is evidence that levels of some glycerophospholipids are elevated in localized cancer but decreased in advanced cancer (Jones et al. 2015). This could be explained by the excess consumption of lipids by rapidly growing tumors or the decrease of HDL in the blood of OC patients (Sun et al. 2016), while glycerophospholipids occur abundantly precisely in HDL particles (Hilvo et al. 2018). However, this phenomenon does not elucidate why there is an increase of some lipid species in OC and indicates that there must be some indeterminate mechanisms.

We are not aware of other such extensive lipid analyses from OC patients. As a validation study, this study shows that lipid alterations exist at all stages of OC, and also in endometrioid and mucinous carcinomas other than HGSOC both in pre- and postmenopausal subjects. Lipid combinations combined with CA125 improved especially the detection of Stage I or II OCs, and could provide possible diagnostic and prognostic biomarkers for OC in the future.

6.5 Strengths and weaknesses

The population in Study I consisted of one hundred women with adnexal tumors which were evaluated preoperatively by various US methods. The study group was small when one takes into account the fact that many validation studies of US methods include hundreds or thousands of patients with ovarian tumors. In addition, some of the US methods were originally not intended for use as preoperative differential diagnostics tools for expert US examiners but, rather, for the triage of adnexal tumors by non-expert examiners. However, in Study I, all of the patients were examined by the same US examiner. To our knowledge, there are no previous publications that include so many different US methods used on the same patients. In addition, another expert evaluated the same data blindly afterwards, and the agreement on results by these two examiners was good. However, one US examiner made a subjective evaluation of the tumor from real-time US and the other from saved static US images. It has been shown that real-time diagnosis is more accurate than a diagnosis based on static images (Van Holsbeke et al. 2008). We estimated tumor vascularity by calculating 3D-PD vascularity indices from the entire tumor. Other possible methods could have been to assess vascularity only from solid vascularized areas (Alcazar et al. 2005) or to use automatic spherical sampling from the most vascularized areas (Jokubkiene et al. 2007). Our method may have influenced the results in the case of large cystic tumors which are not entirely vascularized. However, it has been shown that the size of the calculated spherical area does not affect the 3D-PD indices (Kudla & Alcazar 2010).

In Study II, we were the first to publish a standardized analysis of 12 polyamines in a single run with urine samples of women with ovarian tumors. The results should be regarded as interesting even though they are preliminary, but also the availability of this non-invasive method should increase interest in future validation studies in larger study populations.

The strength of Study III lies in its proof-of-concept nature, which makes the results more interesting and may even offset the quite-small size of its study population. Another advantage of Study III is its non-invasive nature and good sensitivity, which is as yet the first known study to use FAIMS technology in the differential diagnostics of ovarian tumors. We have only found two earlier published studies that utilized FAIMS technology in cancer detection (Arasaradnam et al. 2014; Arasaradnam et al. 2018). The disadvantage of Study III is the long storage time of

the urine samples before analysis: this may have had an influence on VOC emissions and thus on the final results, according to a British study (Esfahani et al. 2016). The black box-approach of FAIMS analysis makes the interpretation of the result challenging for the clinician. In order to validate the method for clinical use, considerable emphasis should be given on evaluation of the repeatability of the method. This underlines the need of a rigorous study on the analytical performance of the technology that could be conducted with a reference sample that is created by spiking pooled urine with known concentrations of target molecules or creating a completely artificial sample that could be used as reference for the method.

It would have been ideal to use the same study population in Studies I, II and III (and partly in Study IV as well). However, Study I included only tumors with a maximum diameter of 10 cm because the entire tumor had to fit into the transvaginal scan. Studies II-IV had no limitations as to the size of the tumor, and they also included women with advanced OC with ascites.

Studies I-III featured relatively many non-epithelial OCs and low malignant potential ovarian tumors as well, making the study group heterogenous, and this may have influenced the results. However, in Studies II and III, the differences in results were seen between women with low malignant potential and benign ovarian tumors and not only in women with advanced OC.

Studies I-III included women who were at least 50 years old, but their menopausal status was not confirmed by laboratory measurements. However, women whose last menstrual periods had occurred more than six months previously were classified as postmenopausal. Study IV included also women of fertile age. Consequently, the different preoperative evaluation methods or potential biomarkers used in our studies cannot be directly compared with each other. As mentioned above, the best option in comparing the accuracy of the methods would have been to have the same large study group in Studies I-III. As it is, only a few women were in all of these three studies.

In Study IV, we were able to validate previously published lipid changes in the serum of patients with HGSOC (Braicu et al. 2017) in a larger and more heterogenous study population, which showed that the lipidomic alterations in OC are seen also beyond HGSOC. Study data sets consisted not only of serum samples, but also plasma ones, but the lipid changes we discovered did not differ in the plasma dataset compared with the serum cohorts. Neither serum lipoprotein levels nor body mass index scores in the study population were available, and they may have had

some effect on lipid results in blood. Also, the blood samples were not collected from patients in a fasting condition, but we assumed that the differences in lipid alterations between patients with OC and with a benign tumor would have been even greater in fasting samples. However, we had study cohorts from Finland and Germany, and the lipid alterations were apparent in all cohorts, which means that the results may be generalizable.

6.6 Future prospects

Future areas of investigation could include a combination of urinary DiAcSpm analysis and FAIMS technology to discover whether elevated DiAcSpm levels correlate with the FAIMS results. On the other hand, it would be relevant to compare urine polyamines, especially DiAcSpm, with serum lipidomic analysis to see whether the main lipidomic changes in serum correlate with the increase in DiAcSpm levels in urine, and whether these two together, combined with serum CA125, would improve the diagnostic value of CA125.

Currently, US findings with serum CA125 are the main diagnostic tools used to estimate ovarian tumor malignancy. In future, it should be studied whether urinary DiAcSpm alone or serum lipidomic changes alone or whether they together combined with US findings would be more sensitive and specific than CA125.

To organize these studies, a large population of women with ovarian tumors should be recruited and systematically examined by US, with serum and urine samples collected from them as well.

7 SUMMARY AND CONCLUSIONS

The goal of this study was to evaluate the performance of traditional US methods in the preoperative diagnostics of adnexal masses, and to search for novel biochemical and biophysical methods to be used in addition to or instead of traditional US. To accomplish this, we evaluated the benefit of 3D-PD examination added to conventional 2D US, serum CA125 and various 2D US scoring methods in the preoperative discrimination between benign and malignant ovarian masses (Study I). In addition, preoperative urine samples from controls and from women with benign and malignant ovarian tumors were analyzed using LC-MS/MS to detect polyamines and compare their concentrations across study groups (Study II). A novel method using FAIMS technology was assessed to detect ovarian malignancies from preoperatively collected urine samples (Study III). Finally, the lipidomic alterations in early- and advanced-stage OC and in various histological subtypes were examined from preoperative blood samples (Study IV).

The main findings and conclusions of this Thesis are as follows:

1. Clinical expert opinion based on 2D US examination discriminates best between malignant and benign ovarian tumors, with an accuracy of 90.8%, a sensitivity of 87.5% and a specificity of 92.4%. The diagnostic value of 3D-PD vascular indices is not significantly better than the RMI. Adding 3D-PD indices to the RMI and other 2D US scoring methods does not provide any noticeable improvement.
2. Six mono- and diacetylated polyamines were found in all urine samples, but only urinary concentrations of DiAcSpm showed significant elevation (p <0.001) in women with malignant ovarian tumors compared with benign ovarian tumors and controls.
3. VOC analysis of urine with FAIMS technology is able to discriminate women with ovarian malignancy from controls and women with benign ovarian tumors with accuracies of 81.3% and 77.3%, respectively.
4. There were parallel alterations in 39 lipids which exist both at early- and late-stage OC. Mostly, these lipid changes are significant as early as in Stages I and

II, but intensify as the cancer advances. Twenty-three of those lipids were altered, not only in serous but also in mucinous and endometrioid OC. The addition of lipids or lipid ratios to serum CA125 increased the AUC values, especially in the case of early-stage OCs.

8 ACKNOWLEDGEMENTS

This study was carried out at the Department of Obstetrics and Gynecology of Tampere University Hospital, the Faculty of Medicine and Life Sciences of the University of Tampere, School of Pharmacy and Biocenter Kuopio of the University of Eastern Finland, and Zora Biosciences Oy in Espoo, Finland.

First of all, I would like to express my deepest gratitude to my supervisor Professor Johanna Mäenpää for her constant encouragement, patience and trust in me. Her extensive experience in scientific research has been priceless for me over these years. I admire her dedication both to research and to treating patients with her incredibly profound knowledge of medicine. She has always found supportive words in my desperate moments and rejoiced with me in the moments of success.

I had a possibility to work with many brilliant professionals in this project. I owe my warm gratitude to Professor Niku Oksala whose role was essential in Studies II and III. His enthusiastic ideas and quick responses to my questions have impressed me. Thank you for introducing me totally new "world" with eNoses and polyamines! The initiator of that co-operation is MD, PhD Antti Roine who has been a very important person and co-author in Studies II and III. I am deeply grateful for all the help and advice during these years. His easygoing and helpful attitude has been invaluable for me and I truly appreciate it.

I want to thank Docent Mika Hilvo for the research idea of Study IV. His profound knowledge on the lipid research was not only essential for me but moreover, his help, advice and messages were always given in such a friendly way which made our collaboration very easy and simple.

All co-authors have been necessary and I am grateful for the contribution of them all. My warm thanks go to my good colleague and friend MD, PhD Sami Saarelainen whose help is always altruistic and kind, with a shared Eastern Finnish sense of humor. I would not have managed without his concrete teaching of 3D ultrasound field and advice with the computer software. Special thanks to: MSc Tiina Luukkaala for her important advice in the statistical analysis in Study I; PhD Merja Häkkinen for the analysis of polyamines; PhD Tuomo Keinänen for guiding me in the field of

polyamines; Professor Jouko Vepsäläinen and Professor Terho Lehtimäki for their contribution in the polyamine study; MSc Pekka Kumpulainen for conducting the statistical analysis in Studies II and III; Medical student Emmi Eräviita for conducting the FAIMS analysis; PhD Kaisa Koistinen for conducting the lipid analysis, and MD, PhD Elena Braicu, MD, PhD Hagen Kulbe, Professor Jalid Sehouli and Professor Ulla Puistola for on one hand providing blood samples and on the other hand participating in writing.

I am very grateful for the official reviewers of this thesis, Docent Maarit Anttila and Professor Kari Punnonen, for their professional evaluation and valuable comments to improve the final result.

I warmly thank Docent Eija Tomás and Docent Kari Nieminen, the members of the follow-up group of my thesis. They have always supported and believed in me, being also significant persons in my whole gynecological career.

The patients who took part in my studies deserve my special gratitude for making this work possible.

Special thanks to my chief and friend Kirsi Kuismanen for understanding and encouraging me. And thanks to all colleagues and coworkers at the Department of Obstetrics and Gynecology in Tampere University Hospital for the humorous and supportive team spirit! I am grateful for easy co-operation to Kati Tihtonen and for cheery company to Synnöve Staff and Piritta Hynninen as also to other "Gynen Ellit". Thanks to Minna Mäenpää for many practical tips when finalizing this doctoral thesis.

I want to thank all my friends from childhood to present time. You have filled my life with joy and happiness. Hopefully you all know that I appreciate our friendship! Especially I am grateful to Pia, my "unbiological sister" and trusty beloved friend. Sharing our lives since medical school has brought me so much pleasure, power and laughter! Thanks for my mental well-being also to my charming friends Leila Alivuotila, Tuija Hämäläinen and sister-in-law Tuija Tarkiainen who have reminded me of life outside the medical world.

My heartfelt gratitude goes to my family which is the most important for me. My mom and dad, Riitta and Heikki, have always encouraged me to study and reach my dreams not forgetting to enjoy life. Your love and concern have been a solid foundation to my life. Thank you for helping us in many ways and being wonderful grandparents!

Finally, my lovely children Helmi, Saimi and Vilho, you are my greatest achievements and number ones. I am very proud of you three! My dear husband Esa, without equal parenting and your caring love I would not have succeeded. You all have taught me so much about love and happiness. Therefore I feel privileged and lucky.

This work has been financially supported by research grants from the competitive research funding of Pirkanmaa Hospital District, Finnish Cancer Foundation, the research funding of Division Four, Tampere University Hospital, and Research Foundation of Obstetrics and Gynecology.

Tampere, January 2019

9 REFERENCES

Abdel-Monem MM, Merdink JL & Theologides A. (1982) Urinary excretion of monoacetyl polyamines in patients with non-Hodgkin's lymphoma. Cancer Research 42(5): 2097.

Abramowicz JS & Timmerman D. (2017) Ovarian mass-differentiating benign from malignant: The value of the international ovarian tumor analysis ultrasound rules. Am J Obstet Gynecol 217(6): 652-660.

Alcazar JL, Galan MJ, Garcia-Manero M, et al. (2003) Three-dimensional sonographic morphologic assessment in complex adnexal masses: Preliminary experience. J Ultrasound Med 22(3): 249-254.

Alcazar JL & Castillo G. (2005) Comparison of 2-dimensional and 3-dimensional power-Doppler imaging in complex adnexal masses for the prediction of ovarian cancer. Am J Obstet Gynecol 192(3): 807-812.

Alcazar JL, Merce LT & Garcia Manero M. (2005) Three-dimensional power Doppler vascular sampling: A new method for predicting ovarian cancer in vascularized complex adnexal masses. J Ultrasound Med 24(5): 689-696.

Alcazar JL. (2006) Tumor angiogenesis assessed by three-dimensional power Doppler ultrasound in early, advanced and metastatic ovarian cancer: A preliminary study. Ultrasound Obstet Gynecol 28(3): 325-329.

Alcazar JL, Garcia-Manero M & Galvan R. (2007) Three-dimensional sonographic morphologic assessment of adnexal masses: A reproducibility study. J Ultrasound Med 26(8): 1007-1011.

Alcazar JL, Rodriguez D, Royo P, et al. (2008) Intraobserver and interobserver reproducibility of 3-dimensional power Doppler vascular indices in assessment of solid and cystic-solid adnexal masses. J Ultrasound Med 27(1): 1-6.

Alcazar JL & Prka M. (2009) Evaluation of two different methods for vascular sampling by three-dimensional power Doppler angiography in solid and cystic-solid adnexal masses. Ultrasound Obstet Gynecol 33(3): 349-354.

Alcazar JL & Jurado M. (2011) Three-dimensional ultrasound for assessing women with gynecological cancer: A systematic review. Gynecol Oncol 120(3): 340-346.

Alcazar JL, Iturra A, Sedda F, et al. (2012) Three-dimensional volume off-line analysis as compared to real-time ultrasound for assessing adnexal masses. Eur J Obstet Gynecol Reprod Biol 161(1): 92-95.

Alcazar JL, Pascual MA, Marquez R, et al. (2017) Malignancy risk of sonographically benign appearing purely solid adnexal masses in asymptomatic postmenopausal women. Menopause 24(6): 613-616.

Alexiou GA, Lianos GD, Ragos V, et al. (2017) Difluoromethylornithine in cancer: New advances. Future Oncol 13(9): 809-819.

Al-Hussaini M, Al-Othman Y, Hijazi E, et al. (2017) A report of ovarian Sertoli-Leydig cell tumors with heterologous intestinal-type glands and alpha fetoprotein elevation and review of the literature. Int J Gynecol Pathol 37(3): 275-283.

Amal H, Shi DY, Ionescu R, et al. (2015) Assessment of ovarian cancer conditions from exhaled breath. Int J Cancer 136(6): 614.

Arasaradnam RP, Quraishi N, Kyrou I, et al. (2011) Insights into 'fermentonomics': Evaluation of volatile organic compounds (VOCs) in human disease using an electronic 'e-nose'. J Med Eng Technol 35(2): 87-91.

Arasaradnam RP, McFarlane MJ, Ryan-Fisher C, et al. (2014) Detection of colorectal cancer (CRC) by urinary volatile organic compound analysis. PLoS One 9(9): e108750.

Arasaradnam RP, Wicaksono A, O'Brien H, et al. (2018) Noninvasive diagnosis of pancreatic cancer through detection of volatile organic compounds in urine. Gastroenterology 154(3): 485-487.

Babic A, Cramer DW, Kelemen LE, et al. (2017) Predictors of pretreatment CA125 at ovarian cancer diagnosis: A pooled analysis in the ovarian cancer association consortium. Cancer Causes Control 28(5): 459-468.

Bachmayr-Heyda A, Aust S, Auer K, et al. (2017) Integrative systemic and local metabolomics with impact on survival in high-grade serous ovarian cancer. Clin Cancer Res 23(8): 2081-2092.

Bae DH, Lane DJR, Jansson PJ, et al. (2018) The old and new biochemistry of polyamines. Biochim Biophys Acta Gen Subj 1862(9): 2053-2068.

Bast RC,Jr, Badgwell D, Lu Z, et al. (2005) New tumor markers: CA125 and beyond. Int J Gynecol Cancer 15(Suppl. 3): 274-281.

Bast RC,Jr & Spriggs DR. (2011) More than a biomarker: CA125 may contribute to ovarian cancer pathogenesis. Gynecol Oncol 121(3): 429-430.

Beloribi-Djefaflia S, Vasseur S & Guillaumond F. (2016) Lipid metabolic reprogramming in cancer cells. Oncogenesis 5: e189.

Bernabei M, Pennazza G, Santonico M, et al. (2008) A preliminary study on the possibility to diagnose urinary tract cancers by an electronic nose. Sensors & Actuators: B. Chemical 131(1): 1-4.

Bharwani N, Reznek RH & Rockall AG. (2011) Ovarian cancer management: The role of imaging and diagnostic challenges. Eur J Radiol 78(1): 41-51.

Bolstad N, Oijordsbakken M, Nustad K, et al. (2012) Human epididymis protein 4 reference limits and natural variation in a Nordic reference population. Tumour Biol 33(1): 141-148.

Bon GG, Kenemans P, Verstraeten R, et al. (1996) Serum tumor marker immunoassays in gynecologic oncology: Establishment of reference values. Am J Obstet Gynecol 174(1 Pt 1): 107-114.

Bonilla-Musoles F, Raga F & Osborne NG. (1995) Three-dimensional ultrasound evaluation of ovarian masses. Gynecol Oncol 59(1): 129-135.

Braicu EI, Darb-Esfahani S, Schmitt WD, et al. (2017) High-grade ovarian serous carcinoma patients exhibit profound alterations in lipid metabolism. Oncotarget 8(61): 102912-102922.

Bristow RE, Tomacruz RS, Armstrong DK, et al. (2002) Survival effect of maximal cytoreductive surgery for advanced ovarian carcinoma during the platinum era: A meta-analysis. J Clin Oncol 20(5): 1248-1259.

Brown J & Frumovitz M. (2014) Mucinous tumors of the ovary: Current thoughts on diagnosis and management. Curr Oncol Rep 16(6): 389.

Brown J, Friedlander M, Backes FJ, et al. (2014) Gynecologic cancer intergroup (GCIG) consensus review for ovarian germ cell tumors. Int J Gynecol Cancer 24(9 Suppl. 3): 48.

Buas MF, Gu H, Djukovic D, et al. (2016) Identification of novel candidate plasma metabolite biomarkers for distinguishing serous ovarian carcinoma and benign serous ovarian tumors. Gynecol Oncol 140(1): 138-144.

Byun JA, Lee SH, Jung BH, et al. (2008) Analysis of polyamines as carbamoyl derivatives in urine and serum by liquid chromatography-tandem mass spectrometry. Biomed Chromatogr 22(1): 73-80.

Byun JA, Choi MH, Moon MH, et al. (2009) Serum polyamines in pre- and post-operative patients with breast cancer corrected by menopausal status. Cancer Lett 273(2): 300-304.

Cai Q, Zhao Z, Antalis C, et al. (2012) Elevated and secreted phospholipase A(2) activities as new potential therapeutic targets in human epithelial ovarian cancer. FASEB J 26(8): 3306-3320.

Campos C, Sarian LO, Jales RM, et al. (2016) Performance of the risk of malignancy index for discriminating malignant tumors in women with adnexal masses. J Ultrasound Med 35(1): 143-152.

Casero RA,Jr, Murray Stewart T & Pegg AE. (2018) Polyamine metabolism and cancer: Treatments, challenges and opportunities. Nat Rev Cancer 18(11): 681-695.

Cha JY & Lee HJ. (2016) Targeting lipid metabolic reprogramming as anticancer therapeutics. J Cancer Prev 21(4): 209-215.

Chan L, Lin WM, Uerpairojkit B, et al. (1997) Evaluation of adnexal masses using three-dimensional ultrasonographic technology: Preliminary report. J Ultrasound Med 16(5): 349-354.

Chang SJ, Bristow RE, Chi DS, et al. (2015) Role of aggressive surgical cytoreduction in advanced ovarian cancer. J Gynecol Oncol 26(4): 336-342.

Chen S, Wang Y & Choi S. (2013) Applications and technology of electronic nose for clinical diagnosis. Open Journal of Applied Biosensor 2: 39-50.

Chen VW, Ruiz B, Killeen JL, et al. (2003) Pathology and classification of ovarian tumors. Cancer 97(Suppl. 10): 2631-2642.

Chen X, Zhang J, Cheng W, et al. (2013) CA-125 level as a prognostic indicator in type I and type II epithelial ovarian cancer. Int J Gynecol Cancer 23(5): 815-822.

Chiva LM, Castellanos T, Alonso S, et al. (2016) Minimal macroscopic residual disease (0.1-1 cm). Is it still a surgical goal in advanced ovarian cancer? Int J Gynecol Cancer 26(5): 906-911.

Coleman RL, Herzog TJ, Chan DW, et al. (2016) Validation of a second-generation multivariate index assay for malignancy risk of adnexal masses. Am J Obstet Gynecol 215(1): e11.

Colombo N, Peiretti M, Garbi A, et al. (2012) Non-epithelial ovarian cancer: ESMO clinical practice guidelines for diagnosis, treatment and follow-up. Ann Oncol 23(Suppl. 7): 6.

Covington JA, van der Schee MP, Edge AS, et al. (2015) The application of FAIMS gas analysis in medical diagnostics. Analyst 140(20): 6775-6781.

Currie E, Schulze A, Zechner R, et al. (2013) Cellular fatty acid metabolism and cancer. Cell Metab 18(2): 153-161.

Dai SY, Hata K, Inubashiri E, et al. (2008) Does three-dimensional power Doppler ultrasound improve the diagnostic accuracy for the prediction of adnexal malignancy? J Obstet Gynaecol Res 34(3): 364-370.

D'Amico A, Di Natale C, Falconi C, et al. (2012) Detection and identification of cancers by the electronic nose. Expert Opinion on Medical Diagnostics 6(3): 175-185.

de Boer RA, Cao Q, Postmus D, et al. (2013) The WAP four-disulfide core domain protein HE4: A novel biomarker for heart failure. JACC Heart Fail 1(2): 164-169.

de Meij TG, Larbi IB, van der Schee MP, et al. (2014) Electronic nose can discriminate colorectal carcinoma and advanced adenomas by fecal volatile biomarker analysis: Proof of principle study. Int J Cancer 134(5): 1132-1138.

Denkert C, Budczies J, Kind T, et al. (2006) Mass spectrometry-based metabolic profiling reveals different metabolite patterns in invasive ovarian carcinomas and ovarian borderline tumors. Cancer Res 66(22): 10795-10804.

Di Natale C, Macagnano A, Martinelli E, et al. (2003) Lung cancer identification by the analysis of breath by means of an array of non-selective gas sensors. Biosens Bioelectron 18(10): 1209-1218.

Dodge JE, Covens AL, Lacchetti C, et al. (2012) Preoperative identification of a suspicious adnexal mass: A systematic review and meta-analysis. Gynecol Oncol 126(1): 157-166.

Duffy MJ, Bonfrer JM, Kulpa J, et al. (2005) CA125 in ovarian cancer: European group on tumor markers guidelines for clinical use. Int J Gynecol Cancer 15(5): 679-691.

Durie BG, Salmon SE & Russell DH. (1977) Polyamines as markers of response and disease activity in cancer chemotherapy. Cancer Res 37(1): 214-221.

Enjoji M, Nakamuta M, Arimura E, et al. (2004) Clinical significance of urinary N^{1},N^{12}-diacetylspermine levels in patients with hepatocellular carcinoma. Int J Biol Markers 19(4): 322-327.

Escudero JM, Auge JM, Filella X, et al. (2011) Comparison of serum human epididymis protein 4 with cancer antigen 125 as a tumor marker in patients with malignant and nonmalignant diseases. Clin Chem 57(11): 1534-1544.

Esfahani S, Sagar NM, Kyrou I, et al. (2016) Variation in gas and volatile compound emissions from human urine as it ages, measured by an electronic nose. Biosensors (Basel) 6(1): 4.

Fahy E, Subramaniam S, Brown HA, et al. (2005) A comprehensive classification system for lipids. J Lipid Res 46(5): 839-861.

Fenchel S, Grab D, Nuessle K, et al. (2002) Asymptomatic adnexal masses: Correlation of FDG PET and histopathologic findings. Radiology 223(3): 780-788.

Ferlay J, Soerjomataram I, Dikshit R, et al. (2015) Cancer incidence and mortality worldwide: Sources, methods and major patterns in GLOBOCAN 2012. Int J Cancer 136(5): 359.

Finnish Cancer Registry. (2018) Syöpätilastot. https://syoparekisteri.fi/tilastot/tautitilastot/

Fischerova D, Zikan M, Dundr P, et al. (2012) Diagnosis, treatment, and follow-up of borderline ovarian tumors. Oncologist 17(12): 1515-1533.

Fischerova D & Burgetova A. (2014) Imaging techniques for the evaluation of ovarian cancer. Best Pract Res Clin Obstet Gynaecol 28(5): 697-720.

Fleischer AC, Rodgers WH, Rao BK, et al. (1991) Assessment of ovarian tumor vascularity with transvaginal color Doppler sonography. J Ultrasound Med 10(10): 563-568.

Fleischer AC, Lyshchik A, Jones HW,Jr, et al. (2008) Contrast-enhanced transvaginal sonography of benign versus malignant ovarian masses: Preliminary findings. J Ultrasound Med 27(7): 1011-18.

Fleischer AC, Lyshchik A, Andreotti RF, et al. (2010) Advances in sonographic detection of ovarian cancer: Depiction of tumor neovascularity with microbubbles. AJR Am J Roentgenol 194(2): 343-348.

Folch J, Lees M & Sloane Stanley GH. (1957) A simple method for the isolation and purification of total lipides from animal tissues. J Biol Chem 226(1): 497-509.

Fong MY, McDunn J & Kakar SS. (2011) Identification of metabolites in the normal ovary and their transformation in primary and metastatic ovarian cancer. PLoS One 6(5): e19963.

Forstner R, Thomassin-Naggara I, Cunha TM, et al. (2016) ESUR recommendations for MR imaging of the sonographically indeterminate adnexal mass: An update. Eur Radiol 27(6): 2248-2257.

Foti PV, Attina G, Spadola S, et al. (2016) MR imaging of ovarian masses: Classification and differential diagnosis. Insights Imaging 7(1): 21-41.

Fujii S, Matsusue E, Kanasaki Y, et al. (2008) Detection of peritoneal dissemination in gynecological malignancy: Evaluation by diffusion-weighted MR imaging. Eur Radiol 18(1): 18-23.

Furuya H, Shimizu Y & Kawamori T. (2011) Sphingolipids in cancer. Cancer Metastasis Rev 30(3-4): 567-576.

Färkkilä A, Koskela S, Bryk S, et al. (2015) The clinical utility of serum anti-Mullerian hormone in the follow-up of ovarian adult-type granulosa cell tumors - A comparative study with inhibin B. Int J Cancer 137(7): 1661-1671.

Gaul DA, Mezencev R, Long TQ, et al. (2015) Highly-accurate metabolomic detection of early-stage ovarian cancer. Sci Rep 5: 16351.

Geomini P, Coppus SF, Kluivers KB, et al. (2007) Is three-dimensional ultrasonography of additional value in the assessment of adnexal masses? Gynecol Oncol 106(1): 153-159.

Geomini P, Kruitwagen R, Bremer GL, et al. (2009) The accuracy of risk scores in predicting ovarian malignancy: A systematic review. Obstet Gynecol 113(2 Pt 1): 384-394.

Gerner EW & Meyskens FL,Jr. (2004) Polyamines and cancer: Old molecules, new understanding. Nat Rev Cancer 4(10): 781-792.

Gershenson DM. (2007) Management of ovarian germ cell tumors. J Clin Oncol 25(20): 2938-2943.

Gershenson DM. (2017) Management of borderline ovarian tumours. Best Pract Res Clin Obstet Gynaecol 41: 49-59.

Glanc P, Benacerraf B, Bourne T, et al. (2017) First international consensus report on adnexal masses: Management recommendations. J Ultrasound Med 36(5): 849-863.

Gordon RT, Schatz CB, Myers LJ, et al. (2008) The use of canines in the detection of human cancers. Journal of alternative and complementary medicine (New York, N.Y.) 14(1): 61-67.

Goyal LD, Kaur S & Kawatra K. (2014) Malignant mixed germ cell tumour of ovary - an unusual combination and review of literature. J Ovarian Res 7: 5.

Greenlee RT, Kessel B, Williams CR, et al. (2010) Prevalence, incidence, and natural history of simple ovarian cysts among women >55 years old in a large cancer screening trial. Am J Obstet Gynecol 202(4): 373.e9.

Guerriero S, Alcazar JL, Coccia ME, et al. (2002) Complex pelvic mass as a target of evaluation of vessel distribution by color Doppler sonography for the diagnosis of adnexal malignancies: Results of a multicenter European study. J Ultrasound Med 21(10): 1105-1111.

Guerriero S, Saba L, Ajossa S, et al. (2013) Assessing the reproducibility of the IOTA simple ultrasound rules for classifying adnexal masses as benign or malignant using stored 3D volumes. Eur J Obstet Gynecol Reprod Biol 171(1): 157-160.

Guerriero S, Saba L, Alcazar JL, et al. (2015) Past, present and future ultrasonographic techniques for analyzing ovarian masses. Womens Health (Lond) 11(3): 369-383.

Hacker NF & Rao A. (2017) Surgery for advanced epithelial ovarian cancer. Best Pract Res Clin Obstet Gynaecol 41: 71-87.

Hajj C, Becker-Flegler KA & Haimovitz-Friedman A. (2015) Novel mechanisms of action of classical chemotherapeutic agents on sphingolipid pathways. Biol Chem 396(6-7): 669-679.

Haltia UM, Hallamaa M, Tapper J, et al. (2017) Roles of human epididymis protein 4, carbohydrate antigen 125, inhibin B and anti-Mullerian hormone in the differential diagnosis and follow-up of ovarian granulosa cell tumors. Gynecol Oncol 144(1): 83-89.

Hamaoki M, Hiramatsu K, Suzuki S, et al. (2002) Two enzyme-linked immunosorbent assay (ELISA) systems for N^1,N^8-diacetylspermidine and N^1,N^{12}-diacetylspermine using monoclonal antibodies. J Biochem 132(5): 783-788.

Han X & Gross RW. (2003) Global analyses of cellular lipidomes directly from crude extracts of biological samples by ESI mass spectrometry: A bridge to lipidomics. J Lipid Res 44(6): 1071-1079.

Hata T, Yanagihara T, Hayashi K, et al. (1999) Three-dimensional ultrasonographic evaluation of ovarian tumours: A preliminary study. Hum Reprod 14(3): 858-861.

Hata T, Hata K, Noguchi J, et al. (2011) Ultrasound for evaluation of adnexal malignancy: From 2D to 3D ultrasound. J Obstet Gynaecol Res 37(10): 1255-1268.

Hauptmann S, Friedrich K, Redline R, et al. (2017) Ovarian borderline tumors in the 2014 WHO classification: Evolving concepts and diagnostic criteria. Virchows Arch 470(2): 125-142.

He ZX, Shi HH, Fan QB, et al. (2017) Predictive factors of ovarian carcinoma for women with ovarian endometrioma aged 45 years and older in China. J Ovarian Res 10(1): 2.

Hellstrom I, Raycraft J, Hayden-Ledbetter M, et al. (2003) The HE4 (WFDC2) protein is a biomarker for ovarian carcinoma. Cancer Res 63(13): 3695-3700.

Hilvo M, de Santiago I, Gopalacharyulu P, et al. (2016) Accumulated metabolites of hydroxybutyric acid serve as diagnostic and prognostic biomarkers of ovarian high-grade serous carcinomas. Cancer Res 76(4): 796-804.

Hilvo M, Simolin H, Metso J, et al. (2018) PCSK9 inhibition alters the lipidome of plasma and lipoprotein fractions. Atherosclerosis 269: 159-165.

Hiramatsu K, Sugimoto M, Kamei S, et al. (1995) Determination of amounts of polyamines excreted in urine: Demonstration of N^1,N^8-diacetylspermidine and N^1,N^{12}-diacetylspermine as components commonly occurring in normal human urine. J Biochem 117(1): 107-112.

Hiramatsu K, Miura H, Sugimoto K, et al. (1997) Preparation of antibodies highly specific to N^1,N^8-diacetylspermidine, and development of an enzyme-linked immunosorbent assay (ELISA) system for its sensitive and specific detection. J Biochem 121(6): 1134-1138.

Hiramatsu K, Miura H, Kamei S, et al. (1998) Development of a sensitive and accurate enzyme-linked immunosorbent assay (ELISA) system that can replace HPLC analysis for the determination of N^1,N^{12}-diacetylspermine in human urine. J Biochem 124(1): 231-236.

Hiramatsu K, Takahashi K, Yamaguchi T, et al. (2005) N^1,N^{12}-diacetylspermine as a sensitive and specific novel marker for early- and late-stage colorectal and breast cancers. Clin Cancer Res 11(8): 2986-2990.

Hiramatsu K, Sakaguchi K, Fujie N, et al. (2014) Excretion of N^1, N^{12}-diacetylspermine in the urine of healthy individuals. Ann Clin Biochem 51(Pt 4): 459-467.

Holcomb K, Vucetic Z, Miller MC, et al. (2011) Human epididymis protein 4 offers superior specificity in the differentiation of benign and malignant adnexal masses in premenopausal women. Am J Obstet Gynecol 205(4): 358.e6.

Horvath G, Jarverud GA, Jarverud S, et al. (2008) Human ovarian carcinomas detected by specific odor. Integr Cancer Ther 7(2): 76-80.

Horvath G, Andersson H & Paulsson G. (2010) Characteristic odour in the blood reveals ovarian carcinoma. BMC Cancer 10: 643.

Horvath G, Chilo J & Lindblad T. (2010) Different volatile signals emitted by human ovarian carcinoma and healthy tissue. Future Oncol 6(6): 1043-1049.

Horvath G, Andersson H & Nemes S. (2013) Cancer odor in the blood of ovarian cancer patients: A retrospective study of detection by dogs during treatment, 3 and 6 months afterward. BMC Cancer 13: 396.

Horvath SE & Daum G. (2013) Lipids of mitochondria. Prog Lipid Res 52(4): 590-614.

Hu R, Xiang H, Mu Y, et al. (2014) Combination of 2- and 3-dimensional contrast-enhanced transvaginal sonography for diagnosis of small adnexal masses. J Ultrasound Med 33(11): 1889-1899.

Huhtinen K, Suvitie P, Hiissa J, et al. (2009) Serum HE4 concentration differentiates malignant ovarian tumours from ovarian endometriotic cysts. Br J Cancer 100(8): 1315-1319.

Hussain T, Tan B, Ren W, et al. (2017) Polyamines: Therapeutic perspectives in oxidative stress and inflammatory diseases. Amino Acids 49(9): 1457-1468.

Häkkinen MR, Roine A, Auriola S, et al. (2013) Analysis of free, mono- and diacetylated polyamines from human urine by LC-MS/MS. J Chromatogr B Analyt Technol Biomed Life Sci 941: 81-89.

Igarashi K & Kashiwagi K. (2010) Modulation of cellular function by polyamines. Int J Biochem Cell Biol 42(1): 39-51.

Jacobs I & Bast RC,Jr. (1989) The CA 125 tumour-associated antigen: A review of the literature. Hum Reprod 4(1): 1-12.

Jacobs I, Oram D, Fairbanks J, et al. (1990) A risk of malignancy index incorporating CA 125, ultrasound and menopausal status for the accurate preoperative diagnosis of ovarian cancer. Br J Obstet Gynaecol 97(10): 922-929.

Jacobs I, Menon U, Ryan A, et al. (2016) Ovarian cancer screening and mortality in the UK collaborative trial of ovarian cancer screening (UKCTOCS): A randomised controlled trial. Lancet 387(10022): 945-956.

Jeevanandam M & Petersen SR. (2001) Clinical role of polyamine analysis: Problem and promise. Curr Opin Clin Nutr Metab Care 4(5): 385-390.

Jia MM, Deng J, Cheng XL, et al. (2017) Diagnostic accuracy of urine HE4 in patients with ovarian cancer: A meta-analysis. Oncotarget 8(6): 9660-9671.

Jokubkiene L, Sladkevicius P & Valentin L. (2007) Does three-dimensional power Doppler ultrasound help in discrimination between benign and malignant ovarian masses? Ultrasound Obstet Gynecol 29(2): 215-225.

Jones CM, Monge ME, Kim J, et al. (2015) Metabolomic serum profiling detects early-stage high-grade serous ovarian cancer in a mouse model. J Proteome Res 14(2): 917-927.

Kahn N, Lavie O, Paz M, et al. (2015) Dynamic nanoparticle-based flexible sensors: Diagnosis of ovarian carcinoma from exhaled breath. Nano Lett 15(10): 7023-7028.

Kaijser J, Bourne T, Valentin L, et al. (2013) Improving strategies for diagnosing ovarian cancer: A summary of the International Ovarian Tumor Analysis (IOTA) studies. Ultrasound Obstet Gynecol 41(1): 9-20.

Kaijser J. (2015) Towards an evidence-based approach for diagnosis and management of adnexal masses: Findings of the International Ovarian Tumour Analysis (IOTA) studies. Facts Views Vis Obgyn 7(1): 42-59.

Kang S, Lee A, Park YS, et al. (2011) Alteration in lipid and protein profiles of ovarian cancer: Similarity to breast cancer. Int J Gynecol Cancer 21(9): 1566-1572.

Kano Y, Soda K, Nakamura T, et al. (2007) Increased blood spermine levels decrease the cytotoxic activity of lymphokine-activated killer cells: A novel mechanism of cancer evasion. Cancer Immunol Immunother 56(6): 771-781.

Karlsen MA, Sandhu N, Hogdall C, et al. (2012) Evaluation of HE4, CA125, risk of ovarian malignancy algorithm (ROMA) and risk of malignancy index (RMI) as diagnostic tools of epithelial ovarian cancer in patients with a pelvic mass. Gynecol Oncol 127(2): 379-383.

Karlsen NS, Karlsen MA, Hogdall CK, et al. (2014) HE4 tissue expression and serum HE4 levels in healthy individuals and patients with benign or malignant tumors: A systematic review. Cancer Epidemiol Biomarkers Prev 23(11): 2285-2295.

Kato M, Onishi H, Matsumoto K, et al. (2014) Prognostic significance of urine N^1, N^{12}-diacetylspermine in patients with non-small cell lung cancer. Anticancer Res 34(6): 3053-3059.

Kawakita M & Hiramatsu K. (2006) Diacetylated derivatives of spermine and spermidine as novel promising tumor markers. J Biochem 139(3): 315-322.

Kawakita M, Hiramatsu K, Yanagiya M, et al. (2011) Determination of N^1,N^{12}-diacetylspermine in urine: A novel tumor marker. Methods Mol Biol 720: 367-378.

Ke C, Hou Y, Zhang H, et al. (2015) Large-scale profiling of metabolic dysregulation in ovarian cancer. Int J Cancer 136(3): 516-526.

Khiewvan B, Torigian DA, Emamzadehfard S, et al. (2017) An update on the role of PET/CT and PET/MRI in ovarian cancer. Eur J Nucl Med Mol Imaging 44(6): 1079-1091.

Kim HJ, Lee SY, Shin YR, et al. (2016) The value of diffusion-weighted imaging in the differential diagnosis of ovarian lesions: A meta-analysis. PLoS One 11(2): e0149465.

Kinde I, Bettegowda C, Wang Y, et al. (2013) Evaluation of DNA from the Papanicolaou test to detect ovarian and endometrial cancers. Sci Transl Med 5(167): 167ra4.

Kinkel K, Lu Y, Mehdizade A, et al. (2005) Indeterminate ovarian mass at US: Incremental value of second imaging test for characterization - meta-analysis and Bayesian analysis. Radiology 236(1): 85-94.

Knapp P, Bodnar L, Blachnio-Zabielska A, et al. (2017) Plasma and ovarian tissue sphingolipids profiling in patients with advanced ovarian cancer. Gynecol Oncol 147(1): 139-144.

Kolakowski BM & Mester Z. (2007) Review of applications of high-field asymmetric waveform ion mobility spectrometry (FAIMS) and differential mobility spectrometry (DMS). Analyst 132(9): 842-864.

Koonings PP, Campbell K, Mishell DR,Jr, et al. (1989) Relative frequency of primary ovarian neoplasms: A 10-year review. Obstet Gynecol 74(6): 921-926.

Koshiyama M, Matsumura N & Konishi I. (2017) Subtypes of ovarian cancer and ovarian cancer screening. Diagnostics (Basel) 7(1): E12.

Kudla MJ & Alcazar JL. (2010) Does sphere volume affect the performance of three-dimensional power Doppler virtual vascular sampling for predicting malignancy in vascularized solid or cystic-solid adnexal masses? Ultrasound Obstet Gynecol 35(5): 602-608.

Kurjak A, Kupesic S, Sparac V, et al. (2001) Preoperative evaluation of pelvic tumors by Doppler and three-dimensional sonography. J Ultrasound Med 20(8): 829-840.

Kurman RJ, Carcangiu ML & Herrington CS. (2014) WHO classification of tumours of female reproductive organs. Lyon: International Agency for Research on Cancer.

Kurman RJ & Shih I. (2016) The dualistic model of ovarian carcinogenesis: Revisited, revised, and expanded. Am J Pathol 186(4): 733-747.

Kuwata G, Hiramatsu K, Samejima K, et al. (2013) Increase of N^1, N^{12}-diacetylspermine in tissues from colorectal cancer and its liver metastasis. J Cancer Res Clin Oncol 139(6): 925-932.

Labidi-Galy SI, Papp E, Hallberg D, et al. (2017) High grade serous ovarian carcinomas originate in the fallopian tube. Nat Commun 8(1): 1093.

Lagarde M, Geloen A, Record M, et al. (2003) Lipidomics is emerging. Biochim Biophys Acta 1634(3): 61.

Lawton F, Griffin M, Slack J, et al. (1989) Urinary polyamine excretion patterns in patients with epithelial ovarian cancer. Gynecol Obstet Invest 28(4): 212-214.

Lee SH, Suh JW, Chung BC, et al. (1998) Polyamine profiles in the urine of patients with leukemia. Cancer Lett 122(1-2): 1-8.

Li F, Tie R, Chang K, et al. (2012) Does risk for ovarian malignancy algorithm excel human epididymis protein 4 and CA125 in predicting epithelial ovarian cancer: A meta-analysis. BMC Cancer 12: 258.

Li J, Xie H, Li A, et al. (2017) Distinct plasma lipids profiles of recurrent ovarian cancer by liquid chromatography-mass spectrometry. Oncotarget 8(29): 46834-46845.

Lippi G & Cervellin G. (2012) Canine olfactory detection of cancer versus laboratory testing: Myth or opportunity? Clin Chem Lab Med 50(3): 435-439.

Liu Q, Luo Q, Halim A, et al. (2017) Targeting lipid metabolism of cancer cells: A promising therapeutic strategy for cancer. Cancer Lett 401: 39-45.

Liu Y, Chen Y, Momin A, et al. (2010) Elevation of sulfatides in ovarian cancer: An integrated transcriptomic and lipidomic analysis including tissue-imaging mass spectrometry. Mol Cancer 9: 186.

Lydic TA & Goo YH. (2018) Lipidomics unveils the complexity of the lipidome in metabolic diseases. Clin Transl Med 7(1): 9.

Manjunath AP, Pratapkumar, Sujatha K, et al. (2001) Comparison of three risk of malignancy indices in evaluation of pelvic masses. Gynecol Oncol 81(2): 225-229.

McCulloch M, Jezierski T, Broffman M, et al. (2006) Diagnostic accuracy of canine scent detection in early- and late-stage lung and breast cancers. Integr Cancer Ther 5(1): 30-39.

Medl M, Ogris E, Peters-Engl C, et al. (1995) TATI (tumour-associated trypsin inhibitor) as a marker of ovarian cancer. Br J Cancer 71(5): 1051-1054.

Meinhold-Heerlein I, Fotopoulou C, Harter P, et al. (2015) Statement by the kommission ovar of the AGO: The new FIGO and WHO classifications of ovarian, fallopian tube and primary peritoneal cancer. Geburtshilfe Frauenheilkd 75(10): 1021-1027.

Meinhold-Heerlein I, Fotopoulou C, Harter P, et al. (2016) The new WHO classification of ovarian, fallopian tube, and primary peritoneal cancer and its clinical implications. Arch Gynecol Obstet 293(4): 695-700.

Melamed A, Manning-Geist B, Bregar AJ, et al. (2017) Associations between residual disease and survival in epithelial ovarian cancer by histologic type. Gynecol Oncol 147(2): 250-256.

Meys EM, Kaijser J, Kruitwagen RF, et al. (2016) Subjective assessment versus ultrasound models to diagnose ovarian cancer: A systematic review and meta-analysis. Eur J Cancer 58: 17-29.

Meys EM, Jeelof LS, Achten NMJ, et al. (2017) Estimating risk of malignancy in adnexal masses: External validation of the ADNEX model and comparison with other frequently used ultrasound methods. Ultrasound Obstet Gynecol 49(6): 784-792.

Miki T, Hiramatsu K & Kawakita M. (2005) Interaction of N^1,N^{12}-diacetylspermine with polyamine transport systems of polarized porcine renal cell line LLC-PK1. J Biochem 138(4): 479-484.

Miller RW & Ueland FR. (2012) Risk of malignancy in sonographically confirmed ovarian tumors. Clin Obstet Gynecol 55(1): 52-64.

Miller-Fleming L, Olin-Sandoval V, Campbell K, et al. (2015) Remaining mysteries of molecular biology: The role of polyamines in the cell. J Mol Biol 427(21): 3389-3406.

Modesitt SC, Pavlik EJ, Ueland FR, et al. (2003) Risk of malignancy in unilocular ovarian cystic tumors less than 10 centimeters in diameter. Obstet Gynecol 102(3): 594-599.

Mogensen O, Mogensen B & Jakobsen A. (1990) Tumour-associated trypsin inhibitor (TATI) and cancer antigen 125 (CA 125) in mucinous ovarian tumours. Br J Cancer 61(2): 327-329.

Moore RG, Brown AK, Miller MC, et al. (2008) The use of multiple novel tumor biomarkers for the detection of ovarian carcinoma in patients with a pelvic mass. Gynecol Oncol 108(2): 402-408.

Moore RG, McMeekin DS, Brown AK, et al. (2009) A novel multiple marker bioassay utilizing HE4 and CA125 for the prediction of ovarian cancer in patients with a pelvic mass. Gynecol Oncol 112(1): 40-46.

Moore RG, Miller MC, Eklund EE, et al. (2012) Serum levels of the ovarian cancer biomarker HE4 are decreased in pregnancy and increase with age. Am J Obstet Gynecol 206(4): 349.e7.

Morice P, Uzan C, Fauvet R, et al. (2012) Borderline ovarian tumour: Pathological diagnostic dilemma and risk factors for invasive or lethal recurrence. Lancet Oncol 13(3): 103.

Muinao T, Deka Boruah HP & Pal M. (2018) Diagnostic and prognostic biomarkers in ovarian cancer and the potential roles of cancer stem cells - an updated review. Exp Cell Res 362(1): 1-10.

Muller CY. (2010) Doctor, should I get this new ovarian cancer test-OVA1? Obstet Gynecol 116(2 Pt 1): 246-247.

Murray-Stewart TR, Woster PM & Casero RA,Jr. (2016) Targeting polyamine metabolism for cancer therapy and prevention. Biochem J 473(19): 2937-2953.

Nakajima T, Katsumata K, Kuwabara H, et al. (2018) Urinary polyamine biomarker panels with machine-learning differentiated colorectal cancers, benign disease, and healthy controls. Int J Mol Sci 19(3): E756.

Nakayama Y, Torigoe T, Minagawa N, et al. (2012) The clinical usefulness of urinary N^1,N^{12}-diacetylspermine (DiAcSpm) levels as a tumor marker in patients with colorectal cancer. Oncol Lett 3(5): 970-974.

Oza AM, Cook AD, Pfisterer J, et al. (2015) Standard chemotherapy with or without bevacizumab for women with newly diagnosed ovarian cancer (ICON7): Overall survival results of a phase 3 randomised trial. Lancet Oncol 16(8): 928-936.

Park CH, Jung MH & Ji YI. (2015) Risk factors for malignant transformation of mature cystic teratoma. Obstet Gynecol Sci 58(6): 475-480.

Pegg AE & Casero RA,Jr. (2011) Current status of the polyamine research field. Methods Mol Biol 720: 3-35.

Peng G, Hakim M, Broza YY, et al. (2010) Detection of lung, breast, colorectal, and prostate cancers from exhaled breath using a single array of nanosensors. Br J Cancer 103(4): 542-551.

Pickel D, Manucy GP, Walker DB, et al. (2004) Evidence for canine olfactory detection of melanoma. Applied Animal Behaviour Science 89(1): 107-116.

Piek A, Meijers WC, Schroten NF, et al. (2017) HE4 serum levels are associated with heart failure severity in patients with chronic heart failure. Journal of Cardiac Failure 23(1): 12-19.

Pineda L, Salcedo E, Vilhena C, et al. (2014) Interobserver agreement in assigning IOTA color score to adnexal masses using three-dimensional volumes or digital videoclips: Potential implications for training. Ultrasound Obstet Gynecol 44(3): 361-364.

Prahm KP, Novotny GW, Hogdall C, et al. (2016) Current status on microRNAs as biomarkers for ovarian cancer. APMIS 124(5): 337-355.

Prat J & FIGO Committee on Gynecologic Oncology. (2014) Staging classification for cancer of the ovary, fallopian tube, and peritoneum. Int J Gynaecol Obstet 124(1): 1-5.

Pyragius CE, Fuller M, Ricciardelli C, et al. (2013) Aberrant lipid metabolism: An emerging diagnostic and therapeutic target in ovarian cancer. Int J Mol Sci 14(4): 7742-7756.

Pöyhönen MJ, Uusitalo UM, Kari A, et al. (1990) Urinary excretion of polyamines: Importance of circadian rhythm, age, sex, menstrual cycle, weight, and creatinine excretion. Am J Clin Nutr 52(4): 746-751.

Qiu W, Lu H, Qi Y, et al. (2016) Dietary fat intake and ovarian cancer risk: A meta-analysis of epidemiological studies. Oncotarget 7(24): 37390-37406.

Raine-Fenning NJ, Nordin NM, Ramnarine KV, et al. (2008a) Determining the relationship between three-dimensional power Doppler data and true blood flow characteristics: An in-vitro flow phantom experiment. Ultrasound Obstet Gynecol 32(4): 540-550.

Raine-Fenning NJ, Nordin NM, Ramnarine KV, et al. (2008b) Evaluation of the effect of machine settings on quantitative three-dimensional power Doppler angiography: An in-vitro flow phantom experiment. Ultrasound Obstet Gynecol 32(4): 551-559.

Reid BM, Permuth JB & Sellers TA. (2017) Epidemiology of ovarian cancer: A review. Cancer Biol Med 14(1): 9-32.

Ren J, Xiao YJ, Singh LS, et al. (2006) Lysophosphatidic acid is constitutively produced by human peritoneal mesothelial cells and enhances adhesion, migration, and invasion of ovarian cancer cells. Cancer Res 66(6): 3006-3014.

Roine A, Veskimäe E, Tuokko A, et al. (2014) Detection of prostate cancer by an electronic nose: A proof of principle study. J Urol 192(1): 230-234.

Royal College of Obstetricians and Gynaecologists. (2016) The management of ovarian cysts in postmenopausal women (Green-top Guideline no 34).

Ruiz de Gauna B, Sanchez P, Pineda L, et al. (2014) Interobserver agreement in describing adnexal masses using the International Ovarian Tumor Analysis simple rules in a real-time setting and using three-dimensional ultrasound volumes and digital clips. Ultrasound Obstet Gynecol 44(1): 95-99.

Russell DH, Levy CC, Schimpff SC, et al. (1971) Urinary polyamines in cancer patients. Cancer Res 31(11): 1555-1558.

Russell DH. (1983) Clinical relevance of polyamines. Crit Rev Clin Lab Sci 18(3): 261-311.

Sala E, Rockall A, Rangarajan D, et al. (2010) The role of dynamic contrast-enhanced and diffusion weighted magnetic resonance imaging in the female pelvis. Eur J Radiol 76(3): 367-385.

Salem S, White LM & Lai J. (1994) Doppler sonography of adnexal masses: The predictive value of the pulsatility index in benign and malignant disease. AJR Am J Roentgenol 163(5): 1147-1150.

Santos AL & Preta G. (2018) Lipids in the cell: Organisation regulates function. Cell Mol Life Sci 75(11): 1909-1927.

Santos CR & Schulze A. (2012) Lipid metabolism in cancer. FEBS J 279(15): 2610-2623.

Saunders BA, Podzielinski I, Ware RA, et al. (2010) Risk of malignancy in sonographically confirmed septated cystic ovarian tumors. Gynecol Oncol 118(3): 278-282.

Sayasneh A, Wynants L, Preisler J, et al. (2013) Multicentre external validation of IOTA prediction models and RMI by operators with varied training. Br J Cancer 108(12): 2448-2454.

Schelling M, Braun M, Kuhn W, et al. (2000) Combined transvaginal B-mode and color Doppler sonography for differential diagnosis of ovarian tumors: Results of a multivariate logistic regression analysis. Gynecol Oncol 77(1): 78-86.

Sedlakova I, Vavrova J, Tosner J, et al. (2008) Lysophosphatidic acid: An ovarian cancer marker. Eur J Gynaecol Oncol 29(5): 511-514.

Sedlakova I, Vavrova J, Tosner J, et al. (2011) Lysophosphatidic acid (LPA) - a perspective marker in ovarian cancer. Tumour Biol 32(2): 311-316.

Seiler N. (2004) Catabolism of polyamines. Amino Acids 26(3): 217-233.

Sethi S & Brietzke E. (2017) Recent advances in lipidomics: Analytical and clinical perspectives. Prostaglandins Other Lipid Mediat 128-129: 8-16.

Sevinc A, Adli M, Kalender ME, et al. (2007) Benign causes of increased serum CA-125 concentration. Lancet Oncol 8(12): 1054-1055.

Shan L, Chen YA, Davis L, et al. (2012) Measurement of phospholipids may improve diagnostic accuracy in ovarian cancer. PLoS One 7(10): e46846.

Sharma SK, Nemieboka B, Sala E, et al. (2016) Molecular imaging of ovarian cancer. J Nucl Med 57(6): 827-833.

Siegel RL, Miller KD & Jemal A. (2016) Cancer statistics, 2016. CA Cancer J Clin 66(1): 7-30.

Silverberg SG, Bell DA, Kurman RJ, et al. (2004) Borderline ovarian tumors: Key points and workshop summary. Hum Pathol 35(8): 910-917.

Silvestre L, Martins WP & Candido-Dos-Reis FJ. (2015) Limitations of three-dimensional power Doppler angiography in preoperative evaluation of ovarian tumors. J Ovarian Res 8: 47.

Sladkevicius P, Jokubkiene L & Valentin L. (2007) Contribution of morphological assessment of the vessel tree by three-dimensional ultrasound to a correct diagnosis of malignancy in ovarian masses. Ultrasound Obstet Gynecol 30(6): 874-882.

Sladkevicius P & Valentin L. (2013) Intra- and interobserver agreement when describing adnexal masses using the International Ovarian Tumor Analysis terms and definitions: A study on three-dimensional ultrasound volumes. Ultrasound Obstet Gynecol 41(3): 318-327.

Soda K, Kano Y, Sakuragi M, et al. (2009) Long-term oral polyamine intake increases blood polyamine concentrations. J Nutr Sci Vitaminol (Tokyo) 55(4): 361-366.

Soda K. (2011) The mechanisms by which polyamines accelerate tumor spread. J Exp Clin Cancer Res 30: 95.

Sonoda H, Kohnoe S, Yamazato T, et al. (2011) Colorectal cancer screening with odour material by canine scent detection. Gut 60(6): 814-819.

Spencer JA, Forstner R, Cunha TM, et al. (2010) ESUR guidelines for MR imaging of the sonographically indeterminate adnexal mass: An algorithmic approach. Eur Radiol 20(1): 25-35.

Sugimoto M, Hiramatsu K, Kamei S, et al. (1995) Significance of urinary N^1,N^8-diacetylspermidine and N^1,N^{12}-diacetylspermine as indicators of neoplastic diseases. J Cancer Res Clin Oncol 121(5): 317-319.

Suh JW, Lee SH, Chung BC, et al. (1997) Urinary polyamine evaluation for effective diagnosis of various cancers. J Chromatogr B Biomed Sci Appl 688(2): 179-186.

Suh-Burgmann E. (2006) Long-term outcomes following conservative surgery for borderline tumor of the ovary: A large population-based study. Gynecol Oncol 103(3): 841-847.

Sun Y, Meng H, Jin Y, et al. (2016) Serum lipid profile in gynecologic tumors: A retrospective clinical study of 1,550 patients. Eur J Gynaecol Oncol 37(3): 348-352.

Sutphen R, Xu Y, Wilbanks GD, et al. (2004) Lysophospholipids are potential biomarkers of ovarian cancer. Cancer Epidemiol Biomarkers Prev 13(7): 1185-1191.

Swinnen JV, Brusselmans K & Verhoeven G. (2006) Increased lipogenesis in cancer cells: New players, novel targets. Curr Opin Clin Nutr Metab Care 9(4): 358-365.

Takahashi Y, Horio H, Sakaguchi K, et al. (2015) Significant correlation between urinary N^1, N^{12}-diacetylspermine and tumor invasiveness in patients with clinical Stage IA non-small cell lung cancer. BMC Cancer 15: 65.

Takahashi Y, Sakaguchi K, Horio H, et al. (2015) Urinary N^1, N^{12}-diacetylspermine is a non-invasive marker for the diagnosis and prognosis of non-small-cell lung cancer. Br J Cancer 113(10): 1493-1501.

Tania M, Khan MA & Song Y. (2010) Association of lipid metabolism with ovarian cancer. Curr Oncol 17(5): 6-11.

Tekay A & Jouppila P. (1992) Validity of pulsatility and resistance indices in classification of adnexal tumors with transvaginal color Doppler ultrasound. Ultrasound Obstet Gynecol 2(5): 338-344.

Tempany CM, Zou KH, Silverman SG, et al. (2000) Staging of advanced ovarian cancer: Comparison of imaging modalities - report from the radiological diagnostic oncology group. Radiology 215(3): 761-767.

Testa AC, Ferrandina G, Fruscella E, et al. (2005) The use of contrasted transvaginal sonography in the diagnosis of gynecologic diseases: A preliminary study. J Ultrasound Med 24(9): 1267-1278.

Testa AC, Timmerman D, Van Belle V, et al. (2009) Intravenous contrast ultrasound examination using contrast-tuned imaging (CnTI) and the contrast medium SonoVue for discrimination between benign and malignant adnexal masses with solid components. Ultrasound Obstet Gynecol 34(6): 699-710.

Testa AC, Kaijser J, Wynants L, et al. (2014) Strategies to diagnose ovarian cancer: New evidence from phase 3 of the multicentre international IOTA study. Br J Cancer 111(4): 680-688.

Thomas T & Thomas TJ. (2003) Polyamine metabolism and cancer. J Cell Mol Med 7(2): 113-126.

Thomassin-Naggara I, Darai E, Cuenod CA, et al. (2008) Dynamic contrast-enhanced magnetic resonance imaging: A useful tool for characterizing ovarian epithelial tumors. J Magn Reson Imaging 28(1): 111-120.

Thomassin-Naggara I, Darai E, Cuenod CA, et al. (2009) Contribution of diffusion-weighted MR imaging for predicting benignity of complex adnexal masses. Eur Radiol 19(6): 1544-1552.

Thomassin-Naggara I, Toussaint I, Perrot N, et al. (2011) Characterization of complex adnexal masses: Value of adding perfusion- and diffusion-weighted MR imaging to conventional MR imaging. Radiology 258(3): 793-803.

Thomassin-Naggara I, Aubert E, Rockall A, et al. (2013) Adnexal masses: Development and preliminary validation of an MR imaging scoring system. Radiology 267(2): 432-443.

Timmerman D, Valentin L, Bourne TH, et al. (2000) Terms, definitions and measurements to describe the sonographic features of adnexal tumors: A consensus opinion from the International Ovarian Tumor Analysis (IOTA) group. Ultrasound Obstet Gynecol 16(5): 500-505.

Timmerman D, Testa AC, Bourne T, et al. (2005) Logistic regression model to distinguish between the benign and malignant adnexal mass before surgery: A multicenter study by the International Ovarian Tumor Analysis group. J Clin Oncol 23(34): 8794-8801.

Timmerman D, Testa AC, Bourne T, et al. (2008) Simple ultrasound-based rules for the diagnosis of ovarian cancer. Ultrasound Obstet Gynecol 31(6): 681-690.

Timmerman D, Ameye L, Fischerova D, et al. (2010a) Simple ultrasound rules to distinguish between benign and malignant adnexal masses before surgery: Prospective validation by IOTA group. BMJ 341: c6839.

Timmerman D, Van Calster B, Testa AC, et al. (2010b) Ovarian cancer prediction in adnexal masses using ultrasound-based logistic regression models: A temporal and external validation study by the IOTA group. Ultrasound Obstet Gynecol 36(2): 226-234.

Timmons J, Chang ET, Wang JY, et al. (2012) Polyamines and gut mucosal homeostasis. J Gastrointest Dig Syst 2(Suppl. 7): 11-21.

Tingulstad S, Hagen B, Skjeldestad FE, et al. (1996) Evaluation of a risk of malignancy index based on serum CA125, ultrasound findings and menopausal status in the pre-operative diagnosis of pelvic masses. Br J Obstet Gynaecol 103(8): 826-831.

Tingulstad S, Hagen B, Skjeldestad FE, et al. (1999) The risk-of-malignancy index to evaluate potential ovarian cancers in local hospitals. Obstet Gynecol 93(3): 448-452.

Tsujinaka S, Soda K, Kano Y, et al. (2011) Spermine accelerates hypoxia-initiated cancer cell migration. Int J Oncol 38(2): 305-312.

Turner AP & Magan N. (2004) Electronic noses and disease diagnostics. Nat Rev Microbiol 2(2): 161-166.

Ueda SM, Yap KL, Davidson B, et al. (2010) Expression of fatty acid synthase depends on NAC1 and is associated with recurrent ovarian serous carcinomas. J Oncol 2010: 285191.

Uehara N, Shirakawa S, Uchino H, et al. (1980) Elevated contents of spermidine and spermine in the erythrocytes of cancer patients. Cancer 45(1): 108-111.

Ueland FR, Desimone CP, Seamon LG, et al. (2011) Effectiveness of a multivariate index assay in the preoperative assessment of ovarian tumors. Obstet Gynecol 117(6): 1289-1297.

Umemori Y, Ohe Y, Kuribayashi K, et al. (2010) Evaluating the utility of N^1,N^{12}-diacetylspermine and N^1,N^8-diacetylspermidine in urine as tumor markers for breast and colorectal cancers. Clin Chim Acta 411(23-24): 1894-1899.

Valentin L. (1997) Gray scale sonography, subjective evaluation of the color Doppler image and measurement of blood flow velocity for distinguishing benign and malignant tumors of suspected adnexal origin. Eur J Obstet Gynecol Reprod Biol 72(1): 63-72.

Valentin L, Hagen B, Tingulstad S, et al. (2001) Comparison of 'pattern recognition' and logistic regression models for discrimination between benign and malignant pelvic masses: A prospective cross validation. Ultrasound Obstet Gynecol 18(4): 357-365.

Valentin L, Ameye L, Savelli L, et al. (2011) Adnexal masses difficult to classify as benign or malignant using subjective assessment of gray-scale and Doppler ultrasound findings: Logistic regression models do not help. Ultrasound Obstet Gynecol 38(4): 456-465.

Van Calster B, Van Hoorde K, Valentin L, et al. (2014) Evaluating the risk of ovarian cancer before surgery using the ADNEX model to differentiate between benign, borderline, early and advanced stage invasive, and secondary metastatic tumours: Prospective multicentre diagnostic study. BMJ 349: g5920.

Van Calster B, Van Hoorde K, Froyman W, et al. (2015) Practical guidance for applying the ADNEX model from the IOTA group to discriminate between different subtypes of adnexal tumors. Facts Views Vis Obgyn 7(1): 32-41.

Van Holsbeke C, Yazbek J, Holland TK, et al. (2008) Real-time ultrasound vs. evaluation of static images in the preoperative assessment of adnexal masses. Ultrasound Obstet Gynecol 32(6): 828-831.

Van Holsbeke C, Van Calster B, Bourne T, et al. (2012) External validation of diagnostic models to estimate the risk of malignancy in adnexal masses. Clin Cancer Res 18(3): 815-825.

van Meer G, Voelker DR & Feigenson GW. (2008) Membrane lipids: Where they are and how they behave. Nat Rev Mol Cell Biol 9(2): 112-124.

van Nagell JR,Jr & Miller RW. (2016) Evaluation and management of ultrasonographically detected ovarian tumors in asymptomatic women. Obstet Gynecol 127(5): 848-858.

Venäläinen MK, Roine AN, Häkkinen MR, et al. (2018) Altered polyamine profiles in colorectal cancer. Anticancer Res 38(6): 3601-3607.

Wang J, Lv F, Fei X, et al. (2011) Study on the characteristics of contrast-enhanced ultrasound and its utility in assessing the microvessel density in ovarian tumors or tumor-like lesions. Int J Biol Sci 7(5): 600-606.

Wang J, Gao J, Yao H, et al. (2014) Diagnostic accuracy of serum HE4, CA125 and ROMA in patients with ovarian cancer: A meta-analysis. Tumour Biol 35(6): 6127-6138.

Wang S & Johnson S. (2012) Prediction of benignity of solid adnexal masses. Arch Gynecol Obstet 285(3): 721-726.

Warburg O. (1956) On the origin of cancer cells. Science 123(3191): 309-314.

Webber K & Friedlander M. (2017) Chemotherapy for epithelial ovarian, fallopian tube and primary peritoneal cancer. Best Pract Res Clin Obstet Gynaecol 41: 126-138.

Weber CM, Cauchi M, Patel M, et al. (2011) Evaluation of a gas sensor array and pattern recognition for the identification of bladder cancer from urine headspace. Analyst 136(2): 359-364.

Weir JM, Wong G, Barlow CK, et al. (2013) Plasma lipid profiling in a large population-based cohort. J Lipid Res 54(10): 2898-2908.

Williams H & Pembroke A. (1989) Sniffer dogs in the melanoma clinic? Lancet 1(8640): 734.

Willis CM, Church SM, Guest CM, et al. (2004) Olfactory detection of human bladder cancer by dogs: Proof of principle study. BMJ 329(7468): 712.

Wilson AD & Baietto M. (2011) Advances in electronic-nose technologies developed for biomedical applications. Sensors (Basel) 11(1): 1105-1176.

Xiang H, Huang R, Cheng J, et al. (2013) Value of three-dimensional contrast-enhanced ultrasound in the diagnosis of small adnexal masses. Ultrasound Med Biol 39(5): 761-768.

Xiao Y, Chen Y, Kennedy AW, et al. (2000) Evaluation of plasma lysophospholipids for diagnostic significance using electrospray ionization mass spectrometry (ESI-MS) analyses. Ann N Y Acad Sci 905: 242-259.

Xu Y, Shen Z, Wiper DW, et al. (1998) Lysophosphatidic acid as a potential biomarker for ovarian and other gynecologic cancers. JAMA 280(8): 719-723.

Xue R, Dong L, Zhang S, et al. (2008) Investigation of volatile biomarkers in liver cancer blood using solid-phase microextraction and gas chromatography/mass spectrometry. Rapid Commun Mass Spectrom 22(8): 1181-1186.

Yamaguchi K, Nakamura M, Shirahane K, et al. (2005) Urine diacetylspermine as a novel tumour maker for pancreatobiliary carcinomas. Dig Liver Dis 37(3): 190-194.

Yamamoto Y, Yamada R, Oguri H, et al. (2009) Comparison of four malignancy risk indices in the preoperative evaluation of patients with pelvic masses. Eur J Obstet Gynecol Reprod Biol 144(2): 163-167.

Yang K & Han X. (2016) Lipidomics: Techniques, applications, and outcomes related to biomedical sciences. Trends Biochem Sci 41(11): 954-969.

Yellen P & Foster DA. (2014) Inhibition of fatty acid synthase induces pro-survival akt and ERK signaling in K-ras-driven cancer cells. Cancer Lett 353(2): 258-263.

Young RC, Walton LA, Ellenberg SS, et al. (1990) Adjuvant therapy in Stage I and Stage II epithelial ovarian cancer. Results of two prospective randomized trials. N Engl J Med 322(15): 1021-1027.

Zannoni L, Savelli L, Jokubkiene L, et al. (2013) Intra- and interobserver reproducibility of assessment of Doppler ultrasound findings in adnexal masses. Ultrasound Obstet Gynecol 42(1): 93-101.

Zeppernick F & Meinhold-Heerlein I. (2014) The new FIGO staging system for ovarian, fallopian tube, and primary peritoneal cancer. Arch Gynecol Obstet 290(5): 839-842.

Zhang T, Wu X, Yin M, et al. (2012) Discrimination between malignant and benign ovarian tumors by plasma metabolomic profiling using ultra performance liquid chromatography/mass spectrometry. Clin Chim Acta 413(9-10): 861-868.

Zhang Y, Liu Y, Li L, et al. (2016) High resolution mass spectrometry coupled with multivariate data analysis revealing plasma lipidomic alteration in ovarian cancer in Asian women. Talanta 150: 88-96.

Zhang Z & Li G. (2010) A review of advances and new developments in the analysis of biological volatile organic compounds. Microchemical Journal 95(2): 127-139.

Zhao YY, Cheng XL, Lin RC, et al. (2015) Lipidomics applications for disease biomarker discovery in mammal models. Biomark Med 9(2): 153-168.

Zhao Z, Cai Q & Xu Y. (2016) The lipidomic analyses in low and highly aggressive ovarian cancer cell lines. Lipids 51(2): 179-187.

10 ORIGINAL PUBLICATIONS

Niemi et al. Journal of Ovarian Research (2017) 10:15
DOI 10.1186/s13048-017-0309-4

Journal of Ovarian Research

RESEARCH Open Access

Reliability of preoperative evaluation of postmenopausal ovarian tumors

Riikka Johanna Niemi[1*], Sami Kristian Saarelainen[1], Tiina Hannele Luukkaala[2] and Johanna Unelma Mäenpää[1,3]

Abstract

Background: Preoperative evaluation of ovarian tumors is challenging. This study was undertaken to evaluate the performance of conventional two-dimensional (2D) ultrasound and CA125 in predicting malignant or benign nature of pelvic masses, and to investigate if three-dimensional power Doppler (3DPD) ultrasound provides any added value. Ninety-six postmenopausal and four perimenopausal women with supposed ovarian tumors were examined by standardized 2D and 3DPD ultrasounds preoperatively. The tumors were evaluated using the risk of malignancy index (RMI), International Ovarian Tumors Analysis (IOTA) group simple rules, expert opinion, IOTA logistic regression model 2 (LR2) and 3D vascular indices, and were postoperatively compared to histopathological results.

Results: Ninety-eight tumors turned out to be ovarian in origin. Of these, 66 were benign and 32 malignant. RMI (cut-off value 200), simple rules, expert opinion and LR2 (cut-off value 25) were used to predict malignant nature of the tumors and had sensitivities of 71.9, 90.6, 87.5 and 90.6%, and specificities of 80.3, 84.6, 92.4 and 77.3%, respectively. When the 3D vascularization flow index (VFI) was added to RMI and LR2, the accuracy of the test improved from 77.6 to 81.4% and from 81.6 to 86.5%, respectively, at the expense of sensitivity, while VFI gave no added benefit for simple rules and expert opinion. Agreement between two examiners using expert opinion was good (Cohen's kappa = 0.89).

Conclusions: The subjective opinion of an expert seems to be the most reliable method in assessing ovarian tumors, and the 3DPD indices seem to provide no significant added value.

Keywords: Expert opinion, IOTA LR2, IOTA simple rules, Ovarian cancer, Ovarian tumor, Power doppler, Three-dimensional ultrasound

Background

Ovarian cancer has the leading mortality rate of all gynecological cancers, and the incidence of ovarian cancer is at its peak among postmenopausal women. The optimal treatment of ovarian neoplasms requires correct preoperative characterization of tumors. The surgical treatment of ovarian cancer should be reserved for gynecological oncologists, while benign tumors can be operated on less radically by general gynecologists, or even managed conservatively.

Preoperatively ultrasound features combined with the measurements of CA125 has been used to predict the malignancy of a pelvis mass (Risk of Malignancy Index, RMI) since early 1990's [1]. However, subjective assessment by an experienced ultrasound examiner has been considered to be the best diagnostic method for ovarian tumors [2, 3]. While not all gynecologists are so well accustomed to ultrasound examinations, in 2008 the International Ovarian Tumors Analysis (IOTA) group presented simple ultrasound-based rules that include five rules for predicting malignant tumors (M-rules) and five for predicting benign tumors (B-rules). If one or more M-rules with absence of B-rules or B-rules with absence of M-rules are present, the tumor is supposed to be malignant or benign, respectively. In a multicenter study, these rules were applicable for 76% of all tumors and showed a sensitivity of 95% and specificity of 91% [4]. If none of the rules is valid or if both M- and B-rules are present, a tumor is considered to be inconclusive [4, 5]. In that case the opinion of an expert ultrasound examiner is needed, which is called a two-step strategy [6]. In addition, the IOTA group developed two logistic regression models (LR1 and LR2) [7]. LR1 is based on 12 different variables, and LR2 is

* Correspondence: riikka.niemi@pshp.fi
[1]Department of Obstetrics and Gynecology, Tampere University Hospital, P.O. Box 2000FI-33521 Tampere, Finland
Full list of author information is available at the end of the article

based on 6, including patient history, clinical signs and ultrasound features. These models have shown sensitivities of 92–95% and 89–95% with specificities of 74–87% and 73–86% in detecting ovarian malignancies, respectively [8]. Nevertheless, in several studies, the impression of an expert ultrasound examiner has still been considered to be the best method, or at least equivalent to LR1 and LR2, for diagnosing ovarian pathology [8, 9].

An increased density of microvessels and abnormal vascular tree of the tumor are characteristic of malignant ovarian processes [10, 11]. These phenomena have given new insight for the use of three-dimensional (3D) ultrasound and 3D power Doppler (3DPD) in evaluating the vascularization of ovarian tumors to discriminate between benign and malignant tumors. Unfortunately, there are no clear cut-off rules for 3D ultrasound features, limiting their clinical utility [12].

The purpose of this study was to examine if 3DPD ultrasound can offer additional benefits over conventional two-dimensional ultrasound and other diagnostic methods as a useful tool for predicting malignancy of an adnexal mass. The aim was to find the most applicable and reliable preoperative diagnostic approach for postmenopausal women.

Methods

Between February 2011 and November 2014, one hundred women over 50 years of age presenting with an abnormal adnexal mass(es) at the Department of Obstetrics and Gynecology of Tampere University Hospital, were recruited to the study. All patients were destined for surgery. Overtly benign or malignant looking tumors like unilocular simple ovarian cysts and tumors associated with marked ascites (depth of the greatest pool over 10 cm) were excluded. In principle, the maximum allowed diameter of the tumors was 10 cm, allowing the entire tumor to be assessible transvaginally. However, there were five tumors, the maximum diameter of which exceeded 10 cm at the final examination, but it never exceeded 12 cm.

According to preoperative findings, the patients were operated on by either a gynecological oncologist or a general gynecologist, using either laparoscopic or open technique.

The patients were assessed within 2 weeks prior to surgery by vaginal two-dimensional (2D) and 3D ultrasound examination with power Doppler. In the case of bilateral ovarian tumors, both masses were examined, and the more complex tumor was assessed for the study. All ultrasound examinations were performed by an experienced gynecologist or the author R.J.N., using a Voluson 730 Expert unit (GE Medical Systems, Zipf, Austria) with a multifrequency transvaginal transducer (5–9 MHz). A normal B-mode ultrasound assessment included the calculation of the size of the adnexal mass. The power Doppler settings were standardized: frequency, 6 MHz; power Doppler gain, -0.6; wall motion filter (WMF), low 1; pulse repetition filter (PRF), 0.6 kHz. The extent of vascularization of the tumor was described by a score from 1 to 4 (1 = no blood flow detected, 4 = high blood flow detected) [13]. 3DPD was used to examine the ovarian tumor after the 2D evaluation. The acquisition sweep angle was set to 85°.

A serum sample was obtained preoperatively, and RMI was calculated by using the original formula of Jacobs et al. in which the serum CA125 level, ultrasound scan result and patient's menopausal status are taken into account [1]. The ultrasound data were stored on a hard disk for later evaluation. Based on the ultrasound examination, the examiner classified the adnexal tumor as benign or malignant (expert opinion), immediately following the actual examination. From the 2D data, the tumors were classified by using the IOTA simple rules. If none of these rules applied or if both M- and B-rules were applicable, the tumor could not be classified. In such case, the tumor was evaluated subjectively by the examiner as benign or malignant.

The IOTA LR2 was implemented by using the Predictive IOTA models for ovarian cancer application software, version 2013 (App for IOS operating systems). In the LR2 model, the six variables used are age of the patient, presence/absence of ascites, presence/absence of papillations/papillary projections with blood flow, maximum diameter of the largest solid component, irregular cyst walls and presence/absence of acoustic shadows. This calculated model yields the probability of malignancy of an ovarian tumor.

The analyses of the stored 3D volumes were performed by the same investigator (R.J.N.) using a virtual organ computer-aided analysis (VOCAL™) imaging program and 4D-View software (GE Healthcare, v 9.1). The volume of each adnexal tumor was measured by manual delineation of the contour of the mass with a 15°-rotation step. Using the VOCAL software's histogram feature, three vascular indices were calculated from the adnexal tumors: vascularization index (VI), flow index (FI) and vascularization flow index (VFI). VI represents the number of vessels in the studied volume and is expressed as a percentage. FI reflects the intensity of blood flow at the time of the 3D sweep. VFI is interpreted to be a combination of VI and FI representing both vascularization and blood flow. FI and VFI are expressed as values ranging from 0 to 100 [12, 14, 15].

To estimate the interobserver agreement, another experienced ultrasound examiner (S.K.S.) re-evaluated the stored ultrasound data and classified the malignancy of tumors (expert opinion), and analysed 3D volumes.

The ultrasound examinations and off-line assessments were performed blinded for each other's results and the histopathological diagnoses while analyzing the tumors. The preoperative findings were finally compared to post-operative histopathological diagnoses. For the purpose of this analysis, the borderline and low grade ovarian tumors were classified as malignant because normally also they are staged surgically. All participants gave their informed consent to the study, which was approved by the Ethics Committee of Tampere University Hospital (ETL R10080, 6 August 2010).

Statistical analysis

No sample size calculation was performed due to the preliminary descriptive nature of this study. All data were analyzed using IBM SPSS Statistics for Windows, version 22 (Armonk, NY, IBM Corp.). The normality of the distributions of continuous variables was evaluated by Kolmogorov-Smirnov tests. Due to the skewness of the distributions, the comparisons of groups were performed using Mann-Whitney U-tests, and correlations were evaluated using Spearman's correlation tests. Receiver operating characteristics curves (ROC) were used for evaluating the performance of serum CA125, RMI, LR2 and 3D vascular indices as predictive tests for malignancy. The best cut-off values of the models were calculated in consideration of sensitivity, specificity, positive predictive value and negative predictive value. Binomial variables were evaluated by Fischer's exact tests or Pearson Chi-Square tests when appropriate.

The agreement of ultrasound features by both ultrasound examiners (R.J.N. and S.K.S.) was estimated by calculating the Cohen's kappa index. A kappa value of less than 0.20 indicates poor agreement, 0.21–0.40 moderate agreement, 0.61–0.80 good agreement and 0.81–1.00 very good agreement [16]. Interobserver agreement of 3DPD indices were analyzed by related-samples Wilcoxon signed rank test.

Results

In 100 patients with supposed adnexal masses, the tumors of 98 patients turned out to be true ovarian tumors, while the remaining two were appendiceal in origin. Of the 98 ovarian tumors, sixty-six (67.3%) were benign, of which 19 were bilateral. Respectively, 32 (32.7%) of the tumors were malignant, of which six were bilateral. Of the malignant tumors, 17 were epithelial serous, five epithelial mucinous, and eight of other pathology. Two of the malignant tumors were metastases of intestinal cancer. The histologic diagnoses of adnexal masses are presented in Table 1.

Table 1 Histology of the tumors

Histologic type	Number	Percent
Benign	66	(67.3)
Serous cystadenoma/adenofibroma	39	
Fibroma/thecoma	5	
Teratoma	7	
Brenner tumor	1	
Endometrioma	3	
Mucinous cystadenoma	3	
Serous/hemorrhagic cyst	7	
Bizarre leiomyoma	1	
Malignant	32	(32.7)
Epithelial tumors		
Serous		
High grade	9	
Low grade	3	
Borderline	5	
Mucinous		
Adenocarcinoma	3	
Borderline	2	
Clear cell carcinoma	1	
Carcinosarcoma	2	
Non-epithelial tumors		
Granulosa cell tumor	4	
Sertoli-Leydig cell tumor	1	
Metastatic[a]	2	
Total	98	(100.0)

[a]Primary tumors: sigmoid carcinoma and carcinoma of the appendix

The median age of the patients was 61 (range, 50–84) years. Tumor pathology did not depend on the age of the women or the bilaterality of the tumors. Three of the women in the benign ovarian tumor group and one in the malignant group were in fact perimenopausal, because they had experienced menstrual bleeding during the previous 6 months. Systemic hormone replacement therapy was used before surgery by 17 women with benign tumors and by five with malignant tumors. The median body mass index was 26 (range, 20–44) for women with benign tumors and respectively 27 (range, 19–39) for women with malignant tumors. The median diameters of the tumors in the groups were 6 (range, 3–11) and 7 (range, 3–12) cm, respectively. The median serum CA125 levels were 15 (range, 6–127) and 50 (range, 9–3195) kU/L, respectively, and the difference between the groups was significant ($p < 0.001$). The calculated median values of RMI for benign and malignant cases were 99 (range, 10–1143) and 360 (range, 27–7488), respectively ($p < 0.001$). The age of the patients, body mass indexes and CA125 levels did not correlate with each other.

The performances of the assessed methods are given in Table 2. Seventy-six (77.6%) of the tumors were

Table 2 Diagnostic performances of different methods at various cut-off values in detecting ovarian malignancy

Diagnostic method Cut-off value	Sensitivity %	95% CI	Specificity %	95% CI	PPV %	95% CI	NPV %	95% CI	Accuracy %
Serum CA125 (kU/L) → Area under the ROC curve = 0.80									
24	71.9	53.3–86.3	78.8	67.0–87.9	62.2	44.8–77.5	85.3	73.8–93.0	76.5
35	59.4	40.6–76.3	84.9	73.9–92.5	65.5	45.7–82.1	81.2	69.9–89.6	76.5
RMI → Area under the ROC curve = 0.81									
200	71.9	53.3–86.3	80.3	68.7–89.1	63.9	46.2–79.2	85.5	74.2–93.1	77.6
220	71.9	53.3–86.3	83.3	72.1–91.4	67.7	49.5–82.6	85.9	75.0–93.4	79.6
Simple rules with expert opinion[a]	90.6	75.0–98.0	84.6	73.9–92.5	74.4	57.9–87.0	94.9	85.9–98.9	86.7
Expert opinion	87.5	71.0–96.5	92.4	83.2–97.5	84.6	68.1–94.9	93.9	85.0–98.3	90.8
Tumor vascularity[b]	90.6	75.0–98.0	77.3	65.3–86.7	65.9	50.1–79.5	94.4	84.6–98.8	81.6
LR2 (%) → Area under the ROC curve = 0.93									
10	100.0	89.1–100.0	36.4	24.9–49.1	43.2	31.8–55.3	100.0	85.8–100.0	57.1
25	90.6	75.0–98.0	77.3	65.3–86.7	65.9	50.1–79.5	94.4	84.6–98.8	81.6
43	81.3	63.6–92.8	90.9	81.3–96.6	81.3	63.6–92.8	90.9	81.3–96.6	87.8

IOTA International Ovarian Tumor Analysis; *CI* Confidential interval; *PPV* Positive predictive value; *NPV* Negative predictive value; *ROC* Receiver operating characteristics; *RMI* Risk of malignancy index; *LR2* Logistic regression model 2
[a]Two-step strategy: as a result of inconclusive findings by simple rules, the expert evaluates the tumor
[b]Two-dimensional ultrasound vascular score 1-2 vs 3-4

classifiable using the simple rules, and 68 of these (89.5%) were correctly classified. Incorrectly classified tumors were all false-positive malignant tumors, and their histopathological diagnoses were serous cystadenoma/-fibroma ($n = 4$), thecoma ($n = 2$), one serous cyst and one Brenner tumor each. The unclassifiable tumors ($n = 22$) were evaluated by expert opinion (R.J.N.), and 77.3% (17 of 22) were classified correctly.

The opinions of the experts (R.J.N. and S.K.S.) differed in five cases, including two serous and one mucinous cystadenoma, one teratoma, and one benign Brenner tumor. In addition, both experts failed in the case of two malignant tumors: one endometrioid adenocarcinoma FIGO Stage IA and one granulosa cell tumor. Two serous borderline cystadenomas were erroneously classified as benign. The interobserver agreement of the malignancy of tumors between both examiners was very good (Cohen's kappa = 0.89, 95% CI 0.79–0.98; percentage of agreement of correct classification = 87.8%).

The tumor vascularity as examined by 2D ultrasound was higher in malignant tumors compared to benign tumors ($p < 0.001$). Predictions of tumor malignancy by scoring the vascularity yielded the same sensitivity (90.6%) as the simple rules with the expert opinion and LR2 with a cut-off value of 25. In comparison, 81.6% (80 of 98) of the tumors were classified correctly by vascularity assessment and LR2 (with a cut-off value 25), whereas the expert opinion correctly diagnosed 90.8% (89 of 98) of the cases. LR2 values and 3D vascular indices (VI, FI and VFI) were significantly different between benign and malignant tumors ($p < 0.001$). VI and VFI were the most sensitive and specific 3DPD indices (Table 3), being at least as specific as RMI, simple rules and LR2 in detecting malignant tumors. The subjective evaluation of tumor vascularity by 2DPD was more sensitive and almost as specific and accurate as 3DPD vascular indices. When 2D vascularity scoring or LR2 was combined to simple rules with the expert opinion, the

Table 3 Diagnostic performances of three-dimensional power Doppler indices at different cut-off values in detecting ovarian malignancy

3DPD indices Cut-off value	Sensitivity %	95% CI	Specificity %	95% CI	PPV %	95% CI	NPV %	95% CI	Accuracy %
VI (%) → Area under the ROC curve = 0.86									
1.00	67.7	48.6–83.3	90.9	81.3–96.6	77.8	57.7–91.4	85.7	75.3–92.9	83.5
FI → Area under the ROC curve = 0.72									
30	83.9	66.3–94.6	51.5	38.9–64.0	44.8	31.7–58.5	87.2	72.6–95.7	61.9
VFI → Area under the ROC curve = 0.87									
0.31	71.0	52.0–85.8	89.4	79.4–95.6	75.9	56.5–89.7	86.8	76.4–93.8	83.5

3DPD Three-dimensional power Doppler; *CI* Confidential interval; *PPV* Positive predictive value; *NPV* Negative predictive value; *ROC* Receiver operating characteristics; *VI* Vascularization index; *FI* Flow index; *VFI* Vascularization flow index

specificity slightly increased, albeit at the expense of sensitivity (data not shown).

The interobserver agreement between the two experts was good also in the case of calculated 3DPD indices, as shown in Table 4.

By combining RMI and LR2 with VFI and using suitable cut-off values, the accuracies and specificities of RMI and LR2 improved, while their sensitivities decreased. On the other hand, combining these 3DPD indices with simple rules or the expert opinion did not improve either method's accuracy. Newly created combination models are given in Table 5.

Discussion

To the best of our knowledge, this is the first study to compare such a large spectrum of various preoperative methods (serum CA125, RMI, simple ultrasound rules, expert opinion, 2DPD and IOTA LR2) along with 3DPD indices for discrimination between benign and malignant ovarian tumors. The results of the present study imply that clinical expert opinion still provides the best method for diagnosing malignant ovarian tumors, with no additional benefit provided by use of 3DPD indices. Regarding the specificity of 3DPD indices, VI and VFI are only as specific as the traditional methods CA125 and RMI, but the combination of them with LR2 and RMI provides a clear improvement of specificity, but unfortunately at the expense of sensitivity.

The present results regarding the superiority of expert opinion are in accordance with previous studies. Timmerman et al. [5] found in their prospective study comparing IOTA-based simple rules, LR1 and LR2, and subjective assessment of the sonologist that expert's opinion is either better or equivalent to the scoring systems.

A weakness of this study is the rather small number of patients, but on the other hand, all the patients were examined by the same investigator, which in turn can be considered to be an advantage. Moreover, the data was assessed by another examiner yielding a very good agreement between both examiners. Another advantage is a quite homogenous patient population, with only four perimenopausal women among 96 postmenopausal patients. A potential bias of the study is that although RMI was originally developed as a triage test for use by a less experienced ultrasound examiner to predict the malignancy of a tumor, in this study it was rather used by an ultrasound expert in parallel with simple rules and LR2 designed to triage patients who should be operated on by a gynecologic oncologist [5, 8]. The main rationale for including also RMI was to provide a reader less experienced in ultrasound, with a familiar comparator for the more specific triage methods.

Table 4 Interobserver agreement between two experts using three-dimensional power Doppler (3DPD) indices

3DPD indices	Expert opinion 1 Median (25–75% quartiles)	Expert opinion 2 Median (25–75% quartiles)	*p*-value[a]
VI	0.337 (0.069–1.098)	0.259 (0.066–0.894)	0.151
FI	31.796 (25.308–35.821)	31.693 (26.351–36.638)	0.839
VFI	0.112 (0.019–0.397)	0.079 (0.019–0.292)	0.257

3DPD Three-dimensional power Doppler; *VI* Vascularization index; *FI* Flow index; *VFI* Vascularization flow index
[a]Calculated by related-samples Wilcoxon signed rank test

CA125 is widely used as a tumor marker for epithelial ovarian cancer. It is quite accurate among postmenopausal women, while the relatively great number of false-positive results limits its utility in premenopausal setting. Our cut-off value was 35 kU/L, whereas some reports have used lower cut-offs, which might explain the lower sensitivity of CA125 (59.4%) in our study. In a review article on seven studies, the pooled sensitivity and specificity of CA125 in postmenopausal women were 85.9 and 85.2%, respectively [17]. We also tested a lower cut-off value of 24 kU/L, which clearly improved sensitivity, while somewhat weakening specificity.

In their original study, Jacobs et al. described a sensitivity of 85% and a specificity of 97% for a RMI cut-off level of 200 [1]. A review of RMI on 13 studies showed that for a cut-off level of 200, the pooled estimate for sensitivity was 78% (95% CI 71–85%) and for specificity was 87% (95% CI 83–91%), which is still better than in our study [18]. The reason for this may be our rather limited sample size, or the fact that the majority of the malignant tumors were of low malignant potential i.e. borderline epithelial, granulosa and Sertoli-Leydig cell tumors, which may have contributed to the less-than-optimal performance of RMI.

An IOTA-based protocol classified a woman as being at high risk for ovarian malignancy if the estimated LR2 risk was at least 25%, at intermediate risk if LR2 was between 5 and 25% and at low risk if LR2 was below 5% [19]. It has been presumed that the LR2-based protocol is more accurate than the RMI-based protocol, and is recommended to be used instead of RMI in discriminating ovarian tumors and concluding treatment protocols [19]. In the multicenter study of Testa et al., LR2 and RMI achieved AUC values of 0.90 and 0.85, respectively in 1,049 postmenopausal patients [6]. The corresponding AUC values in the present study were quite similar, 0.93 and 0.81. We argue that LR2 ≥ 25% risk is the most practical value in clinical work because in our study it achieved a negative predictive value of 94.4%.

Different preoperative scoring systems of ovarian tumors were evaluated in the meta-analysis of Kaijser et al. The pooled sensitivity and specificity of simple rules in five validated studies were found to be 93 and 81%,

Table 5 Diagnostic performances of combined methods to detect malignancy at specific cut-off values

Developed method	Sensitivity %	95% CI	Specificity %	95% CI	PPV %	95% CI	NPV %	95% CI	Accuracy %
RMI > 200 and VFI > 0.31	51.6	33.1–69.9	95.5	87.3–99.1	84.2	60.4–96.6	80.8	70.3–88.8	81.4
Simple rules with expert opinion[a] and VFI > 0.31	71.0	52.0–85.8	95.5	87.3–99.1	88.0	68.8–97.5	87.5	77.6–94.1	86.7
LR2 > 25 and VFI > 0.31	64.5	45.4–80.8	97.0	89.5–99.6	90.9	70.8–98.9	85.3	75.3–92.4	86.5

IOTA International Ovarian Tumor Analysis; *CI* Confidential interval; *PPV* Positive predictive value; *NPV* Negative predictive value; *RMI* Risk of malignancy index; *VFI* Vascularization flow index; *LR2* Logistic regression model 2

[a]Two step-strategy: As a result of inconclusive by simple rules, the expert evaluates the tumor

respectively [20]. However, the inconclusive cases were assessed to be malignant, which differs from our study where in the inconclusive results obtained by the simple rules protocol, the tumors were subjectively classified as being either benign or malignant by the same examiner. This is described as a two-step strategy [6]. In our data 85/98 of tumors were classified correctly by using this two-step strategy. Only three of 13 incorrectly classified tumors were false negative, or they were malignant although they were classified as benign. We reached equivalent results as the meta-analysis by Testa et al., which yielded a sensitivity of 93% and specificity of 83% for the two-step strategy in postmenopausal women [6]. Our results are also in line with a large database of IOTA studies which has shown that the pattern recognition by an experienced clinician is the best method in assessing ovarian tumors [8]. Recently, Piovano et al. showed that when serum CA125 was added to simple rules with subjective assessment for diagnosing ovarian tumors, the diagnostic accuracy increased, with an acceptable cost/benefit ratio [21].

In recent years, several studies have been published, where 3D ultrasound assessment has been used in gynecological cancers, including ovarian cancer. It has been shown that 3DPD vascular indices are elevated in malignant ovarian tumors [22]. Jokubkiene et al. also found this difference, but quantitative 3DPD indices of an ovarian tumor measured by another expert did not add any significant information to subjective quantitation by the original examiner of 2DPD findings [23]. Similarly, Guerriero et al. reported that 3DPD indices failed to improve accuracy as a secondary test for ovarian tumors alongside the evaluation of central vascularization by 2DPD [24]. On the contrary, Geomini et al. found that 3D ultrasonography significantly improved the discrimination of ovarian pathology, when they compared 2D to 3D ultrasound models [25]. Two methods of vascular sampling, manual [22] and spherical [23], have been purported to be alternatives to measuring the vascularity of the whole tumor, but based on our experience, the entire tumor should be taken account. In support of this, Kudla and Alcazar have shown that the size of the sphere volume does not affect power Doppler indices [26].

Our results do not differ from those of the only previous study that compared simple rules and 3DPD. The study of Silvestre et al. assessed 3DPD examination and simple rules in the identification of ovarian tumors [27]. They did not use other preoperative diagnostic methods, and the menopausal status of the patients was ignored. Similar to our study, the ovarian tumors were classified by conventional 2DPD according to IOTA vascular scores. They found that VI and VFI differentiated malignant tumors from benign ones, but they were not more accurate than 2D vascular scores. The use of 3D vascular indices did not decrease the number of false positive results obtained by simple rules.

Conclusions

Combining the 3DPD vascular index VFI with RMI or LR2 may increase the specificity of the diagnostic test, but an ultrasound examination by an experienced clinician still seems to be the most reliable method in the preoperative work-up of ovarian tumors.

Abbreviations

2D: Two-dimensional; 2DPD: Two-dimensional power Doppler; 3D: Three-dimensional; 3DPD: Three-dimensional power Doppler; FI: Flow index; IOTA: International Ovarian Tumors Analysis; LR: Logistic regression model; RMI: Risk of malignancy index; VFI: Vascularization flow index; VI: Vascularization index

Acknowledgements

Not applicable.

Funding

The study was supported by Finnish Cancer Society and Competitive Research Funding of the Tampere University Hospital (Grant 9S040).

Availability of data and materials

The datasets used and analysed during the current study are available and can be provided by the corresponding author upon request.

Authors' contributions

RN did all the ultrasound examinations and wrote the first draft of the manuscript. SS evaluated the stored data as the second investigator and reviewed the manuscript. TL did the statistical analysis. JM presented the original idea, supervised the study, and revised the manuscript. All authors read and approved the final manuscript.

Authors' information

Not applicable.

Competing interests

The authors declare that they have no competing interests.

Consent for publication
Not applicable.

Ethics approval and consent to participate
All participants gave their informed consent to the study, which was approved by the Ethics Committee of Tampere University Hospital (ETL R10080, 6 August 2010).

Publisher's Note

Author details
[1]Department of Obstetrics and Gynecology, Tampere University Hospital, P.O. Box 2000FI-33521 Tampere, Finland. [2]Research and Innovation Center, Tampere University Hospital and Faculty of Social Sciences, University of Tampere, FI-33014 Tampere, Finland. [3]Faculty of Medicine and Life Sciences, University of Tampere, FI-33014 Tampere, Finland.

Received: 22 December 2016 Accepted: 2 March 2017
Published online: 14 March 2017

References

1. Jacobs I, Oram D, Fairbanks J, Turner J, Frost C, Grudzinskas JG. A risk of malignancy index incorporating CA 125, ultrasound and menopausal status for the accurate preoperative diagnosis of ovarian cancer. Br J Obstet Gynaecol. 1990;97(10):922–9.
2. Valentin L, Hagen B, Tingulstad S, Eik-Nes S. Comparison of 'pattern recognition' and logistic regression models for discrimination between benign and malignant pelvic masses: a prospective cross validation. Ultrasound Obstet Gynecol. 2001;18(4):357–65.
3. Timmerman D. The use of mathematical models to evaluate pelvic masses; can they beat an expert operator? Best Pract Res Clin Obstet Gynaecol. 2004;18(1):91–104.
4. Timmerman D, Testa AC, Bourne T, Ameye L, Jurkovic D, Van Holsbeke C, et al. Simple ultrasound-based rules for the diagnosis of ovarian cancer. Ultrasound Obstet Gynecol. 2008;31(6):681–90.
5. Timmerman D, Ameye L, Fischerova D, Epstein E, Melis GB, Guerriero S, et al. Simple ultrasound rules to distinguish between benign and malignant adnexal masses before surgery: prospective validation by IOTA group. BMJ. 2010;341:c6839.
6. Testa A, Kaijser J, Wynants L, Fischerova D, Van Holsbeke C, Franchi D, et al. Strategies to diagnose ovarian cancer: new evidence from phase 3 of the multicentre international IOTA study. Br J Cancer. 2014;111(4):680–8.
7. Timmerman D, Testa AC, Bourne T, Ferrazzi E, Ameye L, Konstantinovic ML, et al. Logistic regression model to distinguish between the benign and malignant adnexal mass before surgery: a multicenter study by the International Ovarian Tumor Analysis Group. J Clin Oncol. 2005;23(34):8794–801.
8. Kaijser J, Bourne T, Valentin L, Sayasneh A, Van Holsbeke C, Vergote I, et al. Improving strategies for diagnosing ovarian cancer: a summary of the International Ovarian Tumor Analysis (IOTA) studies. Ultrasound Obstet Gynecol. 2013;41(1):9–20.
9. Meys EM, Kaijser J, Kruitwagen RF, Slangen BF, Van Calster B, Aertgeerts B, et al. Subjective assessment versus ultrasound models to diagnose ovarian cancer: A systematic review and meta-analysis. Eur J Cancer. 2016;58:17–29.
10. Orre M, Lotfi-Miri M, Mamers P, Rogers PA. Increased microvessel density in mucinous compared with malignant serous and benign tumours of the ovary. Br J Cancer. 1998;77(12):2204–9.
11. Konerding MA, Malkusch W, Klapthor B, van Ackern C, Fait E, Hill SA, et al. Evidence for characteristic vascular patterns in solid tumours: quantitative studies using corrosion casts. Br J Cancer. 1999;80(5-6):724–32.
12. Alcazar JL, Rodriguez D. Three-dimensional power Doppler vascular sonographic sampling for predicting ovarian cancer in cystic-solid and solid vascularized masses. J Ultrasound Med. 2009;28(3):275–81.
13. Timmerman D, Valentin L, Bourne TH, Collins WP, Verrelst H, Vergote I. Terms, definitions and measurements to describe the sonographic features of adnexal tumors: a consensus opinion from the International Ovarian Tumor Analysis (IOTA) Group. Ultrasound Obstet Gynecol. 2000;16(5):500–5.
14. Alcazar JL, Jurado M. Three-dimensional ultrasound for assessing women with gynecological cancer: a systematic review. Gynecol Oncol. 2011;120(3):340–6.
15. Pairleitner H, Steiner H, Hasenoehrl G, Staudach A. Three-dimensional power Doppler sonography: imaging and quantifying blood flow and vascularization. Ultrasound Obstet Gynecol. 1999;14(2):139–43.
16. Brennan P, Silman A. Statistical methods for assessing observer variability in clinical measures. BMJ. 1992;304(6840):1491–4.
17. Wang J, Gao J, Yao H, Wu Z, Wang M, Qi J. Diagnostic accuracy of serum HE4, CA125 and ROMA in patients with ovarian cancer: a meta-analysis. Tumour Biol. 2014;35(6):6127–38.
18. Geomini P, Kruitwagen R, Bremer GL, Cnossen J, Mol BW. The accuracy of risk scores in predicting ovarian malignancy: a systematic review. Obstet Gynecol. 2009;113(2 Pt 1):384–94.
19. Van Calster B, Timmerman D, Valentin L, McIndoe A, Ghaem-Maghami S, Testa AC, et al. Triaging women with ovarian masses for surgery: observational diagnostic study to compare RCOG guidelines with an International Ovarian Tumour Analysis (IOTA) group protocol. BJOG. 2012; 119(6):662–71.
20. Kaijser J, Sayasneh A, Van Hoorde K, Ghaem-Maghami S, Bourne T, Timmerman D, et al. Presurgical diagnosis of adnexal tumours using mathematical models and scoring systems: a systematic review and meta-analysis. Hum Reprod Update. 2014;20(3):449–62.
21. Piovano E, Cavallero C, Fuso L, Viora E, Ferrero A, Gregori G, et al. diagnostic accuracy and cost-effectiveness of different strategies to triage adnexal masses: a prospective study. Ultrasound Obstet Gynecol. 2016; doi: 10.1002/uog.17320.
22. Alcazar JL, Merce LT, Garcia MM. Three-dimensional power Doppler vascular sampling: a new method for predicting ovarian cancer in vascularized complex adnexal masses. J Ultrasound Med. 2005;24(5):689–96.
23. Jokubkiene L, Sladkevicius P, Valentin L. Does three-dimensional power Doppler ultrasound help in discrimination between benign and malignant ovarian masses? Ultrasound Obstet Gynecol. 2007;29(2):215–25.
24. Guerriero S, Ajossa S, Piras S, Gerada M, Floris S, Garau N, et al. Three-dimensional quantification of tumor vascularity as a tertiary test after B-mode and power Doppler evaluation for detection of ovarian cancer. J Ultrasound Med. 2007;26(10):1271–8.
25. Geomini PM, Coppus SF, Kluivers KB, Bremer GL, Kruitwagen RF, Mol BW. Is three-dimensional ultrasonography of additional value in the assessment of adnexal masses? Gynecol Oncol. 2007;106(1):153–9.
26. Kudla MJ, Alcazar JL. Does sphere volume affect the performance of three-dimensional power Doppler virtual vascular sampling for predicting malignancy in vascularized solid or cystic-solid adnexal masses? Ultrasound Obstet Gynecol. 2010;35(5):602–8.
27. Silvestre L, Martins WP, Candido-Dos-Reis FJ. Limitations of three-dimensional power Doppler angiography in preoperative evaluation of ovarian tumors. J Ovarian Res. 2015;8:47. 015-0174-y.

Urinary Polyamines as Biomarkers for Ovarian Cancer

Riikka Johanna Niemi, MD, Antti N. Roine, MD, PhD,† Merja R. Häkkinen, PhD,‡ Pekka S. Kumpulainen, DSc,§ Tuomo A. Keinänen, PhD,‡ Jouko J. Vepsäläinen, PhD,‡ Terho Lehtimäki, MD, PhD,|| Niku K. Oksala, MD, PhD, DSc,¶# and Johanna U. Mäenpää, MD, PhD****

Objectives: Elevated concentrations of polyamines have been found in urine of patients with malignant tumors, including ovarian cancer. Previous research has suffered from poorly standardized detection methods. Our liquid chromatography–tandem mass spectrometry (LC-MS/MS) method is capable of simultaneous standardized analysis of most known polyamines. Liquid chromatography–tandem mass spectrometry has not previously been used in the differential diagnostics of ovarian tumors in postmenopausal women.

Materials and Methods: In this prospective study, postmenopausal women (n = 71) presenting with an adnexal mass and, as controls, women with genital prolapse or urinary incontinence scheduled for surgery (n = 22) were recruited in the study. For analysis of the polyamines, a morning urine sample was obtained before surgery. Preoperative serum CA125 concentrations were determined in the study group.

Results: Twenty-three women with benign and 37 with malignant ovarian tumors were eligible. Of all analyzed polyamines, only urinary N^1,N^{12}-diacetylspermine showed statistically significant differences between all groups except controls versus benign tumors. N^1,N^{12}-diacetylspermine was elevated in malignant versus benign tumors ($P < 0.001$), in high-grade versus low malignant potential tumors ($P < 0.001$), in stage III to IV versus stage I to II cancers ($P < 0.001$), and even in early-stage cancer (stage I–II) versus benign tumors ($P = 0.017$). N^1,N^{12}-diacetylspermine had better sensitivity (86.5%) but lower specificity (65.2%) for distinguishing benign and malignant ovarian tumors than CA125 with a cut-off value of 35 kU/L (sensitivity, 75.7%; specificity, 69.6%).

Conclusions: Urinary N^1,N^{12}-diacetylspermine seems to be able to distinguish benign and malignant ovarian tumors as well as early and advanced stage, and low malignant potential and high-grade ovarian cancers from each other, respectively.

Key Words: LC-MS/MS, Ovarian tumor, Ovarian cancer, DiAcSpm, Polyamine

Received February 6, 2017, and in revised form March 30, 2017.
Accepted for publication April 1, 2017.

(*Int J Gynecol Cancer* 2017;27: 1360–1366)

*Department of Obstetrics and Gynecology, Tampere University Hospital; †Faculty of Medicine and Life Sciences, University of Tampere, Tampere; ‡School of Pharmacy, Biocenter Kuopio, University of Eastern Finland, Kuopio; §Digital Health Solutions; ||Department of Clinical Chemistry, Fimlab Laboratories and Faculty of Medicine and Life Sciences; ¶Department of Surgery, Faculty of Medicine and Life Sciences, University of Tampere; #Department of Vascular Surgery, Tampere University Hospital; and **Department of Obstetrics and Gynecology, Faculty of Medicine and Life Sciences, University of Tampere, Tampere, Finland.

ISSN: 1048-891X
DOI: 10.1097/IGC.0000000000001031

Address correspondence and reprint requests to Riikka Johanna Niemi, MD, Department of Obstetrics and Gynecology, Tampere University Hospital, P.O. Box 2000, FI-33521 Tampere, Finland. E-mail: riikka.niemi@pshp.fi.

This project was financially supported by the Competitive Research Funding of the Tampere University Hospital (grant X51001 to T.L., grant 9S040 to J.M., grant 9S045 to N.O.) and by the strategic funding from University of Eastern Finland (to M.H., T.K., and J.V.), Cancer Foundation of Finland (to J.M., T.L., and N.O.), Elna Kaarina Savolainen's Cancer Research Fund (to N.O.), Seppo Nieminen's Testament Fund (to N.O.), Tampere Tuberculosis Foundation (to N.O.), and Finnish Funding Agency for Technology and Innovation (TEKES) (to N.O.).

The authors declare no conflicts of interest.

N.K.O. and J.U.M. contributed equally in the study.

Ovarian cancer is the leading cause of deaths due to gynecological cancer in the United States and Europe. The lack of specific symptoms makes the diagnosis of ovarian cancer difficult, with ultrasound being typically the first imaging test used to distinguish benign and malignant tumors from each other. Ultrasound features combined with CA125 and menopausal status have been used to calculate the risk of malignancy index.[1] A major problem in ultrasound imaging is the relatively large number of false-positive results. Unfortunately, CA125 antigen lacks sensitivity even in the postmenopausal setting, as it is not expressed by approximately 20% of early-stage ovarian cancers.[2]

Polyamines are molecules essential for nearly all living organisms with critical roles in cell signaling and growth in vertebrates. Putrescine, spermidine, and spermine are the most common polyamines detected in mammals. Polyamines exist in urine mainly in acetylated forms.[3] Increased polyamine concentrations are found during active cellular proliferation, like in patients with cancer.[4] Ovarian cancer was one of the first cancers linked to polyamines.[5] These early studies were hampered by methodological problems, but subsequently, the development of gas chromatography–mass spectrometry enabled quantitation of both free and acetylated polyamines in human urine without hydrolysis of polyamines.[6] Recently, an optimized LC-MS/MS method has been developed, which allows for a simultaneous analysis of up to 14 polyamines in different forms in urine.[7]

The present study was undertaken as a proof of concept study to explore the usefulness of LC-MS/MS in differential diagnostics of ovarian tumors.

MATERIALS AND METHODS

Patients

From May 2013 to March 2016, 71 patients presenting with an abnormal adnexal mass and scheduled for surgery at the Department of Obstetrics and Gynecology of Tampere University Hospital were prospectively recruited to the study. They had to be at least 50 years old, and the only exclusion criterion was an ongoing treatment for cancer. Besides pelvic examination, a vaginal ultrasound scan was performed, and a serum sample for CA125 was obtained from each patient. The final sample size was 60 patients, after exclusion of ineligible patients (Fig. 1).

Twenty-two postmenopausal women scheduled for surgery because of genital prolapse or urinary incontinence from May 2013 to April 2014 were recruited as controls. One patient of the control group had to be excluded because of an incidental endometrial adenocarcinoma. All subjects provided a morning urine sample at the day of operation. The samples were stored at −70°C until analysis for polyamines.

All participants gave their informed consent to the study, which was approved by the ethics committee of Tampere University Hospital (ETL R10066).

Liquid Chromatography–Tandem Mass Spectrometry Analysis

The LC-MS/MS analysis was conducted at the University of Eastern Finland (Kuopio, Finland) and was performed using the previously described method.[7] In short, the chromatographic

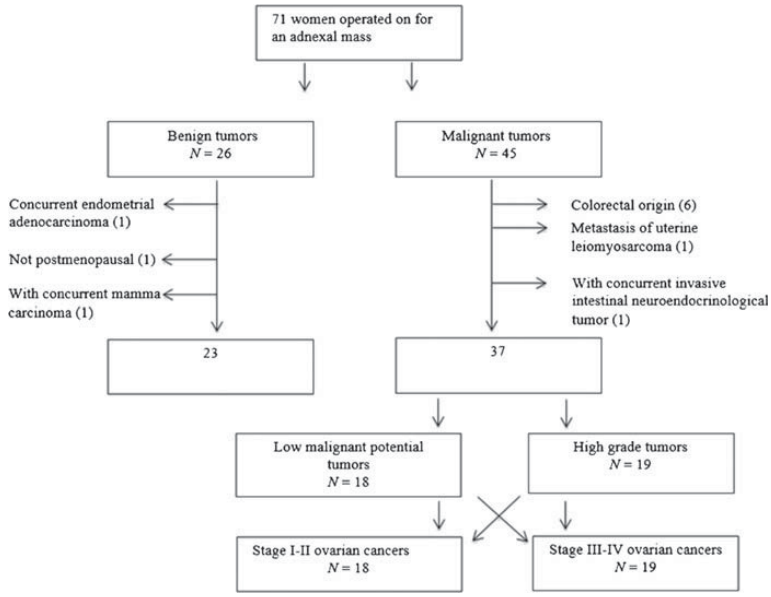

FIGURE 1. Study population.

separations were carried out using a reversed phase column (Phenomenex Kinetex C18 150 × 2.1 mm, 2.6 μm) and 0.1% heptafluorobutyric acid as the evaporative ion-pairing reagent. Detection was performed with Agilent 6410 triple quadrupole mass spectrometry equipped with an electrospray ionization source and using selected reaction monitoring method. Deuterated polyamines were used as stable internal standards in quantification. Polyamine concentrations were normalized using creatinine concentration. The concentrations are expressed as micromole of polyamine per gram of creatinine.

The creatinine concentrations of the urine samples were determined enzymatically using Cobas 6000, C 501-module (Roche diagnostics GmbH, Mannheim, Germany) at Fimlab Laboratories.

Statistical Analysis

No formal sample size calculations were made because of the preliminary nature of the study. The statistical analysis was performed by using MATLAB Version R2016b. The normality of the distributions of continuous variables was evaluated by Kolmogorov-Smirnov tests. Due to the skewness of the distributions, the differences in polyamine concentrations between the distinct groups were analyzed by Wilcoxon rank sum test. The differences in the concentrations of polyamines are visualized by box plots. A probability value of less than 0.05 was considered as statistically significant. All tests were two-sided. To compare the predictive performance of diacetylspermine (DiAcSpm) and CA125, a receiver operating characteristics analysis was accomplished.

RESULTS

Patients and Tumors

All 81 women in the final study population were older than 50 years and postmenopausal. The median age (75 years; range, 55–83 years) in the control group was significantly higher than in the groups with benign (65 years; range, 51–73 years) and malignant tumors (64 years; range, 51–86 years), respectively ($P = 0.02$). Three of the controls and 4 of the cases had used systemic hormonal therapy before surgery. Five patients (1 in the control group, 1 with a benign, and 3 with a malignant ovarian tumor) had previously been treated for breast cancer and 1 patient (with a malignant ovarian tumor) for thyroid cancer, but all of them were disease free at the time of sampling.

Of the ovarian tumors, 23 were benign and 37 were malignant (Fig. 1). The benign group consisted of 11 serous and 2 mucinous cystadenomas, 2 fibromas, 5 simple and 2 endometriotic cysts, and 1 necrotized cyst. Eighteen of the malignant tumors were of low malignant potential (4 serous and 5 mucinous borderline tumors, 3 mucinous adenocarcinomas, 4 granulosa cell tumors, 1 Sertoli-Leydig cell tumor, and 1 endometrioid adenocarcinoma). Eighteen of the high-grade tumors were serous carcinomas (HGSC) and one was a carcinosarcoma. One of the patients with HGSC had 2 primary tumors, or the stage IIIC ovarian cancer and an invasive ductal grade 3 breast cancer, which were operated on at the same session.

The median serum concentrations of CA125 were 18.0 kU/L (range, 5–1984), 53.5 kU/L (range, 7–841), and 546.0 kU/L (range, 22–8152) in the patients with benign tumors, with low malignant potential tumors, and with high-grade tumors, respectively. The difference of the tumor marker concentration between the groups was statistically significant ($P < 0.001$).

Urinary Polyamines and Their Metabolites

The polyamines and their metabolites detected by the LC-MS/MS are given in Table 1. Six polyamines or acetylated putrescine, acetylated cadaverine, N^1-acetylated spermidine (N^1AcSpd), N^8-acetylated spermidine (N^8AcSpd), N^1,N^8-diacetylspermidine (DiAcSpd), and DiAcSpm were constantly found in all urine samples, but only DiAcSpm showed statistically significant differences between all groups except between controls and benign ovarian tumors (Figs. 2, 3). The polyamine concentrations were independent of body mass index (data not shown).

A detailed description of the urinary concentrations of DiAcSpm in different settings is given in Table 2. There were no differences between the women with genital prolapse or urinary incontinence and the women with benign tumors. Of the women with malignant tumors, the ones with high-grade and advanced stage tumors had the highest urinary concentrations of DiAcSpm. However, the concentrations were significantly higher also in women with low malignant potential and early-stage tumors than in the controls.

Besides DiAcSpm, there was also a significant difference in concentrations of DiAcSpd, N^1AcSpd, and N^8AcSpd between low malignant potential and high-grade malignant ovarian tumors ($P = 0.02$, 0.004 and 0.013, respectively) and between benign and malignant ovarian tumors in concentrations of DiAcSpd and N^8AcSpd ($P = 0.015$ and 0.042).

Performance of CA125 and Urinary DiAcSpm

In distinguishing benign tumors from the malignant ones, the specificity and sensitivity of CA125 (using the standard used cut-off value 35 kU/L) were 69.6% and 75.7%, respectively. Correspondingly, the specificity of DiAcSpm (cut-off value of 0.097 μmol/g creatinine) was 65.2% and sensitivity 86.5% (Fig. 4).

DISCUSSION

The main finding of this preliminary study was that urinary concentrations of DiAcSpm are elevated among postmenopausal women with malignant ovarian tumors as compared with women with benign ovarian tumors or genital prolapse. Although DiAcSpm concentrations were higher in the case of high-grade and advanced stage cancers than among low malignant potential and early-stage cancers, respectively, there was still a statistically significant difference in DiAcSpm levels between early-stage (and low malignant potential) and benign tumors.

Previous studies used methodology with limited polyamine array and were unable to measure all polyamines in a single run, which deteriorated repeatability and increased variability of different studies. Another limitation was that acetylated polyamines, which are highly specific for malignant disease, could not be measured. Consequently, the earlier

TABLE 1. The polyamines studied and their urinary concentrations (micromole per gram creatinine) in patients with ovarian tumors and in controls

	Controls (n = 21)		Benign Ovarian Tumors (n = 23)		Low-Grade Malignant Tumors (n = 18)		High-Grade Malignant Ovarian Tumors (n = 19)	
Polyamine	Creatinine, Range, μmol/g	Detection Rate	Creatinine, Range, μmol/g	Detection Rate	Creatinine, Range, μmol/g	Detection Rate	Creatinine, Range, μmol/g	Detection Rate
Cad	NA–2.65	13/21	NA–3.94	19/23	NA–20.19	15/18	NA–48.7	9/19
AcCad	0.04–5.64	21/21	0.08–14.26	23/23	0.11–13.08	18/18	0.17–5.57	19/19
DiAcCad	NA–0.48	13/21	NA–0.28	18/23	NA–1.79	12/18	NA–0.63	8/19
AcPut	6.57–19.28	21/21	5.60–28.1	23/23	9.15–41.45	18/18	8.54–50.16	19/19
DiAcPut	NA–0.24	17/21	NA–0.62	18/23	NA–0.75	16/18	NA–0.25	17/19
Spd	NA–0.30	20/21	0.08–0.27	23/23	0.10–0.28	18/18	0.09–0.56	19/19
N^1AcSpd	1.78–8.92	21/21	1.04–8.17	23/23	1.39–6.50	18/18	2.52–18.50	19/19
N^8AcSpd	1.84–4.75	21/21	1.15–4.69	23/23	1.65–5.03	18/18	2.18–5.99	19/19
DiAcSpd	0.18–0.65	21/21	0.14–1.32	23/23	0.16–1.34	18/18	0.23–1.20	19/19
Spm	NA–0.55	8/21	NA–0.45	12/23	NA–0.25	12/18	NA–0.32	14/19
AcSpm	NA–0.01	3/21	NA–0.01	4/23	NA–0.004	1/18	NA–0.04	7/19
DiAcSpm	0.06–0.20	21/21	0.04–1.02	23/23	0.06–0.37	18/18	0.14–2.37	19/19

NA indicates that analyzed concentration was below the lowest calibration point.

AcSpm, acetylated spermine; Cad, cadaverine; AcCad, acetylated cadaverine; DiAcCad, diacetylated cadaverine; AcPut, acetylated putrescine; DiAcPut, diacetylated putrescine; DiAcSpm, N^1,N^{12}-diacetylspermine.

research focused on less specific unacetylated polyamines.[8] Many methods rely on derivatization techniques where polyamines are conjugated with other molecules to allow extraction and analysis.[9] This technique is not suitable for the analysis of diacetylated polyamines due to acetylation of active amino groups. Our LC-MS/MS method optimized for

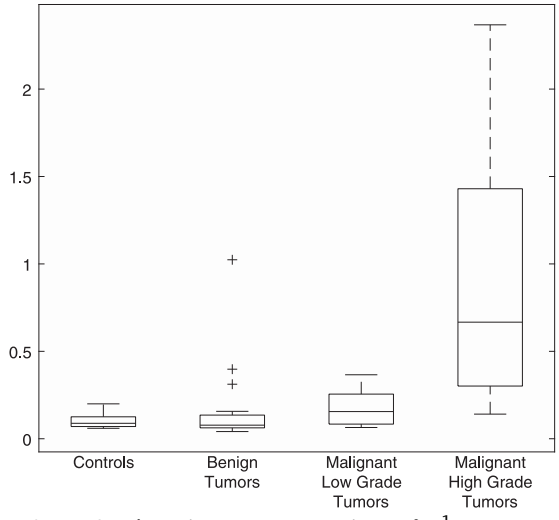

FIGURE 2. The urinary concentrations of N^1, N^{12}-diacetylspermine (DiAcSpm) (micromole per gram creatinine) in controls and in patients with ovarian tumors.

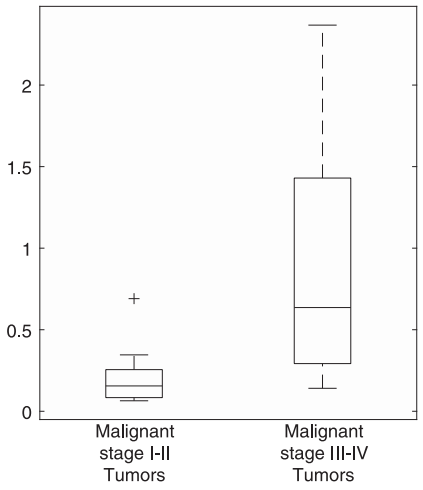

FIGURE 3. The urinary concentrations of N^1, N^{12}-diacetylspermine (DiAcSpm) (micromole per gram creatinine) in the women with stage I to II and stage III to IV ovarian tumors.

TABLE 2. The urinary concentrations of N^1,N^{12}-diacetylspermine (DiAcSpm) (micromole per gram creatinine) in patients with ovarian tumors and in controls and comparisons between the groups

	N^1,N^{12}-diacetylspermine, μmol/g creatinine					
	Mean (SD)	**Median**	**Minimum**	**Maximum**	**Comparison**	***P***
Controls	0.10 (0.04)	0.09	0.06	0.20	Versus benign tumors	NS
Benign tumors	0.15 (0.21)	0.08	0.04	1.02		
All malignant tumors	0.54 (0.62)	0.26	0.06	2.37	Versus benign tumors	<0.001
					Versus controls	<0.001
Low malignant potential tumors	0.17 (0.09)	0.16	0.06	0.37	Versus benign tumors	0.020
High-grade tumors	0.89 (0.72)	0.67	0.14	2.37	Versus low malignant potential tumors	<0.001
Stage I–II tumors	0.19 (0.15)	0.16	0.06	0.69	Versus benign tumors	0.017
Stage III–IV tumors	0.87 (0.72)	0.64	0.14	2.37	Versus Stage I–II tumors	<0.001

NS, not significant.

noninvasive and standardized single-run analysis of urine can be used for simultaneous analysis of up to 14 polyamines in free, mono- and diacetylated forms in human urine, without any derivatization.[7] In the present study, however, 1,3-diaminopropane and putrescine were not detectable. In addition, results concerning diacetylated cadaverine and diacetylated putrescine should be interpreted with caution, because their analysis is only semiquantitative.[7]

Although we are not aware of any subsequent studies since the report by Suh et al,[10] on the urinary polyamine profile in ovarian cancer, our results are in accordance with previous experience with other tumors. Patients with non-Hodgkin lymphoma or urogenital cancer (testicular, prostatic, renal, and bladder carcinoma) have been found to have elevated urinary concentrations of DiAcSpm and those with urogenital cancer also of DiAcSpd.[6,11–13] In breast cancer, even early-stage disease seems to be associated with elevated levels of DiAcSpm in the urine.[13] In colon cancer, urinary DiAcSpm may be a better tumor marker than carcinoembryonic antigen or cancer antigen 19-9.[13,14] Besides being predictive markers, there is a possibility that DiAcSpm and DiAcSpd could be used also as prognostic markers, at least in testicular or prostatic cancer.[11] Urinary DiAcSpm has been shown to be both diagnostic and prognostic marker also for nonsmall cell lung cancer.[15,16]

In the present study, the performance of CA125 used in the preoperative diagnostic work-up of pelvic tumors was poorer than in published large screening studies.[1,17–20] The reason may be by chance only due to the rather limited sample size, but the fact that a large portion of the malignant tumors were of low malignant potential or borderline epithelial, granulosa, and Sertoli-Leydig cell tumors may have contributed to the less than optimal performance. In any case, urinary DiAcSpm was a more sensitive marker of malignant ovarian tumors than CA125 with a cut-off value 35 kU/L, while being less specific.

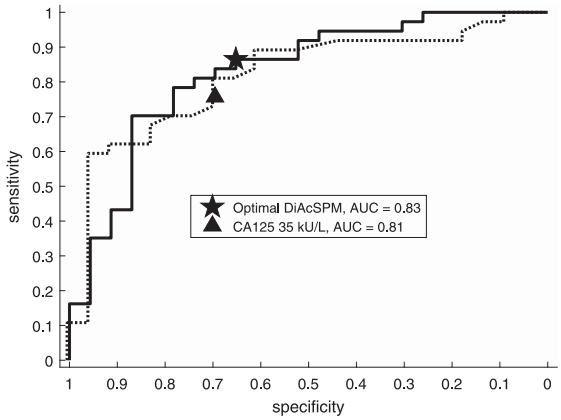

FIGURE 4. Receiver operating characteristic curves for urinary N^1,N^{12}-diacetylspermine (DiAcSpm) and CA125 in benign and malignant ovarian tumors with optimal (DiAcSpm 0.097 μmol/g creatinine) and typically used (CA125 35 kU/L) thresholds.

Although the mechanism underlying elevated concentrations of DiAcSpm in the urine of patients with cancer is not completely understood, an increased synthesis of polyamines in proliferating cells, including malignant cells, is well documented. It has been suggested that the increased secretion of DiAcSpm may reflect a defense mechanism by the organism to lower intracellular polyamine concentrations by acetylating and excreting polyamines and hence decreasing the growth rate of the tumor.[8,13,21] It has also been purported that the production of DiAcSpm in tumorigenesis may be a result of host macrophage activation.[22]

The results of the present study are to be considered as preliminary, to be confirmed in larger patient cohorts. Chronic inflammatory diseases may influence DiAcSpm concentrations. However, in the study of pancreatico-biliary diseases, the levels of DiAcSpm in urine were lower in benign inflammatory conditions than in cancers.[23] Presence of urinary tract infection may also have a confounding influence on urinary polyamines, increasing especially the level of putrescine.[24] The impact of infection cannot totally be ruled out in the present study, because a routine urine sample for diagnosing urinary infection was taken only from the patients of the control group. Moreover, cadaverine in human urine is suggested to be derived from the gut microbial flora.[24] A limitation of the study is that there were no patients with a benign teratoma, because among benign tumors, teratomas have been associated with elevated levels of urinary polyamines.[5] On the other hand, teratomas are typically tumors of adolescents and young adults and not of postmenopausal women, the risk population for ovarian cancer.

Ornithine decarboxylase is one of the key enzymes in polyamine synthesis and is stimulated by estrogens in estrogen-responsive tissues.[25] A previous study found that urinary DiAcSpm values are higher in women than in men, whereas postmenopausal women had lower concentrations than premenopausal ones.[26] Accordingly, Byun et al[27] showed that patients with premenopausal breast cancer had higher (free and monoacetylated) polyamine levels in serum than postmenopausal ones, whose polyamine levels were similar to healthy controls. In our study, all women were postmenopausal, but 7 of them used hormone replacement therapy, creating a potential bias. However, excluding these patients did not alter the results. The control women were older than the ones with tumors, which may have had impact on the results. However, there was no significant difference between DiAcSpm levels of control group and women with benign ovarian tumors. One patient in the malignant tumor group had been treated for breast cancer for 5 years, but she had no signs of recurrence. Another patient had a grade 3 breast cancer concurrently with the stage IIIC HGSC, which may have affected her DiAcSpm level. However, her urinary level of DiAcSpm was of similar magnitude as in the patients with advanced high-grade tumors in general.

We used a morning urine sample in our study, which, however, may not have been necessary. According to a study on healthy people, a spot urine sample at any time of the day represents the true excretion rate of DiAcSpm after creatinine normalization.[26] Although the LC-MS/MS method is very accurate, it is as such not suitable for routine clinical use, at least not for time being.[7] However, if only 1 (DiAcSpm) or a few polyamines need to be analyzed, the analysis could probably be made faster and less expensive to perform. Alternative methods to measure only urinary DiAcSpm in routine clinical practice include an enzyme-linked immunosorbent assay[13,28] or a colloidal gold aggregation procedure.[29]

In conclusion, urinary levels of DiAcSpm were elevated in patients with malignant ovarian tumors, even in patients with tumors of low malignant potential and early-stage tumors. These preliminary findings suggest that urinary DiAcSpm may in the future become a useful diagnostic marker for malignant ovarian tumors in the postmenopausal setting.

ACKNOWLEDGMENT

The authors thank Mrs Tuula Reponen for the technical assistance.

REFERENCES

1. Jacobs I, Oram D, Fairbanks J, et al. A risk of malignancy index incorporating CA 125, ultrasound and menopausal status for the accurate preoperative diagnosis of ovarian cancer. *Br J Obstet Gynaecol*. 1990;97:922–929.
2. Bast RC Jr. Status of tumor markers in ovarian cancer screening. *J Clin Oncol*. 2003;21:200s–205s.
3. Muskiet FA, Dorhout B, van den Berg GA, et al. Investigation of polyamine metabolism by high-performance liquid chromatographic and gas chromatographic profiling methods. *J Chromatogr B Biomed Appl*. 1995;667:189–198.
4. Gerner EW, Meyskens FL Jr. Polyamines and cancer: old molecules, new understanding. *Nat Rev Cancer*. 2004;4:781–792.
5. Russell DH, Levy CC, Schimpff SC, et al. Urinary polyamines in cancer patients. *Cancer Res*. 1971;31:1555–1558.
6. van den Berg GA, Muskiet FA, Kingma AW, et al. Simultaneous gas-chromatographic determination of free and acetyl-conjugated polyamines in urine. *Clin Chem*. 1986;32:1930–1937.
7. Häkkinen MR, Roine A, Auriola S, et al. Analysis of free, mono- and diacetylated polyamines from human urine by LC-MS/MS. *J Chromatogr B Analyt Technol Biomed Life Sci*. 2013;941:81–89.
8. Kawakita M, Hiramatsu K. Diacetylated derivatives of spermine and spermidine as novel promising tumor markers. *J Biochem*. 2006;139:315–322.
9. Byun JA, Lee SH, Jung BH, et al. Analysis of polyamines as carbamoyl derivatives in urine and serum by liquid chromatography-tandem mass spectrometry. *Biomed Chromatogr*. 2008;22:73–80.
10. Suh JW, Lee SH, Chung BC, et al. Urinary polyamine evaluation for effective diagnosis of various cancers. *J Chromatogr B Biomed Sci Appl*. 1997;688:179–186.
11. Hiramatsu K, Sugimoto M, Kamei S, et al. Diagnostic and prognostic usefulness of N1,N8-diacetylspermidine and N1,N12-diacetylspermine in urine as novel markers of malignancy. *J Cancer Res Clin Oncol*. 1997;123:539–545.
12. Sugimoto M, Hiramatsu K, Kamei S, et al. Significance of urinary N1,N8-diacetylspermidine and N1, N12-diacetylspermine as indicators of neoplastic diseases. *J Cancer Res Clin Oncol*. 1995;121:317–319.
13. Hiramatsu K, Takahashi K, Yamaguchi T, et al. N(1), N(12)-Diacetylspermine as a sensitive and specific novel

marker for early- and late-stage colorectal and breast cancers. *Clin Cancer Res*. 2005;11:2986–2990.
14. Umemori Y, Ohe Y, Kuribayashi K, et al. Evaluating the utility of N1,N12-diacetylspermine and N1, N8-diacetylspermidine in urine as tumor markers for breast and colorectal cancers. *Clin Chim Acta*. 2010;411:1894–1899.
15. Takahashi Y, Sakaguchi K, Horio H, et al. Urinary N1, N12-diacetylspermine is a non-invasive marker for the diagnosis and prognosis of non-small-cell lung cancer. *Br J Cancer*. 2015;113:1493–1501.
16. Kato M, Onishi H, Matsumoto K, et al. Prognostic significance of urine N1, N12-diacetylspermine in patients with non-small cell lung cancer. *Anticancer Res*. 2014;34:3053–3059.
17. Jacobs I, Bast RC Jr. The CA 125 tumour-associated antigen: a review of the literature. *Hum Reprod*. 1989;4:1–12.
18. Patsner B, Mann WJ. The value of preoperative serum CA 125 levels in patients with a pelvic mass. *Am J Obstet Gynecol*. 1988;159:873–876.
19. Einhorn N, Sjövall K, Knapp RC, et al. Prospective evaluation of serum CA 125 levels for early detection of ovarian cancer. *Obstet Gynecol*. 1992;80:14–18.
20. Markowska J, Manys G, Kubaszewska M. Value of CA 125 as a marker of ovarian cancer. *Eur J Gynaecol Oncol*. 1992;13:360–365.
21. Park MH, Igarashi K. Polyamines and their metabolites as diagnostic markers of human diseases. *Biomol Ther (Seoul)*. 2013;21:1–9.
22. Hamaoki M, Nagata A. Host macrophages produce diacetylspermine related with tumorigenesis. *Cancer Lett*. 2006;243:128–134.
23. Yamaguchi K, Nakamura M, Shirahane K, et al. Urine diacetylspermine as a novel tumour maker for pancreatobiliary carcinomas. *Dig Liver Dis*. 2005;37:190–194.
24. Satink HP, Hessels J, Kingma AW, et al. Microbial influences on urinary polyamine excretion. *Clin Chim Acta*. 1989;179:305–314.
25. Russell DH, Taylor RL. Polyamine synthesis and accumulation in the castrated rat uterus after estradiol-17-beta stimulation. *Endocrinology*. 1971;88:1397–1403.
26. Hiramatsu K, Sakaguchi K, Fujie N, et al. Excretion of N(1), N(12)-diacetylspermine in the urine of healthy individuals. *Ann Clin Biochem*. 2014;51:459–467.
27. Byun JA, Choi MH, Moon MH, et al. Serum polyamines in pre- and post-operative patients with breast cancer corrected by menopausal status. *Cancer Lett*. 2009;273:300–304.
28. Hiramatsu K, Miura H, Kamei S, et al. Development of a sensitive and accurate enzyme-linked immunosorbent assay (ELISA) system that can replace HPLC analysis for the determination of N1,N12-diacetylspermine in human urine. *J Biochem*. 1998;124:231–236.
29. Kawakita M, Hiramatsu K, Yanagiya M, et al. Determination of N(1),N(1)(2)-diacetylspermine in urine: a novel tumor marker. *Methods Mol Biol*. 2011;720:367–378.

Gynecologic Oncology 151 (2018) 519–524

Contents lists available at ScienceDirect

Gynecologic Oncology

journal homepage: www.elsevier.com/locate/ygyno

FAIMS analysis of urine gaseous headspace is capable of differentiating ovarian cancer

Riikka J. Niemi [a,*], Antti N. Roine [b], Emmi Eräviita [b], Pekka S. Kumpulainen [c], Johanna U. Mäenpää [a,b], Niku Oksala [b,d]

[a] Department of Obstetrics and Gynecology, Tampere University Hospital, P.O. Box 2000, 33521 Tampere, Finland
[b] Faculty of Medicine and Life Sciences, University of Tampere, P.O. Box 100, 33014 Tampere, Finland
[c] Faculty of Biomedical Sciences and Engineering, Tampere University of Technology, P.O. Box 527, 33101 Tampere, Finland
[d] Department of Vascular Surgery, Tampere University Hospital, P.O. Box 2000, 33521 Tampere, Finland

HIGHLIGHTS

- Analysis of volatile organic compounds (VOCs) offers a new diagnostic method.
- VOCs from urine can be analyzed by FAIMS (field asymmetric ion mobility spectrometry).
- FAIMS distinguished urine from ovarian cancer patients compared to controls.
- Patients with high vs. low grade ovarian cancer have also different VOC signatures.

ARTICLE INFO

Article history:
Received 26 July 2018
Received in revised form 15 September 2018
Accepted 18 September 2018
Available online 23 September 2018

Keywords:
FAIMS
Ovarian neoplasm
Ovarian cancer
VOC
Owlstone Lonestar
Urine

ABSTRACT

Aim. We hypothesized that field asymmetric waveform ion mobility spectrometry (FAIMS) as a novel artificial olfactory technology could differentiate urine of women with malignant ovarian tumors from controls and women with benign tumors, based on previous findings on the ability of canine olfactory system to "smell" cancer.

Patients and methods. Preoperative urine samples from 51 women with ovarian tumors, both benign and malignant, and from 18 women with genital prolapse, as controls, were collected. The samples were analyzed by FAIMS device. Data analysis was processed by quadratic data analysis (QDA) and linear discriminant analysis (LDA), and cross-validated using 10-fold cross-validation.

Results. Thirty-three women had malignant ovarian tumors, of which 18 were high-grade cancers. FAIMS distinguished controls from malignancies with the accuracy of 81.3% (sensitivity 91.2% and specificity 63.1%), and benign tumors from malignancies with the accuracy of 77.3% (sensitivity 91.5% and specificity 51.4%). Moreover, low grade tumors were also separated from high grade cancers and benign ovarian tumors with accuracies of 88.7% (sensitivity 87.8% and specificity 89.6%) and 83.9% (sensitivity 73.1% and specificity 92.9%), respectively.

Conclusions. This proof of concept-study indicates that the FAIMS from urine has potential to discriminate malignant ovarian tumors from no tumor-bearing controls and benign tumors.

1. Introduction

Annually 22,000 new ovarian cancer (OC) cases are diagnosed in the United States, and the survival rates are poor due to the majority of OCs being detected at advanced stages [1]. While early diagnosis and adequate cytoreductive surgery improve prognosis, there is a need for better preoperative diagnostic methods for ovarian tumors.

Various ultrasound-based models have been developed for preoperative evaluation of ovarian masses. These include e.g. Risk of Malignancy Index (RMI) [2] and logistic regression analyses and ultrasound-based rules from the International Ovarian Tumor Analysis (IOTA)-study. Although they have relatively high sensitivity and specificity, they are non-applicable for about 20% of tumors [3].

Studies on urinary biomarkers for OC are relatively sparse. Urinary protein biomarkers, human epididymis protein 4 (HE4) and mesothelin, have shown to improve the early detection of serous OC compared to serum biomarkers [4]. Metabolite changes related to OC have been discovered as potential biomarkers [5,6], like N^1,N^{12}-diacetylspermine in

* Corresponding author at: Tampere University Hospital, Department of Obstetrics and Gynecology, P.O. Box 2000, FI-33521 Tampere, Finland.
E-mail address: riikka.niemi@fimnet.fi (R.J. Niemi).

https://doi.org/10.1016/j.ygyno.2018.09.016
0090-8258/

polyamine analyses [7]. In addition, circulating microRNAs have been shown to be abundant in urine of OC patients [8].

Many diseases are linked to distinct odors caused by volatile organic compounds (VOCs) released into exhaled air, urine, blood and stool [9]. Horvath et al. trained dogs to discriminate OC patients and healthy controls from tissue samples [10] and blood samples from cancer patients [11] with high accuracy. The costly training, limited working capacity and cultural factors have prevented the use of "sniffer dogs" in the clinic. Artificial olfaction with electronic devices could be easier to validate and adopt into clinical practice [9].

Gas chromatography-mass spectrometry (GC–MS) has been used extensively in analysis of VOCs but it involves complex technology and has high costs. Electronic nose (eNose) technology provides a more economical and simpler way to qualitatively analyze VOCs. The technology mimics the working principle of mammalian olfactory system (Fig. 1). Ion mobility spectrometry (IMS) works according to the same principles, providing a qualitative VOC spectrum from the sample. Field asymmetric waveform IMS (FAIMS) is a modern and sensitive variant of IMS providing a high sensitivity and stability [12]. The working principle of FAIMS is illustrated in Fig. 2.

There is mounting evidence of the potential of eNose devices in detection of cancer from various sample media [12]. FAIMS specifically has previously been shown to detect colorectal and pancreatic cancers from urine [13,14]. Detection of OC has been only attempted from cancer tissue [15]. Urine is a promising sampling method since it can be obtained non-invasively.

We hypothesized that FAIMS would be capable of differentiating the urine of women with OC from benign ovarian tumors and controls.

2. Materials and methods

2.1. Subjects and study design

Between May 2013 and March 2016, 60 women with an adnexal tumor scheduled for surgery gave a morning urine sample in the operation day at the Department of Obstetrics and Gynecology of Tampere University Hospital. They were all postmenopausal, and none of them had an ongoing treatment for cancer. After operation nine tumors were excluded due to their non-ovarian origin or a concurrent malignant tumor. The final sample size after exclusions was 51. Eighteen women scheduled for urinary incontinence or genital prolapse surgery were recruited as controls. The samples were stored at −70 °C until analysis. Because of the proof-of-concept nature of the study, no power calculations could be done. The size of the study population was based on the experience from previous studies with similar technology [16].

The samples were defrosted and analyzed using Owlstone Lonestar (Owlstone Inc., Cambridge, United Kingdom) device which uses FAIMS technique. The sensor was coupled with ATLAS sampling unit (Owlstone Inc., Cambridge, United Kingdom) that standardizes the analytical conditions by controlling the temperature and dilution of the VOCs evaporated from the sample.

2.2. Protocol of FAIMS

For FAIMS analysis, we used settings previously described by Arasaradnam et al. [13]. The step-by-step analysis protocol was as follows:

1) Urine samples were first thawed at room temperature and analyzed in random order.
2) A 5 ml urine sample was aliquoted to a 30 ml glass vial and warmed to 40 °C.
3) Once the sample achieved the target temperature, three consecutive scans were conducted to minimize the effect of scan-to-scan variation.
4) After the analysis, the sample vial was removed from the sampling unit and a vial of 5 ml of purified water was placed in to the chamber.
5) The vapour released from the purified water acts as a cleaning agent that removes the carry-over effect of trace VOCs from the urine sample that are retained in the sensor. Five consecutive scans with purified water were conducted.

The next urine sample was placed to the sampling chamber and the process was repeated. To ensure stable and clean carrier gas for the system, we utilized standard pressurized clean air that was cleaned from residual humidity with a silica gel filter and from residual VOCs with activated charcoal filter before entering the system. We used the flow settings recommended by the manufacturer for urine samples: The flow rate over the sample was 500 ml/min, which was mixed to 2000 ml/min stream of clean air for a total flow of 2500 ml/min for the sensor. The FAIMS scanning settings used were also ones provided by the manufacturer: Dispersion field from 0 to 90% was scanned in 51 steps and compensation voltage from −6 to +6 V was scanned in 512 steps. Each scan contains two ion windows, one for negative and one for positive ions. One window is produced by the negative ions

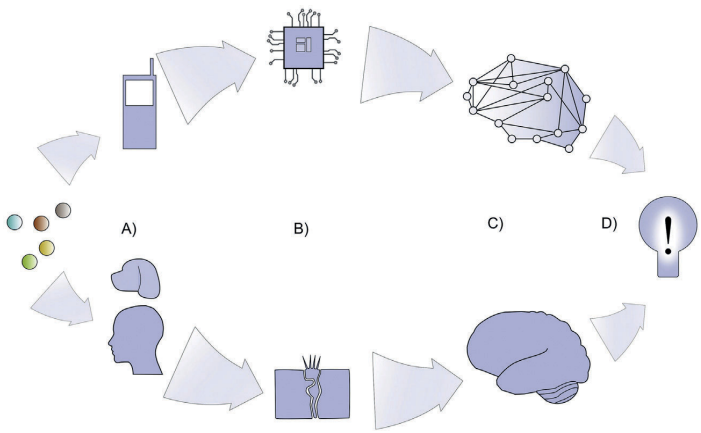

Fig. 1. The working principle of mammary and eNose compared A) VOCs enter a sampling unit where the humidity, the temperature and the concentration of the sample are optimized. B) Optimized sample enters the sensor unit where different VOCs attach to different areas of the sensor and produce electrical currents. C) Electrical currents are referred to a computing system for analysis where they are associated with previously gathered information. D) A result of the analysis is produced.

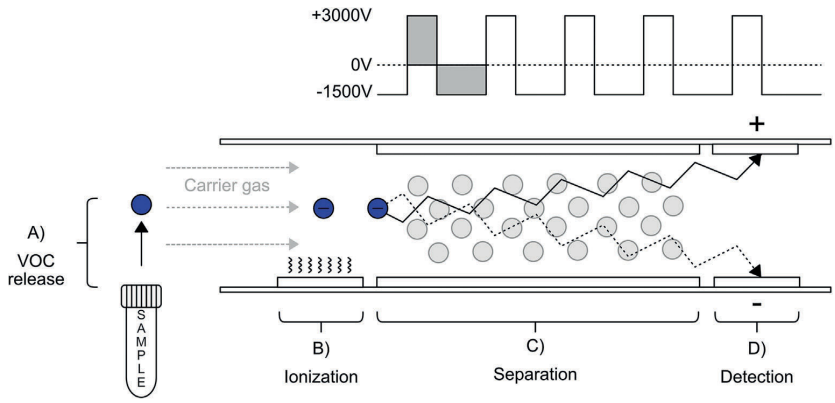

Fig. 2. Illustration on the working principle of FAIMS A) Sample vial is placed in to the sampling chamber where VOCs are released from the sample. VOCs are then transferred to the analyzer by clean air flow. B) In the analyzer, VOCs are first ionized by a radioactive isotope and gain electrical charge. C) Ionized VOCs enter separation area where they are alternately exposed to high and low electric fields between the electric plates. The plates also have a baseline compensation voltage that is periodically adjusted. The different properties of VOCs cause them to travel at different speed in the separation chamber and behave differently in high and low electric fields. This results in separation of the VOCs according to their charge, shape and mass. D) At the last stage of the analysis, VOCs collide with detectors, creating electric currents that create a unique spectrum for each molecular mixture.

that collide the positive detector and the other is produced by the positive ions that collide the negative detector, respectively. The detectors are illustrated in Fig. 2.

The ion window is a spectrum that has compensation voltage on the X axis and dispersion field on the Y axis as seen in Fig. 3. The compensation voltage is the base voltage between the electric plates in the separation part of the FAIMS sensor. This biases the ion flow either towards negative or positive plate. The dispersion field strength represents the strength of the electrical field between the plates as a percentage of the maximum field that can be created by the system. The ion window is compiled by adjusting the dispersion field strength stepwise and on each step scanning the selected compensation voltage range at each step. The scans were saved on the hard drive of the Lonestar system from which they were transferred to an USB drive for statistical analysis.

2.3. Statistical methods

The last of the three scans from the urine sample was found to be equal in performance when compared to the average of three scans, and was taken for analysis. One scan consists of a matrix of 52,200 measurement values, including both positive and negative ion window. The areas with no response were removed and the remaining signal was downsampled, selecting every other line and column of the scan, leaving 1536 points for each measurement.

Forward feature selection with linear discriminant analysis (LDA) and quadratic discriminant analysis (QDA) were utilized to find discriminating features from each group. Both LDA and QDA seek a classifier that is optimal for discrimination of the groups. LDA is a special case of QDA where the covariance of each group is assumed to be equal which results in a linear discriminator whereas QDA allows the covariances to differ which also enables quadratic, parable-shaped discriminators. Because LDA is a simpler method, it is preferred as the first option to test. The results were cross-validated by 10-fold cross-validation to avoid overfitting. In this method, the dataset is divided into 10 groups. One group is then excluded from the dataset and the remaining nine groups are used to create the classification parameters as the training set. The excluded group is then classified using these parameters. Since, due to random division for the cross validation, the classification

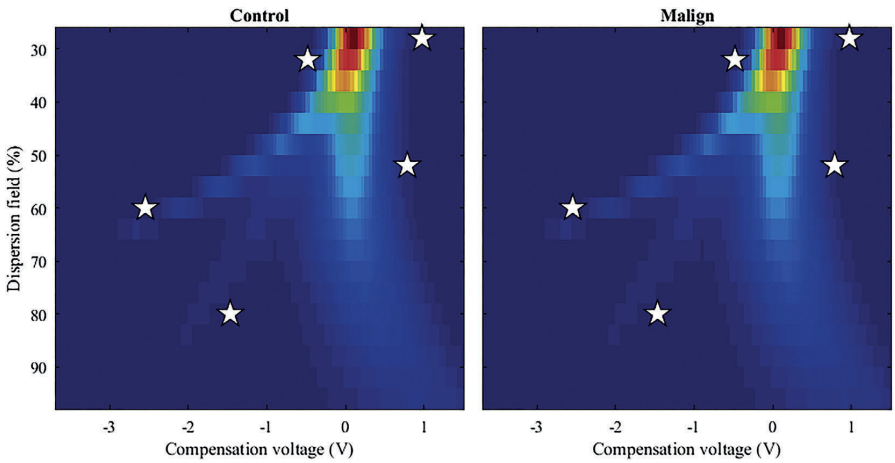

Fig. 3. Average FAIMS spectrum from a patient with ovarian cancer and from a control Stars indicate the areas of the spectrum that yielded optimum discrimination of the two groups. Compensation voltage is on X-axis and dispersion field strength is on Y-axis.

parameters change to a certain extend in every run, the process was repeated 100 times to reduce the effect of variation and to calculate averages and standard deviations for classification results. The analysis was conducted with MATLAB R2017b (MathWorks Inc., Natick, MA, USA).

3. Results

Characteristics of the final study population are presented in Table 1. The averages and standard deviations of the 100 runs of QDA and LDA analysis are given in Table 2. The performances of QDA and LDA seem to be mostly equal yet there is a notable difference in comparisons of benign tumors with low grade vs. high grade malignant tumors, respectively. The data produced by FAIMS is nonlinear by nature [17], and it is likely that nonlinear methods such as QDA yield better results in most cases, especially when the differences between groups are less distinct. By QDA analysis, benign ovarian tumors were distinguished from malignant tumors with sensitivity and specificity of 91.5% and 51.4%, respectively. However, the specificity improved to 79.7% when they were compared only to high-grade ovarian cancers. Even low grade ovarian malignancies were discriminated from high grade ovarian cancers with sensitivity of 87.8% and specificity of 89.6%, and from benign ovarian tumors with sensitivity of 73.1% and specificity of 92.9%, respectively.

Fig. 3 shows average FAIMS outputs from urine sample of a control and of a woman with ovarian cancer.

4. Discussion

This study provides preliminary evidence that FAIMS analysis of VOCs can discriminate urine samples from OC patients, patients with non-malignant tumors and healthy controls. High grade ovarian cancers seem to be separated from low grade ovarian cancers, benign ovarian tumors and controls.

The study further demonstrates that OC is associated with distinct odor [18–20]. The fact that this phenomenon is apparent in urine suggests that a systemic process is involved. It is apparent that metastatic, systemic cancer may elicit profound changes in urine composition that may be an indication of decreasing renal function. However, in the case of colorectal cancer, even early stage cancers could be detected [13]. There is in fact mounting body of evidence that cancer releases VOCs to systemic circulation that consequently are released through alveoli to breath and via glomerular filtration to urine [21]. This suggests that breath and urine can be considered alternative sampling methods for same VOCs. The feasibility of FAIMS/IMS has been demonstrated in both sampling sources [13,22]. Reliable sampling from exhaled breath is challenging [23] and the performance of breath VOC analysis in OC seems to be inferior to our results obtained from urine [18,24]. Since urine can be obtained non-invasively, we consider it as a more promising sampling source for VOC analysis in OC.

VOCs in different sample mediums and cancers seem to have common features, which are related to oxidation such as benzene derivatives [13,18,21]. The metabolic origin and function of most of these VOCs are unclear. They can originate from endogenous and exogenous sources and may thus be a result also from environmental exposure instead of the cancer [21]. In this study we achieved a good discrimination of high grade and low grade cancers. It has been suggested that KRAS and TP3 mutations play a role as a watershed in development of high or low grade serous OC, i.e. type I and II OCs [25]. These single mutations have resulted in VOC changes in cellular model [26] that reflect those found in urine in other cancers [13]. We speculate that the VOC alterations concerning various mutations should be studied in future also in ovarian cancer.

This study must be considered as preliminary, and the results should be verified in larger patient cohorts with this repeatable method. However, there is urgent need for early detection of especially aggressive type II OCs, with an ultimate goal to improve the prognosis of this devastating disease [25]. An important topic in future FAIMS research is to examine if cytoreductive surgery and immunosuppressive therapy have influences on VOC emissions of urine samples. FAIMS technology itself has advantages compared to GC–MS- and eNose implications; the technology by nature is sensitive to trace concentrations of molecules, is considerably more economical than MS-based methods, and does not suffer stability problems of other eNose technologies [27]. In contrast to canine studies, FAIMS is standardized and repeatable, whereas it is almost impossible to replicate research settings of canine studies because of variation in dogs.

Our study has also limitations. First, the present results cannot as such be generalized to unselected populations, but rather should be considered valid in the setting of tertiary hospitals, as part of the diagnostic work-up of adnexal tumors. Second, the number of analyzed urine samples was quite small. However, the proportions of three patient groups (controls, benign and malignant tumors) were balanced. Third, the considerable number of low malignant potential and borderline ovarian tumors in our study certainly has an influence on our results comparing benign and malignant ovarian tumors, and may have contributed to the rather great deviation seen between comparisons of benign tumors and all or low-grade malignant tumors. However, the comparisons between benign ovarian tumors or controls and high grade ovarian tumors are more accurate and specific. Fourth, the storage time of our samples was several years, which may have reduced the VOC emissions and thus differences between groups, as has been shown in a recent study examining the effect of storage on VOC profiles of urine [28]. In addition, the effects of the diet and possible medications may have had influence on the concentration and composition of urine although the samples were collected in the morning after at least 4 h

Table 1
Demographic data of study population.

	Malignant tumors		Benign tumors	Controls
n	33		18	18
Age (years)	64		64	71
Median (range)	(51–82)		(51–73)	(55–83)
Diagnosis (n)	Low grade cancers (15) - mucinous adenocarcinoma Stage IA and IC (1 + 1) - endometrioid adenocarcinoma Stage IA (1) - mucinous borderline Stage IA (5) - serous borderline Stage IA (4) - Sertoli-Leydig cell tumor Stage IIIC (1) - Granulosa cell tumor Stage IA (2)	High grade cancers (18) - carcinosarcoma Stage IIIC (1) - high grade serous adenocarcinoma • Stage IC (1) • Stage IIC (1) • Stage III/IV (15)	Serous cystadenoma (9) Mucinous cystadenoma (1) Fibroma (2) Simple cyst (3) Endometriotic cyst (2) Necrotized cyst (1)	Genital prolapse or urinary incontinence (18)

Table 2
Results of FAIMS signal data and QDA and LDA classification.

Classification pairs	QDA			LDA		
	Accuracy (%) (±2 Std)	Sensitivity (%) (±2 Std)	Specificity (%) (±2 Std)	Accuracy (%) (±2 Std)	Sensitivity (%) (±2 Std)	Specificity (%) (±2 Std)
Benign ovarian tumors vs. controls	91.9 (±9.8)	93.4 (±11.4)	90.4 (±14.4)	86.1 (±9.6)	86.0 (±11.2)	86.1 (±12.2)
Controls vs. malignant ovarian tumors	81.3 (±8.2)	91.2 (±7.2)	63.1 (±16.0)	81.2 (±5.8)	90.4 (±5.2)	64.3 (±12.8)
Controls vs. high grade ovarian cancers	81.9 (±5.2)	89.1 (±2.8)	74.6 (±9.6)	82.1 (±6.0)	88.7 (±3.2)	75.6 (±11.8)
Benign vs. malignant ovarian tumors	77.3 (±13.8)	91.5 (±6.4)	51.4 (±32.0)	65.9 (±13.8)	87.1 (±9.0)	27.1 (±38.6)
Benign ovarian tumors vs. low grade ovarian cancers	83.9 (±23.4)	73.1 (±41.4)	92.9 (±11.4)	59.3 (±7.0)	35.9 (±14.0)	78.8 (±5.8)
Benign ovarian tumors vs. high grade ovarian cancers	82.5 (±10.0)	85.3 (±15.0)	79.7 (±12.0)	82.5 (±9.6)	85.0 (±15.0)	79.9 (±11.2)
Low grade vs. high grade ovarian cancers	88.7 (±11.2)	87.8 (±12.8)	89.6 (±16.6)	82.0 (±10.8)	84.3 (±16.0)	79.7 (±13.4)

QDA, quadratic data analysis; LDA, linear data analysis.

fasting. The fact that the highest discrimination rate was achieved for benign tumors and controls suggests that there is a degree of bias between patient groups. This may also result from the larger and more heterogenous nature of cancer group.

5. Conclusion

According to our results, we propose that the VOC signature of urine of ovarian cancer patients can be recognized by FAIMS and that it has potential for being a non-invasive method in the detection of ovarian malignancy. Our novel study encourages us to examine further possibilities of FAIMS for diagnostics and follow-up of gynecological malignancies.

Funding

The study was supported by the Finnish Cancer Foundation (J.M. Grant MS738), Competitive Research Funding of Tampere University Hospital (J.M. Grant 9U036, N.O. Grants 150618, 9S045, 9T044, 9V044, 151B03 and 9U042), Tampere Tuberculosis Foundation (N.O. Grant) and Emil Aaltonen Foundation (N.O. Grant).

Role of the funding source

Researchers received funding for governmental bodies and non-profit organizations. These parties had no role in planning and execution of the study or in the analysis and writing process of the article.

Conflict of interest statement

RJN, EE and JUM declare no conflicts of interest. NO, PSK and ANR are shareholders of Olfactomics Ltd. which is about to commercialize proprietary technology for the detection of diseases by ion mobility spectrometry.

Ethical conduct of research

All participants gave their informed consent to the study, and the investigation was approved by the Ethic committee of Tampere University Hospital.

Acknowledgements

The authors thank medical student Elina Jokiniitty for technical assistance.

References

[1] K.D. Miller, R.L. Siegel, C.C. Lin, A.B. Mariotto, J.L. Kramer, J.H. Rowland, et al., Cancer treatment and survivorship statistics, 2016, CA Cancer J. Clin. 66 (2016) 271–289.
[2] I. Jacobs, D. Oram, J. Fairbanks, J. Turner, C. Frost, J.G. Grudzinskas, A risk of malignancy index incorporating CA 125, ultrasound and menopausal status for the accurate preoperative diagnosis of ovarian cancer, Br. J. Obstet. Gynaecol. 97 (1990) 922–929.
[3] J. Kaijser, Towards an evidence-based approach for diagnosis and management of adnexal masses: findings of the international ovarian tumour analysis (IOTA) studies, Facts Views Vis. Obgyn. 7 (2015) 42–59.
[4] I. Hellstrom, K.E. Hellstrom, fTwo novel biomarkers, mesothelin and HE4, for diagnosis of ovarian carcinoma, Expert Opin. Med. Diagn. 5 (2011) 227–240.
[5] J.J. Sandow, A. Rainczuk, G. Infusini, M. Makanji, M. Bilandzic, A.L. Wilson, et al., Discovery and validation of novel protein biomarkers in ovarian cancer patient urine, Proteomics Clin. Appl. 12 (2018), e1700135. .
[6] O. Turkoglu, A. Zeb, S. Graham, T. Szyperski, J.B. Szender, K. Odunsi, et al., Metabolomics of biomarker discovery in ovarian cancer: a systematic review of the current literature, Metabolomics 12 (2016) 60.
[7] R.J. Niemi, A.N. Roine, M.R. Hakkinen, P.S. Kumpulainen, T.A. Keinanen, J.J. Vepsalainen, et al., Urinary polyamines as biomarkers for ovarian cancer, Int. J. Gynecol. Cancer 27 (2017) 1360–1366.
[8] V. Mandilaras, M. Vernon, M. Meryet-Figuière, K. Karakasis, B. Lambert, L. Poulain, et al., Updates and current challenges in microRNA research for personalized medicine in ovarian cancer, Expert. Opin. Biol. Ther. 17 (2017) 927–943.
[9] G. Lippi, G. Cervellin, Canine olfactory detection of cancer versus laboratory testing: myth or opportunity? Clin. Chem. Lab. Med. 50 (2012) 435–439.
[10] G. Horvath, G.A. Jarverud, S. Jarverud, I. Horvath, Human ovarian carcinomas detected by specific odor, Integr. Cancer Ther. 7 (2008) 76–80.
[11] G. Horvath, H. Andersson, G. Paulsson, Characteristic odour in the blood reveals ovarian carcinoma, BMC Cancer 10 (2010) 643.
[12] J.A. Covington, M.P. van der Schee, A.S. Edge, B. Boyle, R.S. Savage, R.P. Arasaradnam, The application of FAIMS gas analysis in medical diagnostics, Analyst 140 (2015) 6775–6781.
[13] R.P. Arasaradnam, M.J. McFarlane, C. Ryan-Fisher, E. Westenbrink, P. Hodges, M.G. Thomas, et al., Detection of colorectal cancer (CRC) by urinary volatile organic compound analysis, PLoS One 9 (2014), e108750. .
[14] R.P. Arasaradnam, A. Wicaksono, H. O'Brien, H.M. Kocher, J.A. Covington, T. Crnogorac-Jurcevic, Noninvasive diagnosis of pancreatic cancer through detection of volatile organic compounds in urine, Gastroenterology 154 (2018) 485–487.
[15] G. Horvath, J. Chilo, T. Lindblad, Different volatile signals emitted by human ovarian carcinoma and healthy tissue, Future Oncol. 6 (2010) 1043–1049.
[16] A. Roine, E. Veskimae, A. Tuokko, P. Kumpulainen, J. Koskimaki, T.A. Keinanen, et al., Detection of prostate cancer by an electronic nose: a proof of principle study, J. Urol. 192 (2014) 230–234.
[17] D. Guo, Y. Wang, L. Li, X. Wang, J. Luo, Precise determination of nonlinear function of ion mobility for explosives and drugs at high electric fields for microchip FAIMS, J. Mass Spectrom. 50 (2015) 198–205.
[18] H. Amal, D.Y. Shi, R. Ionescu, W. Zhang, Q.L. Hua, Y.Y. Pan, et al., Assessment of ovarian cancer conditions from exhaled breath, Int. J. Cancer 136 (2015) 614.
[19] G. Horvath, H. Andersson, S. Nemes, Cancer odor in the blood of ovarian cancer patients: a retrospective study of detection by dogs during treatment, 3 and 6 months afterward, BMC Cancer 13 (2013) 396.
[20] G. Horvath, J. Chilo, T. Lindblad, Different volatile signals emitted by human ovarian carcinoma and healthy tissue, Future Oncol. 6 (2010) 1043–1049.
[21] H. Haick, Y.Y. Broza, P. Mochalski, V. Ruzsanyi, A. Amann, Assessment, origin, and implementation of breath volatile cancer markers, Chem. Soc. Rev. 43 (2014) 1423–1449.
[22] M. Westhoff, P. Litterst, L. Freitag, W. Urfer, S. Bader, J.I. Baumbach, Ion mobility spectrometry for the detection of volatile organic compounds in exhaled breath of patients with lung cancer: results of a pilot study, Thorax 64 (2009) 744–748.
[23] C. Lourenco, C. Turner, Breath analysis in disease diagnosis: methodological considerations and applications, Metabolites 4 (2014) 465–498.

[24] N. Kahn, O. Lavie, M. Paz, Y. Segev, H. Haick, Dynamic nanoparticle-based flexible sensors: diagnosis of ovarian carcinoma from exhaled breath, Nano Lett. 15 (2015) 7023–7028.
[25] R.J. Kurman, I. Shih, The origin and pathogenesis of epithelial ovarian cancer: a proposed unifying theory, Am. J. Surg. Pathol. 34 (2010) 433–443.
[26] M.P. Davies, O. Barash, R. Jeries, N. Peled, M. Ilouze, R. Hyde, et al., Unique volatolomic signatures of TP53 and KRAS in lung cells, Br. J. Cancer 111 (2014) 1213–1221.
[27] Z. Ma, G. Luo, K. Qin, N. Wang, W. Niu, Online sensor drift compensation for e-Nose systems using domain adaptation and extreme learning machine, Sensors (Basel) 18 (2018) 742.
[28] S. Esfahani, N.M. Sagar, I. Kyrou, E. Mozdiak, N. O'Connell, C. Nwokolo, et al., Variation in gas and volatile compound emissions from human urine as it ages, measured by an electronic nose, Biosensors (Basel) 6 (2016) 4.

Ovarian tumors of different histologic type and clinical stage induce similar changes in lipid metabolism

Running title: Various ovarian tumors affect blood lipidome

Riikka J Niemi[1,*], Elena I Braicu[2,*], Hagen Kulbe[2], Kaisa M Koistinen[3], Jalid Sehouli[2], Ulla Puistola[4], Johanna U Mäenpää[1,5] and Mika Hilvo[3,#]

[1]Department of Obstetrics and Gynecology, Tampere University Hospital, Tampere, Finland; [2]Charité – Universitätsmedizin Berlin, corporate member of Freie Universität Berlin Humboldt-Universität zu Berlin, and Berlin Institute of Health, Department of Gynecology, Berlin, Germany; [3]Zora Biosciences Oy, Espoo, Finland; [4]Department of Obstetrics and Gynecology, PEDEGO Research Unit, Medical Research Center Oulu, University of Oulu and University Hospital of Oulu, Oulu, Finland; [5]Faculty of Medicine and Life Sciences, University of Tampere, Tampere, Finland

[*]These authors contributed equally to this work

[#]Corresponding author at: Zora Biosciences Oy, Biologinkuja 1, FI-02150 Espoo, Finland.
e-mail: mika.hilvo@zora.fi, tel: +358-50-5347782

Abstract

Background: Previous results obtained from serum samples of late-stage, high-grade serous ovarian carcinoma patients showed large alterations in lipid metabolism. To validate and extend the results, we studied lipidomic changes in early-stage ovarian tumors. In addition to serous ovarian cancer, we investigated whether these changes occur in mucinous and endometrioid histological subtypes as well.

Methods: Altogether, 354 serum or plasma samples were collected from three centers, one from Germany and two from Finland. We performed lipidomic analysis of samples from patients with malignant (N=138) or borderline (N=25) ovarian tumors, and 191 controls with benign pathology. These results were compared to previously published data.

Results: We found 39 lipids that showed consistent alteration both in early- and late-stage ovarian cancer patients as well as in pre- and postmenopausal women. Most of these changes were already significant at an early stage and progressed with increasing stage. Furthermore, 23 lipids showed similar alterations in all investigated histological subtypes.

Conclusion: Changes in lipid metabolism due to ovarian cancer occur in early-stage disease but intensify with increasing stage. These changes occur also in other histological subtypes besides high grade serous carcinoma. Understanding lipid metabolism in ovarian cancer may lead to new therapeutic and diagnostic alternatives.

Key words: ovarian cancer; lipid; lipidomic; diagnostic; early-stage; histology; biomarker

Background

Prognosis of ovarian cancer improves remarkably if the disease is diagnosed at an early-stage, as early detection affords better opportunities for curative treatment. Current diagnostic methods primarily include vaginal ultrasound combined with the blood test to measure cancer antigen 125 (CA 125) levels. These methods lack specificity and sensitivity, especially in non-advanced ovarian cancer.[1] Therefore, there is a demand for new detection methods and biomarkers for distinguishing benign and borderline ovarian tumors, as well as early-stage and advanced ovarian cancer.

Malignant tumors, including ovarian cancer, adopt many metabolic abnormalities to meet the increased energy demand associated with increased cellular proliferation and tumor growth.[2] In ovarian cancer, the metabolic alterations in tissues and body fluids have been investigated by metabolic profiling to identify biomarkers for early detection and reliable prognosis.[3-5] Recently, using liquid chromatography-mass spectrometry (LC-MS), Gaul et al. found from serum 16 diagnostic metabolites, including many lipids and fatty acids, that distinguish early-stage ovarian cancer samples from healthy control samples.[6] In a lipidomic study, Buas et al. showed 34 significantly altered metabolites between serous ovarian carcinoma and benign serous ovarian tumor patients, and the plasma levels of the lipids were reduced in patients with a malignant disease.[7] Recently, our metabolomic analyses of tumor and blood samples from high-grade serous ovarian carcinoma (HGSOC) patients showed elevated concentrations of hydroxybutyric acids, implicating that these molecules could act as diagnostic and prognostic biomarkers.[8] Subsequently, lipidomic profiling of the same samples showed an overall reduction in the levels of most of the lipid species but elevations in specific ceramide (Cer) and triacylglycerol (TAG) lipids in metastatic ovarian cancer patients.[9]

Despite several studies showing lipidomic alterations in ovarian cancer, we are not aware of any studies that confirm which lipid species are the most consistently altered. To this end, as well as to validate our published lipidomic results and extend the analyses to low malignant potential (borderline) ovarian tumors and early-stage ovarian cancers, we applied the same previously used methodology[9] to analyze blood samples from patients with early-stage ovarian cancers. These results were subsequently compared to the results obtained from patients with benign gynecological disease. Our further aim was to investigate whether the lipidomic alterations found in patients with HGSOC can be applied to other histological subtypes, i.e., to mucinous and endometrioid ovarian carcinoma.

Materials and methods

Patients and samples

We performed lipidomic profiling on two study cohorts, one from Charitè (N=189) and another from Finland (N=165, from Tampere (N=111) and Oulu (N=54) University Hospitals). In addition, we used data from an independent, previously published study[9], referred herein as the Charité discovery (N=250). The Charité discovery study included 5 additional samples from patients with endometrioid tumors that were excluded from the original publication.[9] Clinical characteristics of these three study cohorts are shown in **Table 1**. The samples from both Charité studies were serum samples, while the Finnish samples were a mixture of serum and plasma, as shown in **Table 1**. All samples were collected preoperatively. In total, in these three studies, 290 samples were collected from patients with malignant ovarian tumors, 25 samples from subjects with borderline ovarian tumors, and 289 from women with benign gynecological tumors, endometriosis, infection, or other conditions. The diagnosis of invasive and borderline ovarian tumors was based on the WHO Classification.[10] The gynae-pathologists at the respective hospitals (University Hospitals of Oulu and Tampere, Finland, and Charité, Berlin, Germany) did the histological analyses, and immunohistochemistry was used when needed. The Charité samples were collected at the Tumor Bank - Ovarian Cancer Network (www.toc-network.de) at the Charitè Medical University (Berlin, Germany) between 07/2013 and 09/2016. The Finnish samples, from Tampere University Hospital and Oulu University Hospital, were collected between 2/2011-11/2014 and between 01/2009-12/2015, respectively.

Lipidomic analysis of serum samples (LC-MS/MS)

The samples were randomized within each cohort before lipidomic analysis. The lipidomic analysis has been previously described in detail.[9] Briefly, lipidomic analyses were performed using two platforms, a global screening method and a phosphosphingolipid platform. For the screening method, 10 µl of sample was needed for the extraction of the lipids using a modified Folch extraction.[11] For

the phosphosphingolipid method, 25 µl of sample was needed for the extraction of lipids using protein precipitation in methanol.

Lipidomic screening and phosphosphingolipid platforms were both analyzed on a hybrid triple quadrupole/linear ion trap mass spectrometer (QTRAP 5500, AB Sciex, Concords, Canada) equipped with ultra-high-performance liquid chromatography (UHPLC) (Nexera-X2, Shimadzu, Kyoto, Japan). Chromatographic separation of the lipidomic screening platform was performed on an Acquity BEH C18, 2.1 × 50 mm id. 1.7 µm column (Waters Corporation, Milford, MA, USA). Chromatographic separation of the phosphosphingolipid platform was performed on an AQUASIL C18, 2.1 × 50 mm, 5 µm (Thermo Fisher Scientific, Waltham, MA, USA) column set at 60 °C. For the MS analysis, a targeted approach in the positive ion mode was used for both platforms. The data were collected using a scheduled multiple reaction monitoring (sMRM™) algorithm for the lipidomics screening platform[12] and multiple reaction monitoring (MRM) for phosphosphingolipids. The lipidomic data were processed using Analyst and MultiQuant 3.0 software (AB Sciex), and the area or height ratios of the analyte and its corresponding IS peak were normalized with the IS amount and the sample volume. The details of the chromatography and mass spectrometry conditions have been previously described.[9]

The number of lipids and the mean coefficient of variation for each lipid class, determined from the quality control samples (6 in each 96-well plate), are shown in **Supplementary Table S1**. The list of all analyzed lipids has been published previously.[9]

Statistical analyses

Group comparisons (patients vs. controls) were performed by calculating the mean relative difference between the groups, and the p-values were determined by parametric t-tests on log-transformed concentrations. R version 3.4.2 was used for all statistical analyses. Tableau 10.1 was used for

heatmap visualizations. For diagnostic calculations, logistic regression models were developed using all samples in the Charité cohort and tested in the Finnish cohort. The AUC values were determined using the *pROC* package.[13] The top models presented in the article were selected by calculating the sum of the AUC values in both cohorts, and selecting the models with the highest values.

Results

Validation of altered lipidomic profile in ovarian cancer patients

To validate the lipidomic alterations detected in ovarian cancer patients, we determined which lipids were similarly altered between the patients and the controls in the two study cohorts (Charité and Finland), in addition to the previously published Charité discovery cohort (**Table 1**), provided that the change between the patients and the controls was significant in at least two cohorts. The results confirmed that ovarian cancer causes wide lipidomic changes as 155 lipids showed the same direction of change in all cohorts, and most of these changes were also statistically significant in all three independent cohorts (**Supplementary Table S2**). All further analyses were limited to these 155 lipids.

Lipidomic changes emerge in early-stage ovarian cancer patients

To identify which lipids have the best diagnostic potential, or those already altered in early-stage (I/II) cancer, we selected lipids that showed consistent increase or decrease both in stage I/II vs. controls and stage III/IV vs. controls, including all cohorts and histological subtypes. In addition, the lipids had to be significantly altered at least in stage III/IV patients in the Charité and Finnish cohorts. This approach resulted in 39 lipids which are shown in a heatmap in **Figure 1**. Samples from patients with ovarian cancer revealed a consistent decrease in the concentration of most of the analyzed lipid classes and included phospholipids (phosphatidylcholines (PCs), lysophosphatidylcholines (LPCs) and phosphatidylinositols (PIs)), cholesteryl esters (CEs), glucosyl/galactosyl ceramides (Glc/GalCers) and sphingomyelins (SMs). In turn, an increase was observed in many ceramides (Cers) with certain fatty acyl (FA) side chain compositions. Cers with 18:0, 20:0 and 24:1 FAs were increased, while 24:0 FA-containing Cers were decreased. The TAG lipid species also showed a variable trend depending on the FA side chains; TAGs with shorter FA side chains were decreased, whereas those with longer FA side chains were increased. In many lipid species, the alterations were

more significant in advanced stage (III/IV) patients but were already present in early-stage patients (I/II) (**Figure 1**). The lipidomic changes were consistent in both pre- and postmenopausal patient populations (**Figure 1**).

Tumors of various histological subtypes induce similar lipid changes

As the previous results were derived from HGSOC patients only[9], we investigated whether some changes in lipid species are also significant in patients with other histological subtypes (mucinous and endometrioid). Thus, we selected lipids showing the same direction of alteration in all histological subtypes of the Charité and Finnish cohorts. In addition, the selected lipids had to be significant in either mucinous or endometrioid subtypes in either of the cohorts. Twenty-one of 23 lipids were decreased in all histological subtypes (**Figure 2**), and only Cer(d18:1/18:0) and TAG(18:1/18:1/20:4) were increased. The most significant alterations were observed in PCs and LPCs. All lipid changes were significant in the serous subtype, which was expected based on the large number of cases in both cohorts. Interestingly, CA 125 was not significantly altered in mucinous subtype samples, while most lipid changes were significant in the Charité cohort despite a low number of mucinous cases (N=6). For endometrioid histology, none of the lipids were significant in the Charité cohort (N=9), whereas the Finnish cohort, with a slightly greater number of cases (N=14), showed significant alterations.

Fewer lipid changes are seen in borderline tumors than in malignant tumors

We also analyzed whether the observed lipidome alterations are present in borderline ovarian tumors. When only those lipids that were altered in the same direction in both cohorts and significant in at least one of them were selected, there were only a few significant alterations (**Figure 3**). Thus, it appears that borderline tumors do not cause as much of a change to the lipidome as malignant tumors.

Lipids improve the diagnostic value of CA125 for the detection of early-stage cancer

Finally, we investigated whether lipids can improve the diagnostic value of CA 125. As lipid ratios have shown diagnostic value in other diseases[14], we investigated combinations of all lipids and lipid ratios together with CA125. The lipids used for this analysis are shown in **Figure 1**. For the ratio calculations, the increased lipids in ovarian cancer patients and CA 125 were used as numerators, and all other lipids were used as denominators. To find more robust biomarkers, those lipids and lipid ratios were excluded that were significantly different (t-test $p<0.05$ and mean relative change > 10%) between control samples of the Charité and Finland cohorts. The models were generated using all subjects in the Charité cohort, and tested in the stage I/II and III/IV ovarian cancer patients separately, in addition to the validation in the Finnish cohort. As an example, the models with the highest improvement in both the Charité and Finnish cohorts are shown in **Table 2**. In the Charité cohort, CA 125 as a continuous variable instead of using the 35 U/mL cut-off improved the AUC values, and further improvement was seen for the detection of early-stage cases with incorporation of lipids, but not for late-stage cases where already CA 125 alone performed well. In the Finnish cohort, which had a higher proportion of other than serous malignant tumors, the AUC values for CA 125 and also the models with lipids were lower than in the Charité, but again the lipids improved the diagnostic value of CA 125 for the detection of stage I/II cancers.

Discussion

The present global lipidomics study investigating early- and advanced-stage ovarian cancer of various histological subtypes was performed to validate and extend our previous results on lipid changes in HGSOC patients. Altered lipid metabolism seems to be linked to ovarian cancer, but specific findings are still strikingly variable. Our data are in line with those earlier studies showing an overall decrease in the serum/plasma concentration of lipid metabolites[7] and glycerophospholipids[15,16] in ovarian cancer patients. The intensification of lipid changes in the advanced stage ovarian cancer patients suggests that the tumors are exploiting circulating lipids and lipoproteins with proportion to their size. The overall decrease of PCs may be associated with reduction of HDL cholesterol and ApoA1 in the ovarian cancer patients[17,18], as PCs are known to be abundant especially in the HDL particles.[19] However, this phenomenon cannot be used to explain the increase of lipid species in ovarian cancer patients. It has been suggested that changes in lipid metabolism during ovarian cancer pathogenesis reflect higher levels of cell division[20], enhanced fatty acid β-oxidation[5], and increased cellular proliferation or motility due to increased PI3-kinase activity[21], yet there are likely to be additional mechanisms explaining the alterations of specific lipids.

These results confirm our previous report describing an increase in the serum concentration of Cer(d18:1/18:0), Cer(d18:0/18:0) and TAG(18:1/18:1/20:4) in ovarian cancer patients.[9] Moreover, the phenomenon is evident at the early stages of disease development, i.e. stage I/II, but was found to become more pronounced with disease progression. In addition to HGSOC, Cer(d18:1/18:0) and TAG(18:1/18:1/20:4) were also significantly increased in mucinous and endometrioid ovarian cancer samples from the Finnish cohort. However, the number of mucinous and endometrioid carcinoma samples was likely too low in the Charitè cohort to show any significant difference. Interestingly, Cer(d18:1/18:0) and its precursor Cer(d18:0/18:0) have been associated with the development of insulin resistance and type 2 diabetes.[22-24] Taken together, these alterations to the lipid profile and

other metabolic changes, such as increase of ketone bodies[8], suggest that the metabolic profile of ovarian cancer patients resemble a diabetic phenotype.

Sphingolipids, especially Cers, have been linked to the development and progression of cancer[25], but results appear vary depending on the type of tumor.[26] Cers are considered to have anti-cancer properties, to act as second messengers for cell apoptosis[25] and to modulate cell growth.[27] Another sphingolipid, sphingosine-1-phosphate (S1P), has opposing cellular effects to Cers.[26] The role of sphingolipid metabolism in ovarian cancer has been investigated in a recent study in which 74 women with HGSOC were found to have significantly elevated plasma and tissue concentrations of C16-Cer, C18:1-Cer and C18-Cer compared to those of healthy controls[28], which is in line with our results. The researchers speculated that the increased amounts of Cers would be associated with particularly aggressive epithelial ovarian cancer cases and that the increased Cer concentrations would lead to increased conversion to S1P, as they found an elevated S1P concentration in tumor tissue. However, congruent with our data, elevation of S1P could not be observed in blood.

Buas et al. have shown reduction of all measured TAGs in the plasma of ovarian cancer patients.[7] However, in a lipidomic analysis of low and highly aggressive ovarian cancer cell lines, TAGs increased dramatically along aggressiveness of the cells and were assumed to be the largest source of cellular energy.[29] In a mouse model of HGSOC, compared to healthy mice, the serum levels of LPE(16:0) and PIs were decreased, while TAG(55:7) was significantly increased at early-stage cancer development.[30] On the other hand, decreased levels of TAGs in epithelial ovarian cancer patients have been shown to predict early recurrence of cancer.[31] In our study, only the concentrations of TAGs with longer fatty acid chains were increased or not altered, while those TAGs with short fatty acid chains were decreased. Our former study proposed that this result could be explained by genetics

via low expression of the *ABCD1* gene[9] which is associated with transport of long-chain fatty acids into the peroxisome for β-oxidation.[32]

Phospho- and sphingolipids are the most studied lipids in regard to the pathogenesis of ovarian cancer.[33] In 2004, it was shown that plasma levels of lysophospholipids varied between healthy controls and ovarian cancer patients, as well as pre- and postoperatively.[34] Moreover, in a pathway analysis, glycerophospholipid (LPCs and PCs) metabolism was a main dysregulated pathway in the pathogenesis of ovarian carcinoma.[35] Alteration of LPC levels may be caused by the binding and activation of specific cell surface G protein-coupled receptors (GPCRs), which can activate cell growth and proliferation.[36] Altered LPCs and lysophosphatidylethanolamines (LPEs) contribute to genetic instability and cancer initiation via enhanced phospholipase A2 (PLA2) activity[37] and inflammation.[3] Phospholipids are needed in cancer cells to generate the cellular membrane and maintain membrane integrity.[3] A large metabolic profiling study[3] of 448 plasma samples from epithelial ovarian cancer patients identified 53 specific metabolites that distinguished early- and late-stage ovarian cancer with an AUC of 0.88. These metabolites included LPCs and LPEs which were elevated in localized ovarian cancer but reduced in metastasized ovarian cancer. A potential explanation for the reduced levels of LPCs and LPEs in advanced cancer could be that rapidly proliferating tumors consume more phospholipids in their attempt to maintain membrane integrity, leading to an exhaustion of substrates.[30] Also lysophosphatidic acid (LPA) has been purported to be a possible biomarker because some studies have shown LPA to be elevated in plasma samples of ovarian cancer patients.[34,38], but we could not confirm this as we did not monitor LPAs in our lipidomic method.

Borderline ovarian tumors have low malignant potential and elevated mitotic activity without stromal invasion. They commonly occur in younger women compared to ovarian cancer patients and have

lower recurrence rates.[39] Denkert et al. found significantly different metabolite levels (including metabolites from glycerolipid metabolism and free fatty acids) in borderline ovarian tumor tissues compared to invasive ovarian carcinomas using gas chromatography/time-of-flight mass spectrometry.[20] However, they had only nine borderline tumors in their study. Based on the present study, lipid metabolism in borderline ovarian tumors differs from that in invasive cancers. The Charité cohort had more borderline ovarian tumors (N=18) than the Finnish cohort. These samples were mainly serous epithelial tumors. Significant differences were observed only for occasional plasmalogens as compared to benign controls.

In the Charitè cohort, the results were evaluated by menopausal status. Greater alterations in Cer d16:1, d18:0 and d18:1 were observed in postmenopausal women. However, in some PC lipids, premenopausal changes were stronger. A serum lipidomics study of ovariectomized healthy rats showed that Cers and phospholipids increased in response to estrogen deficiency while TAGs decreased, which was contrary to earlier studies.[40] Our study lacks data on possible hormone replacement or hormone therapy in the Charitè premenopausal group. The samples from the Finnish cohort were postmenopausal with no current hormone therapy.

Our study had some limitations. First, changes in lipoprotein levels can at least partly explain the overall decrease of lipids among cancer patients, but unfortunately, we did not have lipoprotein levels available from the patients. Neither did we have the information on BMI, which may also affect lipid levels. Second, in the Finnish cohort, the sample sets contained both serum and plasma samples, which may affect the lipid levels. However, it is worth noting that the lipid changes were consistent with the two other data sets, and thus, it can be assumed that the difference does not significantly affect the results. Moreover, the logistic regression models developed in the Charité cohort showed high AUC values in the Finnish cohort, which also supports the validity of the results. Third, there

was an age imbalance in the cohorts, as the Charité cohort patients were older than the controls. However, the results were consistent with the Finnish cohort, where the controls were older than the patients. This finding and our previous age-adjusted lipidomic analyses[9] suggest that age does not explain the differences in lipid metabolism observed in ovarian cancer patients. Fourth, the blood samples were not collected during a fasting condition, which may affect the results. However, it is worth noting that there were no differences between groups and that it is expected that fasting samples might have given a better separation between the ovarian cancer patients and the subjects with benign disease.

We have shown that blood lipidomic changes occur in several patient cohorts and already at the early-stage ovarian cancer, but intensify with the progression of the disease. Many of the lipid changes are similar in patients with serous, mucinous and endometrioid ovarian carcinoma, suggesting that rewiring of lipid metabolism is an integral part of ovarian carcinogenesis. The results provide an excellent basis for further development of diagnostics and the future investigations should also explore the potential of exploiting the altered ovarian cancer lipid metabolism for therapeutic purposes.

Additional information

Ethics approval and consent to participate

All patients gave their informed consent to the study, and the investigation was approved by the local Ethical Committees of Charité, Oulu and Tampere University Hospitals. The study was performed in accordance with the Declaration of Helsinki.

Availability of data and materials' statement

The datasets generated during and/or analysed during the current study are available for non-commercial use from the corresponding author on reasonable request.

Conflict of interest

MH and KMK are employed by Zora Biosciences Oy, which holds patent disclosures for diagnostic tests of ovarian cancer using small molecules, including lipids. JUM reports grants and personal fees from Roche, AstraZeneca, Tesaro, SOBI and Clovis, outside the submitted work. RJN, EIB, HK, JS and UP declare no conflicts of interest.

Funding

No external funding was used for conducting this study.

Authorship

JUM, EIB, UP, JS, RJN and HK conducted patient enrollment and clinical work. KMK performed lipidomic mass spectrometry experiments, and MH statistical analyses. RJN, MH and JUM wrote the manuscript. All authors have revised and approved the manuscript.

Supplementary information is available at the British Journal of Cancer`s website.

References

1. Gupta D, Lis CG. Role of CA125 in predicting ovarian cancer survival - a review of the epidemiological literature. *J Ovarian Res* 2009; **2:** 13.

2. Sciacovelli M, Gaude E, Hilvo M, Frezza C. The metabolic alterations of cancer cells. *Methods Enzymol* 2014; **542:** 1-23.

3. Ke C, Hou Y, Zhang H, Fan L, Ge T, Guo B, *et al*. Large-scale profiling of metabolic dysregulation in ovarian cancer. *Int J Cancer* 2015; **136:** 516-526.

4. Odunsi K, Wollman RM, Ambrosone CB, Hutson A, McCann SE, Tammela J, *et al*. Detection of epithelial ovarian cancer using 1H-NMR-based metabonomics. *Int J Cancer* 2005; **113:** 782-788.

5. Fong MY, McDunn J, Kakar SS. Identification of metabolites in the normal ovary and their transformation in primary and metastatic ovarian cancer. *PLoS One* 2011; **6:** e19963.

6. Gaul DA, Mezencev R, Long TQ, Jones CM, Benigno BB, Gray A, *et al*. Highly-accurate metabolomic detection of early-stage ovarian cancer. *Sci Rep* 2015; **5:** 16351.

7. Buas MF, Gu H, Djukovic D, Zhu J, Drescher CW, Urban N, *et al*. Identification of novel candidate plasma metabolite biomarkers for distinguishing serous ovarian carcinoma and benign serous ovarian tumors. *Gynecol Oncol* 2016; **140:** 138-144.

8. Hilvo M, de Santiago I, Gopalacharyulu P, Schmitt WD, Budczies J, Kuhberg M, *et al*. Accumulated Metabolites of Hydroxybutyric Acid Serve as Diagnostic and Prognostic Biomarkers of Ovarian High-Grade Serous Carcinomas. *Cancer Res* 2016; **76:** 796-804.

9. Braicu EI, Darb-Esfahani S, Schmitt WD, Koistinen KM, Heiskanen L, Poho P, *et al*. High-grade ovarian serous carcinoma patients exhibit profound alterations in lipid metabolism. *Oncotarget* 2017; **8:** 102912-102922.

10. Carcangiu ML, Kurman RJ, Carcangiu ML, Herrington CS. WHO Classification of Tumours of Female Reproductive Organs. Lyon: International Agency for Research on Cancer (I A R C) (UN); 2014.

11. Folch J, Lees M, Sloane Stanley GH. A simple method for the isolation and purification of total lipides from animal tissues. *J Biol Chem* 1957; **226:** 497-509.

12. Weir JM, Wong G, Barlow CK, Greeve MA, Kowalczyk A, Almasy L, *et al*. Plasma lipid profiling in a large population-based cohort. *J Lipid Res* 2013; **54:** 2898-2908.

13. Robin X, Turck N, Hainard A, Tiberti N, Lisacek F, Sanchez JC, *et al*. pROC: an open-source package for R and S+ to analyze and compare ROC curves. *BMC Bioinformatics* 2011; **12:** 77.

14. Laaksonen R, Ekroos K, Sysi-Aho M, Hilvo M, Vihervaara T, Kauhanen D, *et al*. Plasma ceramides predict cardiovascular death in patients with stable coronary artery disease and acute coronary syndromes beyond LDL-cholesterol. *Eur Heart J* 2016; **37:** 1967-1976.

15. Bachmayr-Heyda A, Aust S, Auer K, Meier SM, Schmetterer KG, Dekan S, *et al*. Integrative Systemic and Local Metabolomics with Impact on Survival in High-Grade Serous Ovarian Cancer. *Clin Cancer Res* 2017; **23:** 2081-2092.

16. Zhang T, Wu X, Yin M, Fan L, Zhang H, Zhao F, *et al*. Discrimination between malignant and benign ovarian tumors by plasma metabolomic profiling using ultra performance liquid chromatography/mass spectrometry. *Clin Chim Acta* 2012; **413:** 861-868.

379 17. Sun Y, Meng H, Jin Y, Shi X, Wu Y, Fan D, *et al*. Serum lipid profile in gynecologic tumors: a
380 retrospective clinical study of 1,550 patients. *Eur J Gynaecol Oncol* 2016; **37:** 348-352.

381 18. Kozak KR, Su F, Whitelegge JP, Faull K, Reddy S, Farias-Eisner R. Characterization of serum
382 biomarkers for detection of early stage ovarian cancer. *Proteomics* 2005; **5:** 4589-4596.

383 19. Hilvo M, Simolin H, Metso J, Ruuth M, Oorni K, Jauhiainen M, *et al*. PCSK9 inhibition alters
384 the lipidome of plasma and lipoprotein fractions. *Atherosclerosis* 2018; **269:** 159-165.

385 20. Denkert C, Budczies J, Kind T, Weichert W, Tablack P, Sehouli J, *et al*. Mass spectrometry-based
386 metabolic profiling reveals different metabolite patterns in invasive ovarian carcinomas and ovarian
387 borderline tumors. *Cancer Res* 2006; **66:** 10795-10804.

388 21. Shayesteh L, Lu Y, Kuo WL, Baldocchi R, Godfrey T, Collins C, *et al*. PIK3CA is implicated as
389 an oncogene in ovarian cancer. *Nat Genet* 1999; **21:** 99-102.

390 22. Meikle PJ, Wong G, Barlow CK, Weir JM, Greeve MA, MacIntosh GL, *et al*. Plasma lipid
391 profiling shows similar associations with prediabetes and type 2 diabetes. *PLoS One* 2013; **8:** e74341.

392 23. Wigger L, Cruciani-Guglielmacci C, Nicolas A, Denom J, Fernandez N, Fumeron F, *et al*. Plasma
393 Dihydroceramides Are Diabetes Susceptibility Biomarker Candidates in Mice and Humans. *Cell Rep*
394 2017; **18:** 2269-2279.

395 24. Hilvo M, Salonurmi T, Havulinna AS, Kauhanen D, Pedersen ER, Tell GS, *et al*. Ceramide stearic
396 to palmitic acid ratio predicts incident diabetes. *Diabetologia* 2018; **61:** 1424-1434.

397 25. Hajj C, Becker-Flegler KA, Haimovitz-Friedman A. Novel mechanisms of action of classical
398 chemotherapeutic agents on sphingolipid pathways. *Biol Chem* 2015; **396:** 669-679.

399 26. Furuya H, Shimizu Y, Kawamori T. Sphingolipids in cancer. *Cancer Metastasis Rev* 2011; **30:**
400 567-576.

401 27. Segui B, Andrieu-Abadie N, Jaffrezou JP, Benoist H, Levade T. Sphingolipids as modulators of
402 cancer cell death: potential therapeutic targets. *Biochim Biophys Acta* 2006; **1758:** 2104-2120.

403 28. Knapp P, Bodnar L, Blachnio-Zabielska A, Swiderska M, Chabowski A. Plasma and ovarian
404 tissue sphingolipids profiling in patients with advanced ovarian cancer. *Gynecol Oncol* 2017; **147:**
405 139-144.

406 29. Zhao Z, Cai Q, Xu Y. The Lipidomic Analyses in Low and Highly Aggressive Ovarian Cancer
407 Cell Lines. *Lipids* 2016; **51:** 179-187.

408 30. Jones CM, Monge ME, Kim J, Matzuk MM, Fernandez FM. Metabolomic serum profiling detects
409 early-stage high-grade serous ovarian cancer in a mouse model. *J Proteome Res* 2015; **14:** 917-927.

410 31. Li J, Xie H, Li A, Cheng J, Yang K, Wang J, *et al*. Distinct plasma lipids profiles of recurrent
411 ovarian cancer by liquid chromatography-mass spectrometry. *Oncotarget* 2017; **8:** 46834-46845.

412 32. van Roermund CW, Visser WF, Ijlst L, Waterham HR, Wanders RJ. Differential substrate
413 specificities of human ABCD1 and ABCD2 in peroxisomal fatty acid beta-oxidation. *Biochim*
414 *Biophys Acta* 2011; **1811:** 148-152.

415 33. Pyragius CE, Fuller M, Ricciardelli C, Oehler MK. Aberrant lipid metabolism: an emerging
416 diagnostic and therapeutic target in ovarian cancer. *Int J Mol Sci* 2013; **14:** 7742-7756.

417 34. Sutphen R, Xu Y, Wilbanks GD, Fiorica J, Grendys EC,Jr, LaPolla JP, *et al*. Lysophospholipids
418 are potential biomarkers of ovarian cancer. *Cancer Epidemiol Biomarkers Prev* 2004; **13:** 1185-1191.

35. Zhang Y, Liu Y, Li L, Wei J, Xiong S, Zhao Z. High resolution mass spectrometry coupled with multivariate data analysis revealing plasma lipidomic alteration in ovarian cancer in Asian women. *Talanta* 2016; **150:** 88-96.

36. Murph M, Tanaka T, Pang J, Felix E, Liu S, Trost R, *et al*. Liquid chromatography mass spectrometry for quantifying plasma lysophospholipids: potential biomarkers for cancer diagnosis. *Methods Enzymol* 2007; **433:** 1-25.

37. Li H, Zhao Z, Wei G, Yan L, Wang D, Zhang H, *et al*. Group VIA phospholipase A2 in both host and tumor cells is involved in ovarian cancer development. *FASEB J* 2010; **24:** 4103-4116.

38. Xu Y, Shen Z, Wiper DW, Wu M, Morton RE, Elson P, *et al*. Lysophosphatidic acid as a potential biomarker for ovarian and other gynecologic cancers. *JAMA* 1998; **280:** 719-723.

39. Trimble CL, Trimble EL. Management of epithelial ovarian tumors of low malignant potential. *Gynecol Oncol* 1994; **55:** 52.

40. Vinayavekhin N, Sueajai J, Chaihad N, Panrak R, Chokchaisiri R, Sangvanich P, *et al*. Serum lipidomics analysis of ovariectomized rats under Curcuma comosa treatment. *J Ethnopharmacol* 2016; **192:** 273-282.

Figure 1. Heatmap showing lipidomic changes in early- (I/II) and late-stage (III/IV) ovarian cancer patients. In addition, the results are shown in pre- and postmenopausal patients of all stages. The difference is calculated relative to controls. The color scale (from -70% to 100%) is adjusted according to the lipids, in cancer patients CA 125 showed mean elevation higher than 100%. ***, $p<0.001$; **, $p<0.01$; *, $p<0.05$. Charité study had 60 premenopausal controls and 17 cancer cases as well as 48 postmenopausal controls and 42 cancer cases.

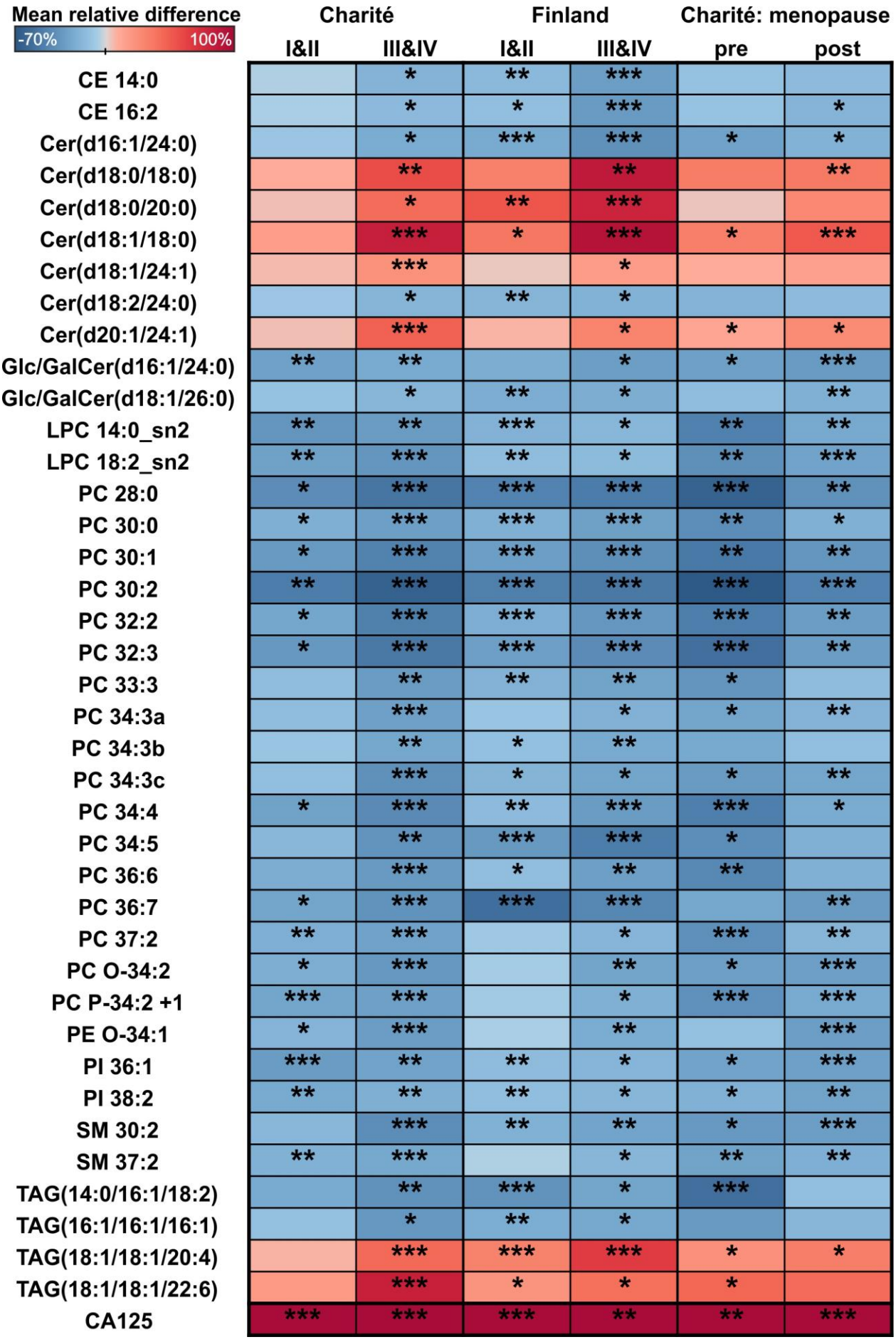
Mean relative difference
-70%
100%
Charité
Finland
Charité: menopause
I&II
III&IV
I&II
III&IV
pre
post
CE 14:0
CE 16:2
Cer(d16:1/24:0)
Cer(d18:0/18:0)
Cer(d18:0/20:0)
Cer(d18:1/18:0)
Cer(d18:1/24:1)
Cer(d18:2/24:0)
Cer(d20:1/24:1)
Glc/GalCer(d16:1/24:0)
Glc/GalCer(d18:1/26:0)
LPC 14:0_sn2
LPC 18:2_sn2
PC 28:0
PC 30:0
PC 30:1
PC 30:2
PC 32:2
PC 32:3
PC 33:3
PC 34:3a
PC 34:3b
PC 34:3c
PC 34:4
PC 34:5
PC 36:6
PC 36:7
PC 37:2
PC O-34:2
PC P-34:2 +1
PE O-34:1
PI 36:1
PI 38:2
SM 30:2
SM 37:2
TAG(14:0/16:1/18:2)
TAG(16:1/16:1/16:1)
TAG(18:1/18:1/20:4)
TAG(18:1/18:1/22:6)
CA125

Figure 2. Heatmap showing lipidomic changes in ovarian cancer patients with different histological subtypes as compared to control subjects. The color scale (from -70% to 100%) is adjusted according to the lipids, in some of the analyses CA 125 showed elevation higher than 100%. ***, p<0.001; **, p<0.01; *, p<0.05.

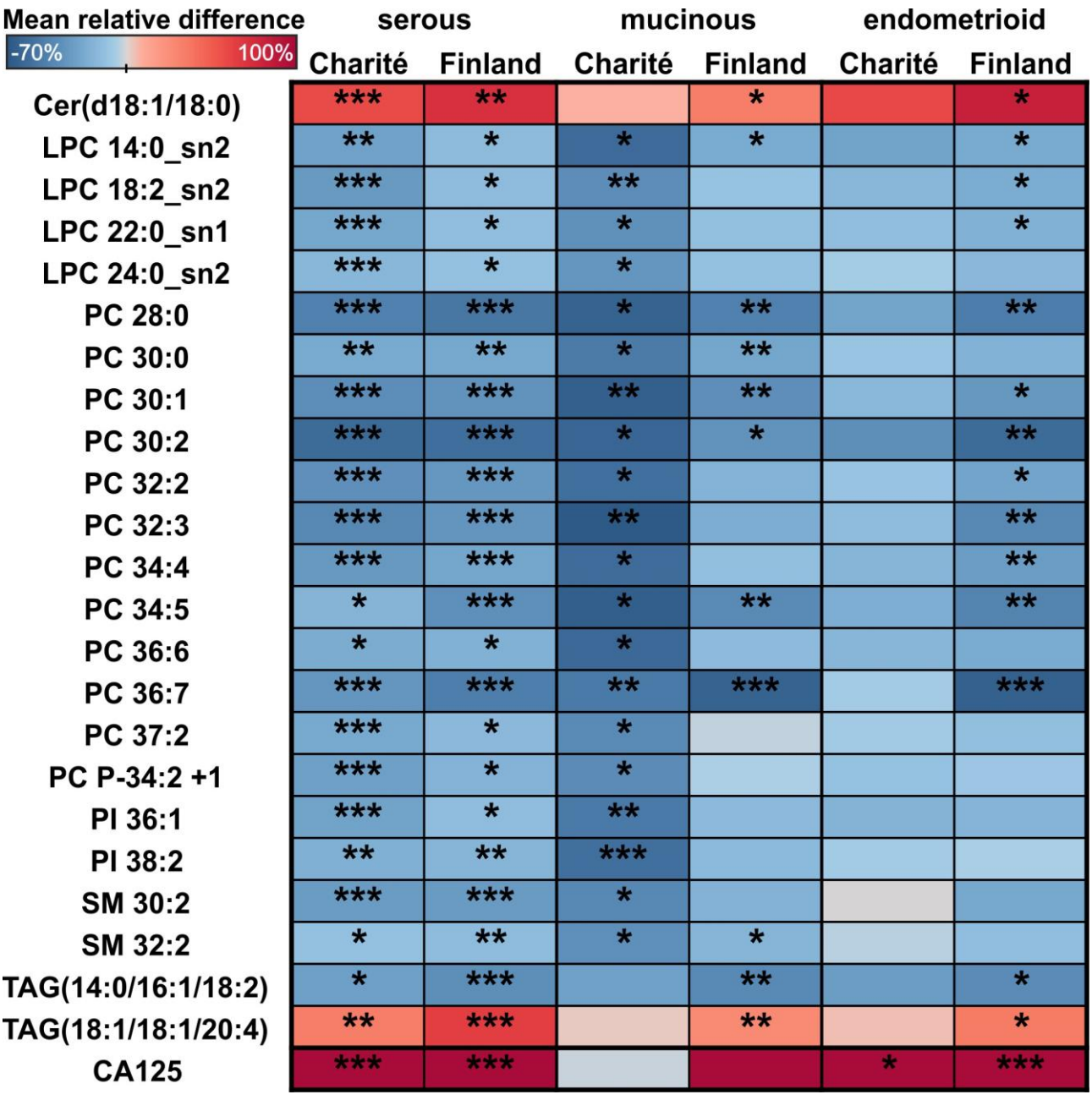

Figure 3. Heatmap showing lipidomic changes in patients with borderline tumors as compared to control subjects. The color scale is adjusted according to the lipids (from -70% to 100%), CA 125 showed elevation higher than 100% in the Charité cohort. ***, p<0.001; **, p<0.01; *, p<0.05.

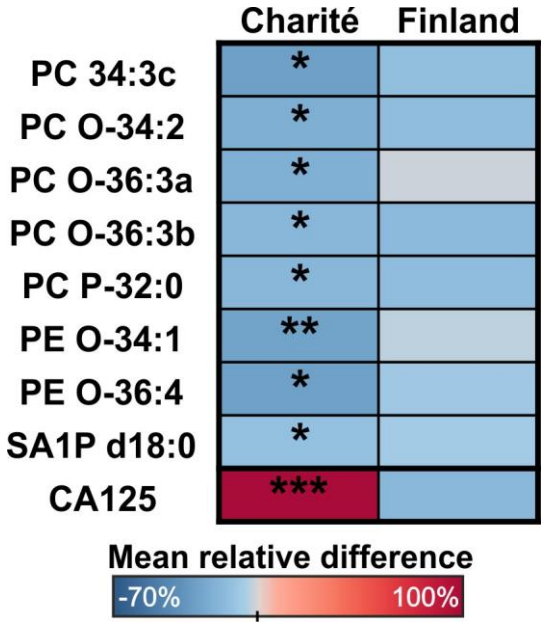

Table 1. Clinical characteristics of the study cohorts. For age, the values represent median and interquartile range and p-values in the comparison against the control group are denoted as follows: ***, p<0.001; **, p<0.01; *, p<0.05; N.S., not significant.

		Charité	Finland	Charité discovery
Malignant		**62**	**76**	**152**
Age		57 (50-72)***	58 (51-64)*	59 (50-67)***
Histology	serous	41	29	147
	mucinous	6	18	
	endometrioid	9	14	5
	other	6	15	
Stage	I&II	26	52	8
	III&IV	33	22	133
	NA	3	2	11
Sample	serum	62	22	152
	plasma		54	
Borderline		**18**	**7**	
Age		51 (44-57) N.S.	63 (56-67) N.S.	
Histology	serous	13	5	
	mucinous	2	2	
	other	3		
Stage	I&II	12	7	
	III&IV	3		
	NA	3		
Sample	serum	18	7	
Benign		**109**	**82**	**98**
Age		49 (40-58)	62 (56-69)	41 (31-55)
Diagnosis	other	7	2	43
	uterine fibroid	7	1	25
	cyst	4	9	1
	cystic teratoma	12	8	5
	functional cyst	22		
	inclusion cyst	3		
	endometrioid cyst	5		
	non-ovarian cyst		4	
	cystadenoma	32	2	4
	mucinous cystadenoma		3	2
	cystadenofibroma	7	10	2
	serous cystadenoma		34	3
	Brenner tumor	1	2	1
	fibroma/thecoma		5	
	fibroadenoma		1	
	incomplete abortion			5
	adnexitis			5
	endometriosis	9	1	2
Sample	serum	109	82	98

Table 2. AUC values with 95% confidence intervals for the logistic regression models. As comparison, the models are shown also for CA 125 alone or CA 125 as binary variable dichotomized by the clinically used 35 U/mL cut off value.

		Charité			Finland		
Variable1	**Variable 2**	**All**	**Stage I/II**	**Stage III/IV**	**All**	**Stage I/II**	**Stage III/IV**
CA125 / Glc/GalCer(d18:1/26:0)	Cer(d18:1/24:1) / LPC 14:0_sn2	0.93 (0.89-0.96)	0.87 (0.80-0.94)	0.98 (0.96-1.00)	0.76 (0.68-0.85)	0.74 (0.64-0.83)	0.93 (0.84-1.00)
Cer(d18:1/24:1) / LPC 14:0_sn2	CA125 / PC 37:2	0.93 (0.89-0.96)	0.87 (0.81-0.94)	0.98 (0.95-1.00)	0.76 (0.68-0.85)	0.73 (0.64-0.83)	0.95 (0.89-1.00)
Cer(d20:1/24:1) / LPC 14:0_sn2	CA125 / PC 37:2	0.92 (0.87-0.96)	0.85 (0.77-0.93)	0.98 (0.95-1.00)	0.77 (0.68-0.85)	0.74 (0.64-0.83)	0.95 (0.90-1.00)
Cer(d18:1/24:1) / LPC 14:0_sn2	CA125 / PI 38:2	0.92 (0.89-0.96)	0.87 (0.81-0.94)	0.97 (0.94-1.00)	0.77 (0.69-0.85)	0.75 (0.66-0.84)	0.95 (0.88-1.00)
CA125	TAG(18:1/18:1/22:6) / LPC 14:0_sn2	0.91 (0.86-0.96)	0.83 (0.73-0.92)	0.98 (0.96-1.00)	0.78 (0.70-0.86)	0.75 (0.66-0.84)	0.89 (0.77-1.00)
TAG(18:1/18:1/22:6) / LPC 14:0_sn2	CA125 / PC 37:2	0.91 (0.86-0.96)	0.83 (0.74-0.91)	0.98 (0.96-1.00)	0.78 (0.70-0.86)	0.75 (0.66-0.84)	0.88 (0.73-1.00)
TAG(18:1/18:1/22:6) / LPC 14:0_sn2	CA125 / PC P-34:2 +1	0.91 (0.86-0.96)	0.83 (0.75-0.92)	0.98 (0.96-1.00)	0.78 (0.70-0.86)	0.75 (0.66-0.84)	0.89 (0.75-1.00)
TAG(18:1/18:1/22:6) / LPC 14:0_sn2	CA125 / SM 37:2	0.91 (0.86-0.95)	0.83 (0.73-0.92)	0.98 (0.96-1.00)	0.78 (0.70-0.86)	0.75 (0.66-0.84)	0.91 (0.80-1.00)
Cer(d20:1/24:1) / LPC 14:0_sn2	CA125 / PI 38:2	0.91 (0.87-0.96)	0.85 (0.76-0.93)	0.97 (0.94-1.00)	0.78 (0.70-0.86)	0.76 (0.67-0.85)	0.95 (0.88-1.00)
TAG(18:1/18:1/22:6) / PC 30:0	CA125 / PC 30:0	0.90 (0.85-0.95)	0.82 (0.73-0.91)	0.98 (0.95-1.00)	0.79 (0.72-0.87)	0.77 (0.68-0.85)	0.91 (0.78-1.00)
CA125		0.90 (0.84-0.95)	0.81 (0.71-0.90)	0.97 (0.94-1.00)	0.72 (0.62-0.81)	0.67 (0.57-0.78)	0.95 (0.91-1.00)
CA125 (35 U/mL cut-off)		0.80 (0.73-0.86)	0.69 (0.59-0.80)	0.89 (0.84-0.94)	0.71 (0.64-0.79)	0.68 (0.60-0.76)	0.91 (0.87-0.95)

Supplementary Table S1. Number of lipids and the mean coefficient of variation (CV) for all the analyzed lipid classes.

Lipid class	Number of lipids	CV
AC	8	15 %
CE	21	24 %
Cer d16:1	8	26 %
Cer d18:0	7	36 %
Cer d18:1	9	25 %
Cer d18:2	9	27 %
Cer d20:1	4	22 %
DAG	18	29 %
Gb3	4	41 %
Glc/GalCer	22	29 %
LacCer	10	28 %
LPC	40	11 %
LPC P/LPC O	13	11 %
LPE	11	12 %
LPE P/LPE O	2	13 %
PC	70	20 %
PC P/PC O	46	23 %
PE	23	27 %
PE P/PE O	15	30 %
PG	4	23 %
PI	19	19 %
S1P/SA1P	4	9 %
SM	41	16 %
TAG	42	11 %

Supplementary Table S2. Lipids that showed consistent alteration in all three and were significant in at least two study cohorts.

		Charité		Finland		Charité Discovery	
Lipid class	Lipid name	Change (%)	p-value	Change (%)	p-value	Change (%)	p-value
CE	CE 14:0	-10,5	0,113	-22,3	**1,2E-05**	-22,3	**4,1E-06**
	CE 14:1	-13,0	0,247	-28,2	**1,5E-04**	-22,0	**4,7E-05**
	CE 16:2	-11,8	0,060	-20,7	**3,3E-04**	-21,1	**2,0E-07**
	CE 18:0	-9,8	0,113	-10,8	**0,020**	-26,7	**4,9E-10**
	CE 18:2	-9,9	**0,028**	-2,1	0,568	-21,9	**7,2E-10**
Cer d16:1	Cer(d16:1/23:0)	-7,0	0,300	-28,5	**2,6E-06**	-24,9	**5,7E-04**
	Cer(d16:1/24:0)	-17,7	**0,027**	-30,2	**6,0E-07**	-29,3	**6,1E-08**
	Cer(d16:1/26:0)	-15,7	0,055	-18,7	**0,003**	-17,1	**0,004**
Cer d18:0	Cer(d18:0/18:0)	36,1	**0,001**	45,0	**0,044**	49,7	**5,7E-05**
	Cer(d18:0/20:0)	28,2	**0,023**	58,2	**4,1E-04**	22,0	**0,018**
	Cer(d18:0/23:0)	-8,8	0,158	-20,4	**0,001**	-17,4	**0,004**
Cer d18:1	Cer(d18:1/18:0)	56,2	**2,9E-06**	52,5	**1,9E-04**	71,4	**7,2E-12**
	Cer(d18:1/20:0)	15,9	**0,027**	24,4	**0,027**	39,7	**9,9E-08**
	Cer(d18:1/24:0)	-4,4	0,570	-13,6	**0,002**	-11,9	**0,009**
	Cer(d18:1/24:1)	18,8	**0,003**	6,9	0,477	30,5	**1,1E-06**
Cer d18:2	Cer(d18:2/18:0)	28,0	**0,005**	20,7	0,063	26,2	**5,2E-04**
	Cer(d18:2/23:0)	-10,9	0,190	-17,9	**7,8E-04**	-18,5	**5,6E-04**
	Cer(d18:2/24:0)	-13,4	0,105	-20,8	**9,9E-05**	-22,4	**1,1E-05**
	Cer(d18:2/26:0)	-10,7	0,298	-9,8	**0,037**	-14,2	**0,040**
Cer d20:1	Cer(d20:1/24:1)	29,1	**6,8E-04**	13,5	0,126	43,9	**2,1E-07**
DAG	DAG(14:0/18:1)	-24,0	0,203	-23,5	**9,6E-04**	-39,1	**6,9E-04**
Gb3	Gb3(d18:1/24:0)	-16,8	**0,011**	-7,7	0,788	-23,1	**8,6E-05**
Glc/GalCer	Glc/GalCer(d16:1/20:0)	-21,6	**0,011**	-25,1	**0,001**	-16,8	**9,7E-04**
	Glc/GalCer(d16:1/22:0)	-19,0	**0,015**	-29,5	**4,2E-05**	-23,4	**1,5E-05**
	Glc/GalCer(d16:1/23:0)	-22,8	**0,003**	-22,5	**0,008**	-19,3	**3,8E-04**
	Glc/GalCer(d16:1/24:0)	-26,9	**4,5E-04**	-25,8	**0,013**	-23,1	**5,0E-06**
	Glc/GalCer(d18:1/20:0)	-15,4	**0,019**	-6,7	0,845	-19,7	**9,2E-05**
	Glc/GalCer(d18:1/22:0)	-18,8	**0,001**	-11,2	0,752	-25,9	**2,6E-07**
	Glc/GalCer(d18:1/23:0)	-19,4	**0,003**	-15,9	0,081	-23,8	**7,8E-07**
	Glc/GalCer(d18:1/24:0)	-17,2	**0,002**	-19,7	**0,047**	-24,2	**4,7E-07**
	Glc/GalCer(d18:1/26:0)	-16,3	**0,016**	-23,7	**0,002**	-21,0	**9,4E-05**
	Glc/GalCer(d18:2/20:0)	-19,9	**0,003**	-11,7	0,587	-23,3	**1,7E-04**
	Glc/GalCer(d18:2/22:0)	-19,2	**0,002**	-19,6	**0,022**	-17,9	**5,0E-04**
	Glc/GalCer(d18:2/23:0)	-22,2	**0,003**	-20,5	**0,012**	-21,6	**5,2E-05**
	Glc/GalCer(d18:2/24:0)	-17,1	**0,002**	-17,5	0,088	-23,9	**4,8E-08**
LacCer	LacCer(d16:1/16:0)	-3,9	0,495	-12,8	**0,016**	-21,1	**5,3E-05**
LPC	LPC 14:0_sn1	-31,2	**1,9E-05**	-13,7	**0,001**	-19,1	**0,002**
	LPC 14:0_sn2	-34,0	**3,1E-05**	-21,0	**3,4E-05**	-30,3	**2,3E-05**
	LPC 18:2_sn1	-32,0	**1,1E-05**	-5,0	0,147	-29,7	**1,9E-07**
	LPC 18:2_sn2	-33,4	**2,9E-06**	-12,8	**0,004**	-34,7	**2,3E-12**
	LPC 20:0_sn1	-24,5	**6,2E-05**	-2,7	0,308	-16,6	**0,003**
	LPC 20:0_sn2	-25,2	**9,9E-06**	-6,9	0,085	-14,6	**0,011**
	LPC 20:2_sn2	-25,4	**6,7E-06**	-7,0	0,067	-16,4	**3,2E-05**
	LPC 20:3_sn2	-19,0	**0,003**	-2,6	0,226	-24,4	**1,4E-06**
	LPC 22:0_sn1	-27,2	**1,6E-07**	-13,3	**0,004**	-28,7	**6,3E-10**
	LPC 24:0_sn1	-21,0	**3,4E-06**	-10,0	**0,015**	-28,7	**1,5E-12**
	LPC 24:0_sn2	-19,0	**2,0E-05**	-11,6	**0,007**	-28,9	**2,3E-13**
LPC O	LPC O-20:0	-19,6	**0,001**	-6,0	0,095	-15,5	**7,1E-04**
	LPC O-22:0	-15,6	**0,007**	-6,6	0,074	-25,3	**4,8E-11**
	LPC O-22:1	-22,3	**3,7E-04**	-5,3	0,113	-17,5	**0,002**
	LPC O-24:1	-15,3	**0,019**	-6,1	0,093	-17,8	**8,2E-05**
	LPC O-24:2	-25,3	**5,5E-05**	-8,5	0,203	-33,0	**1,2E-08**
LPE	LPE 18:2_sn1	-37,7	**5,8E-06**	-1,3	0,288	-40,1	**1,5E-11**
	LPE 18:2_sn2	-37,2	**1,8E-06**	-4,0	0,191	-35,4	**4,6E-10**
LPE P	LPE P-16:0	-9,9	**0,013**	-23,3	**1,5E-07**	-12,4	0,197
	LPE P-18:0	-13,2	**0,005**	-12,8	**9,4E-05**	-7,8	0,382
PC	PC 28:0	-47,2	**5,5E-06**	-47,8	**2,7E-07**	-59,0	**1,5E-15**
	PC 30:0	-26,4	**0,001**	-25,1	**2,1E-05**	-43,4	**4,0E-15**
	PC 30:1	-39,4	**2,1E-04**	-34,6	**1,2E-06**	-52,1	**2,4E-13**
	PC 30:2	-57,6	**4,2E-08**	-48,2	**4,5E-07**	-61,4	**2,1E-14**
	PC 31:1	-14,8	0,311	-23,8	**0,002**	-36,9	**1,9E-08**
	PC 32:1	-12,2	0,795	-15,0	**0,016**	-29,0	**1,9E-06**
	PC 32:2	-38,0	**8,7E-07**	-26,7	**1,9E-06**	-52,5	**4,0E-19**
	PC 32:3	-42,9	**1,1E-05**	-34,3	**2,9E-07**	-58,5	**4,2E-17**
	PC 33:2	-18,0	**0,010**	-7,8	0,098	-35,6	**6,9E-13**
	PC 33:3	-23,3	**0,021**	-23,4	**1,9E-04**	-42,0	**4,2E-11**
	PC 34:2	-15,9	**0,001**	-5,8	0,198	-28,6	**4,5E-10**
	PC 34:3a	-22,1	**5,0E-04**	-14,2	**0,010**	-37,9	**9,7E-14**
	PC 34:3b	-19,2	**0,025**	-17,5	**0,001**	-35,8	**3,9E-12**
	PC 34:3c	-25,4	**0,002**	-21,8	**0,010**	-44,1	**1,2E-13**
	PC 34:4	-35,4	**1,3E-05**	-22,1	**4,5E-05**	-52,1	**5,6E-16**
	PC 34:5	-28,0	**0,006**	-39,4	**2,9E-08**	-41,3	**1,4E-05**
	PC 35:2a	-16,5	**0,036**	-0,4	0,931	-26,3	**2,6E-06**
	PC 35:2b	-16,1	**0,006**	-2,9	0,413	-28,1	**1,1E-09**
	PC 35:3a	-26,7	**1,3E-05**	-5,9	0,151	-39,8	**3,1E-15**
	PC 35:3b	-17,1	**0,019**	-4,5	0,206	-35,9	**2,0E-09**
	PC 36:1	-16,3	**0,033**	-9,5	**0,038**	-12,5	0,053
	PC 36:2	-22,6	**7,2E-05**	-7,7	0,103	-35,1	**2,0E-13**
	PC 36:3a	-30,8	**3,2E-07**	-3,8	0,280	-36,0	**2,2E-14**
	PC 36:3b	-14,6	**0,040**	-4,9	0,186	-29,2	**1,9E-08**
	PC 36:5a	-16,9	**0,030**	-10,6	0,097	-32,1	**1,4E-07**
	PC 36:6	-28,8	**7,7E-04**	-20,3	**7,5E-04**	-46,4	**2,0E-09**
	PC 36:7	-32,8	**9,3E-04**	-52,7	**1,6E-13**	-27,4	**2,1E-05**
	PC 37:1	-16,8	**0,004**	-5,1	0,300	-20,5	**4,6E-06**
	PC 37:2	-26,5	**2,6E-05**	-11,7	**0,022**	-36,3	**6,0E-13**
	PC 37:3	-13,5	**0,031**	-2,2	0,432	-30,4	**7,4E-09**
	PC 38:0	-10,9	**0,049**	-5,9	0,106	-29,1	**5,0E-11**
	PC 38:3	-19,4	**0,007**	-3,0	0,262	-30,6	**1,5E-09**
	PC 38:5b	-4,4	0,564	-19,6	**0,002**	-16,1	**0,003**
	PC 38:6a	-28,1	**9,3E-05**	-9,9	0,051	-35,0	**2,6E-10**
	PC 38:6b	-33,2	**1,3E-06**	-5,8	0,446	-38,0	**7,1E-13**
	PC 40:8	-22,0	**0,004**	-7,7	0,051	-33,4	**6,8E-10**
PC P	PC P-34:2	-29,8	**2,3E-06**	-12,7	**0,035**	-33,3	**2,7E-13**
PC O	PC O-32:1	-17,6	**0,011**	-3,4	0,490	-31,3	**7,1E-10**
	PC O-34:1	-13,4	**0,012**	-0,2	0,968	-22,2	**1,2E-08**
	PC O-34:2	-29,9	**1,0E-05**	-12,6	**0,031**	-39,7	**6,7E-17**
	PC O-36:1	-10,2	0,075	-9,8	**0,026**	-27,6	**1,5E-07**

	PC O-36:2b	-27,1	**4,4E-06**	-2,1	0,924	-36,3	**4,2E-14**
	PC O-36:3a	-28,9	**4,8E-07**	-4,6	0,424	-38,7	**4,8E-16**
	PC O-36:3b	-22,1	**1,5E-04**	-0,2	0,644	-33,2	**4,7E-13**
	PC P 36:2a	-25,8	**1,0E-04**	-9,0	0,235	-26,8	**6,2E-08**
	PC P-32:0	-17,6	**0,001**	-6,8	0,214	-20,2	**8,1E-07**
	PC P-32:1	-16,2	**0,018**	-11,7	0,159	-21,4	**1,6E-05**
	PC P-34:1	-13,8	**0,039**	-3,2	0,815	-13,9	**3,6E-04**
PE	**PE 34:3**	-19,1	0,328	-19,5	**0,009**	-49,7	**8,1E-07**
	PE 36:2	-10,7	0,326	-17,1	**0,010**	-37,9	**1,5E-06**
	PE 36:3a	-31,0	**0,005**	-3,9	0,359	-53,8	**2,0E-07**
	PE 36:3b	-44,6	**0,003**	-5,4	0,674	-54,7	**3,9E-08**
	PE 36:5	-6,4	0,700	-25,9	**4,1E-05**	-26,5	**0,023**
	PE 38:3	-9,7	0,583	-10,6	**0,042**	-40,4	**6,8E-07**
	PE 38:5b	-7,2	0,995	-23,5	**1,0E-04**	-36,9	**1,6E-04**
PE O	**PE O-34:1**	-25,6	**3,8E-05**	-11,7	**0,030**	-12,4	**0,047**
	PE O-36:4	-35,9	**1,3E-05**	-2,6	0,148	-49,1	**4,9E-11**
	PE O-38:5	-35,4	**3,0E-06**	-0,2	0,419	-38,5	**1,3E-09**
	PE O-38:6	-22,7	**0,001**	-4,2	0,259	-16,2	**0,044**
PG	**PG 34:1**	-2,6	0,870	-13,6	**0,024**	-22,9	**0,011**
	PG 36:2	-5,5	0,740	-16,6	**0,007**	-25,6	**3,5E-04**
PI	**PI 32:0**	-22,0	0,181	-19,6	**0,005**	-49,6	**3,0E-04**
	PI 34:1	-18,7	**0,050**	-7,2	0,163	-31,3	**4,7E-04**
	PI 34:2	-17,6	**0,016**	-4,1	0,371	-31,3	**6,4E-06**
	PI 36:1	-30,7	**4,1E-05**	-16,7	**0,001**	-40,1	**3,8E-07**
	PI 36:3a	-42,8	**1,4E-08**	-1,9	0,195	-51,5	**9,9E-10**
	PI 36:3b	-27,7	**2,1E-04**	-3,8	0,223	-39,6	**3,0E-09**
	PI 38:2	-25,1	**2,7E-04**	-16,1	**0,002**	-40,5	**3,5E-07**
	PI 38:3a	-23,5	**4,9E-04**	-4,8	0,104	-33,8	**1,6E-09**
	PI 38:3b	-23,7	**0,007**	-3,9	0,458	-13,3	**0,050**
S1P	**S1P d16:1**	-10,2	**0,045**	-14,2	**1,6E-04**	-20,0	**1,4E-08**
	S1P d18:1	-3,7	0,333	-9,3	**0,001**	-19,3	**1,3E-07**
	S1P d18:2	-11,3	**0,007**	-2,0	0,396	-29,3	**1,2E-13**
SA1P	**SA1P d18:0**	-6,4	0,126	-11,0	**5,6E-04**	-24,8	**5,3E-13**
SM	**SM 30:2**	-29,3	**1,2E-04**	-24,5	**2,5E-04**	-35,8	**2,2E-11**
	SM 31:1	-9,3	0,158	-11,3	**0,033**	-24,7	**1,2E-07**
	SM 32:1	-3,4	0,615	-9,8	**0,004**	-17,3	**7,4E-06**
	SM 32:2	-14,4	**0,006**	-13,7	**9,7E-04**	-28,0	**3,3E-11**
	SM 36:0	27,8	**0,012**	40,0	**0,008**	6,9	0,288
	SM 37:2	-24,7	**4,2E-05**	-9,5	0,069	-34,8	**1,4E-13**
	SM 39:1	-8,9	0,203	-16,5	**1,7E-04**	-27,5	**1,3E-10**
	SM 40:2b	-10,0	**0,044**	-7,9	**0,021**	-27,3	**4,5E-12**
	SM 44:2	12,6	**0,035**	13,1	**0,041**	5,0	0,304
TAG	**TAG(14:0/16:0/18:1)**	-21,2	0,112	-31,0	**6,4E-06**	-37,3	**1,0E-04**
	TAG(14:0/16:0/18:2)	-16,3	0,318	-31,2	**1,7E-05**	-36,5	**2,3E-04**
	TAG(14:0/16:1/18:1)	-23,5	0,085	-30,4	**1,1E-05**	-44,3	**1,5E-04**
	TAG(14:0/16:1/18:2)	-28,1	**0,009**	-35,5	**1,7E-05**	-50,9	**2,4E-06**
	TAG(14:0/17:0/18:1)	-1,9	0,555	-20,4	**0,004**	-22,6	**0,045**
	TAG(14:0/18:0/18:1)	-17,5	0,166	-29,4	**4,4E-05**	-44,4	**1,7E-04**
	TAG(14:0/18:2/18:2)	-26,4	**0,010**	-23,0	**0,013**	-47,7	**3,3E-06**
	TAG(14:1/16:0/18:1)	-18,9	0,528	-30,3	**1,9E-05**	-35,4	**0,005**
	TAG(14:1/16:1/18:0)	-11,6	0,860	-23,7	**0,001**	-28,7	**0,016**
	TAG(14:1/18:0/18:2)	-12,7	0,391	-14,0	**0,008**	-25,3	**0,014**
	TAG(14:1/18:1/18:1)	-9,6	0,408	-15,7	**0,009**	-33,0	**1,2E-04**
	TAG(16:0/18:1/18:1)	18,4	**0,002**	3,0	0,780	9,2	**0,037**
	TAG(16:1/16:1/16:1)	-19,3	0,207	-26,7	**5,2E-04**	-43,7	**5,2E-05**
	TAG(16:1/16:1/18:0)	-19,2	0,108	-27,6	**2,5E-05**	-40,5	**6,6E-05**
	TAG(18:1/18:1/20:4)	30,3	**0,003**	40,5	**9,7E-07**	28,4	**6,7E-06**
	TAG(18:1/18:1/22:6)	52,8	**6,0E-04**	28,6	**0,004**	54,9	**5,4E-08**